Evaluación neurobiológica de electrodos regenerativos como interfase entre nervios lesionados y prótesis biónicas

Natalia Lago Pérez

Memoria de Tesis presentada por Natalia Lago Pérez para optar al grado de Doctora en Biología por la Universidad Autónoma de Barcelona

Director de Tesis:

Dr. Xavier Navarro Acebes
Catedrático de la Unidad de Fisiología Médica
Departamento de Biología Celular, Fisiología e Inmunología
Universidad Autónoma de Barcelona

Bellaterra, Julio de 2006

AGRADECIMIENTOS

Parece mentira que hoy esté escribiendo los agradecimientos. Bueno, a decir verdad, es la tercera vez que lo intento. Las otras dos pasadas, no pasaron el corte de los expertos, así que he decidido volver a intentarlo hasta que todo el mundo quede contento con el resultado. Imposible!

Si comenzamos por el principio, el que yo esté escribiendo ahora los agradecimientos, se lo agradezco, y valga la redundancia, a mi director de tesis, el Dr. Xavier Navarro Acebes, es decir, mi jefe para los amigos. Agradecerle el dejarme pertenecer a su grupo, el enseñarme infinidad de cosas y sobre todo, agradecerle la paciencia que ha mostrado conmigo, siempre. Porque la verdad es que existen pocas personas en el mundo con el aguante necesario para soportar mis cambios de humor y, a veces, mis contestaciones. Pues sí, he tenido la inmensa suerte de rodearme de gente paciente y con muchísimas ganas de enseñar sus conocimientos. También quiero agradecerle el que me haya hecho parte del proyecto en el que hemos estado trabajando todo este tiempo, dándome la oportunidad de conocer "lo que se cuece" fuera de la poyata.

Saltándome este primer agradecimiento, volveré hacia atrás para recordar como empezó todo. Nunca hubiera imaginado hasta dónde llegaría cuando entré en Fisiología Animal para comenzar las prácticas de la carrera. Agradecer a Amalia Molinero, Mercé Giralt y Juan Hidalgo el dejarme pertenecer a su grupo durante, casi, tres años. Junto a ellos aprendí muchísimo a la vez que me lo pasé genial. Y por extensión a todos los compañeros de fisio con los que compartí momentos muy buenos tanto dentro como fuera del laboratorio. Desde Jordi Camats, Quinoche, Javier, Albert, Xava Loca, David, Sheila, Octavi, Cristineta, Laura, Joan Carles, Olguita, Josep ("Betty Boo y el viejo pederasta"-gran torneig de futbolín), Antonio, Lluís…seguro que me dejo a alguien (perdón)…y Cris (buena amiga).

Y con alguno de ellos conocí la AENC, bueno, las neurofarras. Y con ellas a Hugo, Mar, Diego, Carles, Ana, Toni, Guillem, Esther y Rubèn, entre otros. Buenos tiempos aquellos.

Y todo esto me llevó a mi lugar actual en el que he realizado el trabajo que hoy presento. Gracias a Guillem y Rubèn por ser tan buenos compañeros y por esas risas. Y gracias, como no, a Esther (ET-Supermannnn…) de la cual he aprendido muchas de las técnicas que me han llevado a los resultados actuales (menos las inmunos claro, je je). Pero sobre todo, por lo gran compañera y mejor amiga que ha demostrado ser.

Y mis compañeros actuales. Mónica Sofía, Clara y Carolina. A ellas tres muchas gracias porque, a pesar que su trabajo no se parece en nada con el mío, siempre han estado para escucharme, para ayudarme, para reírse de mi…para reírme

de ellas…También a Chesi porque ha sido pieza clave en mi tesis y porque siempre ha estado allí cuando la he necesitado. También acordarme de Caty, Txell, Toni, Laura, Tabare y Eva. Y de Kike, Quim y su antropología social, y Jordi Serra por enseñarme "el secreto del registro de fibras C".

Mención especial a Mónica Espejo y a Maite. Gracias Mónica (alias Mc Giver) por toda tu ayuda, siempre, por escucharme y por esos cafés a las 9 de la mañana. Eres una profesional de los pies a la cabeza de la que he aprendido cada día.

Continuando con la UAB, acordarme de esas pequeñas cosas que hacen más fácil el día a día. Los buenos días a Maite y sus compañeras, y el trato tan cercano con los compañeros del bar. Siempre que los he necesitado para alguna cosa, si han podido, me han ayudado. Y parecerá una tontería, pero al fin y al cabo, ¿que nos queda? Acordarnos de "esas pequeñas cosas".

También a los compis de Farmacología (David, Marta, Myriam, Francesc, Sonia, Laura, Ana…), a los de Histología y a Lydia por esos ánimos que siempre está dispuesta a dar. También a José Miguel Vela, Mar y Sierra por hacerme más fácil mi vida "inmunohistológica".

Bueno, dejando de lado el territorio UAB, pasaremos al territorio Santacolomense. Mi pueblo. Ahí, nacimos y crecimos los que hoy por hoy somos una gran familia: mis amigos. A ellos tengo que agradecerles el esfuerzo tan grande que han realizado para intentar entender mi trabajo. Y también por hacerme ver que existe algo más ahí fuera, tras las columnas de la Autónoma. Me acuerdo de muchos momentos junto a ellos. Mon y nuestros "viajes cruzando la meseta", Brujas y Spiderman-Alba, Calella con su fruta fresca y ese "barco inoportuno", esos esfuerzos "Sevillanísticos" todos los sábados tarde…bodorrios, bautizos, celebraciones Champions (inolvidables!!!), esos Ponces... Para ellos: Alba, Ana, Bruno (nuestro sobrinito), Cristian, Elsa, Encarna, Esther, Fernando, Iván, Jorge, Juan, Luís, Mar, Maribel, Marta Cañadas, Marta Genovés, Marta Gisbert, Mon, Myriam, Óscar, Paquito, Raúl, Sonia (ya te debo dos, por lo menos) y Víctor.

Y a mis padres: final y principio de todo. Los que siempre han estado allí para darme ese aliento necesario para continuar y para creer en mis posibilidades. Habéis sido mi mano derecha y mi mano izquierda, y el pecho sobre el que recostarme para descansar. Este trabajo está dedicado a ellos; a los que siempre creyeron en mí. También acordarme de mi yayita y mi hermano Sergio que cierran esta pequeña pero enorme familia.

Gracias a todos por allanar el camino.

ÍNDICE

INTRODUCCIÓN

El cuerpo humano siempre ha sido atractivo desde el punto de vista de la ingeniería y la robótica como inspiración al diseño de máquinas. En particular, la mano humana es un buen ejemplo de cómo un mecanismo tan complejo puede ser implementado siendo capaz de realizar tareas muy complejas y útiles por medio de una combinación efectiva de mecanismos, sensaciones, acciones y control. La mano humana no solo es una "máquina" efectiva sino que también es un instrumento ideal para adquirir información del ambiente externo. Por toda la información que nos aporta y por su gran utilidad, la falta por amputación provoca graves problemas al individuo que la padece.

La amputación es la separación de un miembro o parte de él del resto del organismo. Sólo en Estados Unidos, se producen unos 50.000 casos de amputaciones de extremidades al año (según información del National Center for Health Statistics). De éstas, aproximadamente una cuarta parte implican la amputación de miembros superiores. Entre las amputaciones de la mano, la pérdida parcial de ésta, como de uno o más dedos, es el tipo más común. Sin embargo, existen unas 45.000 presonas registradas en Estados Unidos con amputación completa de la mano o del brazo. En países escandinavos, las lesiones que implican amputación de extremidades superiores, que requieren potencialmente reimplante o prótesis se presentan con una incidencia de 1,9 por 100.000 personas cada año (3,3 en hombres y 0,5 en mujeres) (Atroshi y Rosberg, 2001). Las causas de la amputación son variables, accidentes traumáticos, enfermedades cardiovasculares, diabetes, infección, etc, siendo los accidentes traumáticos y el cáncer las causas más frecuentes de las amputaciones de mano.

Las consecuencias más importantes de la amputación de la mano son la pérdida de capacidades funcionales y de la información que normalmente recibimos a través de ella, ya que representa uno de los instrumentos fundamentales del organismo humano para la adquisición de información del ambiente externo y para la realización de tareas complejas de la vida cotidiana. La mano es un órgano muy especial. Su nivel de función y versatilidad es único requiriendo una integración sensorial central y un control motor fino, no encontrado en ningún otro sistema del cuerpo. La sensibilidad de la mano es vital; de hecho, se encuentra representada de forma desproporcionada en el cerebro siendo indicativo del grado de importancia.

Nuestras manos son imprescindibles en la manipulación de nuestro ambiente, recibiendo información desde éste, y en la comunicación no verbal entre individuos. Es, además, un sistema complejo y adaptable, capaz tanto de manipular de forma precisa y delicada como de coger objetos pesados con fuerza (Chao et al., 1989; Kapandji, 1982). Para realizar las diferentes funciones, la mano presenta muchas combinaciones de hasta 60 grados de libertad, un gran número de receptores propioceptivos y extereoceptivos y un complejo control jerárquico. A pesar de esta complejidad, los movimientos requeridos para realizar las actividades de la vida diaria (Activities of Daily Living: ADLs) son pocos, más si se tiene en cuenta que esas habilidades se han ido adquiriendo durante años de forma consciente o inconsciente.

Una vez ocurrida la amputación de la mano, existen 2 posibilidades para el reemplazamiento de esta mano perdida: el transplante de mano y la prótesis de mano. La primera opción radica en el reimplante de la mano amputada, pero esto sólo es posible en lesiones limpias y si la extremidad se ha conservado. Mayores posibilidades puede ofrecer el transplante de la mano de donantes fallecidos. En el año 2004, se realizaron 24 transplantes de mano en todo el mundo, la mayoría en Italia y Francia (Hausman et al., 2003; Lanzetta et al., 2004). Desde el punto de vista quirúrgico, el transplante ofrece algunas ventajas técnicas, debido a que el miembro donante puede ser seccionado de forma controlada con el fin de optimizar la anastomosis y la función mecánica. Tras 24 meses de rehabilitación, se ha observado en los pacientes una recuperación de la función motora y sensorial que puede llegar a ser bastante buena. Sin embargo, en la mayoría de los casos se produce rechazo inmunológico, que precisa para su control la administración a largo plazo de tratamiento inmunosupresor. El rechazo inmunológico en este tipo de transplantes es mayor que en el de otros órganos, debido a que está compuesto de varios tipos de tejidos (huesos, nervios, vasos, músculos y piel) aumentando mucho la inmunogenicidad. Por ello, y dado que el transplante de mano no está considerado como un transplante vital, la proporción entre riesgo y beneficio genera un dilema ético (Moore, 2000; Herndon, 2000). Por otra parte, el grado de recuperación de funciones complejas, como tareas motoras de habilidad o la discriminación tactil, suele ser limitado debido a la falta de reinervación adecuada de músculos y receptores cutáneos por parte de los axones regenerados del receptor,

lo que, en todo caso, precisa de la sutura microquirúrgica de los nervios del receptor a los de la mano transplantada.

La alternativa al transplante de mano es la utilización de prótesis con el fin de remedar las funciones perdidas tras la amputación. La mano humana ofrece 2 funciones básicas: la prensión y la sensibilidad (tacto, temperatura, propiocepción…). Las prótesis de brazo o de mano pueden sustituir las funciones básicas de una mano, así como reestablecer el aspecto exterior. Las prótesis actuales se agrupan en manos y garfios, que pueden estar controladas de forma externa o por el propio cuerpo. Las prótesis de garfio, aunque no son cosméticas, ofrecen una buena prensión, especialmente para tareas específicas (de tipo mecánico). Algunas de las prótesis de mano permiten al amputado el intercambio de la terminal con el fin de realizar tareas específicas. A este tipo de prótesis hay que sumar aquellas en las que se han incorporado sensores artificiales en la punta de los "dedos", obteniendo información por retroalimentación para un mayor control de la fuerza de prensión. Las prótesis de mano más avanzadas, sean controladas por la fuerza corporal o mediante sistema de control mioeléctrico, ofrecen aún inconvenientes y limitaciones, principalmente debidos al déficit de control sobre la prensión y al limitado control de un movimiento cada vez (Atkins et al., 1996).

Mediante los avances en las técnicas de microfabricación, durante las dos últimas décadas, ha aumentado el interés en el desarrollo de interfases nerviosas periféricas que permitan conectar una mano artificial con los nervios proximales de la mano amputada previamente, permitiendo al sujeto tener un control neural sobre la mano prostética (Körner, 1979; Kovacs et al., 1992; Kovacs et al., 1994; Dario et al., 1998). De esta manera, se utilizarían las señales nerviosas eferentes motoras para controlar los diferentes grados de libertad de la mano artificial y la estimulación de las fibras aferentes sensoriales para obtener el feed-back sensorial pseudonatural. A pesar de la viabilidad de las conexiones físicas entre la mano artificicial y los nervios seccionados, se desconoce si el sistema puede llegar a ser funcional o no. Existe un número elevado de impedimentos a la hora de interconectar el sistema nervioso con prótesis y ortesis; entre ellos, los cambios a nivel del nervio periférico proximal a la sección, la pérdida de conexiones centrales y los cambios dinámicos en las áreas corticales como resultado de la plasticidad del Sistema Nervioso Central (SNC). Todos estos cambios explicarían, en parte, los pobres resultados en la regeneración del nervio periférico seccionado.

El principal objetivo del presente trabajo ha sido el estudio de los electrodos de tipo regenerativo como potencial interfase neuroelectrónica. Para ello, se han realizado estudios de biocompatibilidad y de regeneración a largo plazo, así como el registro de señales neurales mediante estos electrodos. Este trabajo constituye el análisis neurobiológico y la revisión crítica más extensa hasta la fecha de los problemas que surgen a la hora de aplicar una interfase a un nervio periférico lesionado. Además se aportan indicaciones básicas de los futuros avances necesarios en el ámbito de la microtecnología, para mejorar los electrodos y sistemas de conexión existentes, así como en la neurobiología, en relación a estrategias que aumenten y mejoren las capacidades regenerativas del Sistema Nervioso Periférico (SNP).

Este trabajo ha estado enmarcado dentro del proyecto europeo "CYBERHAND" ("Development of a cybernetic hand prosthesis", IST-2001-35094; www.cyberhand.org), en el cual se ha abordado la realización de una neuroprótesis de mano avanzada, capaz de re-crear la unión natural, perdida, entre el medio ambiente y el paciente que ha sufrido una amputación (Fig. 1).

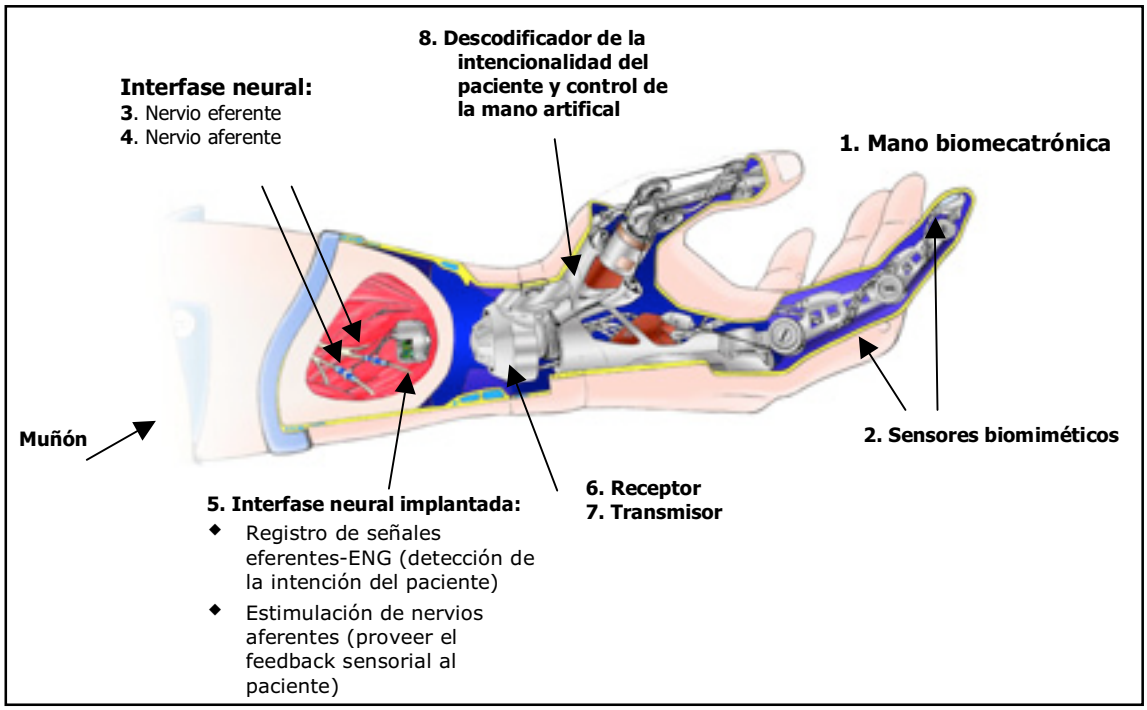

Figura 1. Esquema general de una neuroprótesis de mano avanzada bidireccional capaz de mimetizar el movimiento de la mano de forma natural y de evocar estímulos sensoriales al paciente (Proyecto CYBERHAND).

1.- Las Neuroprótesis

1.1. Prótesis

El campo de las prótesis ha existido desde hace miles de años, aunque las prótesis de mano han evolucionado lentamente, siendo básicamente cosméticas y con un diseño mínimamente funcional hasta muy recientemente. Las prótesis de mano y de brazo actuales que se encuentran en el mercado pueden sustituir las funciones básicas más importantes de una mano, como por ejemplo, abrirla y cerrarla, así como restablecer el aspecto exterior, como las prótesis cosméticas de brazo sin posibilidades funcionales pero con una importancia significativa a nivel psicológico.

Las prótesis funcionales se pueden dividir en prótesis accionadas por tracción y prótesis mioeléctricas. Las primeras se basan en brazos de prehensión activos en los que la función se controla con la propia fuerza, generalmente del hombro o pecho. El movimiento, usualmente efectuado con el hombro o el brazo residual, se transmite mediante un correaje de tracción a un cable conectado a la parte terminal de la prótesis (garfio o mano). Las principales ventajas son la durabilidad, el bajo coste de mantenimiento y el feed-back propioceptivo que los pacientes adquieren con el tiempo al relacionar la presión que ejerce el cable en el hombro con la posición del garfio. Por el contrario, los pacientes suelen quejarse de molestias por el sistema de correaje y del poco control que pueden ejercer sobre la prótesis. En muchos casos, la funcionalidad de la prótesis sólo es adecuada para acciones dirigidas delante del cuerpo entre cintura y cabeza, siendo poco útiles para acciones laterales, inferiores a la cintura o superiores a la cabeza.

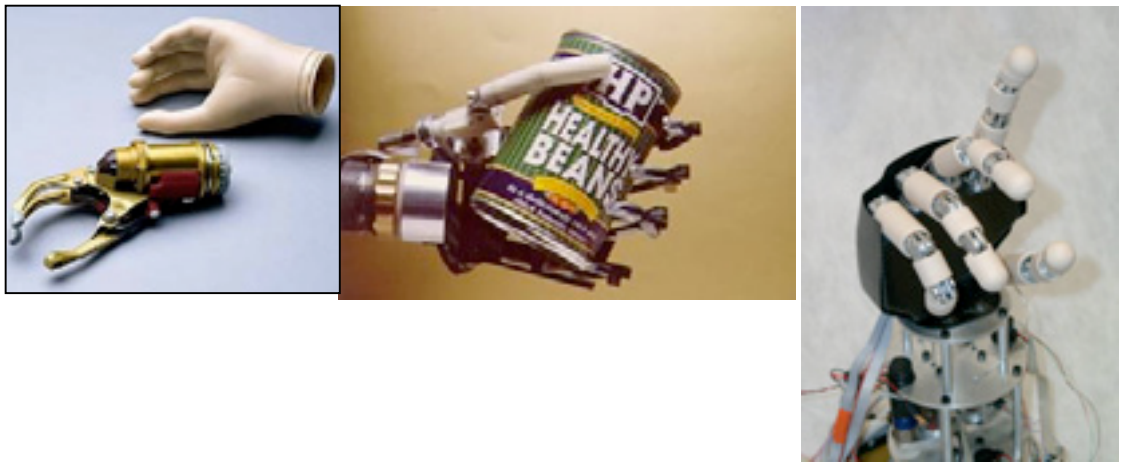

Figura 2. Prótesis de mano comerciales y en investigación. (a) Prótesis comercial Otto Bock con un grado de libertad y controlada por señales electromiográficas. (b) Prototipo de prótesis mioeléctrica con 6 grados de libertad (Southampton-Remedi). (c) Prototipo de neuroprótesis CYBERHAND con 16 grados de libertad.

Las prótesis de brazo mioeléctricas son prótesis con fuerza ajena. Las señales eléctricas de la excitación muscular, previa a la contracción, se pueden registrar mediante electrodos de superficie colocados en la piel por encima del músculo de interés. Estas señales eléctricas generadas por la contracción de músculos residuales (electromiografía, EMG), proximales a la amputación, son aprovechadas para controlar prótesis accionadas eléctricamente. Existen dos tipos de prótesis mioeléctricas: una con un electrodo para la flexión y otro para la extensión de los dedos de la prótesis de mano (Otto Bock) (Fig. 2), y la segunda con un solo electrodo para la flexión y extensión controlándose mediante la aplicación de diferentes grados de fuerza (Utah Arm). Las prótesis mioeléctricas suponen una mejora de funcionalidad y de cosmética respecto a las de tracción, pero resultan más pesadas y caras y requieren mayor mantenimiento.

En resumen, las prótesis disponibles en el mercado así como los diseños de las manos multifuncionales, presentan gran fiabilidad y robustez, pero su rendimiento y funcionabilidad todavía deben ser mejoradas (Cutkosky, 1985).

Tabla 1. Características generales de una mano humana y comparación con la prótesis del Cyberhand.

	Mano humana	**Cyberhand**
Grados de libertad	22	16 (6 grados de movilidad)
Tipo de prensión	Precisión y fuerza	Precisión y fuerza
Fuerza de prensión	> 500 N (edad 20-25) > 300 N (edad 70-75)	< 35 N
Fuerza con 2 dedos	> 100 N	< 10 N
Rango de flexión	100° dependiendo de la articulación	90° dependiendo de la articulación
Número de sensores	Sobre 17000	53
Control proporcional y destreza	Habilidad para regular la fuerza y la velocidad dependiendo del tipo de prensión	Habilidad para regular la fuerza dependiendo de las intenciones del paciente
Volumen total	50 cc. (solo la mano)	50 cc. (solo la mano)
Peso total	400 g sin los músculos extrínsecos	360g (sin los músculos extrínsecos) 1800 g (incluyendo la musculatura extrínseca y el brazo artificial)

Los importantes avances de los sistemas electromecánicos de prótesis han conducido, pues, a la existencia de prótesis que pueden remedar en gran medida el funcionalismo de la mano. Sin embargo, la capacidad de controlar tales prótesis avanzadas requerirá implementar sistemas de control neuro-eléctrico, para conseguir que los impulsos del sistema nervioso gobiernen la actuación de la prótesis y que los sensores de ésta envíen señales apropiadas al sistema nervioso del sujeto.

1.2. Neuroprótesis

En los últimos años, se han invertido muchos esfuerzos en el desarrollo de sistemas biónicos híbridos capaces de unir, vía interfases neurales, el sistema nervioso humano con prótesis, ortesis o incluso máquinas robóticas externas, con el principal objetivo de recuperar las funciones motoras y sensoriales de pacientes con lesiones de médula espinal, cerebrales o enfermedades degenerativas (Agnew y McCreery, 1990; Stein et al., 1992; Chapin y Moxon, 2000; Navarro et al., 2005).

En numerosas neuroprótesis, desarrolladas para sustituir artificialmente o mimetizar funciones sensoriomotoras en pacientes con déficits neurológicos, se incluyen interfases con el SNP o con músculos por medio de diversos tipos de electrodos, los cuales permitirán la estimulación neuromuscular y el registro de señales neurales. El acoplamiento eléctrico es el sistema más común y mejor conocido para estas interfases .

De hecho, gran proporción de los esfuerzos realizados en la investigación sobre neuroprótesis han ido dirigidos hacia el desarrollo y testado experimental de sistemas de interfases neurales, que no dañen al nervio y a los tejidos, permitan el acceso a las señales sensoriales aferentes, la estimulación selectiva de fibras nerviosas y el control del grado de fuerza muscular (Branner et al., 2001). Estos electrodos se implantan adyacentes, alrededor o dentro del nervio o de la raiz espinal. Debido a la proximidad con el nervio, la intensidad del estímulo requerida para la activación es menor comparada con la estimulación muscular o con los electrodos superficiales, con lo cual el consumo energético del sistema se ve reducido (Loeb y Peck, 1996). Junto con este ahorro, una de las características del sistema es la posibilidad de estimulación y registro, de forma específica, de los diferentes fascículos que componen el nervio. Por contra, estos electrodos pueden dañar el nervio en el cual se hayan implantado, mientras que los electrodos

musculares son más seguros. Por todo esto, son necesarios estudios experimentales detallados acerca de las compatibilidades mecánicas, químicas y eléctricas de los electrodos neurales antes de poder ser aplicados a la clínica.

1.3. Aplicaciones clínicas de las neuroprótesis

La construcción y aplicación de una neuroprótesis requiere la colaboración de diferentes campos de la investigación, tales como neurobiología, medicina, informática, microelectrónica y microtecnología. La gran complejidad de la estructura y la función del sistema nervioso es, sin embargo, un obstáculo real para la aplicación de las neuroprótesis simples; aun hoy en día, las neuroprótesis más sofisticadas no consiguen remedar completamente las funciones complejas naturales del sistema nervioso. De todas formas, diversas neuroprótesis son implantadas en la actualidad con éxito en algunas situaciones particulares, consiguiendo una restitución funcional parcial durante largo tiempo (Prochazka et al., 2001). Las aplicaciones más frecuentes (Fig. 3) son los marcapasos cardíacos, los implantes cocleares y los sistemas para el control de la micción en casos de lesiones de médula espinal. En este caso el sistema de estimulación eléctrica funcional (FES) aplicada a distintas vías nerviosas (Schmidt, 1986; Grimes y Nashold, 1974; Brindley et al., 1986) y en concreto la estimulación de las raíces sacras anteriores (SARS) son efectivas para el control de la micción. Otras aplicaciones son las neuroprótesis para el control del dolor, mantenimiento de la ventilación y para el control de músculos paralizados de las extremidades, todo y que no han alcanzado una utilización tan extensa.

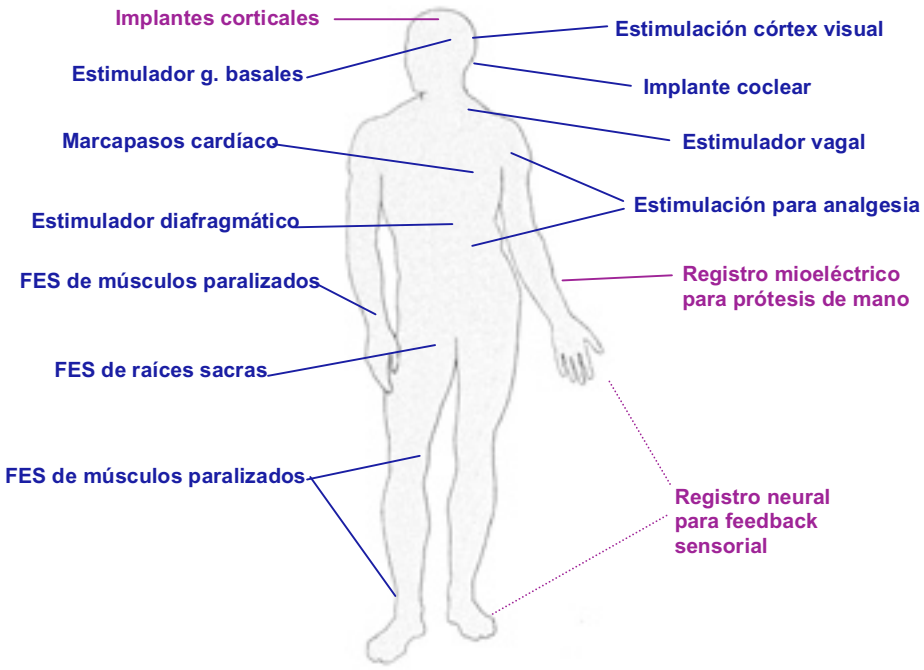

Figura 3. Esquema de los diferentes sistemas de neuroprótesis que actualmente se utilizan en clínica en mayor o menor número.

1.4. Interfases neurales

Los electrodos de interfases con el SNP pueden clasificarse en función del grado de selectividad para la estimulación/registro de fibras o fascículos nerviosos (Navarro et al., 2005). La selectividad de un electrodo aumenta con el grado de invasividad del mismo. Por ejemplo, los electrodos superficiales pueden registrar actividad electromiográfica y estimular solamente aquellos músculos que se encuentran justo debajo del electrodo implantado, mientras que los electrodos intrafasciculares y los electrodos regenerativos, insertados dentro del nervio, podrán registrar y estimular pequeñas poblaciones de axones dentro de un fascículo nervioso (Tabla 2, Fig. 4)

Tabla 2. Clasificación de los electrodos neurales

1. Electrodos no invasivos
    a. Electrodos superficiales
    b. Interfases no eléctricas
2. Electrodos musculares
    a. Electrodos epimisiales
    b. Electrodos intramusculares
3. Electrodos extraneurales

a. Electrodos epineurales y helicoidales
b. Electrodos en libro (*book electrodes)*
c. Electrodos de manguito (*cuff electrodes)*
d. Electrodos planos (*flat electrodes*)
e. Electrodos interfasciculares

4. Electrodos intraneurales
   a. Electrodos intrafasciculares
   b. Electrodos penetrantes (*spike electrodes*)
   c. Electrodos regenerativos

De todos estos tipos de electrodos los que ofrecen mayor potencial de ser utilizados para la interfase entre el SNP y prótesis avanzadas de mano son los de tipo cuff, los intrafasciculares y los regenerativos.

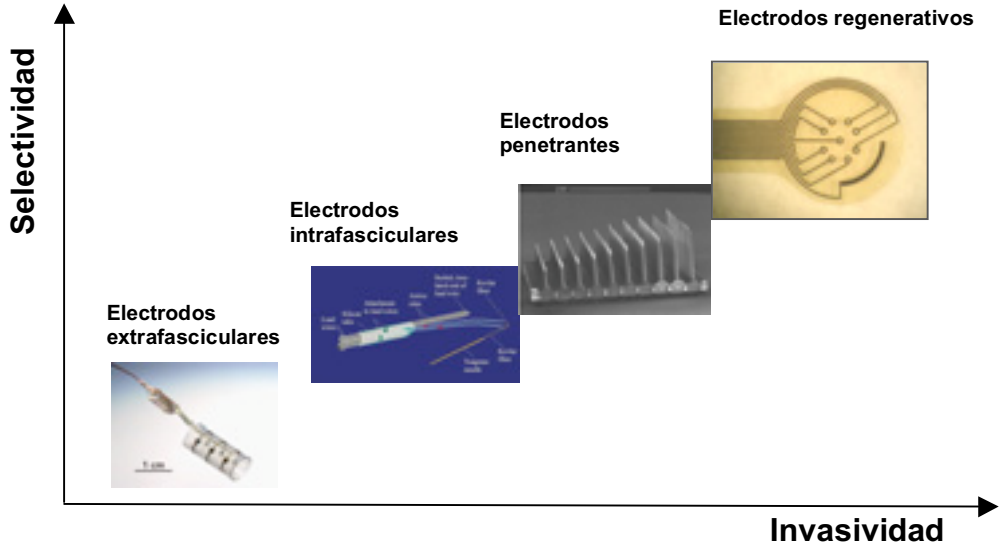

Figura 4. Esquema de algunos de los electrodos utilizados como interfases neurales, desde los más superficiales en contacto con el nervio (extrafasciculares, tipo Cuff), hasta los más invasivos (electrodos regenerativos). Existe una relación directa entre la invasividad del electrodo sobre el sistema nervioso y su selectividad en la estimulación y registro de señales neurales.

Electrodos tipo Cuff

Se basan en un tubo, fabricado con biomateriales, que envuelve al nervio y que puede contener varios electrodos contactando con éste. Son los electrodos más utilizados, tanto en investigación básica como en aplicación clínica.

Este tipo de electrodos presenta varias ventajas con respecto a otros electrodos extraneurales. Permiten un contacto directo con el nervio minimizando la distorsión mecánica. Al estar emplazados los electrodos en la parte interna del cuff, la estimulación queda restringida al propio nervio evitando así la estimulación de nervios de la proximidad y otros tejidos (Loeb y Peck, 1996). La intensidad del estímulo requerida también queda disminuida. A diferencia de otros electrodos más invasivos, como los electrodos regenerativos o intrafasciculares, los electrodos de tipo cuff son menos dañinos para el nervio y más fáciles de implantar.

Electrodos intrafasciculares

Con el objetivo de mejorar la selectividad del registro y la estimulación neural, se han desarrollado electrodos que se pueden implantar dentro del nervio estando en contacto directo con el tejido. Estos permiten, a diferencia de los extraneurales, aumentar la relación entre la señal y el ruido de fondo (signal-to-noise ratio) de los registros. La estimulación a través de ellos activa específicamente el fascículo nervioso en el cual se han implantado con un “cross-talk” muy bajo con los fascículos adyacentes. Se pueden implantar varios electrodos para la estimulación múltiple y además, con una menor intensidad del estímulo se pueden conseguir niveles similares de excitación a los producidos mediante electrodos extraneurales (Yoshida et al., 2000).

Dentro de los electrodos intrafasciculares se ha desarrollado un electrodo longitudinal intrafascicular o *LIFE* (longitudinal intrafascicular electrode). Este electrodo permite ser interfase de una pequeña población de axones en el nervio periférico. Primariamente, se construyeron de materiales rígidos como Pt-Ir o fibras de Kevlar metalizadas (Malagodi et al.,1989; McNaughton y Horch, 1996; Yoshida et al., 2000; Lawrence et al.,2003). Sin embargo, los filamentos flexibles de polímero son preferidos a los filamentos de metal debido a que éstos provocarían una encapsulación fibrosa y un descenso gradual de la amplitud de los potenciales de acción registrados (Lefurge et al., 1991). El estudio histológico de los nervios implantados con LIFEs de metal o de polímero revela que son biocompatibles y que no causan daño neural por la presencia del electrodo al cabo de 6 meses (Lefurge et al., 1991; Lawrence et al., 2002).

Varios estudios experimentales han demostrado que los LIFE son útiles para la estimulación selectiva (Nannini y Horch, 1991; Yoshida y Horch, 1993) y para el

registro multiunitario extracelular (Goodall y Horch, 1992; McNaughton y Horch, 1994). Estas propiedades hacen, este tipo de electrodos, útiles para la aplicación en sistemas FES y también en estudios básicos para la codificación y control neural. Se ha registrado la actividad de los receptores cutáneos en respuesta a estímulos, aunque debido al ruido de fondo, puede ser difícil diferenciar la señal registrada (Malmstrom et al., 1998; Yoshida et al., 2000).

Electrodos regenerativos

Los electrodos regenerativos se diseñaron con el fin de interconectar un número elevado de fibras nerviosas por medio de una serie de orificios, algunos de los cuales están rodeados por electrodos, y que se implantan entre los muñones de un nervio periférico seccionado (Llinás et al., 1973; Edell, 1986; Kovacs et al., 1992; Dario et al., 1998). Una vez implantado el electrodo, los axones regeneran a través de los múltiples orificios (Fig. 5), haciendo posible el registro de potenciales de acción desde estos electrodos a la vez que la estimulación de axones individuales o de pequeños fascículos. La aplicabilidad de estos electrodos depende del grado de regeneración axonal del nervio, del posible daño nervioso provocado por la carga mecánica impuesta al nervio o de las fuerzas constrictivas dentro de cada uno de los agujeros, y de la biocompatibilidad de los componentes (Rosen et al., 1990; Navarro et al., 1996).

En los últimos 30 años se han utilizado, en la construcción de los electrodos regenerativos, diferentes técnicas y materiales. Los primeros electrodos se hicieron de materiales no-semiconductores por perforación mecánica de los orificios en módulos de epoxi (Mannard et al., 1974). Con el avance de la microelectrónica, se hizo posible la construcción de electrodos de silicio de mayores dimensiones y un número más elevado de orificios (Akin et al., 1994; Kovacs et al., 1994; Navarro et al., 1996; Wallman et al., 2001). Mediante la utilización de este tipo de electrodos, se demostró la regeneración y el registro de actividad neural en nervios periféricos de rata, rana y pez (Kovacs et al., 1994; Navarro et al., 1996; Bradley et al., 1997; Della Santina et al., 1997; Mensinger et al., 2000). Sin embargo, este tipo de electrodo provoca con frecuencia axonopatía constrictiva y constituye una barrera física a la elongación de los axones regenerativos dependiendo del tamaño de los orificios (Edell, 1986; Rosen et al., 1990; Navarro et al., 1996; Zhao et al., 1997). El diseño del electrodo ideal sería aquel que tuviera orificios tan pequeños que sólo

regenerara un axón por cada agujero, del orden de 2-10 µm de diámetro. Sin embargo, en esta situación la regeneración no se da, con lo cual es necesario encontrar un equilibrio entre el número de orificios y su diámetro (del orden de 40-65 µm). Recientemente, se han diseñado electrodos regenerativos fabricados en poliamida (Stieglitz et al., 1997; Navarro et al., 1998). Este material es biocompatible y estable a lo largo del tiempo y permite una mejor regeneración que los electrodos fabricados en silicio (Navarro et al., 1998; Ceballos et al., 2002).

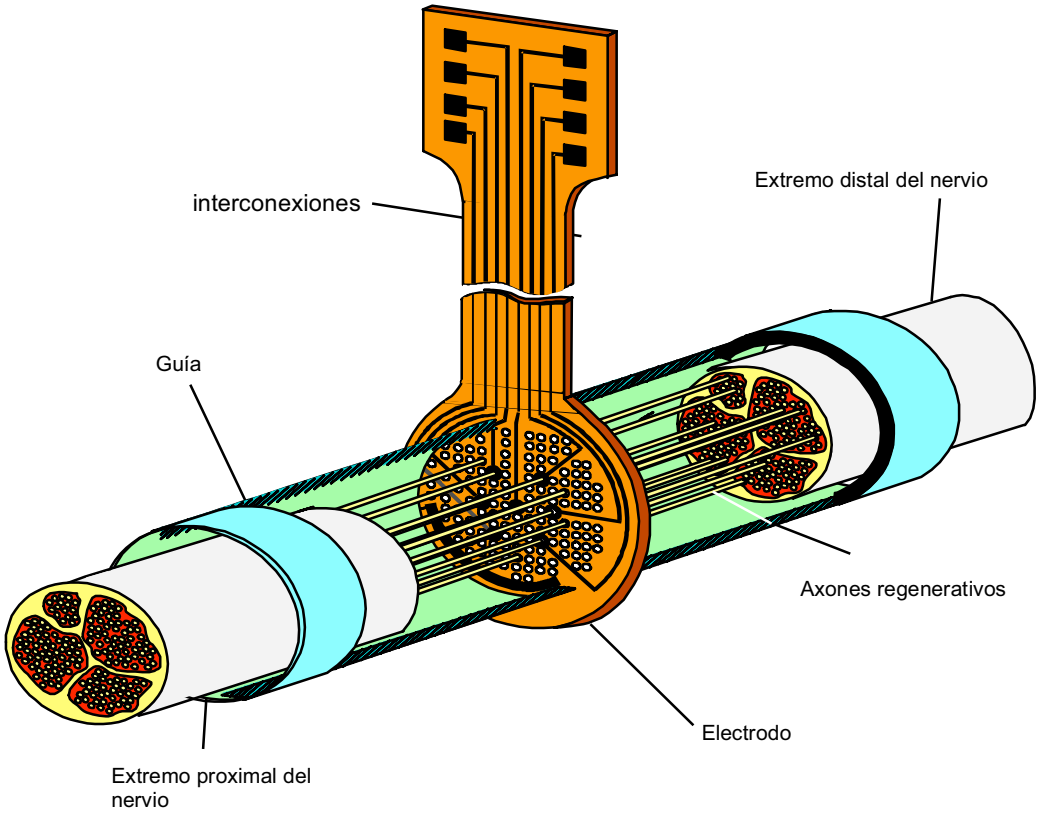

Figura 5. Representación esquemática de un electrodo regenerativo implantado con una guía entre los dos extremos de un nervio seccionado. Los axones regenerativos del extremo proximal crecen a través de los micro-orificios del electrodo.

Una de las aplicaciones más lógicas de estos electrodos regenerativos consiste en su implantación en nervios lesionados de una extremidad amputada con el fin de actuar como una interfase bidireccional en una neuroprótesis. Por una parte, el registro de señales eferentes puede ser usado para el control locomotor de la prótesis mecánica (Edell, 1986) mientras que las señales registradas a partir de sensores táctiles y mecánicos podrían ser evocadas al paciente por medio de la estimulación de fibras nerviosas aferentes (Riso, 1999). Desafortunadamente, este

tipo de electrodos regenerativos sólo son aplicables a nervios seccionados excluyéndose, por tanto, posibles experimentos agudos. En experimentos crónicos se ha podido estimular diferentes agrupaciones axonales y registrar potenciales de acción en respuesta a la estimulación funcional (Navarro et al., 1998; Ceballos et al., 2002), aunque hay que tener en cuenta algunas variables para estudios futuros como que el electrodo esté emplazado alrededor de la fibra y no en paralelo, el diámetro de cada uno de los orificios y el hecho de que el grosor de la mielina es menor en los axones regenerativos que en los intactos.

2.- Lesiones nerviosas

Las acciones naturales del cuerpo están controladas por medio de señales neurales eferentes, desde el SNC hasta el SNP para reclutar diversos músculos. Al mismo tiempo, la información transducida por los sensores naturales (mecanoreceptores, propioceptores, etc.) se conduce hacia el SNC por la activación de las fibras nerviosas aferentes. Las señales se transmiten por los axones correspondientes en series de impulsos o potenciales de acción, con intensidad de las señales codificadas principalmente en frecuencias de impulsos a lo largo del axón periférico.

Cuando se produce una lesión del nervio periférico hay una pérdida parcial o total de las funciones motoras, sensoriales y autonómicas del segmento diana denervado debido a la interrupción de la continuidad del axón, la degeneración distal de las fibras nerviosas y la muerte de neuronas axotomizadas. Estos déficits pueden ser compensados por la reinervación de los órganos diana mediante tres mecanismos: la regeneración de los axones previamente lesionados, la ramificación colateral de los axones intactos del entorno y la reorganización estructural y funcional de los circuitos del sistema nervioso implicados en sus acciones. Sin embargo, las evidencias clínicas y experimentales muestran como estos mecanismos no son suficientes para que haya una recuperación funcional idónea, especialmente tras lesiones graves, haciéndose necesaria en muchos casos la aplicación de procedimientos terapéuticos con el fin de potenciar los efectos de la regeneración, la colateralización y la reorganización mejorando las posibilidades de una adecuada recuperación funcional.

La lesión del nervio periférico puede ser el resultado de una variedad de causas que comportan en última instancia lesiones estructurales y funcionales de los

axones que lo componen. Entre las diferentes causas, cabe destacar las lesiones por isquemia, agentes neurotóxicos, afectaciones por radiaciones, desórdenes metabólicos, ataque inmunitario, cambios extremos de temperatura y lesiones mecánicas. Las lesiones mecánicas son las afectaciones más frecuentes pudiendo ser por compresión, fricción o lesión parcial o total de los nervios periféricos debido a accidentes traumáticos o como consecuencia de intervenciones quirúrgicas.

2.2. Manifestaciones clínicas de las lesiones nerviosas

Clínicamente, las lesiones del nervio periférico se manifiestan por la pérdida de las diferentes funciones mediadas por los axones afectados. Así, en el caso de la lesión de las fibras eferentes motoras se observa parálisis o paresia muscular seguida de la atrofia del músculo denervado. La afectación de las fibras sensoriales aferentes provoca una anestesia o hipoestesia de las diferentes modalidades sensoriales, conformando el conjunto de *síntomas negativos* del trastorno.

Paralelamente, se producen una serie de *síntomas positivos*, derivados de la denervación de los órganos periféricos o de los cambios en la transmisión de los estímulos periféricos. De esta forma, en el músculo esquelético se detecta excitación espontánea de fibras musculares aisladas (fibrilaciones), unidades motoras completas (fasciculaciones) o de la totalidad del músculo (espasmos). A nivel autonómico, se presenta una hipersensibilidad de los órganos denervados frente a los neurotransmisores o agonistas (Cannon, 1939), pudiendo provocar aumentos exagerados del tono vascular periférico, así como una actividad sudomotora o vasoconstrictora incrementada compensatoria en regiones intactas (Seddon, 1943).

En la vía aferente sensorial, junto con la pérdida de sensibilidad, se refieren sensaciones dolorosas espontáneas en ausencia de estímulo, dolores mayores en presencia de estímulos dolorosos de baja intensidad (hiperalgesia), sensaciones dolorosas frente a estímulos no dolorosos como el frío, el calor o el tacto (alodinia) y hasta el síndrome del miembro fantasma, caracterizado por la percepción de poseer una extremidad amputada y de dolor referido a ésta al estimular otras zonas (Omer et al., 1998).

2.3. Clasificación de las lesiones nerviosas

Entre las diferentes causas de lesión nerviosa, la mecánica puede provocar diferentes grados de lesión dependiendo de su morfología, sus requerimientos

terapéuticos y su pronóstico. Las clasificaciones clínicas más habitualmente empleadas son las de Seddon y la de Sunderland (Seddon, 1943; Sunderland, 1951) (Tabla 3).

Tabla 3. Clasificación de las lesiones nerviosas según Seddon y según Sunderland.

Clasificación de Seddon

- Neuropraxia: bloqueo de la conducción en un nervio con los axones preservados manteniéndose la excitabilidad en el segmento distal a la lesión. Generalmente se da por una compresión del nervio.
- Axonotmesis: pérdida de la continuidad del axón pero preservación de los tubos endoneurales.
- Neurotmesis: pérdida de la continuidad tanto del axón como de los elementos conectivos del nervio. En esta situación, no se da regeneración espontánea efectiva.

Clasificación de Sunderland

- Primer grado: corresponde a la neurapraxia de Seddon
- Segundo grado: corresponde a la axonotmesis de Seddon
- Tercer grado: discontinuidad de los axones y tubos endoneurales pero mantenimiento del perineuro que envuelve los fascículos.
- Cuarto grado: discontinuidad también del perineuro
- Quinto grado: pérdida total de la continuidad del tronco nervioso, corresponde a la neurotmesis.

2.4. Métodos de reparación del nervio periférico

Después de producirse una lesión del nervio periférico, la capacidad de los axones de regenerar y alcanzar sus tejidos diana es dependiente del lugar y tipo de lesión, y de la distancia que tienen que recorrer los axones para avanzar a través de la lesión. Así por ejemplo, en una lesión por aplastamiento, la regeneración es bastante buena debido a que la continuidad de los tubos endoneurales queda preservada, mientras que cuando queda un espacio entre los muñones después de una sección total del nervio, el éxito de la regeneración dependerá de la distancia entre los extremos.

2.4.1. Sutura directa

Cuando la lesión es una sección limpia del nervio, la sutura epineural de los muñones proximal y distal, es el método clásico de reparación. No obstante, no asegura el correcto alineamiento fascicular. La sutura fascicular intenta asegurar este alineamiento suturando los fascículos individualmente pudiendo mejorar la especificidad de la reinervación (Brushart et al., 1993). A pesar de esto, plantea una serie de inconvenientes como es el hecho de que hay que disecar los diferentes fascículos provocando un trauma quirúrgico añadido, la dificultad de identificar los fascículos del nervio, y que no es recomendable en lesiones muy distales debido al elevado grado de fasciculación del nervio (Sunderland, 1991).

2.4.2. Injerto nervioso

En lesiones con gran pérdida de tejido nervioso se recomienda la interposición de un injerto nervioso que evite una tensión excesiva al unir los dos extremos. Los injertos nerviosos son buenos sustratos para la regeneración ya que los tubos endoneurales servirán de guía para los axones en crecimiento y habrá un gran número de células de Schwann (CS) reactivas. El más utilizado en clínica es el autólogo, utilizándose un nervio de menor jerarquía (habitualmente el nervio sural). Esta opción comporta una segunda intervención quirúrgica con pérdida funcional, junto con el hecho que el nervio donante no se corresponde en calibre con el receptor. La utilización de injertos alogénicos junto con el tratamiento con inmunosupresores como la Ciclosporina A o el FK506 es una de las posibilidades en las que se está trabajando en los últimos años. Así, a nivel experimental, la interposición de un injerto alogénico y el tratamiento con FK506 permite alcanzar unos niveles de regeneración parecidos a los de un injerto autólogo (Udina et al., 2004a).

2.4.3. Tubulización nerviosa

Una alternativa a la utilización de material autólogo o alogénico es la tubulización nerviosa, es decir, la interposición de un tubo biocompatible entre los extremos del nervio con el fin de que haga de guía a los axones regenerativos evitando que éstos se desvíen a tejidos adyacentes, y facilite, al condensar los factores tróficos liberados por los extremos seccionados, la creación de un

microambiente favorable en la promoción de la regeneración (Lundborg et al., 1982; Fields et al., 1989).

Se han utilizado materiales biológicos con el fin de unir los extremos nerviosos siendo los vasos sanguíneos y los músculos esqueléticos los que han recibido mayor atención de los investigadores. Aunque la efectividad de los vasos sanguíneos como cámaras tubulares ha sido demostrada (Lundborg, 2003; Meek y Coert, 2002), tanto a nivel experimental como clínico, se ha demostrado su eficacia sólo en separaciones interneurales cortas (Chiu, 1999). Este hecho, unido a la dificultad de obtener material biológico a partir del receptor, ha hecho perder su interés como opción en clínica. La aparición de materiales sintéticos biocompatibles permitió sustituir los materiales biológicos, aportando además un modelo experimental ideal para el estudio del proceso regenerativo en nervios periféricos (Lundborg, 1982a; 1982b; Williams et al.,1983; Le Beau et al., 1988; Fields et al., 1989). Entre estos materiales destacan, por su adecuación y utilización tanto experimental como en la clínica, las guías de silicona y las guías de colágeno.

La regeneración de un nervio seccionado a través de un espacio vacío dentro de una guía neural implica la reconstitución de un nuevo segmento del nervio. En las etapas iniciales, los extremos nerviosos secretan al interior de la cámara un fluido compuesto por elementos sanguíneos, de la matriz extracelular y factores neurotróficos. La polimerización de la fibrina de este exudado permite constituir una matriz o cordón enlazante de los dos extremos nerviosos, bañado en una solución promotora de la supervivencia neuronal y la activación y proliferación de células no neurales (Uzman y Villegas, 1983; Williams et al., 1983; Le Beau et al 1988; Liu, 1996).

En la siguiente etapa, células procedentes de ambos extremos nerviosos, principalmente macrófagos, fibroblastos y CS, infiltran el cordón regenerativo (Williams et al., 1983; Scaravilli, 1984; Williams y Varon, 1985; Le Beau et al., 1988). Por un lado, las CS se activan y proliferan en respuesta a los factores mitógenos acumulados en el interior de la cámara nerviosa, secretados entre otros por macrófagos infiltrados (Heumann et al., 1987; Lindholm et al., 1987; Perry y Brown, 1992; Goodrum y Bouldin, 1996). Por otro lado, los fibroblastos llenan espacios que no contienen CS, pudiendo condicionar y dirigir la migración de estas células, por lo que se cree que estos dos tipos celulares podrían participar en la configuración de las estructuras endoneurales (Scaravilli, 1984; Fields et al., 1989). A las 3 semanas,

ya se han formado las unidades regenerativas que avanzarán hasta las dianas sinápticas periféricas (Fawcett y Keynes, 1990). Finalmente, a las 4 semanas, la elongación axonal es seguida por la mielinización y maduración de los axones regenerados en la guía neural (Le Beau et al., 1988). El nervio regenerado aumenta de calibre con el tiempo permaneciendo en el centro del tubo, compuesto de fascículos pequeños con axones mielínicos y amielínicos, rodeados por un fino perineurio.

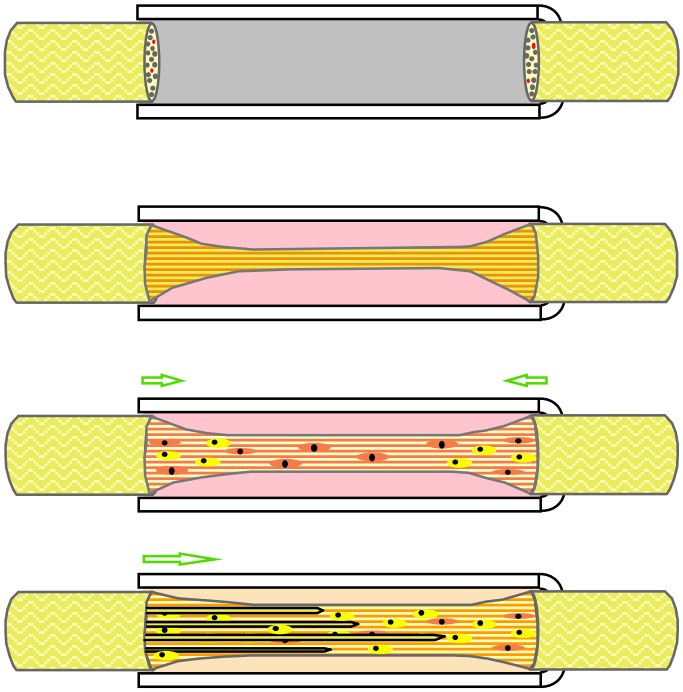

Figura 6 : Fases de la regeneración en guías neurales. Tras lesión y reparación por tubulización se produce extravasación de plasma (a) y formación de un cable de fibrina entre los 2 segmentos nerviosos (b). Tras este primer proceso, se produce la migración de células no neurales hacia el interior de la cámara desde los dos extremos del nervio (c) y, por último, la elongación axonal (d).

El éxito de la regeneración intratubular depende de la capacidad del nervio lesionado de proporcionar suficientes elementos humorales y celulares que constituyen el cordón regenerativo inicial. Las características físico-químicas del tubo, principalmente la dimensión, permeabilidad, durabilidad y la composición de la pared, influyen en el grado de regeneración axonal. La principal limitación de la tubulización es la distancia interneural a la que tiene que ser aplicada. La distancia limitante varía entre especies. Diferentes estudios experimentales describen como la regeneración es exitosa cuando se utiliza un tubo de silicona en distancias de 4 mm en ratón (Henry et al., 1985; Butí et al., 1996), 10 mm en rata (Lundborg et al.,

1982b) y 30 mm en primates (Dellon y Mackinnon, 1988; Archibald et al., 1995), no alcanzándose en muchos casos en distancias más largas. En el ámbito clínico, las reparaciones por tubulización se han limitado a la reparación de nervios distales, como nervios digitales (Mackinnon y Dellon, 1990) o nervios en el antebrazo (Lundborg et al., 2004) con una separación interneural promedio de hasta 20 mm, observándose una recuperación funcional comparable a la de un autoinjerto.

3.- Regeneración del nervio periférico

Cuando los axones se desconectan del soma neuronal tras la lesión, su segmento distal degenera hasta desaparecer en la llamada degeneración walleriana (Waller, 1850), que se caracteriza por una desintegración progresiva de los axones y las vainas de mielina, y por una serie de cambios metabólicos en el soma neuronal conocidos genéricamente como reacción axonal y cromatolisis (Selzer, 1980; Fawcett y Keynes, 1990). El significado funcional de la degeneración walleriana es el de crear un microambiente en el segmento distal a la lesión favorable para la posterior regeneración de los axones de las neuronas supervivientes, mientras que la reacción axonal y la cromatolisis constituyen los cambios metabólicos necesarios para la regeneración. La regeneración constituye el conjunto de mecanismos celulares que permite la elongación de los axones (Selzer, 1980; Fawcett y Keynes, 1990; Fu y Gordon, 1997), con el objetivo funcional de reemplazar el extremo distal del axón que se ha perdido durante la degeneración y reinervar los órganos diana denervados, permitiendo el restablecimiento de su función y control neural.

3.1. Degeneración walleriana

Los primeros signos de degeneración walleriana se observan a las 24 horas de la lesión prolongándose durante dos semanas. A las 48 horas los axones muestran una disrupción total de su estructura interna con desintegración del citoesqueleto y la consecuente acumulación de orgánulos en la zona de lesión. A su vez, las CS sufren hipertrofia y forman invaginaciones hacia el axón, lo que provoca la fragmentación de la mielina que posteriormente fagocitan. El resultado final es la acumulación en el interior de los tubos endoneurales distales a la lesión de material detrítico compuesto por la desintegración de los axones y las vainas de mielina. Las CS comienzan la fagocitosis de las vainas de mielina a las 24 h postlesión, aunque la principal vía de fagocitosis es el reclutamiento de macrófagos infiltrados a partir de

los 2-3 días de la lesión. Esta infiltración viene dada por la secreción de factores quimiotácticos, como el factor inhibitorio de leucemia (LIF) e interleuquina-1 (IL-1-α, IL-1β), por las CS reactivas. Los macrófagos también secretan potentes activadores como IL-1, y agentes mitógenos de las CS (PDGF, FGF y TGF) provocando la desdiferenciación de las CS.

Una vez degradados los materiales residuales, los macrófagos son eliminados por apoptosis, mientras que las CS reactivas, que han proliferado hasta 3-4 veces su número normal, permanecen dentro de los túbulos endoneurales formando las denominadas bandas de Büngner (Cajal, 1928).

3.2 Reacción neuronal y cromatolisis

Si la degeneración walleriana sirve para crear un microambiente distal a la lesión que favorece el crecimiento axonal de las neuronas supervivientes, la reacción axonal y la cromatolisis representan los cambios metabólicos de la neurona para sostener la regeneración del axón. Los cambios morfológicos más importantes en el cuerpo neuronal después de axotomía son la disolución de los gránulos de Nissl, la migración excéntrica del núcleo, aumento del tamaño del nucleolo y retracción de las dendritas (Lieberman, 1971). La entrada masiva de calcio y la supresión del transporte retrógrado de factores neurotróficos debido a la lesión inducen la expresión de genes tempranos (immediate early genes, IEGs) (Lunn et al., 1990) en el soma neuronal. Su activación conducirá a la síntesis de proteínas que, a su vez, activarán a los genes tardíos (late response genes, LRGs), encargados de sintetizar proteínas con función específica (Sheng y Greenberg, 1990).

3.3. Regeneración axonal

Los axones regenerativos producen múltiples conos de crecimiento que tienden a crecer desde el segmento proximal a la lesión hacia el segmento distal hasta llegar a los tejidos diana (Ann et al., 1994). La columna de CS en el nervio degenerado es un soporte indispensable para que los axones regenerativos crezcan hasta alcanzar su diana. Si los axones regenerativos evaden la CS y entran en el tejido conectivo, la regeneración cesa después de haber crecido unos pocos milímetros dentro de este tejido. Las CS, por tanto, proveen al axón de un ambiente favorable para el crecimiento, por la expresión de moléculas de adhesión en la

superficie de la membrana plasmática y por la producción de factores tróficos para los axones regenerativos (Bunge, 1993). El conjunto formado por la interacción de la membrana basal de la CS con los conos de crecimiento de una neurona constituye la denominada unidad regenerativa (Fawcett y Keynes, 1990).

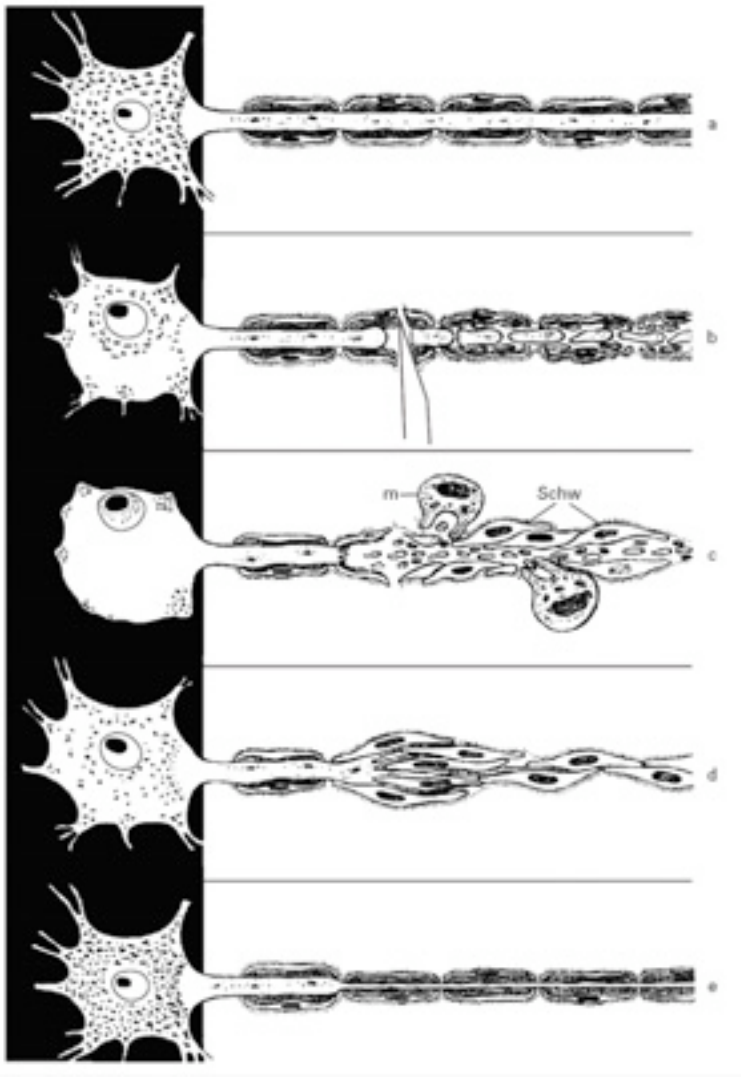

Figura 7. Degeneración y regeneración de una fibra mielínica. Tras lesión de la fibra, se produce la disolución de las envueltas de mielina y la degeneración axoplasmática distalmente a la lesión; invasión de macrófagos y proliferación de células de Schwann; crecimiento de colaterales axonales proximales a la lesión; elongación de los axones en las columnas de células de Schwann; remielinización axonal. (Lundborg. Nerve injury and repair regeneration 2005. Elsevier Inc.)

Para la elongación del axón regenerativo, los conos de crecimiento viajan a lo largo del nervio degenerado en respuesta a moléculas guía del ambiente que les rodea (Tessier-Lavigne y Goodman, 1996; Dickson, 2002). La motilidad del cono de crecimiento está regulada por la reorganización y la dinámica de la actina y de los microtúbulos (Dent y Gertler, 2003). La región central del cono de crecimiento

contiene haces de microtúbulos mientras que en la periferia se encuentran los filamentos de actina que formarán tanto los lamelipodios como los filopodios (Pollard y Borisy, 2003). La actividad mecánica de las proteínas contráctiles actina y miosina, hace que los filopodios se estiren o encojan explorando el ambiente que encuentran en su avance. La elongación se produce por la unión o anclaje de estos filopodios a moléculas trópicas de la matriz extracelular mediante receptores de moléculas de matriz extracelular como integrinas o N-CAM, en la membrana de los mismos (Letorneau y Shattuck, 1989). El avance del cono se dará por el anclaje entre estas moléculas mientras que la presencia de iones calcio y de kinasas permitirá la estabilización del nuevo citoesqueleto formado al fosforilar las tubulinas y sus proteínas asociadas o MAPs.

Durante la extensión del axón regenerativo éste contacta con las CS y su lámina basal. El cono de crecimiento exhibe selectivamente diferentes moléculas de adhesión en la membrana plasmática. El contacto entre la CS y el axón está mediado por varias moléculas de adhesión incluyendo la superfamilia de las inmunoglobulinas, como por ejemplo N-CAM y L1, y la superfamilia de las cadherinas (N-cadherina y E-cadherina), mientras que el contacto entre la lámina basal y el axón viene mediado principalmente por la laminina (Bixby y Harris, 1991; Letourneau et al., 1994). Tras denervación, las moléculas de adhesión N-CAM y L1 aumentan su expresión en las superficies en contacto entre las CSs y la membrana plasmática de la unión entre el axón (Martini y Schachner, 1988; Rathjen, 1988; Rutishauser et al., 1988). Sin embargo, cuando las CS comienzan el proceso de remielinización de los axones, estas dos moléculas rápidamente bajan su expresión hasta llegar a ser indetectables (Martini y Schachner, 1988). Este fenómeno sugiere que estas moléculas de adhesión ayudan a la interacción entre CS y axón promoviendo el crecimiento axonal a lo largo de la membrana plasmática de la CS. La laminina interviene en el crecimiento del frente regenerativo por contacto entre la lámina basal y el axón, así como en la velocidad de la regeneración axonal (Werner et al., 2000; Chen y Strickland, 2003).

En un nervio intacto, los factores tróficos se producen a nivel del órgano diana distal y se transportan retrógradamente hacia el soma neuronal. Cuando la comunicación entre el axón y su cuerpo neuronal queda interrumpida por una lesión, las CS reactivas producen diversos factores neurotróficos como NGF, BDNF, GDNF. Estas neurotrofinas se liberan desde las CS y se difunden de tal manera que forman

un gradiente de concentraciones alrededor del axón regenerativo. Estos axones se extienden a lo largo del gradiente de densidad de neurotrofinas hacia el segmento distal (Kuffler, 1986). Los patrones de expresión entre las diferentes neurotrofinas varía pero en general, se mantienen a niveles bajos de expresión en las CS y tras lesión del nervio aumentan su expresión. El pico máximo de expresión varía desde las primeras 24 horas tras axotomía para el NGF (Heumann et al., 1987) hasta las 4 semanas en el caso del BDNF (Meyer et al., 1992). Estas neurotrofinas promueven la supervivencia y crecimiento de diferentes poblaciones axonales como se ha visto para el caso del NGF y GDNF (Whitworth et al., 1996; Bloch et al., 2001; Fine et al., 2002), y del BDNF y NT-3 aumentando la regeneración axonal periférica y la supervivencia de neuronas motoras y sensoriales (Utley et al., 1996; Shirley et al., 1996; Sterne et al., 1997; Bloch et al., 2001). No obstante, los trabajos son inconsistentes variando los resultados dependiendo de cómo se libera el factor neurotrófico y en qué concentraciones (Jones et al., 2001).

3.4. Reinervación periférica

La reinervación de los órganos dianas viene determinada por una serie de señales que se establecen bidireccionalmente, entre los axones regenerativos y los tejidos periféricos. Además de los cambios en la membrana del órgano diana al producirse el contacto entre el axón y la célula diana (Bowe y Fallon, 1995), su reinervación supone importantes cambios estructurales de las neuronas regenerativas ya que deben transformar sus conos de crecimiento en botones presinápticos. La fosforilación de la GAP-43 por parte de una proteína Kinasa-C (PKC), sería la determinante en la inhibición del avance del axón regenerativo (Skene, 1989; Strittmatter et al., 1994).

4.- Especificidad de la regeneración

La correcta restitución funcional después de una lesión nerviosa vendrá determinada no sólo por el éxito de la regeneración axonal y de la reinervación de las dianas periféricas, sino también por la reconexión apropiada entre neurona y órgano diana, con un patrón similar al normal o compatible con el desarrollo de la función. La capacidad de los axones de reconectar con sus dianas originales está condicionada simultáneamente por cuatro tipos de mecanismos: neurotropismo, guía por contacto, neurotrofismo y alineamiento quirúrgico.

El neurotropismo es la regeneración de un axón dirigida por un gradiente de concentraciones de factores hasta reinervar una diana específica, frente a otros tipos celulares y órganos no afines (Brushart, 1991). Dentro de la teoria neurotrópica, hay que distinguir los diferentes niveles de especificidad. De esta manera, la especificidad de tejido es la capacidad de los axones regenerativos de dirigirse hacia un segmento distal nervioso y no hacia estructuras conectivas u otros tejidos no neurales. La especificidad fascicular o troncular describe la capacidad de los axones de un fascículo determinado de encontrar su correspondiente extremo distal. La especificidad sensorio-motora es la que separa los axones aferentes de los eferentes. En este contexto, la capacidad topográfica demuestra la capacidad de los axones que proyectaban sobre una región corporal de reinervar la misma zona después de la lesión. Finalmente, la especificad de órgano diana se produce cuando una neurona reinerva preferentemente el tipo de diana que originalmente inervaba y por lo cual ocupa una disposición anatómica y presenta conexiones específicas con vías y nucleos centrales (Brushart, 1998). Los datos de los estudios realizados hasta el momento confirman la especial afinidad de los axones regenerativos por su extremo distal frente a otros tejidos (Abernethy et al., 1994; Kuffler, 1989), ponen en duda la existencia de un neurotropismo fascicular (Doolabh et al., 1996), y confirman en un modelo de nervio mixto la afinidad especial de los axones motores por fascículos distales musculares (Brushart, 1988; 1990; 1993) y de los sensoriales por los cutáneos (Madison et al., 1996).

4.1. Reinervación motora preferencial

La selectividad de la regeneración de un nervio mixto hacia sus dianas musculares y cutáneas ha permitido analizar los mecanismos de la selección de tubos endoneurales en caso de acierto y error. Así, se han descrito axones motores que penetran en tubos endoneurales sensoriales rodeados de CS, así como axones sensoriales regenerando a través de fascículos motores (Zalewski, 1970) que en ambos casos no conseguían reestablecer sinapsis funcionales y eran eliminados.

En 1988, Brushart (Brushart, 1988) introdujo el término de *reinervación motora preferencial (PMR)* como la capacidad de los axones motores regenerativos en un nervio mixto, como el nervio femoral, de reinervar preferentemente un músculo (Brushart, 1988) o un nervio motor (Brushart, 1993). Proximalmente al lugar de reparación, los axones musculares y cutáneos crecen juntos teniendo acceso libre a

los túbulos endoneurales que se dirigen hacia tejidos musculares y cutáneos. La especificidad de la regeneración se evalúa a nivel distal, donde el nervio se bifurca en la rama del músculo cuadriceps y en la del nervio safeno. Durante los primeros estadíos de la regeneración del nervio femoral seccionado, un número similar de motoneuronas proyectan exclusivamente a los nervios cutáneos y musculares, mientras que un tercer grupo de motoneuronas proyectan ramas colaterales hacia ambas vías simultáneamente (Brushart, 1990). El número de motoneuronas que proyectan correctamente al músculo aumenta con el tiempo mientras que las que proyectan colaterales hacia las dos ramas descienden. Estas observaciones sugirieron la hipótesis del "prunning" (Brushart, 1993): los axones motores regenerativos generan múltiples colaterales los cuales reinervan de manera aleatoria cualquiera de las dos vías; con el tiempo, se generan proyecciones específicas por eliminación (prunning) de los colaterales desde la rama cutánea manteniéndose en la rama muscular.

4.2. Moléculas relacionadas con la reinervación específica

Los mecanismos moleculares por los cuales se daría esta reinervación motora preferencial no están bien establecidos. Martini et al. (1988; 1992; 1994) observaron como el péptido L2/HNK1 se expresa preferencialmente por las CS de las raíces ventrales y nervios musculares mientras que raramente se expresa en las raíces dorsales y nervios cutáneos. L2/HNK1 es detectable en la mielina compacta, lámina basal y en la superficie de las CS, los lugares que los axones motores prefieren para regenerar tras lesión del nervio.

Otros trabajos sugieren la molécula NCAM junto con su ácido polisiálico (PSA) como los posibles responsables de la especificidad ya que están expresados por axones motores regenerativos después de lesión del nervio periférico (Zhang et al., 1995; Rutishauser and Landmesser, 1996). En este sentido, mientras que los animales control presentan PMR, cuando se utilizan ratones *knockout* para el NCAM, o se elimina enzimáticamente el ácido polisiálico (PSA), las motoneuronas reinervan tanto la rama muscular como la cutánea indistintamente (Franz et al., 2005).

Por último, otros trabajos han demostrado como la administración exógena de BDNF aumenta el número de motoneuronas revertiendo los efectos de una axotomía crónica y que la combinación de BDNF y GDNF es beneficioso para la regeneración axonal motora selectiva (Boyd y Gordon, 2003).

5.- Neuroma por amputación

Cuando se da una amputación de un miembro, se forma un neuroma en el extremo distal del nervio seccionado. Los axones seccionados generan múltiples brotes regenerativos, que no pueden elongarse por el nervio distal, al haber éste desaparecido. El neuroma representa una masa de axones que han quedado atrapados en tejido conectivo, formándose un ovillo de colaterales axonales. El desarrollo, forma y tamaño del neuroma dependerá de cómo los axones escapan de sus tubos endoneurales interrumpidos y van hacia el tejido conectivo. En los muñones amputados, sin embargo, estas características asumen particularmente importancia debido a que estos muñones quedan desprotegidos en la extremidad estando sujetos a golpes repetidos, presión e irritación. La irritación crónica de este muñón nervioso hace aumentar el tamaño y la sensibilidad de éste. Bajo estas condiciones desfavorables esta mayor sensibilidad se acaba convirtiendo en una hipersensibilidad aguda volviéndose dolorosa. Algunos de los neuromas acaban siendo dolorosos y otros no pero igualmente es suficiente para incapacitar al sujeto. Es por esto que es necesario encontrar medidas paliativas dirigidas a disminuir la regeneración incontrolada de las fibras nerviosas y la formación del neuroma (Sunderland, 1991)

5.1 Dolor neuropático asociado al neuroma

Estudios electrofisiológicos muestran como los axones atrapados en un neuroma tienden a volverse más sensibles a estímulos mecánicos, químicos, físicos y metabólicos, presentando algunos, descargas espontáneas de impulsos ectópicos (Devor, 1993).

Cuando hay una lesión de las fibras sensoriales, se produce inmediatamente un tren de impulsos de duración variable entre segundos y algunos minutos, que contribuye a iniciar la reacción neuronal pero también a la sensibilización central. Posteriormente aparecen notables cambios en la excitabilidad de membrana de las neuronas motoras y sensoriales debidos a modificaciones en la expresión de canales iónicos, principalmente para el sodio. Particularmente, las neuronas aferentes primarias presentan una sobre-expresión de canales de sodio tipo III, que es sensible a la tetrodotoxina y no se encuentra normalmente en las neuronas del ganglio espinal, y una reducción de la expresión de genes para canales de sodio

SNS/PN3 y NaN, que son resistentes a tetrodotoxina (Waxman et al., 1999). Estos cambios, que también se han demostrado en modelos de dolor inflamatorio, parecen ser dependientes del déficit de aporte de factores neurotróficos, como NGF y GDNF. También se ha descrito la reducción de canales de calcio de tipo N en las neuronas sensoriales lesionadas. Estos cambios de canales de sodio y calcio en respuesta a la lesión nerviosa incrementan la excitabilidad de las neuronas, lo que conduce a una predisposición a excitarse espontáneamente y a elevada frecuencia, resultando no sólo en dolor espontáneo sino también en una sensibilización central (Zimmermann, 2001).

La génesis de descargas de impulsos ectópicos, originados en el neuroma, puede deberse a la hipersensibilidad de los brotes regenerativos a estímulos mecánicos, térmicos, químicos e inflamatorios que ocurren en el microambiente local. Los impulsos ectópicos y la sensación de dolor consiguiente pueden persistir durante periodos largos de tiempo como consecuencia de los cambios de excitabilidad neuronal. Una proporción de fibras sensoriales lesionadas, tanto A como C, muestran oscilaciones del potencial de membrana que conduce a excitación ectópica. Estas descargas pueden amplificarse por diversos mecanismos que incluyen: aumento de las postdescargas, excitación cruzada a otras fibras por cambios iónicos locales o liberación de neuropéptidos, y excitación efáptica debida a la aposición de membrana de axones regenerativos y desmielinizados (Devor, 1993). Se ha sugerido que los macrófagos que quedan atrapados dentro del neuroma podrían contribuir a las anomalías electrofisiológicas, ya sea por liberación de factores que intervienen en la regeneración o por la creación de zonas amielínicas susceptibles a estímulos externos (Frisen et al., 1993).

5.2 Terapéutica

El problema principal del neuroma es el del dolor neuropático que provoca. Se han utilizado varias terapias para el tratamiento del dolor neuropático con diferentes grados de éxito. Estas terapias incluyen la utilización de fármacos antiinflamatorios no esteroidales (AIDEs), opioides, anticonvulsionantes, antiarrítmicos, antidepresivos tricíclicos y agentes tópicos como la capsaicina, dependiendo de la naturaleza del dolor. Hay que tener en cuenta que todos estos tratamientos presentan muchos efectos secundarios además de actuar más como paliativos que no como curativos, con lo que el estado patofisiológico del sistema nervioso persiste y progresa.

Evidencias recientes indican que los factores neurotróficos podrían representar los nuevos tratamientos revertiendo el proceso. De entre los factores neurotróficos, cabría destacar NGF, BDNF, NT-3 y GDNF (Sah et al., 2003). Otro tipo de aproximación para evitar tanto la formación de un neuroma como la aparición de dolor neuropático, es la cirugía. Estas medidas van dirigidas a promover la dispersión de los axones regenerados, a suprimir la regeneración axonal y a limitar el crecimiento del muñón nervioso final, mediante la implantación del muñón distal dentro de un músculo próximo al nervio con el fin de proveerle de un mejor ambiente en el cual poder extenderse o el encapsulamiento del muñón para evitar el crecimiento axonal incontrolado (Sunderland, 1991).

OBJETIVOS GENERALES

1. **Evaluar la regeneración nerviosa periférica a través de electrodos regenerativos implantados crónicamente en el nervio ciático de rata.**

   La aplicabilidad de los electrodos regenerativos depende básicamente del éxito de la regeneración axonal a través de ellos y de la biocompatibilidad de sus componentes, especialmente en implantaciones crónicas. Si el objetivo final es conseguir aplicar este tipo de interfase en humanos, es necesario, junto con la biocompatibilidad del material, conocer los cambios funcionales y morfológicos que ocurren crónicamente en el nervio seccionado.

   Este estudio pretende evaluar funcional y morfológicamente la regeneración del nervio ciático tras implante de electrodos regenerativos de poliamida, investigar los posibles efectos a largo plazo y comprobar si los axones regenerativos pueden adquirir y mantener características funcionales y morfológicas normales. Junto con el primer objetivo de evaluar la regeneración nerviosa periférica, se propuso estudiar la regeneración diferencial de las dos poblaciones axonales principales, motora y sensorial, a través del electrodo.

2. **Evaluar la capacidad de los electrodos regenerativos para estimular y registrar señales neurales.**

   Se han desarrollado un número elevado de electrodos neurales que varían en su forma, invasividad y selectividad de estimulación y registro. Desde los electrodos superficiales a los regenerativos, se han utilizado electrodos para diferentes aplicaciones permitiendo, la mayoría de ellos, la estimulación y el registro de señales neurales con mayor o menor selectividad. Los electrodos regenerativos, implantados entre los dos extremos nerviosos seccionados, permiten el registro y estimulación de un número pequeño de axones siendo, entre la variedad de electrodos, los que mayor selectividad pueden ofrecer. El siguiente objetivo fue el implante de electrodos regenerativos y la obtención de señales neurales evocadas por estimulación eléctrica o en respuesta a estímulos funcionales.

3. **Estudiar la regeneración nerviosa del nervio ciático de rata en un modelo de amputación**

   La aplicabilidad de los electrodos regenerativos como interfase neural aumenta si se trata de miembros amputados y el fin último es implantar una prótesis de mano y controlarla mediante señales neurales. Para ello, es necesario evaluar el comportamiento de los axones en un modelo de amputación y la capacidad de éstos de mantenerse a lo largo del tiempo sin reconectar con los tejidos diana. Con el fin de alcanzar este objetivo, se ha diseñado un modelo experimental de amputación nerviosa mimetizando una situación de amputación de una extremidad.

   Debido a que la regeneración axonal puede estar obstaculizada por la pérdida de reconexión con los tejidos distales, en otros grupos se evaluó el mantenimiento y supervivencia de los axones mediante algunas estrategias, entre ellas el transplante de células de Schwann primarias o inmortalizadas sobreexpresando el factor neurotrófico GDNF, dado que las células de Schwann sirven de soporte a la regeneración nerviosa mediante la liberación de factores tróficos, entre otros componentes, hacia el ambiente regenerativo.

4. **Evaluar la regeneración de axones motores en lesión del nervio periférico. Estrategias para promover la regeneración específica motora y sensorial.**

   Tras lesión del nervio periférico, el determinante más importante de la recuperación funcional es la precisión de los axones para volver a reinervar órganos diana originales. Desafortunadamente, los axones regenerados se equivocan a la hora de reinervar dando como resultado que, a pesar que a nivel morfológico pueda alcanzar valores normales en el número de fibras regeneradas, a nivel funcional no se recupera nunca una situación normal. Las principales razones por las que se mantienen los déficits funcionales son el número limitado de axones que regeneran y la pérdida de especificidad de la reinervación distal. El siguiente objetivo se propuso con el fin de correlacionar los déficits funcionales con la pérdida de la topografía intrafascicular tras diferentes grados de lesión del nervio periférico e investigar estrategias para aumentar la regeneración específica diferencial de axones sensoriales y motores.

DISEÑO EXPERIMENTAL

1.- Evaluación de la regeneración nerviosa periférica a través de electrodos regenerativos implantados crónicamente en el nervio ciático de rata

Publicaciones:

1. Lago N, Ceballos D, Rodríguez FJ, Stieglitz T, Navarro X. Long term assessment of axonal regeneration through polyimide regenerative electrodes to interfase the peripheral nerve. Biomaterials 2005, 26:2021-2031.
2. Negredo P, Castro J, Lago N, Navarro X, Avendaño C. Differential growth of axons from sensory and motor neurons through a regenerative electrode: a stereological, retrograde tracer, and functional study in the rat. Neuroscience 2004, 128:605-615.

Objetivos:

1.1. Estudio de la regeneración del nervio ciático de rata tras implantación de electrodos regenerativos a largo plazo, por medio de tests funcionales y morfológicos.

1.2. Estudio de la regeneración diferencial de axones motores y sensoriales a través del electrodo regenerativo. Estudio del número de axones motores en el nervio ciático y de motoneuronas y neuronas sensoriales a nivel central.

Metodología:

- Implante de electrodos regenerativos en nervio ciático de rata
- Grupos experimentales:
    - Grupo sieve
    - Grupo control
- Evaluación funcional a 2, 3, 4, 6, 9 y 12 meses
    - Algesimetría plantar
    - Walking track
    - Electrofisiología: conducción motora y sensorial
- Evaluación morfológica a 2, 6 y 12 meses
    - Recuento de fibras mielínicas
    - Recuento de fibras ChAT-positivas
    - Recuento de motoneuronas y neuronas sensoriales regeneradas mediante marcaje con retrotrazadores (2 meses)

2.- Registro de señales neurales mediante electrodos regenerativos

Publicaciones:

3. Lago N, Udina E, Navarro X. Regenerative electrodes for interfacing injured peripheral nerves: neurobiological assessment. IEEE BioRob2006. 06EX1254D. ISBN:1-4244-0040-6.

Objetivos:

2.1. Evaluar si es posible registrar señales neurales de pequeñas agrupaciones axonales regeneradas a través de los electrodos regenerativos.
2.2. Evaluar si se puede diferenciar entre señales aferentes y eferentes

Metodología:

- Lesión del nervio ciático de rata e implante de electrodos regenerativos
- Registro de señales neurales

3.- Estudio de la regeneración nerviosa en un modelo de amputación

Publicaciones:

4. Lago N, Navarro X. Evaluation of nerve regeneration in an experimental amputee model. (Manuscrito, enviado a J Periph Nerv System)
5. Lago N, Casas C, Rodríguez FJ, Muir EM, Rogers J, Navarro X. Effects of Schwann cell transplantation in an experimental amputee model. (Manuscrito)

Objetivos:

3.1. Evaluación de la regeneración axonal a largo plazo tras sección del nervio ciático de rata y reparación por tubulización en un modelo experimental de amputación.
3.2. Evaluación de los cambios morfológicos de los axones regenerados en el modelo de amputación crónica.
3.3. Efecto del transplante de células de Schwann (CS) en el modelo de amputación sobre la morfología y el mantenimiento de los axones regenerados.

Metodología:

- Cultivo de células de Schwann de rata
- Modelo de amputación nerviosa
- Grupos experimentales (Trabajo 4)
    - Grupo Amputación (Amp): Amp-2.5, Amp-6 y Amp-9
    - Grupo reinervación (Rei): Rei-2.5, Rei-6 y Rei-9
- Grupos experimentales (Trabajo 5):
    - Grupo Amputación + SC (Amp+SC)
    - Grupo Amputación+SCTM41
    - Grupo Amputación+SCTM41-GDNF
- Evaluación morfológica a 2.5, 6 y 9 meses

- Recuento de fibras mielínicas
- Inmunohistoquímica: ChAT, CGRP, GAP-43, GDNF, S-100, BrdU

4.- Evaluación de la regeneración de axones motores en lesión del nervio periférico. Estrategias para promover la regeneración específica motora y sensorial.

Publicaciones:

6. Lago N, Navarro X. Correlation between target reinnervation and distribution of motor axons in the injured rat sciatic nerve. J Neurotrauma 2006, 23:227-240.
7. Lago N, Rodríguez FJ, Jaramillo J, Navarro X. Effects of motor and sensory nerve transplants on the amount and specificity of sciatic nerve regeneration. (Manuscrito).

Objetivos:

4.1. Caracterización de la regeneración de los axones motores tras diferentes lesiones del nervio ciático de rata.

4.2. Evaluación de la promoción de las diferentes poblaciones axonales mediante transplante de raiz ventral y dorsal.

Metodología:

- Lesión del nervio ciático de rata
- Grupos experimentales (Trabajo 6):
  - Grupo CON: grupo control
  - Grupo Crush: lesión por aplastamiento
  - Grupo SUT: sección y reparación por sutura
  - Grupo SIL: sección y reparación con tubo de silicona
  - Grupo COL: sección y reparación con tubo de colágeno
- Grupos experimentales (Trabajo 7):
  - Grupo S: solución salina
  - Grupo VR: injerto de raíz ventral
  - Grupo DR: injerto de raíz dorsal
- Evaluación funcional:
  - Algesimetría plantar
  - Walking track
  - Electrofisiología
- Evaluación morfológica:
  - Recuento de fibras mielínicas
  - Recuento de fibras ChAT-positivas /NF-200-positivas

RESULTADOS

1

Evaluación de la regeneración nerviosa periférica a través de electrodos regenerativos implantados crónicamente en el nervio ciático de rata

Lago N, Ceballos D, Rodríguez FJ, Stieglitz T, Navarro X.
Long term assessment of axonal regeneration through polyimide regenerative electrodes to interfase the peripheral nerve.
Biomaterials 2005, 26: 2021-2031

[a]Negredo P, [a]Castro J, Lago N, Navarro X, [a]Avendaño C.
Differential growth of axons from sensory and motor neurons through a regenerative electrode: a stereological, retrograde tracer, and functional study in the rat.
Neuroscience 2004, 128: 605-615.

(Trabajo realizado en colaboración con el Dpto de Morfología de la Universidad Autónoma de Madrid (UAM)[a]. Nuestro grupo realizó la cirugía animal y el seguimiento funcional de los animales, mientras que el grupo de la UAM participó en la evaluación morfológica)

Available online at www.sciencedirect.com
SCIENCE DIRECT
Biomaterials 26 (2005) 2021–2031
Biomaterials

Long term assessment of axonal regeneration through polyimide regenerative electrodes to interface the peripheral nerve

Natalia Lago[a], Dolores Ceballos[a], Francisco J Rodríguez[a], Thomas Stieglitz[b], Xavier Navarro[a,*]

[a] *Department of Cell Biology, Physiology and Immunology, Institute of Neuroscience, Universitat Autònoma de Barcelona, Edif M, Campus UAB, E08193 Bellaterra, Spain*

[b] *Neural Prosthetics Unit, Fraunhofer Institute for Biomedical Engineering, St. Ingbert, Germany*

Received 1 June 2004; accepted 15 June 2004

Available online 20 July 2004

Abstract

Polyimide sieve electrodes were implanted between the severed ends of the sciatic nerve in rats. The degree of axonal regeneration through the electrode was examined by physiological and histological methods from 2 to 12 months postimplantation. Regeneration was successful in the 30 animals implanted. Functional reinnervation of hindlimb targets progressed to reach maximal levels at 6 months. Comparatively, the reinnervation of distal plantar muscles was lower than that of proximal muscles and of digital nerves. The number of regenerated myelinated fibers increased from 2 to 6 months, when it was similar to control values. The majority of myelinated fibers crossing the via holes and regenerated through the distal nerve had a normal appearance. However, in a few cases decline of target reinnervation and loss of regenerated nerve fibers was found from 6 to 12 months postimplantation. Motor axons labeled by ChAT immunoreactivity regenerated scattered within minifascicles, although they were found at higher density at the periphery of the regenerated nerve. The number of ChAT-positive axons was markedly lower distally than proximally to the sieve electrode.

Keywords: Interface; Motor axons; Nerve regeneration; Neural prosthesis; Peripheral nerve; Polyimide; Regenerative electrode

1. Introduction

A number of neuroprostheses, developed to artificially substitute or mimic sensorimotor functions in patients with neurological impairment, include interfacing the peripheral nervous system by means of appropriate electrodes, which may allow neuromuscular stimulation and neural signal recording. For such purpose, a variety of electrode designs, including cuff, intrafascicular, penetrating and regenerative electrodes have been developed and tested [1,2]. Regenerative electrodes are designed to interface a high number of nerve fibers by using an array of via holes, with electrodes built around them, implanted between the severed stumps of a peripheral nerve [3,4]. One of the most logical and challenging applications of regenerative electrodes will be its implantation in severed nerves of an amputee limb for a bi-directional interface in a feedback-controlled neuroprosthesis. On the one hand, recording of neural efferent signals can be used for the motion control of a mechanical prosthesis [5], and on the other, sensory feedback from tactile and force sensors might be provided to the user through stimulation of afferent nerve fibers within the residual limb [6].

The applicability of regenerative electrodes is dependent upon the success of axonal regeneration through the perforations or via holes, the possible nerve damage from the mechanical load imposed by the electrode or from constrictive forces within the via holes, and the biocompatibility of the components, especially over long term implantation [7,8]. Different techniques and materials have been used during the last 30 years in the construction of regenerative electrodes. With the advent of microelectronic technologies, it became

*Corresponding author. Tel.: +34-935-811-966; fax: +34-935-812-986.

E-mail address: xavier.navarro@uab.es (X. Navarro).

0142-9612/$ - see front matter © 2004 Elsevier Ltd. All rights reserved.
doi:10.1016/j.biomaterials.2004.06.025

possible to construct silicon electrodes with dimensions and number of via holes compatible with the characteristics of peripheral nerves. Using multiple holes silicon arrays, axonal regeneration and even neural activity recording was demonstrated in peripheral nerves of rat, frog and fish [8–12]. However, such silicon interfaces cause frequent signs of axonopathy [5,8], and constitute a physical barrier that limits the elongation of regenerating axons depending on the size of the via holes [7,8,13]. Because of their more adaptive physical characteristics, polyimide-based electrodes were introduced more recently [14,15]. Polyimide allows to make a higher number of holes than silicon dice of the same total area and to be micromachined in a variety of designs suitable for implantation in different nerve models. Polyimide-based electrodes have been shown to be biocompatible [14,16] and stable over several months of in vivo implantation and testing [15,17].

In previous studies we evaluated the adequate design of a regenerative electrode based on polyimide substrate [14] and its suitability for allowing axonal regeneration in the sciatic nerve of the rat [15]. The proportion of regenerates and the quality of the regenerated nerves were better than those found through silicon dice [8]. In a more recent study we reported that nerve regeneration was sustained at long term, up to 12 months, and that the electrodes allowed for selective stimulation of different regenerated nerve fascicles [18]. However, there were few cases evaluated at such a long interval (3 rats at 12 months). The knowledge of the long-term functional and structural changes in the nerve due to implanted electrodes is highly relevant if they have to become a valuable tool for providing an interface between peripheral nerves and distal target organs or limb prosthetic devices in humans [7,19]. In this work, we further evaluated, by functional and morphological analysis, the regeneration of the rat peripheral nerve through polyimide regenerative electrodes implanted from 2 to 12 months in order to investigate the possible effects of chronic implantation and to assess if regenerated axons may acquire and maintain normal morphological and functional features. Furthermore, in order to assess if motor and sensory fibers, representing the two main types of axons that should be selectively interfaced, tend to grow separately or intermingled within the small fascicles that regenerate through each via hole, motor axons were identified by immunohistochemistry against cholin-acetyl transferase (ChAT).

2. Material and methods

2.1. Regenerative electrode and implantation

The regenerative electrodes were micromachine fabricated using a polyimide resin (PI2611, DuPont) as substrate and insulation material with a single metallization layer, as previously described in detail [14,15]. The used polyimide has low water absorption, it is biocompatible, and it has been shown to be mechanically stable after long in vitro and in vivo testing [15,17,18,20]. The regenerative electrode is a flexible structure, with a thickness of 10 μm and a weight of 4 mg. It consists of three portions: a round sieve interface (2 mm diameter), a narrow ribbon cable (1 mm wide, 21 mm long) and an ending connector (2 mm × 3 mm). The sieve part of the interface has 281 round via holes of 40 μm diameter, with nine integrated Pt electrodes arranged around via holes, occupying an area of 1473 μm^2. The Pt electrodes were connected through integrated leads in the ribbon to nine-squared connects placed at the ending pad. The sieve portion was placed between two silicone tubes (2 mm i.d., 4 mm length) and glued by plasma etching, and the interconnection covered with silicone glue (Fig. 1). Silicone tubes served for implantation and as guidance for nerve regeneration.

Operations were performed under pentobarbital anesthesia (40 mg/kg i.p.) on 30 adult Sprague–Dawley rats (aged 3 months). The sciatic nerve was exposed at the thigh and freed from surrounding tissues from the sciatic notch to the knee. The sciatic trunk was transected and each nerve stump fixed into one end of the silicone guide with one stitch of 10-0 suture, leaving a short gap of about 3 mm between the stumps. The electrode ribbon was routed to the upper thigh region, where the ending part was secured under the skin. The muscles and the skin were sutured and the wound disinfected. In order to avoid autotomy after denervation, the sciatic nerve was blocked by local application of bupivacaine proximal to the lesion site, and the animals were treated by administering amitriptyline in the drinking water [21]. A group of 5 rats with intact sciatic nerve were used as controls. The experimental procedures were approved by the Ethical Committee of our institution.

2.2. Functional evaluation

At intervals of 1, 2, 3, 4, 6, 9 and 12 months postimplantation the rats were evaluated by noninvasive tests to assess the success of distal target reinnervation by the sciatic nerve regenerating through the sieve electrode. Regeneration of large myelinated nerve fibers was assessed by nerve conduction tests. With the animals under anesthesia (pentobarbital 40 mg/kg i.p.), the nerve was stimulated through a pair of needle electrodes placed at the sciatic notch with single electrical pulses of 0.05 ms duration. The compound muscle action potentials (CMAPs) were recorded from the medial gastrocnemius muscle and from the plantar muscles (at the third interosseus space) with small needle

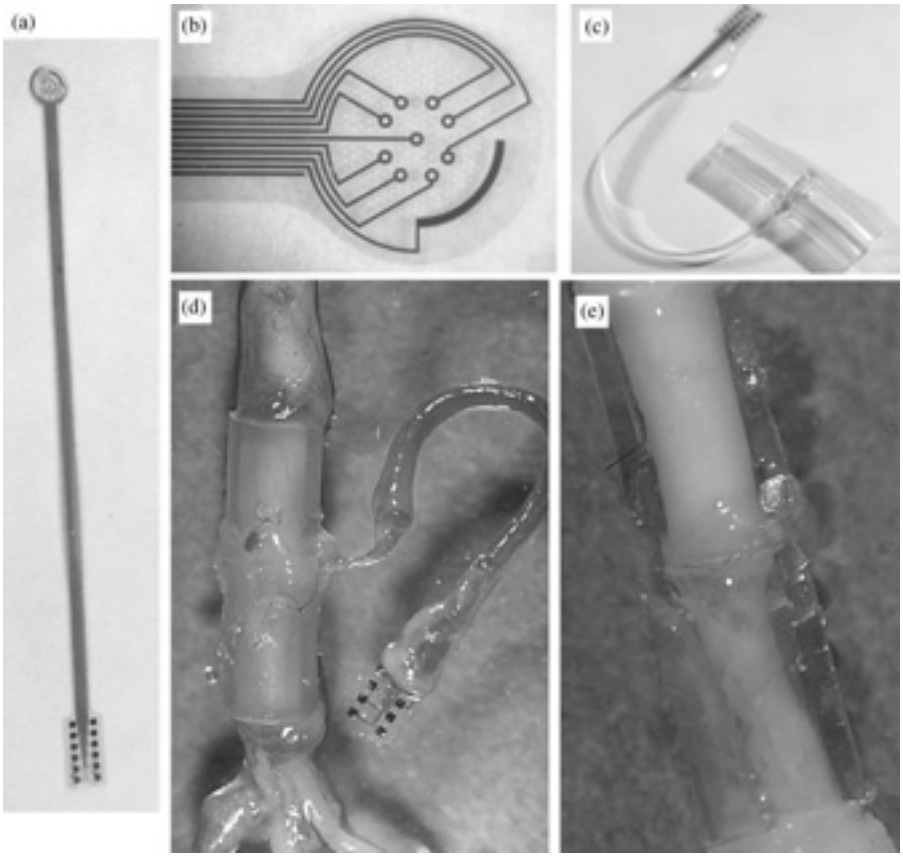

Fig. 1. Photomicrographs of (a) a polyimide regenerative electrode, (b) enlarged view of the sieve portion of the regenerative electrode, (c) the silicone guide with the sieve electrode encased, (d) a sciatic nerve regenerated through the polyimide sieve electrode after removal at 6 months postimplantation, and (e) view of the regenerated nerve after opening the silicone tube. In d and e the proximal side is at the top and the distal side at the bottom. The regenerated nerve shows a conic-shape enlargement at both sides of the sieve, most evident at the distal site. Note the thin fibrous tissue covering the polyimide ribbon.

electrodes [22–24]. Similarly, sensory compound nerve action potentials (CNAPs) were recorded by electrodes placed near the tibial nerve at the ankle and near the digital nerves of the fourth toe. The evoked action potentials were displayed on a storage oscilloscope at settings appropriate to measure the amplitude from baseline to peak and the latency to the onset.

The extension of pain sensitivity in the hindpaw was tested by light pricking with a needle in five areas, from the most proximal pawpad to the tip of the second digit on the plantar surface. The animal response was scored as no response (0), reduced (1) or normal reaction (2) in each area tested, and the 5 scores added into a pinprick score (PP). Recovery of nociception was also quantitated by plantar algesimetry [25]. Rats were placed into a plastic box with an elevated glass floor. The beam of a projection lamp was focused from the bottom of the box onto the plantar surface of the hindpaw. The time spent until withdrawal of the heated paw was measured through a time-meter coupled with IR detectors directed to the plantar surface. The value for a test was the mean of three trials separated by 30 min resting periods. The values were normalized as the percentage with respect to the withdrawal latency of the contralateral intact hindpaw each testing day.

2.3. Morphological evaluation

At 2.5, 6 and 12 months postimplantation, subgroups of animals were anesthetized and perfused transcardially with 4% paraformaldehyde in phosphate-buffer saline solution (PBS, 0.1 M, pH 7.4). The sciatic nerve was harvested and a segment of the nerve just distal to the silicone tube was postfixed in 3% glutaraldehyde-3% paraformaldehyde in cacodylate-buffer solution (0.1 M, pH 7.4) overnight at 4°C, and then processed for embedding in Epon resin. Semithin sections 0.5 μm thick were stained with toluidine blue and examined by light microscopy. Images of the whole sciatic nerve were acquired at 10x with an Olympus DP50 camera attached to computer, while sets of images chosen by systematic random sampling of squares representing at least 30% of the nerve cross-sectional area were acquired at 100x. Measurements of the cross-sectional area of the whole

nerve, area of bundles of regenerated fibers, as well as counts of the number of myelinated fibers were carried out by using NIH Image software. Morphometric evaluation of the regenerated myelinated fibers was performed by measuring 500 fibers from the set of images chosen at a final magnification of 2600x. The outline of each axon and its myelin sheath in the sample was drawn with a digitizing pen and captured on the screen by means of a computer-linked digitizing tablet and specific software.

2.4. Immunohistochemistry

Segments of the regenerated sciatic nerves inside the silicone guide, about 2 mm proximal and distal to the sieve were collected and postfixed in the same perfusion solution for 4 h. Then samples were washed in PBS and stored in the same buffer with azide 0.1% for embedding in paraffin. The control rats were perfused and postfixed in the same solution, and an equivalent segment of the sciatic nerve was collected and processed in parallel. Transverse sections (4 μm) were cut, mounted in silane-coated slides and dried overnight. The sections were deparaffinized and rehydrated before antigen retrieval with sodium citrate during 20 min at 95°C. Then immunocytochemical staining methods were employed with two types of primary antibodies: anti-NF200 (Chemicon; 1:400) which reacts with the 200-kDa neurofilament regions, and goat polyclonal antiserum to ChAT (Chemicon; 1:50) were applied to the tissue sections for 24 h at 4°C. Slides were washed with TBST (5% Tween-20) and incubated with biotynilated secondary antibodies (Vector) for 1 h at room temperature. After further washing the slides were incubated with ABC (avidin-biotin complex, Vector) for 1 h at room temperature. After TBS washing slides were incubated for 3 min with DAB, counterstained with hematoxylin, dehydrated and mounted with DPX. Images of the whole sciatic nerve were acquired at 10x, while sets of systematic randomly chosen images representing at least 30% of the nerve cross-sectional area were acquired at 100x. Measurements of the whole nerve area and counts of the number of ChAT-positive axons were carried out by using NIH Image software.

2.5. Statistical analysis

All results are expressed as mean ± SE. Statistical comparisons between groups and intervals were made by nonparametric tests, and differences were considered significant when $p < 0.05$.

3. Results

3.1. Functional results

Functional tests performed during follow-up after operation indicated successful reinnervation of distal targets by the regenerating sciatic nerve in all the rats that had a regenerative electrode implanted. Table 1 shows the values for the neurophysiological tests at the different follow-up intervals postimplantation.

The percentage recovery achieved maximal values by 6 months. The amplitude of CMAPs increased with time from 2 to 6 months postimplant up to values that were about 46% of control values in the gastrocnemius muscle and 18% in the plantar muscle, whereas

Table 1
Neurophysiological results of target reinnervation by nerves regenerated through regenerative electrodes

(*n*)	Baseline (30)	2 months (30)	3 months (18)	4 months (18)	6 months (18)	9 months (10)	12 months (10)
Gastrocnemius muscle Latency (ms)	1.3 ± 0.02	3.8 ± 0.2	2.7 ± 0.1	1.9 ± 0.1	1.8 ± 0.1	1.7 ± 0.2	1.7 ± 0.2
CMAP (mV)	60.2 ± 1.5	9.4 ± 1.2	18.0 ± 1.6	25.3 ± 1.5	26.2 ± 1.2	24.0 ± 2.0	22.3 ± 2.7
Plantar muscle Latency (ms)	3.1 ± 0.1	12.6 ± 1.2	6.9 ± 0.3	5.2 ± 0.2	5.2 ± 0.2	6.1 ± 0.9	6.5 ± 1.2
CMAP (mV)	9.02 ± 0.28	0.09 ± 0.02	0.36 ± 0.05	1.30 ± 0.21	1.61 ± 0.34	1.33 ± 0.35	1.04 ± 0.45
Tibial nerve Latency (ms)	1.2 ± 0.02	1.4 ± 0.1	1.2 ± 0.1	1.4 ± 0.1	1.4 ± 0.1	1.4 ± 0.1	1.4 ± 0.1
CNAP (μV)	209 ± 5.6	24.3 ± 3.3	49.1 ± 10.8	93.4 ± 12.6	90.7 ± 10.7	77.0 ± 10.6	78.2 ± 11.0
Digital nerve Latency (ms)	2.2 ± 0.03	4.6 ± 0.4	4.9 ± 0.6	4.8 ± 0.2	5.0 ± 0.3	5.0 ± 0.4	4.4 ± 0.4
CNAP (μV)	24.3 ± 1.2	1.66 ± 0.43	3.40 ± 0.98	5.33 ± 0.70	9.50 ± 1.35	7.04 ± 2.01	5.20 ± 1.27
Nociception PP score	10 ± 0	2.7 ± 0.3	3.0 ± 0.4	5.6 ± 0.5	6.8 ± 0.5	7.4 ± 1.1	8.0 ± 0.4
Withdrawal (%)	100 ± 4	180 ± 8	163 ± 9	155 ± 9	157 ± 8	144 ± 6	133 ± 10

Values are mean ± SEM.

the CNAPs amplitude increased to 44% in the tibial nerve and to 39% in the more distal digital nerve (Fig. 2). The low reinnervation achieved in the distal plantar muscle in comparison with the other targets suggests that large alphamotor fibers may have more limited regeneration through the regenerative electrode than large myelinated sensory fibers. The latency of CMAPs and CNAPs shortened with time but remained longer than control values, by about 30% in proximal targets (gastrocnemius muscle and tibial nerve) and by 100% in distal targets (plantar muscle and digital nerve). The time to paw withdrawal found during the algesimetry was longer (180–133%) in the operated hindlimb than in the intact contralateral hindlimb during follow-up. Pain sensibility recovered progressively from proximal to distal areas of the paw with time, but was still incomplete at 12 months.

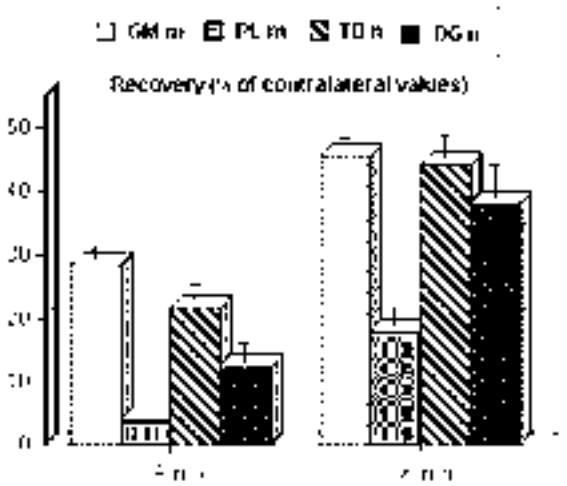

Fig. 2. Percentage recovery of the amplitude of the CMAP of gastrocnemius (GM) and plantar (PL) muscles and of the CNAP of tibial (TB) and digital (DG) nerves at 3 and 6 months postoperation (dpo).

From 6 to 12 months postimplant there was a mild decrease in the degree of functional reinnervation, particularly in distal targets, i.e. plantar muscle and digital nerve. Changes of electrophysiological parameters in the same ten rats followed up to 12 months postimplantation are shown in Fig. 3. The decline affected 3 rats that showed a moderate reduction in plantar CMAP and digital CNAP amplitude and 1 rat with marked loss at 12 months.

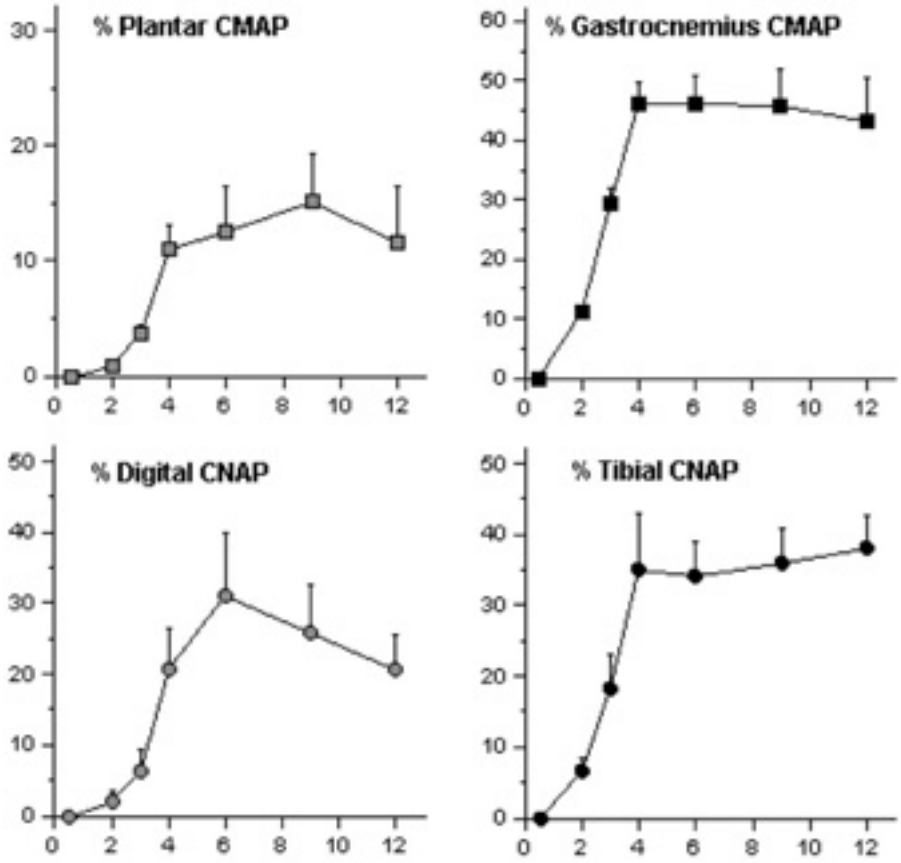

Fig. 3. Plots of the amplitude of CMAP of plantar and gastrocnemius muscles and of CNAP of digital and tibial nerves, expressed as percentage of contralateral values, along time in the ten rats with a 12 months follow-up after implantation of a regenerative electrode in the transected sciatic nerve. The X-axis scale is in months postimplantation. The Y-axis scale is in percentage of the contralateral control response.

3.2. Morphological evaluation

The morphological evaluation performed at 2, 6 and 12 months postimplant corroborated that the sciatic nerve had grown through the sieve portion of the electrode. The silicone guide and the polyimide ribbon were covered by well vascularized fibrous tissue, without signs of inflammatory reaction. The regenerated nerves had variable thickness, and showed a conic-shape enlargement at both sides of the sieve (Fig. 1b). At the distal nerve level, the regenerated nerves were organized in multiple small fascicles. The transverse nerve area was smaller than that of the intact sciatic nerve, whereas the number of regenerated myelinated fibers increased significantly from 2 to 6 months, reaching mean values similar to controls (Table 2). The morphological appearance of the myelinated fibers indicated progressive increase of axonal size and myelin sheath from 2 to 6 months, but the mean values were still far below normal (Table 2, Fig. 4).

From 6 to 12 months postimplantation there was a decline in the endoneurial area and in the mean number of regenerated myelinated fibers. While looking at individual values, 4 of the nerves at 12 months showed numbers of regenerated fibers in the range of those found at 6 months (6000–9800), 3 nerves had lower numbers (3000–4600), and 1 had a very low number (220). The cases with low regenerated myelinated fibers corresponded to the rats that showed a decrease in target reinnervation from 6 to 12 months in functional

Table 2
Cross-sectional area, number of myelinated fibers and morphometric results in the nerves regenerated through a regenerative electrode taken at the distal nerve level

(*n*)	Control (10)	2 months (5)	6 months (8)	12 months (10)
Nerve area (mm^2)	0.66 ± 0.06	$0.29 \pm 0.06^*$	$0.35 \pm 0.05^*$	$0.29 \pm 0.03^*$
No. myelinated fibers	8266 ± 258	$4940 \pm 1455^*$	8848 ± 1033	$4650 \pm 838^*$
Axonal diameter (μm)	4.58 ± 0.12	1.86 ± 0.13	2.35 ± 0.17	2.20 ± 0.14
Myelin thickness (μm)	1.69 ± 0.04	0.64 ± 0.02	0.71 ± 0.03	0.68 ± 0.03

Control values are also shown for comparison. Values are mean ± SEM.
$^*p < 0.05$ with respect to control values.

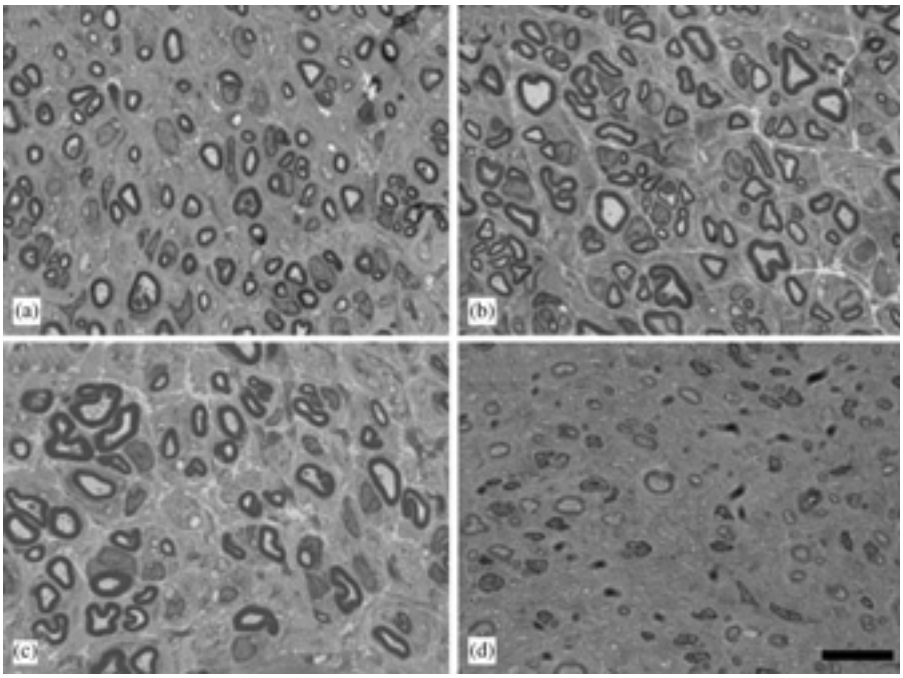

Fig. 4. Micrographs of semithin sections of nerves regenerated through polyimide sieve electrodes. Cross section of the distal nerve at 2 (a), 6 (b) and 12 (c and d) months postimplantation. Note the appearance of the myelinated fibers showing progressive increase of axonal size and myelin sheath from 2 to 6 months. At 12 months postimplantation there were some nerves with numbers in the range of those found at 6 months (c) and some with a low number of fibers (d). Bar = 10 μm.

Table 3
Number of ChAT labeled myelinated fibers in the regenerated nerves proximal and distal to the sieve portion of the regenerative electrode

No. ChAT+ MF (n)	Control (5)	2 months (5)	6 months (5)	12 months (5)
Proximal nerve	1655±79	5048±1333	5243±1033*	4197±1029*
Distal nerve		892±509	1244±187**	758±222*,**

Control values are also shown for comparison. The proportion of ChAT positive fibers with respect to the toal number of myelinated fibers can be derived by comparing with values given in Table 2. Values are mean±SEM.
*$p<0.05$ with respect to control values; **$p<0.05$ with respect to proximal nerve values.

tests. Transverse histological sections made near the sieve electrode distal level showed that there were high numbers of regenerated nerve fibers, but some had no or only very thin myelin sheath and others were swollen and with signs of degeneration. These findings consistent with loss and damage of nerve fibers that had initially regenerated, most likely due to compressive axonopathy at the sieve electrode level affecting some of the nerves studied.

3.3. Immunohistochemistry

The number of ChAT-positive axons counted in the intact rat sciatic nerve averaged 1655±79, i.e. about 20% of the number of myelinated fibers. In the regenerated nerves, there was a marked increase in the number of ChAT positive axons at the level just proximal to the sieve (Table 3), whereas at the distal level there was about 5 times less. The number increased slightly from the 2 months to the 6 months samples but decreased in those taken at 12 months. The percentage of ChAT positive fibers was around 18–14% of the number of myelinated fibers found regenerated at the distal nerve, about 2 mm more distally (see Tables 2 and 3).

Regarding the distribution of ChAT-labeled fibers, in the normal sciatic nerve they tended to group in fascicles together with other large myelinated fibers, like muscular afferents. In contrast, in regenerated nerves they were scattered throughout the cross-sectional area within the small fascicles. The density of ChAT positive profiles was higher in the periphery of the regenerated nerve, at both levels proximal and distal to the sieve (Fig. 5).

4. Discussion

Contemporary research in developing a motor neuroprosthesis has concentrated on addressing the development and experimental testing of interfaces to the peripheral nervous system that do not damage the nerve, allow access to information from sensory afferents, selectively stimulate multiple nerve fibers and provide graded control of muscle force [26]. Since electrodes that may be integrated with the peripheral nerve can be used for stimulation of nerve fibers as well as for recording of neural impulses, they hold great interest for the development of bi-directional interfaces with the nervous system. Intraneural microelectrode arrays made of silicon with up to 100 individual needle electrodes can be inserted into a peripheral nerve, and it has been shown that they provide a good electrical interface with individual or small groups of axons within nerve fascicles [26–28]. However, the rigid structure of such electrodes and the tethering forces produced by the lead wires may induce problems when applied to limb nerves, and no long-term study of the biocompatibility of the array in a peripheral nerve has been done yet. On another hand, multichannel regenerative electrodes can be applied only to transected nerves and some time is needed for interfacing the regenerated axons, thus precluding acute experiments. Regenerative electrodes fabricated with silicon dice also presented problems derived from the rigid structure of the sieve and the lead connectors [8,9], which motivated the development of electrodes based on polyimide that are thin and highly flexible [14,15].

4.1. Regeneration through regenerative electrodes

In this study we extensively investigated the fate of nerve regeneration across polyimide sieve electrodes implanted in the transected rat sciatic nerve for 2 to 12 months. We found that regeneration of peripheral nerve fibers through the array of via holes took place in all the 30 animals implanted. These findings corroborate and extend our previously reported results in smaller numbers of rats [15,18]. Regenerative polyimide electrodes have also been shown to be useful for stimulation of different regenerated nerve bundles and for recording nerve action potentials in response to functional stimulation [15,18], further indicating that it is an adequate device for creating an interface with the regenerated fibers of transected peripheral nerves. These results are comparatively better than those reported for silicon-based regenerative electrodes, in which regeneration usually fails in a proportion of animals, the number of axons present in the distal nerve stump is low and a significant proportion of them show morphological

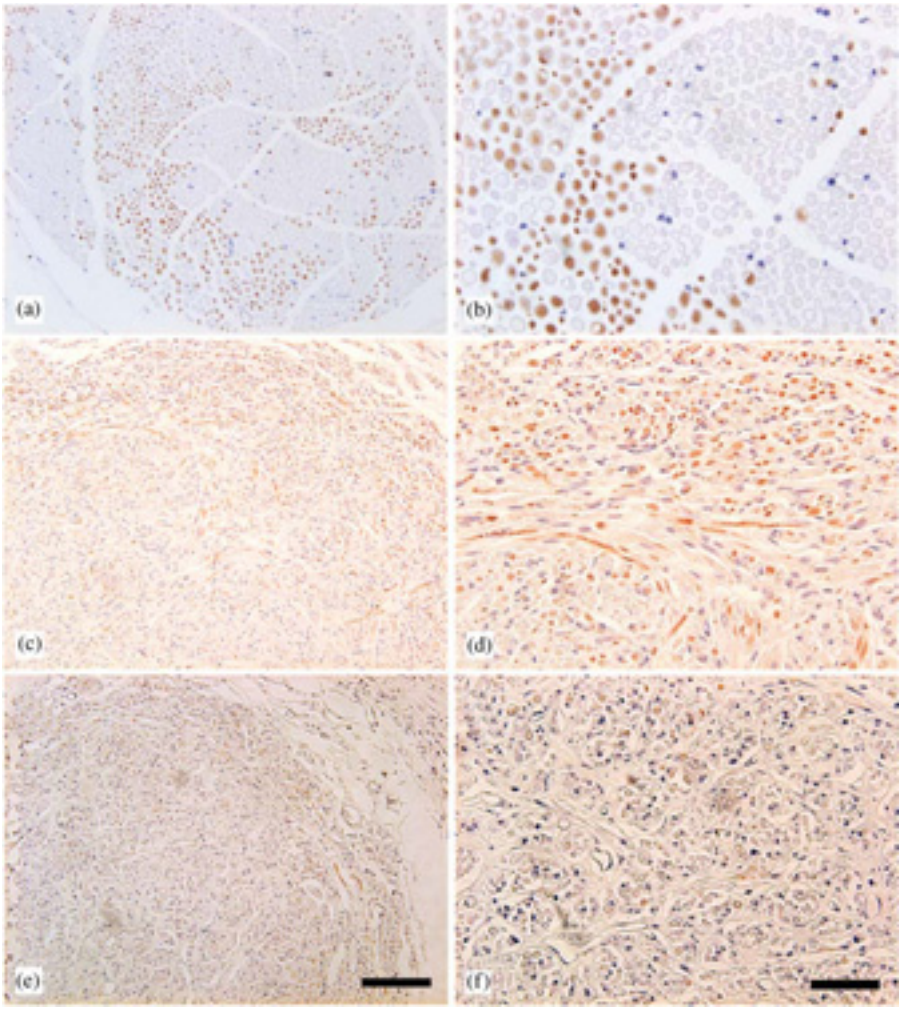

Fig. 5. Immunohistochemical labeling against ChAT in transverse sections of a control sciatic nerve (a and b), and of a representative regenerated nerve at 6 months postimplantation at levels proximal (c and d) and distal (e and f) to the sieve electrode. Note the higher number of ChAT-positive fibers at the level just proximal to the sieve than at the distal level. The density of ChAT positive profiles was higher in the periphery of the regenerated nerve. Bar = 100 μm in a, c, e, and 40 μm in b, d, f.

abnormalities likely derived from constriction within the rigid perforations [8–10,12,13].

We found that the degree of regeneration progressed with time until 6 months postimplantation of the regenerative electrode as judged by the increasing numbers of regenerated axons, and the progressive increase in amplitude of evoked compound muscle and nerve action potentials and in nerve conduction velocity in neurophysiological tests. However, distal reinnervation was slightly delayed and decreased in comparison with results found after simple silicone tube repair leaving a similar gap (about 4 mm) in the rat sciatic nerve [24]. The number of myelinated fibers found distal to the sieve electrode was about 8800 at 6 months postimplantation, i.e. slightly more than the number present in the normal rat sciatic nerve (see Table 2). Nevertheless, this number may overrepresent the number of neurons that actually regenerated their axons across the electrode, since even long time after injury regenerating neurons support multiple sprouts, branching from the lesion site in the distal nerve stump [29,30]. Thus, transverse placement of a sieve electrode constitutes a microperforated barrier that may disturb the initial phases of the regenerating cable, delays and may impede the elongation of growing axons.

In animals evaluated at long-term, from 6 to 12 months postimplantation, there was a decline in levels of target reinnervation and in the number of myelinated fibers in the distal regenerated nerve. This loss affected markedly only one rat, and mildly other 3 of the 10 rats followed until 12 months. In the majority of cases the histological study showed that the myelinated fibers crossing the sieve via holes had a normal appearance for a regenerated nerve, i.e. with smaller caliber and thinner myelin sheath than in intact nerves, whereas a few showed signs of compressive axonopathy (see also [18]). In those rats with loss of functional reinnervation, the number of regenerated fibers was reduced, and a

variable percentage showed evidence of damage, such as demyelination and axonal degeneration. These findings are attributable to compressive axonopathy at the sieve electrode level affecting nerve fibers that had initially regenerated and enlarged caliber and myelination as they matured. Klinge et al. [20] reported on axonal regeneration across a similar polyimide sieve electrode directly sutured to the transected sciatic nerve of rats without a distal nerve insert. They found that axonal sprouts readily grew through the via holes, increasing in number from 5 weeks to 11 months after implantation, although no quantitation was performed.

A quantitative long-term characterization of the outcome of nerve regeneration and stability of the electrode itself is relevant for subsequent application of electrodes since it will provide experimental evidences contributing to modified implantation procedures and electrode designs. It has been reported that the size and structure of the implanted device as well as the size of the perforated via holes play a notable influence on nerve regeneration [8,10,13]. The polyimide regenerative electrodes used had a high number of via holes of 40 μm in diameter, allowing regeneration of small bundles of axons through them. With larger via holes regeneration may be less difficult, but the purpose of selective accessing of a small number of axons will be limited [5]. Additionally, a large number of small sieve holes with integrated electrodes needs much more space for the interconnect lines from the sieve to the connecting pad. Thereby, the distance between holes must be increased or at least kept constant with respect to larger holes, thus decreasing the hole to material relation of the implant. On the view of the present results, minor modifications may be suggested, such as increasing the diameter of via holes and enlarging the total open area within the sieve electrode in order to facilitate regeneration of a larger number of axons and to reduce potential chronic damage to regenerated axons. In spite of some loss of selectivity, recorded action potentials from larger hole electrodes will be higher in amplitude due to more fibers contributing to the signal, thus the signal-to-noise ratio will increase and will be more robust as input signal for envisioned artificial limb control.

4.2. Regeneration of motor nerve fibers

Ideally, the number of via holes in the sieve electrode should match or be close to the average number of axons in the nerve to be implanted, thus increasing the probability of regeneration of one or only a few axons per hole and allowing for selective identification of individual signals [7]. However, holes with diameters within the micrometer range are usually occupied by several regenerating axons, which initially are of small size and grow together in regenerating units. In fact, immediately adjacent to the sieve interface the regenerated nerves were organized in minifascicles corresponding to the grid pattern of the via holes and covering in most cases the whole area of the sieve portion. These small fascicles contain a number of myelinated and unmyelinated fibers, which were intermingled at short term, but tend to segregate at long term, with unmyelinated fibers mostly localized to the periphery of each via hole [18,20]. It has been shown that nerve fibers have some somatotopic organization as well as fiber segregation by modality within the normal peripheral nerve [31,32]. In order to assess if regenerating fibers maintain such organization and, therefore, the fibers grown together through one via hole are functionally related, we have used ChAT immunoreactivity to identify motor myelinated axons in transverse sections taken near the sieve electrode. To confirm that the number of ChAT-immunoreactive axons was representative of the number of motor axons, we made counts in control sciatic nerves, and found that they represented a 20% of myelinated fibers, in agreement with previous data [33]. In regenerated nerves there were high numbers of ChAT-positive fibers proximal to the sieve, about 4 times those of the intact sciatic nerve, which may be attributed to sprouting of regenerating fibers at the lesion site and when facing the physical sieve barrier. In contrast, distal to the sieve motor axons were reduced in number at all times analyzed, representing about 15% of the number of myelinated fibers in the same nerves. Large alphamotor axons seem to have a lower capability for growing through the regenerative electrode in comparison other types of axons as indicated by a retrograde tracing study [34], and suggested also by the low degree of reinnervation achieved in the distal plantar muscle in comparison with that of the digital nerve.

The majority of ChAT-immunoreactive motor axons grew up by the periphery of the nerve, and we could not delineate a clear map of muscular nerve fascicles, as observed in control nerves. The abundant proximal sprouting and the reduced distal regeneration of motor axons, and their spatial distribution may be explained by a faster rate of regeneration for small than for large diameter fibers and for sensory than for motor myelinated axons during the initial stages of regeneration [35,36]. Therefore, small sensory and sympathetic fibers growing in the regenerative front would occupy the center of the regenerative nerve cable facing the sieve electrode; motor fibers regenerating with more delay would be confined to the outer layers of the cable and have more difficulties to find paths across the sieve perforations. Neurobiological strategies to be investigated and applied will focus on enhancing regeneration of motor axons [37], needed for the use of regenerative interfaces to detect efferent signals in the sectioned nerves of amputees, and also to rescue regenerated axons from compressive forces within the via holes [38].

Despite these critical problems, nerve regeneration through the polyimide sieve electrodes was satisfactory, further indicating that they can be adequate part on the design of interface systems, that may allow simultaneous access to a high number of neural signals in the peripheral nerve. Evidences have been previously reported that polyimide electrodes were useful for stimulation of peripheral nerves inducing excitation of different regenerated nerve fascicles and for recording bursts of nerve action potentials in response to functional stimulation [15,18,39].

Acknowledgements

This research was supported by Grant IST-2001-35094 from the EC. The authors thank Jessica Jaramillo for technical assistance in the morphological studies, and Drs. Martí Pumarola and José M. Vela for advice and support in the immunohistochemical methods.

References

[1] Heiduschka P, Thanos S. Implantable bioelectronic interfaces for lost nerve functions. Prog Neurobiol 1998;55:433–61.
[2] Rutten WLC. Selective electrical interfaces with the nervous system. Annu Rev Biomed Eng 2002;4:407–52.
[3] Llinás R, Nicholson C, Johnson K. Implantable monolithic wafer recording electrodes for neurophysiology. In: Phillips MI, editor. Brain unit activity during behaviour. Illinois: Charles Thomas; 1973. p. 105–10.
[4] Kovacs GTA, Storment CW, Rosen JM. Regeneration microelectrode array for peripheral nerve recording and stimulation. IEEE Trans Biomed Eng 1992;39:893–902.
[5] Edell DJ. A peripheral nerve information transducer for amputees: long-term multichannel recordings from rabbit peripheral nerves. IEEE Trans Biomed Eng 1986;33:203–14.
[6] Riso RR. Strategies for providing upper extremity amputees with tactile and hand position feedback—moving closer to the bionic arm. Technol Health Care 1999;7:401–9.
[7] Rosen JM, Grosser M, Hentz VR. Preliminary experiments in nerve regeneration through laser-drilled holes in silicon chips. Restor Neurol Neurosci 1990;2:89–102.
[8] Navarro X, Calvet S, Butí M, Gómez N, Cabruja E, Garrido P, Villa R, Valderrama E. Peripheral nerve regeneration through microelectrode arrays based on silicon technology. Restor Neurol Neurosci 1996;9:151–60.
[9] Kovacs GTA, Storment CW, Halks-Miller M, Belczynski CR, Della Santina CC, Lewis ER, Maluf NI. Silicon-substrate microelectrode array for parallel recording of neural activity in peripheral and cranial nerves. IEEE Trans Biomed Eng 1994;41:567–77.
[10] Della Santina CC, Kovacs GTA, Lewis ER. Multi-unit recording from regenerated bullfrod eighth nerve using implantable silicon-substrate microelectrodes. J Neurosci Methods 1997;72:71–86.
[11] Bradley RM, Cao X, Akin T, Najafi K. Long term chronic recordings from peripheral sensory fibers using a sieve electrode array. J Neurosci Methods 1997;73:177–86.
[12] Mensinger AF, Anderson DJ, Buchko CJ, Johnson MA, Martin DC, Tresco PA, Silver RB, Highstein SM. Chronic recording of regenerating VIIIth nerve axons with a sieve electrode. J Neurophysiol 2000;83:611–5.
[13] Zhao Q, Drott J, Laurell T, Wallman L, Lindström K, Bjursten LM, Lundborg G, Montelius L, Danielsen N. Rat sciatic nerve regeneration through a micromachined silicon chip. Biomaterials 1997;18:75–80.
[14] Stieglitz T, Beutel H, Meyer J-U. A flexible, light-weight multichannel sieve electrode with integrated cables for interfacing regenerating peripheral nerves. Sensor Actuators 1997;60:240–3.
[15] Navarro X, Calvet S, Rodríguez FJ, Stieglitz T, Blau C, Butí M, Valderrama E, Meyer JU. Stimulation and recording from regenerated peripheral nerves through polyimide sieve electrodes. J Peripher Nerv System 1998;2:91–101.
[16] Stieglitz T, Navarro X, Calvet S, Blau C, Meyer UW. Interfacing regenerating peripheral nerves with a micromachined polyimide sieve electrode. Proceedings of the 18th Annual International Conference IEEE Engineering in Medicine an Biology Society. Amsterdam, 1996. p. 417 (on CD-ROM).
[17] Rodríguez FJ, Ceballos D, Schüttler M, Valderrama E, Stieglitz T, Navarro X. Polyimide cuff electrodes for peripheral nerve stimulation. J Neurosci Methods 2000;98:105–18.
[18] Ceballos D, Valero-Cabré A, Valderrama E, Schüttler M, Stieglitz T, Navarro X. Morphological and functional evaluation of peripheral nerve fibers regenerated through polyimide sieve electrodes over long term implantation. J Biomed Mater Res 2002;60:517–28.
[19] Lundborg G, Drott J, Wallman L, Reimer M, Kanje M. Regeneration of axons from central neurons into microchips at the level of the spinal cord. Neuroreport 1998;9:861–4.
[20] Klinge PM, Vafa MA, Brinker T, Brandis A, Walter GF, Stieglitz T, Samii M, Wewetzer K. Immunohistochemical characterization of axonal sprouting and reactive tissue changes after long-term implantation of a polyimide sieve electrode to the transected adult rat sciatic nerve. Biomaterials 2001;22:2333–43.
[21] Navarro X, Verdú E, Butí M. Autotomy prevention by amitriptyline after nerve section in different strains of mice. Restor Neurol Neurosci 1994;6:151–7.
[22] Navarro X, Verdú E, Butí M. Comparison of regenerative and reinnervating capabilities of different functional types of nerve fibers. Exp Neurol 1994;129:217–24.
[23] Valero-Cabré A, Tsironis K, Skouras E, Perego G, Navarro X, Neiss WF. Superior muscle reinnervation after autologous nerve graft and poly L-lactide-ε-caprolactone (PLC) tube implantation in comparison to silicone tube repair. J Neurosci Res 2001;63:214–23.
[24] Valero-Cabré A, Tsironis K, Skouras E, Navarro X, Neiss WF. Peripheral and spinal motor reorganization after nerve injury and repair. J Neurotrauma 2004;21:95–108.
[25] Hargreaves K, Dubner R, Brown F, Joris J. A new and sensitive method for measuring thermal nociception in cutaneous hyperalgesia. Pain 1988;32:77–88.
[26] Branner A, Stein RB, Normann RA. Selective stimulation of cat sciatic nerve using an array of varying-length microelectrodes. J Neurophysiol 2001;85:1585–94.
[27] Branner A, Normann RA. A multielectrode array for intrafascicular recording and stimulation in sciatic nerve of cats. Brain Res Bull 2000;51:293–306.
[28] Warwick K, Gasson M, Hutt B, Goodhew I, Kyberd P, Andrews B, Teddy P, Shad A. The application of implant technology for cybernetic systems. Arch Neurol 2003;60:1369–73.
[29] Horch K, Lisney SJW. On the number and nature of regenerating myelinated axons after lesions of cutaneous nerves in the cat. J Physiol 1981;313:275–86.
[30] Jenq CB, Coggeshall RE. Numbers of regenerating axons in parent and tributary peripheral nerves in the rat. Brain Res 1985;326:27–40.

[31] Hallin RG. Microneurography in relation to intraneural topography: somatotopic organization of median nerve fascicles in man. J Neurol Neurosurg Psychiatry 1990;53:736–44.
[32] Ekedahl R, Frank O, Hallin RG. Peripheral afferents with common function cluster in the median nerve and somatotopically innervate the human palm. Brain Res Bull 1997;42:367–76.
[33] Schmalbruch H. Fiber composition of the rat sciatic nerve. Anat Rec 1986;215:71–81.
[34] Avendaño C, Castro J, Negredo P, Lago N, Navarro X. Regrowth of sensory and motor axons through a regenerative electrode: stereological and retrograde tracer study in the rat. Soc Neurosci 2003; Abstract No. 152.12.
[35] Krarup C, Loeb GE, Pezeshkpour GH. Conduction studies in peripheral cat nerve using implanted electrodes: II. The effects of prolonged constriction on regeneration of crushed nerve fibers. Muscle Nerve 1988;11:933–44.
[36] Suzuki G, Ochi M, Shu N, Uchio Y, Matsuura Y. Sensory neurons regenerate more dominantly than motoneurons during the initial stage of the regenerating process after peripheral axotomy. Neuroreport 1998;9:3487–92.
[37] Natsume A, Wolfe D, Hu J, Huang S, Puskovic V, Glorioso JC, Fink DJ, Mata M. Enhanced functional recovery after proximal nerve root injury by vector-mediated gene transfer. Exp Neurol 2003;184:878–86.
[38] Boyd JG, Gordon T. Glial cell line-derived neurotrophic factor and brain-derived neurotrophic factor sustain axonal regeneration of chronically axotomized motoneurons in vivo. Exp Neurol 2003;183:610–9.
[39] González C, Rodríguez M. A flexible perforated microelectrode array probe for action potential recording in nerve and muscles tissues. J Neurosci Methods 1997;72:189–95.

Neuroscience 128 (2004) 605–615

DIFFERENTIAL GROWTH OF AXONS FROM SENSORY AND MOTOR NEURONS THROUGH A REGENERATIVE ELECTRODE: A STEREOLOGICAL, RETROGRADE TRACER, AND FUNCTIONAL STUDY IN THE RAT

P. NEGREDO,[a] J. CASTRO,[a] N. LAGO,[b] X. NAVARRO[b] AND C. AVENDAÑO[a]*

[a]*Department of Morphology, Autonoma University, Medical School, c/ Arzobispo Morcillo s/n, 28029 Madrid, Spain*

[b]*Department of Cell Biology, Physiology and Immunology, and Institute of Neuroscience, Autonomous University of Barcelona, 08193 Bellaterra, Spain*

Abstract—Polyimide regenerative electrodes (RE) constitute a promising neural interface to selectively stimulate regenerating fibers in injured nerves. The characteristics of the regeneration through an implanted RE, however, are only beginning to be established. It was recently shown that the number of myelinated fibers distal to the implant reached control values 7 months postimplant; however, the functional recovery remained substantially below normal [J Biomed Mater Res 60 (2002) 517]. In this study we sought to determine the magnitude, and possible selectivity, of axonal regeneration through the RE by counting sensory and motor neurons that were retrogradely labeled from double tracer deposits in the sciatic nerve. Adult rats had their right sciatic nerves transected, and the stumps were placed in silicone tubes; some simply were filled with saline (*Tube* group), and others held a RE in its center (*RE* group). Simultaneously, the proximal stump was exposed to Diamidino Yellow. Two months later the nerves were bilaterally excised distal to the implant, and exposed to Fast Blue. Electrophysiological recordings, and skin nociceptive responses confirmed previous findings of partial functional recovery. In controls, an average of 20,000 and 3080 neurons were labeled in L4–L5 dorsal root ganglia (with minor contributions from L3 and/or L6), and in the ventral horn of the lumbar spinal cord, respectively. In the regenerating side, 35% of the DRG neurons were double-labeled, without differences between groups. In contrast, only 7.5% of motoneurons were double-labeled in the *RE* group, vs. 21% in the *Tube* group. Moreover, smaller ganglion cells regenerated better than large neurons by a significant 13.8%. These results indicate that the RE is not an obstacle for the re-growth of sensory fibers, but partially hinders fiber regeneration from motoneurons. They also suggest that fine fibers may be at an advantage over large ones to regenerate through the RE.

Key words: fluorochromes, stereology, nerve regeneration, sieve electrode, sciatic.

*Corresponding author. Tel: +34-91-497-5335; fax: +34-91-497-5338.
E-mail address: carlos.avendano@uam.es (C. Avendaño).

Abbreviations: CE, coefficient of error; CMAP, compound muscle action potential; CNAP, compound nerve action potential; DRG, dorsal root ganglia; DY, Diamidino Yellow; FB, Fast Blue; RE, regenerative electrode.

Neuroprostheses, defined as artificial systems capable of restoring or improving neural functions that have been lost due to injuries, are nowadays a therapeutic option for spinal cord- and nerve-injured patients. A variety of neuroprostheses has been developed in order to gain control on the traffic of sensory and motor signals through peripheral nerves. They are aimed at interfacing the peripheral nervous system by means of different stimulation and/or recording devices. For this purpose, a panoply of electrode designs, such as cuff, intrafascicular, shaft and regenerative electrodes has been introduced and tested (for a review, see Rutten, 2002).

Regenerative electrodes (RE) are designed to access a high number of nerve fibers by using an array of via holes, with electrodes built around some of them, implanted between the severed stumps of a peripheral nerve (Bradley et al., 1997; Kovacs et al., 1994; Llinas et al., 1973; Mensinger et al., 2000; Navarro et al., 1998). It has been recently demonstrated that the axon stumps in a severed sciatic nerve of the rat are able to regenerate through the via holes of a polyimide RE (Ceballos et al., 2002; Klinge et al., 2001; Navarro et al., 1996). The number of myelinated fibers in the nerve trunk distal to the implant increased with time, slightly exceeding control values by 7 months postimplantation. Regenerated fibers reinnervated hindlimb muscle and nerve targets, but the functional features were far from normal, and were reduced in comparison with nerves that regenerated through a nerve guide without an interposed RE (Navarro et al., 1998). The apparent normalization in the numerical recovery of myelinated axons, however, is only a limited measure of the regenerating scenario. First, it may be due to branching of regenerating axons (Cajal, 1914; Jenq and Coggeshall, 1985), each of which may give rise to over 10 axonal sprouts in the first few weeks (Brushart and Witzel, 2003). Secondly, no quantitative data are available on unmyelinated fibers, which are a substantial component of peripheral nerves. Moreover, it cannot be excluded that some of these may represent early stages of regeneration of axons which will eventually become myelinated (Williams et al., 1983). Finally, it is possible that different axonal classes display different regenerating capabilities (Maki, 2002; Suzuki et al., 1998), thus resulting in an imbalance in the net contribution of each nerve fiber type to the reinnervation of peripheral tissues.

This study was therefore aimed at quantitatively assessing the recruitment of previously axotomized sensory

0306-4522/04$30.00+0.00
doi:10.1016/j.neuroscience.2004.07.017

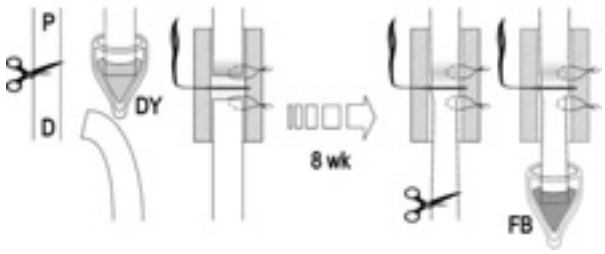

Fig. 1. Summary of the experimental design. The right sciatic nerve is transected at mid-thigh, and its proximal stump (P) is placed for 30 min in a well containing a solution of DY. Then both stumps are introduced into a silicone tube carrying the regenerative sieve electrode in its center, and secured by single stitches. Two months later the nerve is transected again several millimeters distal to its emergence from the tube, and a solution of a second tracer (FB) is applied to the cut end. On the left side, only steps 1 and 2 are performed, and FB is used instead of DY. To test the specific effects induced on the regenerative process by the presence of the sieve electrode, the same procedure is followed in another group of animals, except that an empty silicone tube is used in steps 3–5.

and motor neurons into the regenerative process that takes place through a polyimide RE. This was achieved by combining the use of retrograde tracers and functional tests with stereological approaches. The active uptake of a second tracer by pre-labeled neurons, and the detection of electrophysiological responses in target structures are sure markers of functional axonal regrowth. Stereological methods enabled not only to obtain reliable quantitative estimates with a known precision, but also to evaluate differential regenerative properties among neuronal populations. A part of this work was recently presented in abstract form (Avendaño et al., 2003).

EXPERIMENTAL PROCEDURES

Subjects

Two groups of young adult female Sprague–Dawley rats were used. The first group (Group *RE*; $n=7$) sustained a transection of the right sciatic nerve, followed by a RE implant, and the application of the retrograde fluorescent tracer Diamidino Yellow (DY). Two months later both sciatic nerves were transected at a level distal to the implant, and the tracer Fast Blue was applied on both sides. The second group (Group *Tube*; $n=6$) was similarly treated, but omitting the RE implant; instead, the stumps of the sectioned right sciatic nerve were placed into an empty silicone tube (Fig. 1). Animal procedures were carried out in accordance with the European Community's Council Directive 86/609/EEC, and were approved by the Ethical Committee of our institution. All efforts were made to minimize animal suffering and to keep the number of animals used at the very minimum deemed necessary to produce reliable data.

Electrode implantation and tracer injections

The sieve electrodes used were the same design as in our previous studies (Ceballos et al., 2002; Navarro et al., 1998). They were made using a polyimide resin (PI2611; DuPont, Bad Homburg, Germany) as substrate and insulation material with a single metallization layer (Stieglitz et al., 1997) The electrodes have 10 μm thickness and consist of a round sieve interface (2 mm diameter), a ribbon cable (1 mm wide, 21 mm long) and an ending connector (2×3 mm). The sieve part of the interface has 281

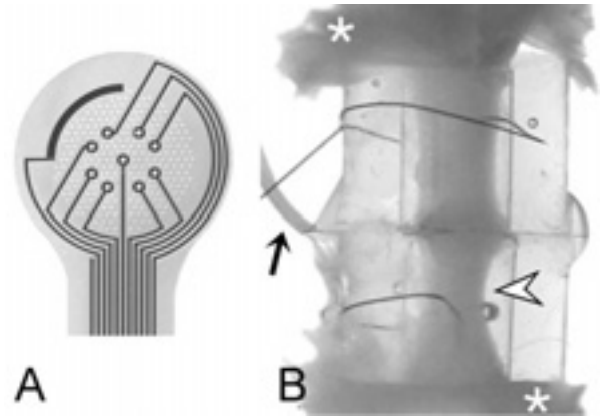

Fig. 2. (A) Enlarged view of the sieve portion of the RE, with nine ring electrodes around via holes and a larger counter electrode. (B) Transillumination view of a silicone tube containing in its center a RE, removed from a rat that received the implant 2 months earlier. The connecting leads are seen emerging to the left (arrow). The proximal stump of the sciatic nerve regenerated successfully through the perforations of the RE, reconnecting with the distal stump (arrowhead). Stitches used to secure the nerve ends inside the tube are clearly seen. Gray masses capping the tube ends (asterisks) correspond to abundant connective and adipose tissue that surrounds the incoming and outgoing nerves.

round via holes of 40 μm diameter, with nine integrated platinum electrodes arranged around some of the holes (Fig. 2A). The sieve portion was placed and glued between silicone tubes (2 mm i.d., 4 mm length), to serve as guidance for implantation to the nerve and subsequent regeneration in rats of group *RE*.

Under pentobarbital anesthesia (40 mg/kg i.p.) and local application of the anesthetic bupivacaine (0.5%), the right sciatic nerve trunk was exposed at the midthigh, freed from surrounding connective tissue, and transected with fine surgical scissors. The proximal stump was exposed for 30 min to a 5% aqueous solution of DY (Sigma, St. Louis, MO, USA). The area was rinsed with saline to eliminate any excess of dye. Both stumps were then introduced along the corresponding ends of the silicone tube containing a RE and were secured to the tube by single knots of 9–0 monofilament suture, leaving a 3–4 mm gap between stumps. The tube was filled with physiological saline, and the wound was sutured by layers.

After a 2-month survival period, the rats were anesthetized again, and the right sciatic nerve was exposed at a level 10 mm distal to the implant. A similar procedure was carried out on the left side. The nerves were transected and their proximal stumps were exposed for 30 min to a 5% solution of Fast Blue (FB; EMS-Polyloy, GmbH, Germany). After cleaning the area, the skin was sutured and the animals were allowed to recover. The rats of Group *Tube* received a similar treatment, except for the RE implant. After the first nerve transection and DY application, the right sciatic nerve stumps were fixed by a stitch to a simple silicone tube leaving a 3–4 mm gap between the stumps.

Functional evaluation

At 60 days postimplantation the rats were evaluated by non-invasive tests to assess the success of regeneration and distal target reinnervation. For nerve conduction studies, the sciatic nerve was percutaneously stimulated with single electrical pulses of 50 μs duration through a pair of needle electrodes placed at the sciatic notch. Compound muscle action potentials (CMAPs) were recorded from the medial gastrocnemius muscle and from the plantar muscles with small needle electrodes (Navarro et al., 1996; Valero-Cabré et al., 2001). Similarly, compound nerve ac-

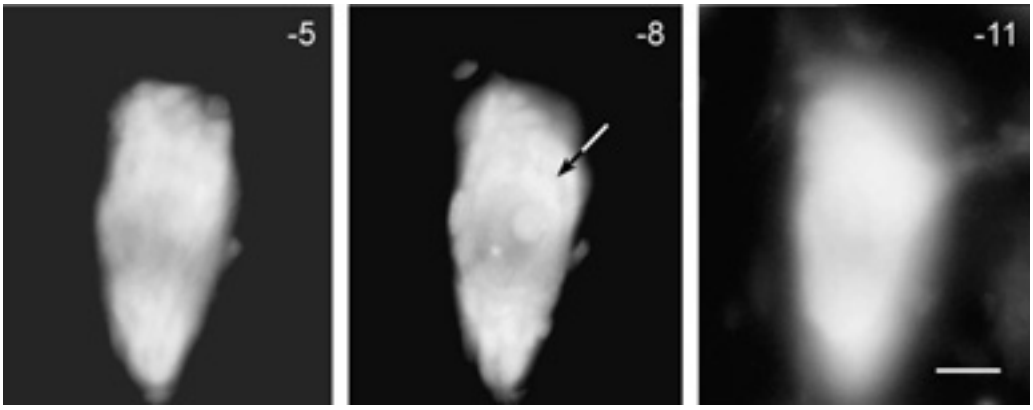

Fig. 3. An example of using the FB-unlabeled cell nucleus as the stereological counting unit. The sequence shows pictures of a FB-positive motoneuron at three 3-μm intervals depths. The images were taken with a PlanApo 100× oil-immersion lens with 1.35 n.a. under ultraviolet illumination. The best focus of the nuclear membrane is obtained when the nucleus is at its maximum girth, or nuclear 'equator' (arrow; in this case, 8 μm below the section surface). The relative darkness of the unlabeled nucleus is here partially dampened by the presence of a prominent, FB-labeled, nucleolus. For most FB-positive neurons, the nuclear profile can be sharply identified within a 1 μm focus change. Scale, 10 μm.

tion potentials (CNAPs) were recorded by electrodes placed near the tibial nerve at the ankle and near the digital nerves of the fourth toe. The evoked action potentials were displayed on a storage oscilloscope (Sapphyre 4M; Oxford Instruments) at settings appropriate to measure the amplitude from baseline to peak and the latency from stimulus to peak onset. During electrophysiological tests, the animals were placed over a warm flat coil controlled by a hot water circulating pump to maintain body temperature.

Recovery of pain sensitivity was tested by light pricking with a needle in five areas, from the most proximal paw pad to the tip of the fourth digit on the plantar surface. The animal response was scored as no response (0), reduced (1) or normal reaction (2) in each area tested, and the five scores were added into a pinprick nociceptive score.

The same tests were performed the same day on the contralateral intact hindlimb to obtain normal control values. For normalization, the results on the injured nerve were expressed as the percentage with respect to the results on the intact nerve for each rat.

Fixation and histology

Seven days after the application of FB, animals were deeply anesthetized with sodium pentobarbital (60 mg/kg i.p.), and were perfused through the ascending aorta with 4% paraformaldehyde and 0.2% glutaraldehyde in 0.1 M phosphate buffer, pH 7.4. After 24–48 h postfixation in 4% paraformaldehyde, the L2–S1 dorsal root ganglia (DRG) were removed, cryoprotected in 30% sucrosed phosphate buffer, embedded in albumin-gelatin and frozen-cut at 40 μm. The lumbosacral part of the spinal cords was similarly treated, but the embedding step was omitted. Before extraction, segmental levels were identified in the spinal cord by checking the location of the incoming dorsal roots, and placing fiduciary marks at identified spots. The cords were longitudinally cut, also at 40 μm. The sciatic nerves, silicone tubes and RE were removed, photographed (Fig. 2B), and kept for separate studies.

All sections were collected in two alternate series. They were mounted on gelatinized glass slides, briefly dehydrated in ethanol, defatted in xylene, coverslipped with DePeX, and stored in the dark at 4 °C. The sections were studied under fluorescence illumination in an Olympus BX51 microscope using the same U-MNU filter (excitation wavelength 360–370 nm) for analyzing FB and DY labeling.

DRG neurons have been classified into two basic morphological types, A and B, according to widely accepted criteria (Andres, 1961; Lagares and Avendaño, 1999; Lawson, 1992). Since morphological details in fluorescent neurons differ from those produced by Nissl-staining, a parallel analysis was carried out in two rats to assess the reliability of the cell type distribution carried out on fluorochrome-labeled neurons. Fluorescent neurons were counted and assigned to one type or the other in one of the DRG section series. The coverslips were then removed and the series was Nissl-stained. After this procedure, a substantial proportion of FB fluorescence remains, but DY fluorescence practically vanishes. A new stereological count and cell type assignment was performed on the Nissl-stained sections. We found a good correlation between the cell type assignment carried out on Nissl-stained and on FB single- or FB/DY double-labeled neurons. Cell typing was harder to make among DY single-labeled neurons, in which a crisp yellow nucleus stands out within a faint and featureless yellowish cytoplasm. Because of these limitations, we opted for classifying DRG neurons into type A (those unambiguously recognizable as such), and type B+ (those clearly corresponding to classic B-type cells, plus those of uncertain ascription).

Stereology

All stereological analyses were carried out in an Olympus BX51 microscope, with the help of an interactive computer system comprising a high-precision motorized microscope stage, a 0.5 mm resolution microcator (Heidenhain VZR401), a solid-state JVC TK-C1380 video camera and a high-resolution video monitor. The main objectives used were a planachromatic 4× dry lens and a planapochromatic 100× oil-immersion lens with high numerical aperture (1.35). The control of the stage movements and the interactive test grids (rectangular unbiased disector frames) were provided by the CAST-GRID stereological software package (Olympus Denmark) running on a Dell OptiPlex computer.

The total number of labeled neurons (FB-, DY-, or FB/DY-double labeled) in the DRG and the ventral horn of the spinal cord was estimated by means of the optical fractionator, that combines the optical disector with a fractionator sampling scheme (Gundersen et al., 1988; Lagares and Avendaño, 1999; West et al., 1991). The nucleus's equatorial plane was used as the counting unit (Fig. 3; Bermejo et al., 2003). The final or total volume fraction (f_T) where neurons are counted is the product of partial fractions at three sampling steps: 1, the numerical fraction of the sections used (f_s=1/2 or 1/4); 2, the areal fraction of the structure covered by the sampling grid (f_a, calculated by the ratio of the counting frame area—1186 μm^2—and the size of each systematic x,y step movement of the stage: 160×160 μm for the DRG, 100×100 for

the spinal cord); and 3, the linear fraction of section thickness covered by the height of the disectors (f_h).

The last fraction f_h requires fair estimates of the *final* section thickness. This is accomplished by taking depth measurements at several random places within the region studied. It is well known (Bermejo et al., 2003; Gardella et al., 2003) that frozen sections shrink markedly and unevenly, yielding substantial variances in the thickness measurements. In our material there was a 57% mean observed shrinkage in the *z*-axis (range: 49%–64%). The variability of real thickness introduces substantial noise in the number estimations. This may be countered by taking thickness measurements at each sampling spot, and weighting the contribution of each section to the final estimate (Dorph-Petersen et al., 2001). As a simpler variant of this procedure, we took an average of eight random readings per section, and estimated the mean thickness for the whole neuronal sample as

$$\bar{t}_{Q^-} = \frac{\sum_{s_1}^{s_n} \left(\bar{t}_i \Sigma q_i\right)}{\sum_{s_1}^{s_n} Q^-} \quad (1)$$

where $\bar{t}_{Q^-}$ is the mean value over the sections of the mean thickness per section, $\bar{t}_i$, weighted by the neuron count per section, q_i, and ΣQ^- is the total number of cells counted in all the disectors (Bermejo et al., 2003).

The chosen disector height was 10 or 12 μm, with an upper guard distance of two or 4 μm. The total number of neurons in each nucleus is then estimated as

$$N = \sum Q^- f_T^{-1} \quad (2)$$

The precision of the individual cell count estimates was determined by computing the coefficient of error ($CE[N]$). The total *estimated* CE is a function of two independent factors: 1, the variance of the cells counted for each section, which, over the sections and for sampling fractions $\ll 1$, leads to a "cumulative measurement error," equal to ΣQ^-; and 2, the variance due to the systematic sampling of sections $\left(Var_{SRS}\left[\bar{Q}^-\right]\right)$, which depends on how—not on how much—the individual counts vary from one section to the next, and is obtained from the equation

$$Var_{SRS}[\sum a] = \frac{1}{240}\{3[\sum (Q_i^- Q_i^-) - \sum Q^-] - 4 \sum (Q_i^- \times Q_{i+1}^-) + \sum (Q_i^- \times Q_{i+2}^-)\} \quad (3)$$

where the subindex *i* refers to section number. Then the estimated CE is computed as

$$CE[N] = \frac{\sqrt{\sum Q^- + Var_{SRS}[\bar{Q}^-]}}{\sum Q^-} \quad (4)$$

A more complete explanation of the theoretical grounds and relevant formulae concerning the evaluation of the precision and error of stereological estimates may be found in Howard and Reed (1998), Gundersen et al. (1999), and García-Fiñana and Cruz-Orive (2000).

On average, 215±55 labeled neurons were counted per side in the DRG (range: 140–310), in six to 13 sections. Corresponding values for spinal motoneurons were 126±30 (range: 69–169), in nine to 11 sections. The mean CEs for total neuron estimates per side ranged between 8% and 12%. Larger relative errors were obtained for small subpopulations of labeled neurons; in particular for double-labeled motoneurons in the *RE* group (mean CE=46%).

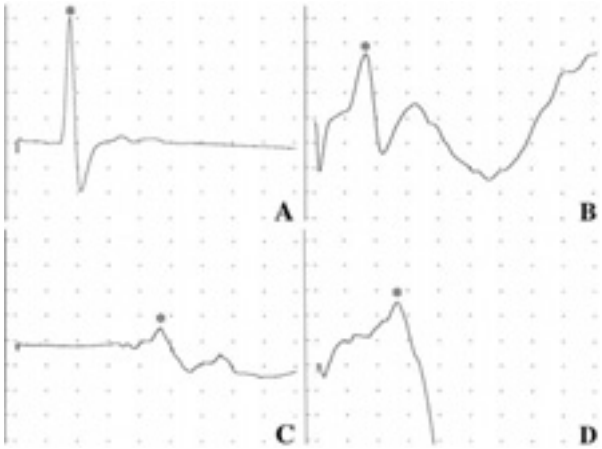

Fig. 4. Representative recordings of compound action potentials in plantar muscles (A, C) and in digital nerves (B, D) of the contralateral intact hindlimb (A, B), and of the operated hindlimb (C, D) of one rat of group RE. Asterisks indicate the corresponding CMAPs and CNAPs. Horizontal scale: 2 ms/square; vertical scale: 2 mV/square in A, 0.2 mV/square in C, 10 μV/square in B, and 5 μV/square in D.

Additional statistics

A two-tailed *t*-test was used to compare functional test results and the labeled neuron numbers between the *RE* and *Tube* groups. Comparison of functional test results between the implanted and the contralateral intact nerve was made with paired *t*-test. Differential labeling between different cell types, and between sides, was evaluated by means of the two-tailed Wilcoxon test.

RESULTS

Functional results

Electrophysiological tests performed after operation evidenced successful reinnervation of distal muscles and nerves by the regenerating axons in all rats, except in one of group *RE,* which did not show reinnervation of plantar muscle and digital nerve and was excluded from further analyses. Nevertheless, the degree of reinnervation was significantly lower than control values (Figs. 4 and 5). Table 1 shows the values for the electrophysiological tests from both intact and injured sciatic nerves at 2 months postoperation. The latency of compound action potentials, indicative of the conduction velocity of impulses by the regenerated fibers, was longer than normal and not significantly different between the two groups. Also, the amplitudes of CMAPs and CNAPs were in general lower in group *RE* than in group *Tube*, with significant differences for the plantar muscle, but they were similar for more proximal targets, such as the gastrocnemius muscle. When comparing the different parameters analyzed, normalized with respect to contralateral values, the mean amplitudes of gastrocnemius and plantar CMAPs in the *RE* group were about 91% and 22%, respectively, of those in group *Tube* whereas the corresponding *RE* over *Tube* ratios of CNAP amplitudes of tibial and digital nerves averaged 62% and 71%, respectively. In contrast, the nociceptive responses showed a substantially larger recovery (nearly

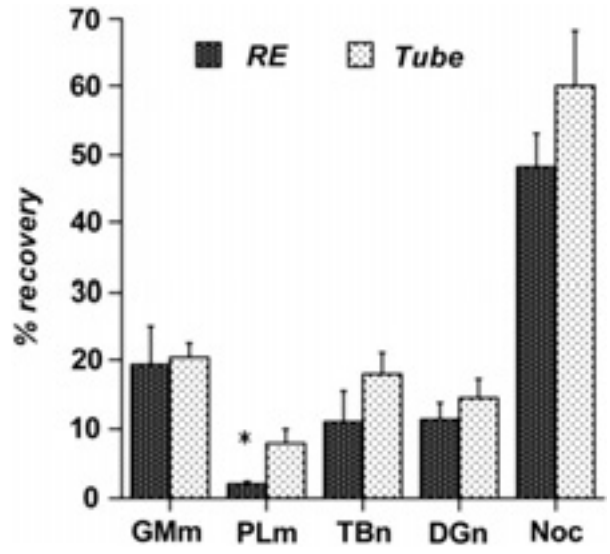

Fig. 5. Histogram of percentage recovery of CMAP amplitude of gastrocnemius and plantar muscles, of CNAP amplitude of tibial and digital nerves, and of nociceptive responses at 2 months postimplantation in groups *RE* and *Tube*. * $P<0.01$ with respect to group *Tube*.

50% of controls), with little differences between groups (mean responses in *RE* averaged 80% of those in *Tube*).

Neuronal labeling and control neuron numbers

DRG L4 and L5 were those most consistently and heavily labeled in all rats (Fig. 6A,B). Ganglia L3 or L6 also showed small groups of labeled neurons in some cases. In the spinal cord, labeled motoneurons formed a continuous, spindle-shaped group spanning segments L3–L6 (Fig. 6C, D). Dot diagrams are used in Fig. 7 to represent the total neuron counts. Values for each subpopulation of labeled neurons are presented in Table 2 and Fig. 8.

An average of 20,000 DRG neurons (range: 15,430–24,670) and 3080 (2480–3730) motoneurons were labeled by FB on the left (control) side, with no differences between groups. Neurons labeled by the first tracer applied in the right (regenerating) side totaled 20,620 (16,090–25,370) in the DRG, a figure that did not differ significantly from the control side. However, the total number of labeled motoneurons in the right side was 20% (*RE* group) or 8% (*Tube* group) lower than in the left. This decrease was statistically significant for all the animals pooled, and for the *RE* group ($P=0.028$ and $P=0.026$, respectively; Wilcoxon, two-tailed), but not for the *Tube* group.

Regenerating neurons

Neurons labeled by the second tracer (FB) in the right side have been able to re-grow their severed axons through the RE and/or the neural gap within the silicone tube, and take up the tracer that was deposited 10 mm distal to the former transection. On average, 35% of the DRG neurons were double-labeled, without intergroup differences. In contrast, the fraction of motoneurons that regenerated was significantly lower ($P=0.037$ for the *Tube* group and $P=0.005$ for the *RE* group, two-tailed *t*-test for correlated groups), and also displayed significant differences between groups: 7.5% motoneurons were double-labeled in the *RE* group, vs. 21% in the *Tube* group ($P=0.027$, two-tailed *t* test).

A separate analysis of the retrograde labeling of A and B+ neuron types explored the possibility that different sensory axons also express differential abilities to regenerate through the RE. By comparing the proportions of double-labeled cells within each DRG neuron class (Fig. 9), it was found that the fraction of B+ cells that were double-labeled exceeded that of A-type cells by a significant 13.8% ($P=0.041$, two-tailed Wilcoxon test).

DISCUSSION

The results found in this study confirm that peripheral nerve fibers are able to regenerate through the perforations of a polyimide RE in practically all cases, as previously reported (Ceballos et al., 2002; Navarro et al., 1998). Also, our findings showed that the number of neurons sustaining axonal regeneration through the polyimide sieve electrode is diminished, when compared with that

Table 1. Electrophysiological results of nerve conduction tests in the left intact and in the right injured sciatic nerves at 2 months postoperation for the two groups of rats evaluated[a]

	Group *RE* ($n=6$)		Group *Tube* ($n=6$)	
Intact sciatic nerve	Latency	Amplitude	Latency	Amplitude
Gastrocnemius CMAP	1.37±0.07	64.0±3.4	1.40±0.03	64.7±1.8
Plantar CMAP	3.08±0.08	9.6±0.6	3.00±0.07	9.6±0.5
Tibial CNAP	1.23±0.02	198.3±10.7	1.26±0.02	192.7±10.4
Digital CNAP	2.25±0.09	19.5±1.9	2.26±0.05	19.7±1.6
Injured sciatic nerve				
Gastrocnemius CMAP	3.09±0.37	11.9±2.9	2.90±0.22	13.0±1.4
Plantar CMAP	9.83±1.45	0.17±0.04*	6.51±0.50	0.76±0.16
Tibial CNAP	1.52±0.04	21.2±7.6	1.56±0.05	34.0±6.4
Digital CNAP	4.72±0.65	1.97±0.31	3.56±0.45	2.77±0.38

[a] Values are the mean±S.E.M. Latency is in ms, and amplitude in mV for CMAPs and in microvolts for CNAPs.
* $P<0.05$ vs Group *Tube*.

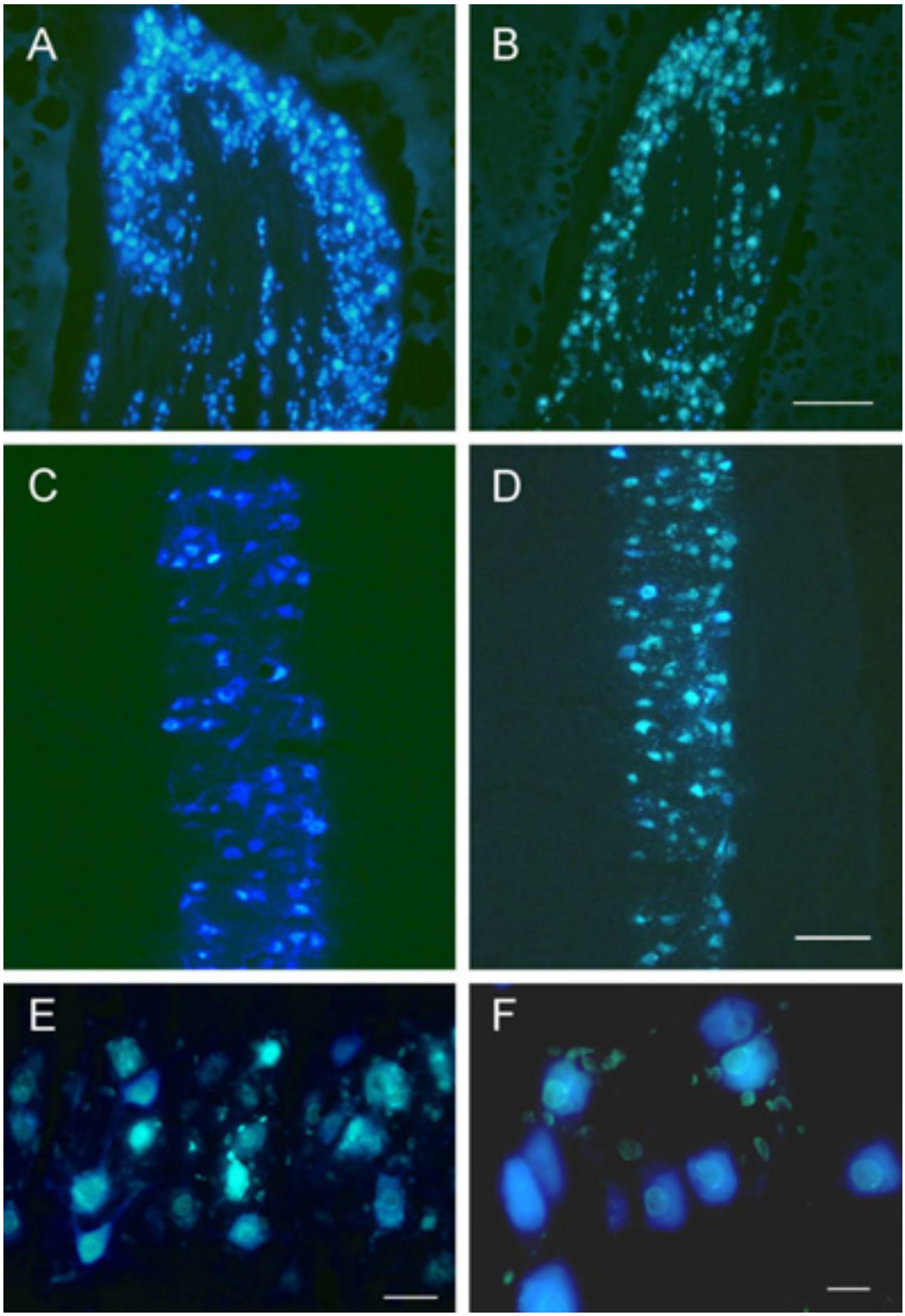

Fig. 6. Fluorescence microscopy, under ultraviolet illumination, of DRG L4 (A, B), and the spinal motoneuron pool at segmental level L5 (C, D). This rat received a RE implant and a two-staged DY-FB deposit in the right sciatic nerve (B, D). The left, or control sciatic of the same rat (A, C), was transected and single-labeled by FB. (E) Higher power view of the motoneuron column in another case, from a selected spot that contains a substantial number of double-labeled neurons. (F) Image from L4 DRG from the same case as in E, showing most neurons double-labeled by FB and DY. In E and F the small bright profiles correspond to nuclei of satellite perineuronal cells, which take up the tracer (particularly DY) that slowly diffuses from the labeled neurons. Scale bars=500 μm (A, B), 200 μm (C, D), 50 μm (E), 20 μm (F).

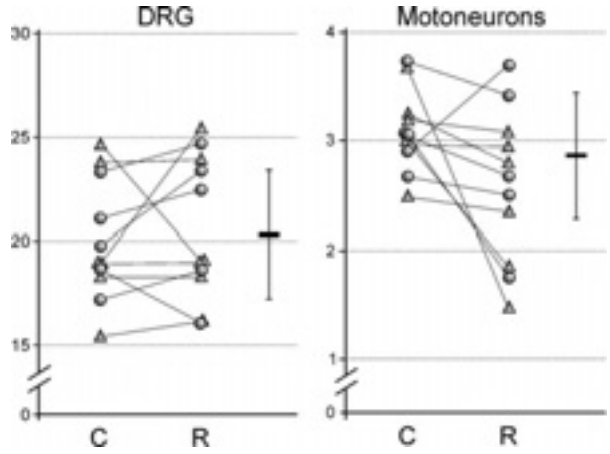

Fig. 7. Dot diagram showing the total number of labeled neurons (in thousands) for each individual. Triangles represent data for rats receiving a RE implant; circles represent cases in which sciatic regeneration occurred through a simple tube. Lines join values from the control (C) and regenerating (R) sides of the same subject. Overall means (averages from both sides from all cases) are indicated by short horizontal bars (error bars: S.D.).

found using a simple silicone tube without the RE. This observation supports the fact that the degree of functional reinnervation was significantly lower than in controls (see also Ceballos et al., 2002). Moreover, we demonstrate that not all types of fibers showed the same regenerative capabilities, the proportion of regenerating α motor fibers being comparatively reduced in comparison with that of sensory fibers.

Comments on methods

Functional evaluation. The functional tests performed are designed to assess reinnervation by different types of peripheral nerve fibers. The protocol allows serial evaluation in the same animal at desired intervals, although comparison of the degree of recovery may be hampered by differences in sensitivity between the tests (Navarro et al., 1994). The reappearance of compound muscle and nerve action potentials reflects functional reinnervation by large myelinated fibers (A$\alpha\beta$), either of motor or sensory origin, whereas the nociceptive response to

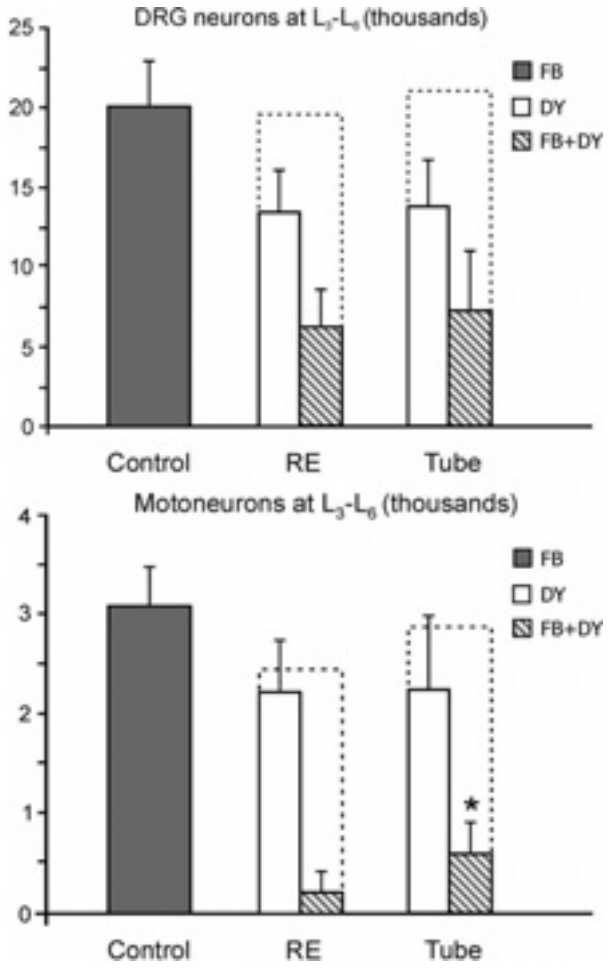

Fig. 8. Total number of neurons single labeled in the control side in all cases (Control), and in the regenerating side in the *RE* and *Tube* groups (empty bars). Numbers of double-labeled neurons, representing those neurons that successfully sent regenerating axons through the electrode and/or the tube, are indicated by shaded bars. A dashed outline represents the mean total numbers of neurons in the regenerating side. The fraction of regenerating neurons in the DRG is independent of the presence or absence of a RE interposed between the nerve stumps. However, there is a three-fold difference in the regenerative capabilities of motoneurons (21% in the *Tube* group vs. 7% in the *RE* group; $P=0.027$, two-tailed *t*-test).

Table 2. Total number of labeled neurons corresponding to each target population

	Structure	DRG								Motoneurons			
	Side	Left (control side)			Right (regenerating side)					Left	Right		
	Cell type				A		B+						
	Labeling	A	B+	All	Single	Double	Single	Double	All	All	Single	Double	All
Group RE	Mean	4666	15331	19997	2844	1221	10103	6015	20183	3085	2206	201	2408
	S.D.	1403	4062	3530	1511	999	3074	2383	3560	389	528	213	650
Group *Tube*	Mean	4732	15286	20018	3209	944	10608	6263	21025	3077	2233	578	2811
	S.D.	1862	1309	2320	1297	583	2579	3549	3565	399	743	308	775

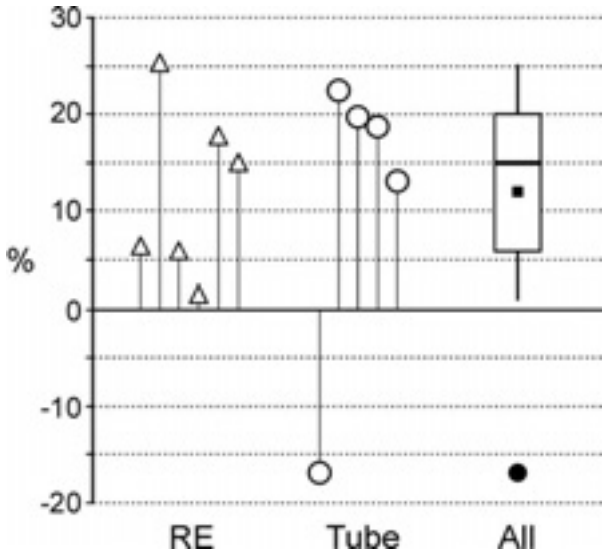

Fig. 9. Differential ability of large (A-type) and small (extended B-type; see Experimental Procedures) DRG neurons to regenerate through the RE and the silicone tube. The diagram shows that in all but one case (in the *Tube* group) the fraction of B+ cells that were double-labeled exceeded that of A cells. As summarized in the box-and-whisker diagram on the right, the mean excess was 13.8%, a value that could be higher if the only outlier (filled circle below the box) is ignored. This difference is statistically significant ($P=0.041$, two-tailed Wilcoxon test).

pinprick reflects reinnervation by small nociceptive fibers (Aδ and C). The nerve conduction velocity is an index of the degree of myelination and maturation of the regenerated fibers, and it usually remains lower than normal for a long time after severe nerve injuries. The degree of reinnervation, expressed by the amplitude of compound action potentials and the nociceptive score, is dependent on the number of fibers of each type that are able to regenerate and reconnect with appropriate tissue targets, as well as on their capabilities for collateral and terminal sprouting. However, a functionally complete recovery does not mean that all the original axons in the injured nerve successfully regenerated. Failure of certain numbers of axons to reach their end-organ permits regenerating axons to express their capacity for collateral branching, increasing the ratio of target end-organ to axon several times the normal ratio (Devor et al., 1979; Diamond and Foerster, 1992; Thompson and Jansen, 1977). Failure of achieving a near normal degree of reinnervation after nerve injury is, thus, an indication that the capacity for regeneration and for collateral reinnervation was limited.

Use of sequential multiple retrograde labeling as a means to evaluate nerve regeneration. The sequential application of various fluorescent tracers has been often used to assess peripheral nerve regeneration over the last two decades (Fritzsch and Sonntag, 1991; Hendry et al., 1986). The usefulness of this method, however, relies on a number of assumptions that have recently been addressed in detail (Puigdellívol-Sánchez et al., 2002, 2003): the tracers used and the administration procedure chosen have to label successfully all, or at least a vast majority of the axons; neither of them should produce significant axonal damage; and fading (particularly long-term) of the retrogradely transported tracer should be minimal. It was demonstrated that the combination of DY and FB is optimal to prevent, or keep at a minimum, these limitations. Another potential confounding factor in regeneration studies is the persistence of the first tracer in the application site, which could label re-directed axons arising from neurons which did not originally project through the target nerve (Puigdellívol-Sánchez et al., 2003). This problem is unlikely to occur in our study, given the absence of incoming or outgoing branches of the sciatic nerve between the injection sites. On the other hand, a decrease in neuron counts due to axotomy-dependent cell death is expected to occur, to a variable degree that is contingent upon a variety of factors (Aldskogius et al., 1992; Hart et al., 2002; Törnqvist and Aldskogius, 1994). In long term regeneration studies, cell loss can only be indirectly assessed by the use of reliable procedures to count neurons (see below) and carrying out statistical comparisons between intact and regenerating populations in the same subjects (to detect side differences) or between different groups.

Stereology. Despite the unbiasedness and high efficiency of the optical fractionator, the dimensional distortions of the tissue due to the fixation and histological processing, and the use of fluorescence microscopy, introduce some difficulties which must be addressed when designing the quantitative protocol and assessing the results (Bermejo et al., 2003; Dorph-Petersen et al., 2001; Guillery, 2002). The first difficulty originates in the tissue shrinkage occurring along the *z*-axis. Frozen-cut sections display a certain amount of inter-section variability in thickness, and normally have uneven upper and lower surfaces, which are responsible for intra-section variations in thickness. To account for this variation, individual section thickness readings at each sampling location were weighted with the corresponding individual neuron counts, using the average to compute the height sampling fraction (Bermejo et al., 2003; see Eq. 1, above).

Other difficulties arise from two limitations inherent to the study of fluorescent tracers: 1, the upper and lower surfaces of the section are often invisible under epi-illumination. This led to substantial interobserver variability in the first stages of the study, in contrast with the low variability found among trained observers working under bright-field (Bermejo et al., 2003). The problem was tackled by systematically crosschecking the readings obtained on the same tissue spots under epi-illumination with u.v. light, or weak illumination with transmitted visible light. With practice, this approach yielded highly consistent results. And 2, the information on cell body features provided by DY fluorescence is insufficient to reliably type the neurons, and is incompatible with Nissl counterstaining. These limitations forced us to adopt a conservative classification of DRG neurons.

Finally, it must be remarked that the sampling and counting scheme chosen contributed a reasonably low proportion of noise (estimated by the computed CE^2 of the

neuron number estimates) to the overall variance [calculated by the observed interanimal, $CV^2=(mean/S.D.)^2$, cf. Table 2] in most cases. The ratio CE^2/CV^2 ranged between 10% and 44% in 22 out of the 24 groups of measurements, and slightly exceeded 50% in the other two cases. These values are within the range generally recommended by other authors (Geinisman et al., 1997; West et al., 1991).

Nerve regeneration through polyimide RE

The clinical applicability of regenerative-type neural interfaces depends on a proven biocompatibility of the implanted device, on an extensive demonstration in experimental models of the success and effectiveness of axonal regeneration, and on the absence of possible nerve damage from the mechanical and constrictive forces imposed by the electrode perforations. Concerning compatibility, it has been shown that the polyimide RE displays a good degree of stability and biocompatibility over a 1-year postimplantation period in the rat (Ceballos et al., 2002; Klinge et al., 2001).

When implanted between the stumps of a severed nerve, RE may constitute a physical obstacle to nerve regeneration (Bradley et al., 1992; Navarro et al., 1996; Zhao et al., 1997). In this respect, the polyimide sieve device behaves much better than RE made on silicon substrate. Problems arising from silicon dice, which are mostly due to electrode failure from broken interconnects, failure of axonal regeneration in a significant proportion of animals, and compressive axonopathy induced by the rigid perforated structure (Kovacs et al., 1994; Navarro et al., 1996; Rosen et al., 1990; Zhao et al., 1997), are largely eluded by the use of polyimide electrodes (Ceballos et al., 2002). Yet, the number of axons present in the distal nerve stump was lower, and distal reinnervation was decreased when compared with simple tube repair of the transected nerve, as also shown in this report. Therefore, it may be concluded that placement of a microperforated die constitutes a physical barrier that is likely to disturb the initial phases of the regenerating process, and consequently make difficult the elongation of growing axons.

An additional advantage of the polyimide-based RE is the flexible and soft nature of the polyimide, which permits to obtain histological sections of the regenerated nerve at the level of the sieve. This facilitates performing detailed studies of the morphological appearance of regenerated fibers when crossing the via holes (Ceballos et al., 2002; Klinge et al., 2001; Navarro et al., 1998). Immediately adjacent to the interface, the regenerated nerves are organized in fascicles corresponding to the grid pattern of the via holes and covering in most cases the whole circle area of the sieve portion. These small fascicles contain myelinated and unmyelinated fibers, which appear intermingled at short term periods (5 weeks), but tend to segregate at longer terms, with unmyelinated fibers mostly localized to the periphery of each via hole (Klinge et al., 2001)

The number of myelinated fibers found a few mm distal to the sieve electrode was about 5900 at 2 months postimplantation (Ceballos et al., 2002), i.e. about 70% of the number present in the normal rat sciatic nerve (Jenq and Coggeshall, 1985). Nevertheless, this number is likely to overrepresent the number of neurons that really regenerated their axons across the gap, since, even a long time after injury, regenerating neurons support multiple sprouts that invade the distal stump of the nerve after branching from the lesion site (Horch and Lisney, 1981; Jenq and Coggeshall, 1985). Unmyelinated axons are nearly twice as many as myelinated in the normal sciatic nerve (Jenq and Coggeshall, 1985), but they outnumber by several times the myelinated axons in the RE-regenerated nerve (Negredo et al., 2003). The size of myelinated fibers regenerated distally to the sieve was much lower than normal, 89% of them being smaller than 5 μm. However, no conclusion may be derived from those measurements regarding the type of nerve fiber that they represent, since axons regenerated across a gap or a nerve graft never achieve their normal original size (Giannini et al., 1989; Le Beau et al., 1988), and may undergo late atrophy if they do not reinnervate target tissues.

Differential regeneration among neuron classes

Significant differences were observed in the regenerative capacity of axons arising from different neuron types. It has been proposed that regeneration of sensory axons dominates that of motor axons, as indicated by the incidence and intensity of retrograde fluorogold labeling in the first 2 weeks after sciatic nerve transection and immediate end-to-end suture (Suzuki et al., 1998). Our findings confirm these results at a longer post-transection time, and show in addition that this phenomenon also occurs when nerve stumps are kept a few millimeters apart inside a silicone tube. The presence of a RE in the tube represents an additional obstacle to motor axon regeneration, as shown by a significant three-fold reduction in the number of motoneurons labeled by the second tracer in the *RE* compared with the *Tube* groups. It is worth noting that the low degree of reinnervation achieved in the distal plantar muscle in comparison with that of the digital nerve, suggests that α motor fibers have more limited capabilities for regeneration through the sieve electrode than sensory fibers. Reinnervation of more proximal targets, such as gastrocnemius muscle, did not seem to be so much affected. Probably the regenerating motor axons preferentially reinnervated the most proximal muscles within a short time and, by intramuscular sprouting, increased the size of their motor units and, thus, of the CMAP. Significantly lower levels of reinnervation of distal plantar muscles in comparison with those of tibial and digital nerves have been found in a functional follow-up study of 12 months in rats with a sieve electrode implanted (Lago and Navarro, unpublished observations), further suggesting that the present findings at 2 months will strongly determine the situation at later time points in this model.

The percentage differences detected between motoneuron and DRG axonal regeneration could actually be substantially larger, because the proportion of double-labeled neurons is referred to the population displaying the first tracer (DY) after 2 months, and not to the original population. It was found that DY-labeled motoneurons, but not DRG neurons,

were significantly fewer in the implanted side than in the control side. This decline could be due to tracer fading or cell death. Fading is unlikely, because it should also have happened in the DRG. Motoneuron death, however, could well account for the reduction, particularly when many motor axons are unable to cross the RE and thus are permanently disconnected from appropriate targets (Puigdellívol-Sánchez et al., 2002; Törnqvist and Aldskogius, 1994).

Among the double-labeled, regenerating DRG neurons, we found relatively fewer A than B+ neurons in all but one case. This could be due to either an actual advantage of smaller cells in successfully reinnervating the distal stump, or to a shift from A to B+ morphology due to cell body shrinkage. While a contribution from the latter can never be excluded, in previous studies with different types of sciatic nerve injuries we have consistently found that small nerve fibers (nociceptive and sympathetic) are able to achieve slightly earlier and significantly higher levels of functional reinnervation of targets at the distal paw than large motor and sensory myelinated fibers (Navarro et al., 1994; Rodríguez et al., 1999; Verdú and Navarro, 1997). These differences may be explained by a lesser difficulty of crossing the lesion site, and by a faster rate of regeneration for thinner than for thicker fibers. Krarup et al. (1988) found, in serial *in vivo* electrophysiological observations after a crush, that small myelinated fibers regenerated in front of large fibers; smaller myelinated or unmyelinated fibers, which might have grown even faster, were not detectable by their method. Thereafter, however, the rate of regeneration along the distal segment of the nerve has been estimated to be similar for different types of myelinated and unmyelinated nerve fibers when reinnervation is measured at target tissues located approximately at the same distance (Gutmann and Young, 1944; Verdú and Navarro, 1997). The reduced representation of large neurons, mainly motoneurons, among those whose axons regenerate through the RE may be explained by a delayed growth of large fibers in comparison with small fibers during the initial phase of regeneration. Therefore, small sensory and sympathetic fibers growing in the regenerative front are at an advantage to occupy the open holes in the sieve portion of the electrode; large fibers regenerating with slight delay would have more difficulties to find paths across the sieve perforations. A redesign of the RE, by making more and somewhat larger via holes, may allow to compensate for this problem.

Acknowledgments—This work was supported by projects IST-2001-34892, IST-2001-35094 and IST-001917 of the E.C.

REFERENCES

Aldskogius H, Arvidsson J, Grant G (1992) Axotomy-induced changes in primary sensory neurons. In: Sensory neurons: diversity, development and plasticity (Scott SA, eds), pp 363–383. New York: Oxford University Press.

Andres KH (1961) Untersuchungen den Feinbau von Spinal Ganglien. Z Zellforsch mikr Anat 55:1–48.

Avendaño, C, Castro, J, Negredo, P, Lago, N, Navarro, X (2003) Regrowth of sensory and motor axons through a regenerative electrode: stereological and retrograde tracer study in the rat. Soc Neurosci Abst Abstract Viewer no. 152.12.

Bermejo PE, Jiménez CE, Torres CV, Avendaño C (2003) Quantitative stereological evaluation of the gracile and cuneate nuclei and their projection neurons in the rat. J Comp Neurol 463:419–433.

Bradley RM, Cao XG, Akin T, Najafi K (1997) Long term chronic recordings from peripheral sensory fibers using a sieve electrode array. J Neurosci Methods 73:177–186.

Bradley RM, Smoke RH, Akin T, Najafi K (1992) Functional regeneration of glossopharyngeal nerve through micromachined sieve electrode arrays. Brain Res 594:84–90.

Brushart, TM, Witzel, C (2003) The morphology of early peripheral axon regeneration. Soc Neurosci Abst Viewer/Itinerary Planner 152.10.

Cajal SR (1914) Estudios sobre la degeneración y regeneración de los centros nerviosos. Madrid: Moya.

Ceballos D, Valero-Cabré A, Valderrama E, Schuttler M, Stieglitz T, Navarro X (2002) Morphologic and functional evaluation of peripheral nerve fibers regenerated through polyimide sieve electrodes over long-term implantation. J Biomed Mater Res 60:517–528.

Devor M, Schonfeld D, Seltzer Z, Wall PD (1979) Two modes of cutaneous reinnervation following peripheral nerve injury. J Comp Neurol 185:211–220.

Diamond J, Foerster A (1992) Recovery of sensory function in skin deprived of its innervation by lesion of the peripheral nerve. Exp Neurol 115:100–103.

Dorph-Petersen KA, Nyengaard JR, Gundersen HJG (2001) Tissue shrinkage and unbiased stereological estimation of particle number and size. J Microsc 204:232–246.

Fritzsch B, Sonntag R (1991) Sequential double labelling with different fluorescent dyes coupled to dextran amines as a tool to estimate the accuracy of tracer application and of regeneration. J Neurosci Methods 39:9–17.

García-Fiñana M, Cruz-Orive LM (2000) New approximations for the variance in Cavalieri sampling. J Microsc 199:224–238.

Gardella D, Hatton WJ, Rind HB, Glenn GD, Von Bartheld CS (2003) Differential tissue shrinkage and compression in the z-axis: implications for optical disector counting in vibratome-, plastic- and cryosections. J Neurosci Methods 124:45–59.

Geinisman Y, Gundersen HJG, Van der Zee E, West MJ (1997) Towards obtaining unbiased estimates of the total number of synapses in a brain region: problems of primary and secondary importance: response. J Neurocytol 26:711–713.

Giannini C, Lais AC, Dyck PJ (1989) Number, size, and class of peripheral nerve fibers regenerating after crush, multiple crush, and graft. Brain Res 500:131–138.

Guillery RW (2002) On counting and counting errors. J Comp Neurol 447:1–7.

Gundersen HJG, Bagger P, Bendtsen TF, Evans SM, Korbo L, Marcussen N, Møller A, Nielsen K, Nyengaard JR, Pakkenberg B, Sørensen FB, Vesterby A, West MJ (1988) The new stereological tools: disector, fractionator, nucleator and point sampled intercepts and their use in pathological research and diagnosis. APMIS 96:857–881.

Gundersen HJG, Jensen EBV, Kiêu K, Nielsen J (1999) The efficiency of systematic sampling in stereology: reconsidered. J Microsc 193:199–211.

Gutmann E, Young PZ (1944) The re-innervation of muscle after various periods of atrophy. J Anat 78:15–43.

Hart AM, Brannstrom T, Wiberg M, Terenghi G (2002) Primary sensory neurons and satellite cells after peripheral axotomy in the adult rat: timecourse of cell death and elimination. Exp Brain Res 142:308–318.

Hendry IA, Hill CE, Watters DJ (1986) Long-term retention of Fast Blue in sympathetic neurones after axotomy and regeneration: demonstration of incorrect reconnections. Brain Res 376:292–298.

Horch KW, Lisney SJ (1981) On the number and nature of regenerating myelinated axons after lesions of cutaneous nerves in the cat. J Physiol (Lond) 313:275–286.

Howard CV, Reed MG (1998) Unbiased stereology: three-dimensional measurement in microscopy. Oxford: BIOS Scientific Publ.

Jenq C-B, Coggeshall RE (1985) Numbers of regenerating axons in parent and tributary peripheral nerves in the rat. Brain Res 326:27–40.

Klinge PM, Vafa MA, Brinker T, Brandis A, Walter GF, Stieglitz T, Samii M, Wewetzer K (2001) Immunohistochemical characterization of axonal sprouting and reactive tissue changes after long-term implantation of a polyimide sieve electrode to the transected adult rat sciatic nerve. Biomaterials 22:2333–2343.

Kovacs GTA, Storment CW, Halks-Miller M, Belczynski CR, Della Santina CC, Lewis ER, Maluf NI (1994) Silicon-substrate microelectrode array for parallel recording of neural activity in peripheral and cranial nerves. IEEE Trans Biomed Eng 41:567–577.

Krarup C, Loeb GE, Pezeshkpour GH (1988) Conduction studies in peripheral cat nerve using implanted electrodes: II. The effects of prolonged constriction on regeneration of crushed nerve fibers. Muscle Nerve 11:933–944.

Lagares A, Avendaño C (1999) An efficient method to estimate cell number and volume in multiple dorsal root ganglia. Acta Stereol 18:185–195.

Lawson SN (1992) Morphological and biochemical cell types of sensory neurons. In: Sensory neurons: diversity, development and plasticity (Scott SA, eds), pp 27–59. New York: Oxford University Press.

Le Beau JM, Ellisman MH, Powell HC (1988) Ultrastructural and morphometric analysis of long-term peripheral nerve regeneration through silicone tubes. J Neurocytol 17:161–172.

Llinas R, Nicholson C, Johnson K (1973) Implantable monolithic wafer recording electrodes for neurophysiology. In: Brain unit activity during behaviour (Phillips MI, eds), pp 105–110. Springfield, IL: Charles Thomas.

Maki Y (2002) Specificity in peripheral nerve regeneration: a discussion of the issues and the research. J Orthop Sci 7:594–600.

Mensinger AF, Anderson DJ, Buchko CJ, Johnson MA, Martin DC, Tresco PA, Silver RB, Highstein SM (2000) Chronic recording of regenerating VIIIth nerve axons with a sieve electrode. J Neurophysiol 83:611–615.

Navarro X, Calvet S, Butí M, Gómez N, Cabruja E, Garrido P, Villa R, Valderrama E (1996) Peripheral nerve regeneration through microelectrode arrays based on silicon technology. Restor Neurol Neurosci 9:151–160.

Navarro X, Calvet S, Rodríguez FJ, Stieglitz T, Blau C, Butí M, Valderrama E, Meyer JU (1998) Stimulation and recording from regenerated peripheral nerves through polyimide sieve electrodes. J Periph Nerv Sys 3:91–101.

Navarro X, Verdú E, Butí M (1994) Comparison of regenerative and reinnervating capabilities of different functional types of nerve fibers. Exp Neurol 129:217–224.

Negredo P, Castro J, Avendaño C (2003) Análisis cuantitativo de nervios periféricos mediante inmunohistoquímica múltiple postinclusión, microscopía óptica y electrónica, y estereología. Rev Neurol 37:1169

Puigdellívol-Sánchez A, Prats-Galino A, Ruano-Gil D, Molander C (2003) Persistence of tracer in the application site-a potential confounding factor in nerve regeneration studies. J Neurosci Methods 127:105–110.

Puigdellívol-Sánchez A, Valero-Cabré A, Prats-Galino A, Navarro X, Molander C (2002) On the use of fast blue, fluoro-gold and diamidino yellow for retrograde tracing after peripheral nerve injury: uptake, fading, dye interactions, and toxicity. J Neurosci Methods 115:115–127.

Rodríguez FJ, Gómez N, Perego G, Navarro X (1999) Highly permeable polylactide-caprolactone nerve guides enhance peripheral nerve regeneration through long gaps. Biomaterials 20:1489–1500.

Rosen JM, Grosser M, Hentz VR (1990) Preliminary experiments in nerve regeneration through laser-drilled holes in silicon chips. Restor Neurol Neurosci 2:89–102.

Rutten WLC (2002) Selective electrical interfaces with the nervous system. Annu Rev Biomed Eng 4:407–452.

Stieglitz T, Beutel H, Meyer J-U (1997) A flexible, light-weight multichannel sieve electrode with integrated cables for interfacing regenerating peripheral nerves. Sensor Actuators 60:240–243.

Suzuki G, Ochi M, Shu N, Uchio Y, Matsuura Y (1998) Sensory neurons regenerate more dominantly than motoneurons during the initial stage of the regenerating process after peripheral axotomy. Neuroreport 9:3487–3492.

Thompson W, Jansen JKS (1977) The extent of sprouting of remaining motor units in partly denervated immature and adult rat soleus muscle. Neuroscience 2:525–535.

Törnqvist E, Aldskogius H (1994) Motoneuron survival is not affected by the proximo-distal level of axotomy but by the possibility of regenerating axons to gain access to the distal nerve stump. J Neurosci Res 39:159–165.

Valero-Cabré A, Tsironis K, Skouras E, Perego G, Navarro X, Neiss WF (2001) Superior muscle reinnervation after autologous nerve graft or poly-L-lactide-epsilon-caprolactone (PLC) tube implantation in comparison to silicone tube repair. J Neurosci Res 63:214–223.

Verdú E, Navarro X (1997) Comparison of immunohistochemical and functional reinnervation of skin and muscle after peripheral nerve injury. Exp Neurol 146:187–198.

West MJ, Slomianka L, Gundersen HJG (1991) Unbiased stereological estimation of the total number of neurons in the subdivisions of the rat hippocampus using the optical fractionator. Anat Rec 231:482–497.

Williams LR, Longo FM, Powell HC, Lundborg G, Varon S (1983) Spatial-temporal progress of peripheral nerve regeneration within a silicone chamber: parameters for a bioassay. J Comp Neurol 218:460–470.

Zhao Q, Drott J, Laurell T, Wallman L, Lindström K, Bjursten LM, Lundborg G, Montelius L, Danielsen N (1997) Rat sciatic nerve regeneration through a micromachined silicon chip. Biomaterials 18:75–80.

(Accepted 7 July 2004)
(Available online 2 September 2004)

2

Registro de señales neurales mediante electrodos regenerativos

Lago N, Udina E, Navarro X.
Regenerative electrodes for interfacing injured peripheral nerves: neurobiological assessment.
IEEE BioRob 2006, 06EX1254D. ISBN: 1-4244-0040-6

Regenerative electrodes for interfacing injured peripheral nerves: neurobiological assessment *

Natalia Lago, Esther Udina, and Xavier Navarro
Group of Neuroplasticity and Regeneration, Institute of Neurosciences
Universitat Autònoma de Barcelona
08193 Bellaterra, Spain
xavier.navarro@uab.es

***Abstract* – Regenerative electrodes are designed to interface regenerated axons from a sectioned peripheral nerve that grow through an array of holes with metal electrodes. Applicability of regenerative electrodes is dependent on its biocompatibility, the success of axonal regeneration through the sieve electrode, the possible secondary nerve damage, and the adequacy of electronic component to interface regenerated axons. Polyimide-based regenerative electrodes have been fabricated that are highly flexible, do not cause substantial nerve damage, and provide a high number of holes. A first design of polyimide sieve electrodes were chronically implanted between the severed ends of the sciatic nerve in 30 rats. Regeneration was successful in all the animals implanted. The number of regenerated myelinated fibers increased from 2 to 6 months, when it was similar to control values. However, in a few cases decline of target reinnervation and loss of regenerated fibers was found from 6 to 12 months postimplantation. Large motor and sensory axons regenerate through the sieve with more difficulties than small axons. A second design of the electrode with 27 ring electrodes coated with Pt black was also implanted to assess the capabilities for nerve signal recordings. Recordings were obtained from a low proportion of electrodes on the sieve in response to functional stimulation of the paw. Difficulties inherent to recording impulses with regenerative electrodes are discussed, considering that regenerated axons have for long time smaller size than normal, and show notable changes in membrane excitability properties and in target reconnection.**

Index Terms - nerve regeneration, neural prosthesis, peripheral nerve, sieve electrode.

I. Introduction

A variety of neuroprostheses, developed to substitute or mimic sensorimotor functions in patients with neurological deficits, include interfacing the peripheral nervous system by means of electrodes that may allow nerve stimulation and neural signal recording. Regenerative or sieve electrodes are envisioned to interface a high number of nerve fibers by using an array of holes with electrodes built around them, implanted between the cut stumps of a peripheral nerve [1]. Regenerating axons from the proximal nerve stump eventually grow through the holes, making it possible to record action potentials from and to stimulate individual axons or small fascicles. The applicability of regenerative electrodes is, however, dependent upon the success of axonal regeneration through the perforations or holes, the possible secondary nerve damage induced by mechanical load imposed by the electrode or by constriction within the holes, the biocompatibility of the components, and the adequacy of electronic components to interface regenerated axons.

From the first theoretical concept presented more than 30 years ago [2], evolving techniques and materials have been used in the construction of regenerative electrodes. With the incorporation of microelectronic technologies, regenerative electrodes of small dimensions and high number of holes were made on silicon substrate [3-7]. Using multiple holes silicon arrays, axonal regeneration and neural activity recordings were reported in experimental animals, such as rat, frog and fish [5, 6, 8-10]. However, silicon electrodes constituted a physical barrier limiting the growth of regenerating axons and induced frequent signs of axonopathy depending on the size of the holes [6, 7, 11]. Ideally a one-to-one design would allow access to each individual regenerated axon (1-12 μm in diameter) grown through one hole. However, this has been proved impossible, because nerve regeneration fails with holes of such small size. An equilibrium has been considered between the number of holes in the dice and their diameter in the range of 40-65 μm. Polyimide-based electrodes were introduced later and tested in injured rat sciatic nerves [12, 13]. Polyimide can be micromachined in a variety of designs suitable for nerve interfaces, including cuff and intrafascicular electrodes. Polyimide electrodes are biocompatible, stable over months after in vivo implantation, do not cause substantial foreign body response, and allow for better regeneration than silicon electrodes [13-16].

A challenging application of regenerative electrodes consists on interfacing severed nerves of an amputee limb for a bidirectional interface in a feedback-controlled advanced neuroprosthesis. Recording of neural efferent signals can eventually be used for the control of motion of the mechanical prosthesis [17], whereas sensory feedback from tactile and force sensors embedded in the prosthesis may be provided to the user through stimulation of afferent nerve fibers within the residual limb nerves [18]. Such a "cybernetic prosthesis" should be felt by an amputee as the lost natural limb delivering sensory feedback by means of the stimulation of specific afferent nerves, re-creating the "life-like" perception of the natural hand. Moreover, it should be controlled in the most natural way possible by processing the efferent neural signals coming from the central nervous system, thus trying to replicate the movements of the natural hand.

II. Axonal Regeneration through Regenerative Electrodes

A. Regenerative Electrode Design

* This work is supported by grants IST-2001-35094 (CYBERHAND) and IST-001917 (NEUROBOTICS) from the EC.

Regenerative electrodes were micromachined using polyimide resin PI2611 (DuPont) as substrate and insulation material with a single metallization layer, as described in detail [12]. The regenerative electrode design consists of three parts: a round sieve interface (2 mm diameter), a narrow ribbon cable (1 mm wide, 21 mm long) and an ending connector (2 mm x 3 mm). The sieve part of the first design interface has 281 round via holes of 40 μm diameter, evenly distributed over the sieve area, with 9 integrated Pt electrodes arranged around via holes, occupying a total area of 1473 μm2. The Pt electrodes are connected through integrated leads in the ribbon to nine squared connects at the ending pad.

For implantation, the sieve portion was placed between two silicone tubes (2 mm i.d., 4 mm length), glued by plasma etching and the junction covered with silicone glue. The silicone tubes are used for securing the electrode to the nerve, and for guidance for nerve regeneration.

B. In vivo Implantation and Evaluation

Regenerative electrodes were implanted between the cut stumps of the sciatic nerve in 30 rats for assessment of biocompatibility and nerve regeneration over long term (2 to 12 months). The sciatic nerve was cut at midthigh and each nerve stump fixed into one end of the silicone tube with one suture stitch, leaving a short gap of 3 mm between stumps (Fig. 1A). The electrode ribbon was routed to the upper thigh region, and the wound was sutured and disinfected.

At monthly intervals after implantation we evaluated, by means of a battery of neurophysiological techniques, the degree of axonal regeneration and reinnervation of distal target organs. Reinnervation of muscles by motor nerve fibers and of sensory nerves by large sensory fibers was monitored by electrophysiological recordings of compound muscle and nerve action potentials (CMAPs and CNAPs), evoked by electrical stimulation of the sciatic nerve proximal to the tube. Nociceptive reinnervation was estimated from withdrawal responses induced by pinpricking discrete areas of the distal paw. At the end of follow-up the regenerated nerve was fixed and embedded in epoxy resin to obtain semithin sections. Morphometrical assessment of the number and size of myelinated axons was performed in the regenerated nerve under light microscopy.

Functional evidences of nerve regeneration and reinnervation of distal targets were found in all the rats that had a regenerative electrode implanted. The percentage recovery achieved maximal values by 6 months. The amplitude of CMAPs increased from 2 to 6 months postimplant up to 46% of control values in the gastrocnemius muscle and 18% in the plantar muscle, whereas the CNAPs amplitude increased to 44% in the tibial nerve and to 39% in the more distal digital nerve. The latency of CMAPs and CNAPs shortened with time but remained longer than control values. Pain sensibility recovered progressively from proximal to distal areas of the paw with time, but was still incomplete at 12 months. However, from 6 to 12 months postimplant there was a mild decrease in the degree of functional reinnervation, particularly in distal targets. The decline affected 3 rats that showed a moderate reduction in plantar CMAP and digital CNAP amplitude and 1 rat with marked loss at 12 months.

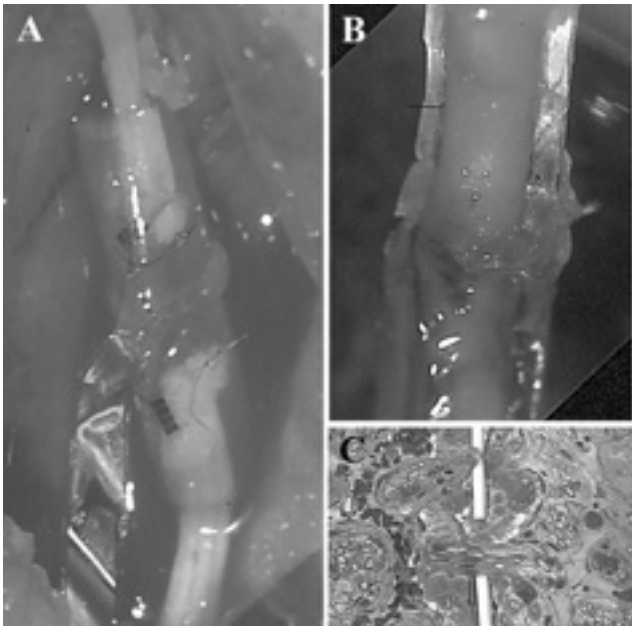

Fig. 1 (A) Implantation of a sieve electrode, encased in silicone tubes, in the transected sciatic nerve of a rat. (B) Macroscopical aspect of a regenerated nerve 6 months postimplant; the silicone tube was opened for visualization. (C) Microscopic image of regenerated axons crossing a via hole of the sieve electrode (X1000).

Morphological studies performed in subgroups of rats at 2, 6 and 12 months postimplant showed that the sciatic nerve had regenerated through the sieve electrode. The regenerated nerves had variable thickness, and showed a conic-shape enlargement at both sides of the sieve. Distally to the sieve, the regenerated nerves were organized in multiple small fascicles (Fig. 2A). The transverse nerve area was smaller than that of the intact sciatic nerve, whereas the number of regenerated myelinated fibers from 2 to 6 months, reaching mean values of 8848 (SE 1033) similar to control nerves (mean 8266, SE 258). From 6 to 12 months there was a decline in the endoneurial area and in the mean number of regenerated myelinated fibers. The rats with low regenerated myelinated fibers were those that showed a decrease in target reinnervation from 6 to 12 months in functional tests. In these cases, there were high numbers of regenerated nerve fibers near the sieve electrode, but some had very thin myelin sheath and others were swollen and with signs of degeneration.

Immunohistochemistry against cholin-acetyl transferase (ChAT) used to label regenerated motor nerve fibers, showed a marked increase in the number of ChAT positive axons proximal to the sieve due to terminal sprouting, but considerably lower numbers distal to the sieve. The number increased slightly from 2 to 6 months but decreased at 12 months. In regenerated nerves ChAT positive axons were scattered throughout the cross-sectional area within the small fascicles (Fig. 2B), but their density was higher in the periphery than in the center of the regenerated nerve [16].

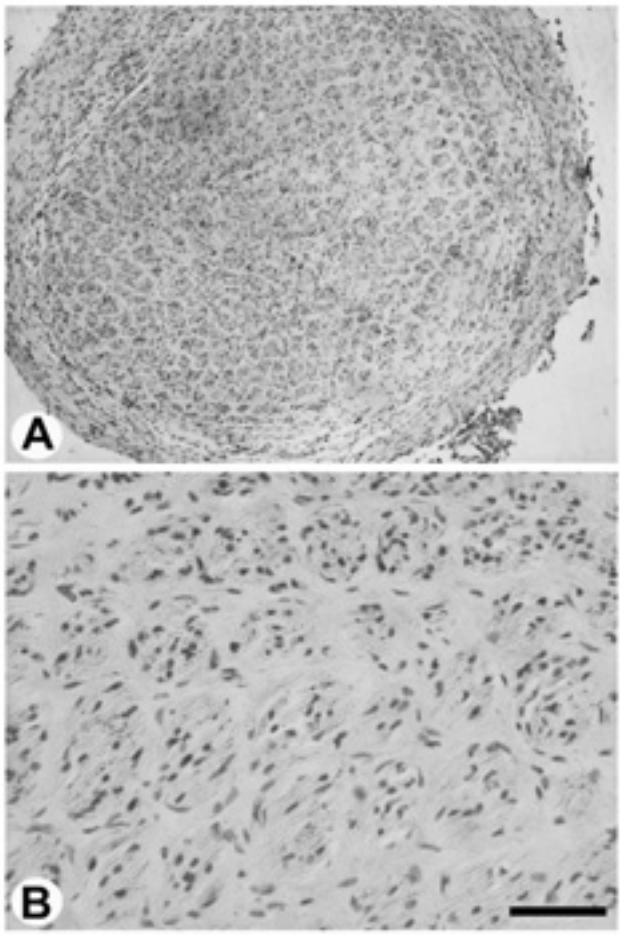

Fig. 2 Representative micrographs of a regenerated sciatic nerve transverse section immediately distal to the sieve electrode. A shows the number of minifascicles matching the sieve via holes. B shows the scattered regeneration of motor axons in the minifascicles. Immunohistochemical labeling against ChAT. Bar in B = 50 μm.

III. Nerve Signal Recording with Regenerative Electrodes

A. *Regenerative Electrode Design*

To increase the chances for neural signal recordings, a design of the sieve electrode with a higher number of via-holes and 27 electrodes around holes was created [19]. This new polyimide-based sieve electrode is 57.6 mm long and 0.15 g in weight. The actual sieve area is circular in shape with a diameter of 1.8 mm. The 571 holes of the sieve are also 40 μm in diameter and hexagonally arranged. Ring-shaped electrodes encircling 27 of the holes are evenly distributed over the sieve area (see Fig. 4 top). The ring electrodes are made of 300 nm thick platinum and electrical connection lines and interconnection pads are made of 300 nm thick gold, deposited by sputtering on to a spin coated polyimide. The platinum electrodes were then coated with platinum black to reduce the electrode impedance. In addition, two electrode contacts are arranged in the center of the sieve, to be used as the second pole for bipolar recordings, and two large-sized electrode contacts are positioned on flexible arms that are bent and glued to the silicone tubes, so they can be used as reference electrodes for neural recording. For protecting the connection lines and contact pads the polyimide ribbon was covered with a thin layer of silicone, whereas the ending pad was sealed within a silicone bag.

B. *In vivo Implantation and Evaluation*

These new regenerative electrodes, encased in silicone tubing, have been implanted in 12 rats. The fate of nerve regeneration through the sieve electrode was assessed by nerve conduction tests performed at 2 to 7 months postimplantation, and by morphological techniques in 4 rats at 7 months, as detailed above. Functional tests performed at 2 months indicated reinnervation of distal targets by the regenerating sciatic nerve in 7 of 12 rats with a polyimide sieve electrode implanted. At 7 months, of the 8 rats tested regeneration progressed in 4 rats but had failed in the other 4 rats. The number of regenerated myelinated fibers distal to the sieve ranged between 7700 and 19500 in the 4 nerves assessed so far. The failure of nerve regeneration through this second design of regenerative electrode in some cases, in comparison with the first design (see Section IIB), might be due to the changes in the fabrication process, including the presence of platinum black on the electrode sites, the larger size of the polyimide ribbon needed to accommodate the higher number of interconnect lines and the increased rigidity of the silicone chamber containing the two counter electrodes.

Nerve signal recordings have been performed in rats with successful distal regeneration, under ketamine-xylacine anesthesia. The ending electrode pad is accessed through an opening in the skin and connected by means of a clamp-like designed ceramic connector to an isolated high input impedance amplifier (3+ Cell Isolated Microamplifier, FHC Inc.), band-pass filtered (at 100 Hz and 10 kHz) and fed to a noise eliminator (Hum Bug, Quest Scientific). The signal was then digitized at 20 kHz and recorded on the hard drive of a PC running Chart software (PowerLab Systems, ADInstruments). Nerve impulses are recorded in response to functional sensory stimuli (mechanical touch and brushes on the hindlimb skin) and evoked by electrical stimuli delivered to the regenerated tibial nerve at the ankle by means of two monopolar small needles. Successful recordings were obtained in 50% of the rats tested; a low proportion of the electrodes on the sieve provided recordable signals. In such cases short bursts of action potentials distinguishable above background noise were evoked by mechanical stimuli applied to the distal limb skin (Fig. 3).

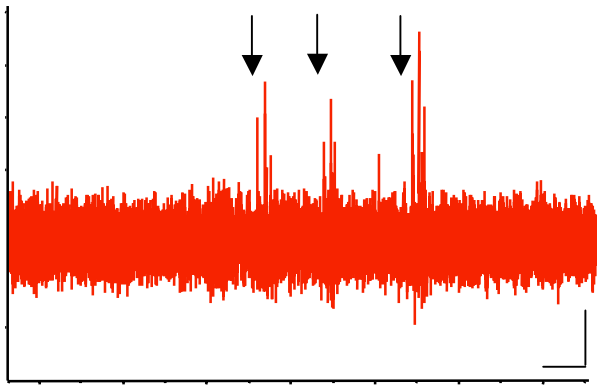

Fig. 3 Sample recording from one ring electrode in the sieve electrode from a regenerated sciatic nerve at 4 months. Brief bursts of impulses elicited by mechanical stimuli on a pawpad. Time bar = 1 s; voltage bar = 5 μV.

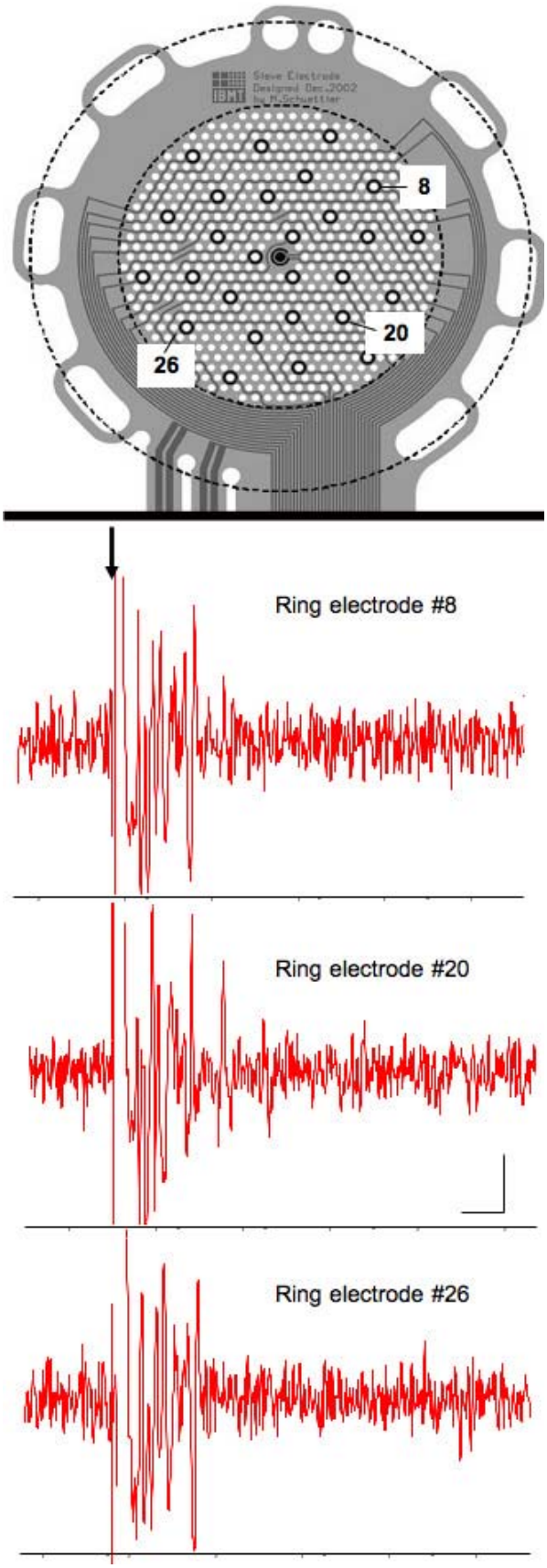

Fig. 4 Recording from three different ring electrodes (#8, 20 and 26) in the sieve electrode (see top panel) from a regenerated sciatic nerve after electrical stimulation (arrow) to the distal nerve at the ankle. Bursts of compound action potentials with slow conduction velocities are recorded. The different shapes and components indicate that different populations of axons are recorded from each ring electrode. Time bar = 1 s; voltage bar = 5 μV.

Moreover, in most cases nerve signals were only evoked by electrical stimulation (see Fig. 4), since functional activation on the paw skin did no elicit responses, probably because insufficient reinnervation. In the other animals in which no signals were recordable, during final surgical exploration we found breaks of the polyimide ribbon, mainly located at sites subjected to friction forces during the animal' movements.

IV. Discussion and Conclusions

Contemporary research in developing neuroprostheses has addressed the development and testing of interfaces to the peripheral nervous system that are biocompatible, do not damage the nerve, allow access to information conveyed by nerve fibers, and can stimulate selective groups of nerve fibers for actuation control. Regenerative electrodes can be applied only to transected nerves, thus requiring some time for effectively interfacing the regenerated axons, and precluding acute experiments. Regenerative electrodes fabricated with silicon presented problems derived from the rigid structure of the sieve and the lead connectors [5, 6], that are partially overcome by sieve electrodes based on polyimide that are thin and highly flexible [12, 13]. Furthermore, a larger number of holes can be practiced in the polyimide substrate, thus providing a larger open area for axons to grow through. The size of the holes (40 μm) was chosen based on previous works on silicon electrodes [5-7, 11]. With larger via holes, regeneration may be less difficult, but the purpose of selectively interfacing a small number of axons will be limited.

Regeneration of peripheral nerve fibers through the polyimide regenerative electrode took place in all the animals implanted. The electrode has also been shown to be useful for stimulation of different nerve bundles and for recording nerve action potentials in response to functional stimulation [13, 15], indicating that it is adequate for creating an interface with the regenerated fibers of transected peripheral nerves. Nevertheless, at long-term a proportion of animals showed a decline of functional recovery and loss of nerve fibers, likely due to compressive axonopathy at the sieve electrode level affecting some fibers that had initially regenerated and enlarged caliber and myelination as they matured [16]. Quantitative long-term characterization of the outcome of nerve regeneration and stability of the electrode is important for the application of electrodes since it may provide useful evidences contributing to modified implantation procedures and electrode designs. The second electrode design (described in Section IIIA) was made to increase the total open surface of the sieve area by incorporating a double number of via holes, thus providing more chances for regeneration of the axons through the sieve [6, 7]. Nevertheless, in view of our results (see Section IIB) it may be suggested that increasing also the diameter of the via holes will be helpful to increase axonal regeneration and to reduce potential chronic damage to regenerated axons. In spite of some loss in selectivity, recorded signals from larger hole electrodes may be higher in amplitude due to more fibers contributing, thus improving the signal-to-noise ratio.

For improving the chances of interfacing the injured nerve, the whole electrode device has to be resistant within the body during chronic implantation. Further improvements are still needed for the interconnect ribbon and for implant-

able connectors that should be more robust but still highly flexible. An important point, usually not considered, regarding the use of regenerative electrodes consists in the difficulties inherent to recording impulses from regenerated axons. Regenerative axons remain for long time with smaller caliber and thinner myelin sheath than normal, and have chronic changes in membrane excitability properties. In addition, nerves that regenerate after complete severance show a loss of the normal fascicular architecture [20], and inadequate reinnervation of targets, leading to defective recovery and transduction of peripheral stimuli. Large motor and sensory axons have a lower capability for growing through the regenerative electrode in comparison with small axons, as indicated by immunohistochemical and retrograde tracing studies [16, 21]. Large motor fibers regenerating with delay are confined to the periphery of the nerve and have more difficulties to find paths across the sieve perforations. Therefore, electrophysiological recordings from targeted large fibers are intrinsically more difficult.

In order to refine the regenerative electrodes as a suitable device for long-term implants in humans different neurobiological and technological strategies have to be investigated and solved, particularly for enhancing regeneration of motor axons, for the use of regenerative interfaces to detect efferent signals in the sectioned nerves of amputees, for guiding selective separate growth of different axonal populations, and also to protect or rescue regenerated axons from compressive forces within the via holes.

ACKNOWLEDGMENT

The authors thank Dr. Dolores Ceballos and Jessica Jaramillo for assistance in the morphological studies, and Dr. Jordi Serra for help in electrophysiological recordings.

REFERENCES

[1] X. Navarro, et al, "A critical review of interfaces with the peripheral nervous system for the control of neuroprostheses and hybrid bionic systems," *J. Periph. Nerv. System*, vol. 10, pp.229-258, 2005.

[2] R. Llinás, C. Nicholson, K. Johnson, "Implantable monolithic wafer recording electrodes for neurophysiology," in Brain Unit Activity during Behaviour, M.I. Phillips, Ed. Illinois: Charles Thomas, 1973, pp. 105-110.

[3] T. Akin, K. Najafi, R.H. Smoke, R.M. Bradley, "A micromachined silicon sieve electrode for nerve regeneration applications," *IEEE Trans. Biomed. Eng.*, vol. 41, pp. 305-313, 1994.

[4] G.T. Kovacs, C.W. Storment, J.M. Rosen, "Regeneration microelectrode array for peripheral nerve recording and stimulation," *IEEE Trans. Biomed. Eng.*, vol. 39, pp. 893-902, 1992.

[5] G.T. Kovacs, et al, "Silicon-substrate microelectrode array for parallel recording of neural activity in peripheral and cranial nerves," *IEEE Trans. Biomed. Eng.*, vol. 41, pp. 567-577, 1994.

[6] X. Navarro, et al, "Peripheral nerve regeneration through microelectrode arrays based on silicon technology," *Restor. Neurol. Neurosci.*, vol. 9, pp. 151-160, 1996.

[7] L. Wallman, Y. Zhang, T. Laurell, N. Danielsen, "The geometric design of micromachined silicon sieve electrodes influences functional nerve regeneration," *Biomaterials*, vol. 22, pp. 1187-1193, 2001.

[8] C.C. Della Santina, G.T. Kovacs, E.R. Lewis, "Multi-unit recording from regenerated bullfrod eighth nerve using implantable silicon-substrate microelectrodes," *J. Neurosci. Methods*, vol. 72, pp. 71-86, 1997.

[9] R.M. Bradley, X. Cao, T. Akin, K. Najafi, "Long term chronic recordings from peripheral sensory fibers using a sieve electrode array," *J. Neurosci. Methods*, vol. 73, pp. 177-186, 1997.

[10] A.F. Mensinger, et al, "Chronic recording of regenerating VIIIth nerve axons with a sieve electrode," *J. Neurophysiol.*, vol. 83, pp. 611-615, 2000.

[11] J.M. Rosen, M. Grosser, V.R. Hentz, "Preliminary experiments in nerve regeneration through laser-drilled holes in silicon chips," *Restor. Neurol. Neurosci.*, vol. 2, pp. 89-102, 1990.

[12] T. Stieglitz, H. Beutel, J.-U. Meyer, "A flexible, light-weight multichannel sieve electrode with integrated cables for interfacing regenerating peripheral nerves," *Sensor Actuators*, vol. 60, pp. 240-243, 1997.

[13] X. Navarro, et al, "Stimulation and recording from regenerated peripheral nerves through polyimide sieve electrodes," *J. Periph. Nerv. System*, vol. 2, pp. 91-101, 1998.

[14] P.M. Klinge, et al, "Immunohistochemical characterization of axonal sprouting and reactive tissue changes after long-term implantation of a polyimide sieve electrode to the transected adult rat sciatic nerve," *Biomaterials*, vol. 22, pp. 2333-2343, 2001.

[15] D. Ceballos et al, "Morphological and functional evaluation of peripheral nerve fibers regenerated through polyimide sieve electrodes over long term implantation," *J. Biomed. Mat. Res.*, vol. 60, pp. 517-528, 2002.

[16] N. Lago, D. Ceballos, F.J. Rodríguez, T. Stieglitz, X. Navarro, "Long term assessment of axonal regeneration through polyimide regenerative electrodes to interface the peripheral nerve," *Biomaterials*, vol. 26, pp. 2021-2031, 2005.

[17] D.J. Edell, "A peripheral nerve information transducer for amputees: Long-term multichannel recordings from rabbit peripheral nerves," *IEEE Trans. Biomed. Eng.*, vol. 33, pp. 203-214, 1986.

[18] R.R. Riso, "Strategies for providing upper extremity amputees with tactile and hand position feedback – moving closer to the bionic arm," *Technol. Health Care*, vol. 7, pp. 401-409, 1999.

[19] A. Ramachandran, O. Brueck, S. Kammer, K.P. Koch, T. Stieglitz, "System test of a smart, bidirectional interface for regenerating peripheral nerves," 9th Annual Conference International FES Society, 2004.

[20] N. Lago, X. Navarro, "Target reinnervation and distribution of motor axons in the regenerated rat sciatic nerve," *J. Periph. Nerv. System*, vol. 10, suppl. 1, p. 49, 2005.

[21] P. Negredo, J. Castro, N. Lago, X. Navarro, C. Avendaño, "Differential growth of axons from sensory and motor neurons through a regenerative electrode: a stereological, retrograde tracer, and functional study in the rat," *Neuroscience*, vol. 128, pp. 605-615, 2004.

3

Estudio de la regeneración nerviosa en un modelo de amputación

Lago N, Navarro X.
Evaluation of nerve regeneration in an experimental amputee model.
(Manuscrito, J Periph Nerv System. En revisión).

Lago N, Casas C, Rodríguez FJ, Muir EM, Rogers J, Navarro X.
Effects of Schwann cell transplantation in an experimental amputee model.
(Manuscrito).

EVALUATION OF THE LONG-TERM REGENERATIVE POTENTIAL IN AN EXPERIMENTAL NERVE AMPUTEE MODEL

Natalia Lago, and Xavier Navarro

Group of Neuroplasticity and Regeneration, Department of Cell Biology, Physiology and Immunology, and Institute of Neuroscience, Universitat Autònoma de Barcelona, Bellaterra, Spain

Corresponding author: Xavier Navarro, Group of Neuroplasticity and Regeneration, Faculty of Medicine, Universitat Autònoma de Barcelona, E-08193 Bellaterra, Spain.
Tel.: +34-935811966; E-mail: xavier.navarro@uab.es

ABSTRACT

In this study we evaluated the long-term capabilities for axonal regeneration in an experimental nerve amputee model in the rat sciatic nerve. The sciatic nerve was transected and repaired with a silicone tube leaving a short gap; the distal nerve segment was again transected 10 mm distally and the distal stump either introduced in a capped silicone chamber (amputee group) or connected to denervated targets (tibial branch into the gastrocnemius muscle and peroneal nerve apposed to skin) (reinnervation group). Morphological studies were performed at 2.5, 6 and 9 months after surgery. In all cases axons regenerated across the silicone tube and grew in the distal nerve segment. In the amputee group, the morphological results show the expected features of a neuroma that is formed when regenerating axons are prevented from reaching the end organs, with a large number of axonal profiles indicative of regenerative sprouting. The number of myelinated axons counted at the distal nerve was sustained over 9 months follow-up, indicating that regenerated axons are maintained chronically. Immunohistochemical labeling showed maintained expression of ChAT, CGRP and GAP-43 in the distal neuroma at 6 and 9 months. Reconnection of the distal nerve to foreign targets mildly improved the pattern of nerve regeneration, decreasing the number of excessive sprouts. These results indicate that axons regenerated through a sieve electrode may be eventually interfaced with external input-output systems over long time, even if ending in the absence of distal targets as will occur in amputee limbs.

Key words: nerve regeneration, neuroma formation, axon sprouting

INTRODUCTION

More than 50000 limb amputations occur every year in the USA and in Europe. Nowadays limb amputation derives in important social and clinical problems. Commercial prosthetic limb devices are unable to provide enough functionality and to deliver appropriate sensory-motor information to the user so as to functionally replace the lost limb. The situation might be considerably improved if the prosthesis could be driven by neural control, by using efferent signals conveyed by the sectioned peripheral nerves (disconnected now from the targets), and conversely provide neural sensory feedback, evoking sensations to the individual by stimulating afferent nerve fibers within the residual limb from signals detected by sensors embedded in the prosthesis. The application of neural interfaces to injured nerves seems a necessary and effective path for the selective stimulation of nerve fibers and for the selective recording of nerve signals. Regarding that, regenerative-type interfaces are designed to allow access to a high number of neural signals by using an array of via holes, with electrodes built around them, implanted between the severed stumps of a peripheral nerve (Navarro et al 2005). Severed axons eventually grow through the via holes, making the possibility to record action potentials from and to stimulate individual axons or small fascicles. This concept has been demonstrated feasible, and extensive demonstration of effective axonal regeneration through regenerative electrodes made on polyimide substrate (Stieglitz et al 1997) has been provided in previous reports (Navarro et al 1998, Ceballos et al 2002, Klinge et al 2001; Lago et al., 2005). One of the most logical and challenging applications of regenerative electrodes consists of their implantation in severed nerves of an amputee's limb for bidirectional interface in a feedback controlled neuroprosthesis.

If the ultimate goal is to make a device that may be chronically implanted into the severed nerve stumps in an amputated limb to control limb prosthesis, it is necessary to previously assess the behavior of the axons in the severed stump, and their capability for sustaining regeneration over long time. In order to address this objective, we have designed an amputee nerve model in rats to mimic a limb amputation situation. The results will give information about the limits for nerve regeneration and about the time period that regenerating axons can survive without the possibility of reconnecting with target organs.

In addition, the nerve amputee model may be suitable for developing and testing new neurobiological procedures for improving regeneration in chronically injured nerves. The growth–supportive environment of the distal nerve stump, mainly provided by the Schwann cells, is maintained only if axonal contact is reestablished within certain time. The growth-supportive environment progressively deteriorates when axonal regeneration is not effective,

as well as when nerve repair is delayed or neurons have to regenerate over long distances (Fu and Gordon, 1995). Some works on chronic denervation models have demonstrated that sectioned axons are able to regenerate during 6 months of denervation, when the proximal stump was re-sutured to the distal nerve stump, although many neurons failed to regenerated their axons into the distal nerve stump (Gordon et al 2003). The capabilities of Schwann cells for supporting axonal regeneration also decline over time (Hall 1999) On the other hand muscle targets can accept reinnervation even after long-term chronic denervation, and regenerated axons may be well myelinated by the chronically denervated Schwann cells (Sulaiman and Gordon, 2000).

In the present experiments, we combined chronic denervation with a proximal lesion with the aim of evaluate if it is possible to sustain the axonal regenerative potential after chronic denervation when there is no the growth supportive target. We have studied histologically the amputee model at three time points: 2.5, 6 and 9 months. In another group of rats the sciatic nerve was sutured directly to distal targets (as frequently done in clinical approaches for limb amputations). We evaluated the number of myelinated fibers, as well as the expression of neurotransmitter markers (ChAT and CGRP) and growth-related peptides (GAP43) in the lesioned nerves to assess the maintenance and phenotypic changes of regenerating nerves on the long term. In addition we have assessed changes in size and proportion of different classes of sensory neurons of the dorsal root ganglia (DRG).

MATERIAL AND METHODS

Surgical procedure

Female Sprague-Dawley rats, aged 2.5 months, were divided in two groups of 12 animals each. In all of them the sciatic nerve was sectioned and repaired with a standard silicone guide. In one group rats (amputee group) were submitted to the nerve amputation model and 4 animals evaluated at 2.5, 6 and 9 months. In the second group (reinnervation group) the distal tibial branch was implanted into the gastrocnemius muscle. An additional control group had the distal sciatic nerve intact to allow for distal target reinnervation, (see Fig. 1).

Operations were performed under pentobarbital anesthesia (40 mg/kg i.p.). With the aid of a dissecting microscope, the sciatic nerve was exposed at the lateral side of the thigh and carefully freed from surrounding tissues from the sciatic notch to below the knee. The sciatic trunk was transected and the nerve stumps fixed in a silicone guide (2 mm i.d, 8 mm long), with one stitch of 10-0 monofilament suture at each end, leaving a short gap of 4 mm

between the stumps (Fig. 2a). The lumen of the silicone guide was filled with saline solution. For the nerve amputee model, the distal nerve was transected again at a distance of 10 mm distally to the silicone guide and the nerve stump fixed inside a silicone blind-end chamber, with one stitch of 10-0 monofilament suture. This silicon chamber was made with a piece of tube 6 mm long that was capped at one end with silicone adhesive. The blind chamber was filled with saline solution.

For comparison of this nerve amputee model with a nerve lesion in which target reinnervation was possible, we included two other groups of rats. In a foreign target reinnervation model, the sciatic trunk was transected and repaired with a silicone guide, and the distal tibial branch was sectioned and directly reconnected with a distal target muscle, the denervated medial gastrocnemius muscle. A small incision was made at the middle of the muscle bulk, into which the tibial nerve stump was gently inserted and secured with one stitch of 10-0 suture. The peroneal nerve branch was sectioned and directed to the denervated skin at the lateral side of the thigh. In a control group with sciatic nerve section and tube repair, the distal nerve was not transected, so it was in continuity to normal distal targets.

After nerve surgery, the muscles overlying the repaired nerve were reapproximated with 5-0 sutures and the skin was closed with 2-0 sutures and disinfected with povidone iodine. In order to avoid autotomy after denervation, the sciatic nerve was blocked by local application of bupivacaine proximal to the lesion site, and the animals were treated by administering amitriptyline in the drinking water (Navarro et al 1994).

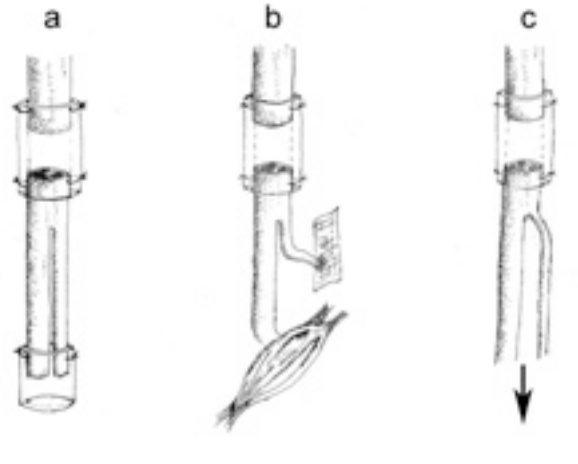

Figure 1. Schematic representation of the nerve lesion paradigms performed in this study. In the amputee group (a) the distal sciatic nerve stump was fixed into a silicone blinded chamber, in the forced reinnervation group (b) the distal tibial branch was implanted into the gastrocnemius muscle whereas the peroneal branch was apposed to the skin, and in a control group (c) the distal nerve was left intact in continuity to normal distal targets.

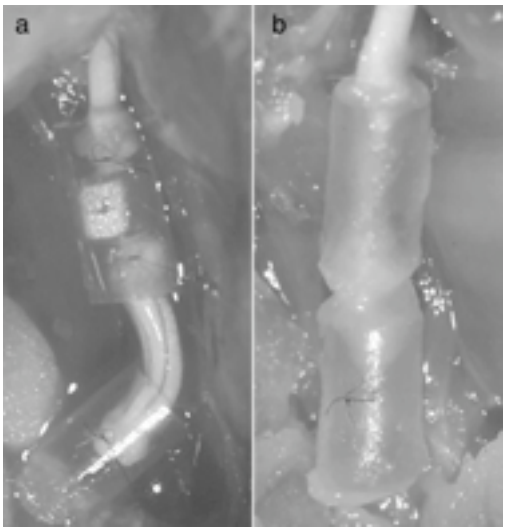

Figure 2. Photomicrographs of (a) the nerve amputee model with the distal nerve stump ending in a blinded silicone chamber at the time of implantation, and (b) a regenerated nerve (amputee model) after removal 2.5 months postimplantation.

Electrophysiological tests

Functional reinnervation of target muscles was tested postoperatively by nerve conduction tests. With the animals under anesthesia (pentobarbital 40 mg/kg i.p.), the sciatic nerve was stimulated through a pair of needle electrodes placed at the sciatic notch. Compound muscle action potentials (CMAP) were recorded from gastrocnemius medialis and plantar muscles with monopolar needle electrodes. The latency and amplitude of the M and H waves were measured. The contralateral limb was tested for control values.

Morphological evaluation

After postoperation intervals of 2.5, 6 and 9 months, the animals were deeply anesthetized and perfused transcardially with 4% paraformaldehyde in phosphate-buffer saline solution (PBS, 0.1M, pH 7.4). After perfusion, the nerve was harvested and sectioned in several pieces: the medial nerve segment (mid level, M) inside the silicone guide and the distal nerve segment (distal level, D1) 5 mm distal to the silicone guide were postfixed with 3% glutaraldehyde-3% paraformaldehyde in cacodylate-buffer solution (0.1 M, pH 7.4). These segments were oriented to obtain transverse sections. The samples were postfixed in osmium tetroxide (2%, 2 h, 4°C), dehydrated through ascending series of ethanol, contrasted with uranyl acetate (2.5%, overnight) and embedded in Agar 100 resin.

Nerves were sectioned using a LKB III 6802 ultramicrotome (Leica). Semithin sections (0.5 μm) were stained with toluidine blue and examined by light microscopy (Olympus BX-40). Images of the whole sciatic nerve were acquired at 4x with a digital

camera, while sets of images chosen by systematic random sampling of squares representing at least 30% of the nerve cross-sectional area were acquired at 100x. Measurements of the cross-sectional area of the whole nerve, as well as counts of the number of myelinated fibers were carried out by using NIH Image software.

Immunohistochemistry of lesioned nerves

Segments of the nerve inside the silicone guide and inside the ending chamber were collected and postfixed in the same perfusion solution for 4 h. Samples were washed in phosphate-buffer (PB; 0.1M, pH 7.4) and stored in the same buffer with azide 0.1% for embedding in paraffin. Transverse sections (4 μm thick) were cut with a microtome, mounted on (3-aminopropyl)triethoxysilane-coated slides and dried overnight. The sections were deparaffinized and rehydrated before staining. Antigen retrieval was performed with sodium citrate (pH 6.1) during 20 minutes at 95ºC. Then sections were washed with Trizma buffer solution (TBS, 0.05M, pH 7.4; Sigma) and TBS plus 0.05% Tween-20 (Fluka) (TBST) before blocking nonspecific binding with 2% BSA in TBST for 1 hour. After washing with TBST, sections were incubated for 24h at 4ºC with antibodies directed against choline acetyltransferase (ChAT; AB144P Chemicon; 1:50), calcitonin gene related peptide (CGRP; AB1971 Chemicon; 1:400) or growth-associated protein (GAP-43; AB5220 Chemicon; 1:500). After washes, sections were incubated with Cy2 or Cy3 conjugated immunoglobulin G (1:200, Jackson Immunoresearch) for 3 h at room temperature. Following additional washes with TBS, sections were dehydrated in ethanol and coverslipped with DPX (Fluka). For negative controls, some sections were processed as described with the omission of primary antibodies. Immunoreactivity against GAP43 was quantified from digitized transverse nerve sections using NIH Image software. The ratio between the area of immunolabeling above threshold and the area of the total sciatic transverse section was calculated.

Immunohistochemistry of DRG neurons

Dissected L4 DRG were post-fixed in 4% PFA for 3 h then stored in 30% sucrose in PBS solution. Cryostat sections (10 μm thick) were processed for immunohistochemistry as above. Different sections were stained using primary antibodies anti- protein gene product 9.5 (PGP9.5; RA95101 UltraClone Limited; 1:200), anti-parvalbumin (PV; MAB1572 Chemicon; 1:3500) and anti-CGRP (1:400), and with Griffonia simplicifolia Lectin I Isolectin B4 (IB4;

L-1104 Vector; 20 μg/ml) followed by anti-IB4 polyclonal antibody (AS2104 Vector; 1:500). After washes, sections were incubated with Cy2 or Cy3 conjugated immunoglobulin G.

For each DRG, 6 sections 100 μm apart were selected for immunostaining. Immunofluorescence was visualized under an Olympus BX-40 fluorescence microscope at x20 objective magnification. Cells counts were performed for neurons positively stained to PGP, PV, CGRP and IB4. The size distribution of positive cell profiles was determined using NIH Image software. The somas of neurons of interest were outlined manually, and their sizes determined. Only neurons with a clear nucleus were counted. To distinguish changes in subpopulations of DRG neuron profiles, cell size criteria set by Noguchi and colleagues (Fukuoka et al., 2001; Obata et al., 2003) were followed, dividing the DRG neuron profiles into small-sized (<600 μm^2), medium-sized (600-1200 μm^2) and large-sized (>1200 μm^2) according to their cross-sectional area. For comparisons, L4 DRG from intact control rats were processed in parallel.

Statistical analysis

Quantitative results are expressed as mean±SEM. Statistical comparisons between groups and intervals were made by one-way ANOVA followed by posthoc Scheffé test and by nonparametric Kruskal-Wallis and Mann-Whitney *U* tests, and differences were considered significant when $p< 0.05$.

RESULTS

Electrophysiological results

Electrical stimulation of the proximal sciatic nerve did not evoke any recordable CMAP of the gastrocnemius and plantar muscles over the 9 months follow-up, thus indicating that no axons that could escape the blinded chamber were able to reinnervate effectively distal muscles. In contrast, in the forced reinnervation group CMAPs were recorded in the gastrocnemius muscle (Fig. 3), but not in the plantar muscle, from 1 month. The latency of the M wave tended to decrease over time and the amplitude increased up to about a third of the normal values (Table 1). The H wave also increased in amplitude with time of reinnervation; the H/M amplitude ratio was larger (20 to 35%) in the reinnervation side than in the contralateral intact side (12%).

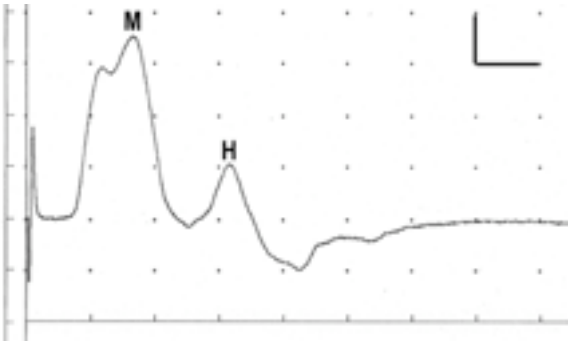

Figure 3. Representative recording of CMAPs (M and H waves) evoked in the gastrocnemius muscle by stimulation of the proximal sciatic nerve in one rat of the reinnervation group at 6 months. Horizontal scale: 2 ms/square; vertical scale: 5 mV/square.

Table 1. Neurophysiological results of reinnervation of gastrocnemious muscle by tibial nerve after forced reinnervation over time after surgery.

	Baseline	1 mo	2 mo	4 mo	6 mo	9 mo
(n)	*(12)*	*(12)*	*(12)*	*(8)*	*(8)*	*(4)*
Latency (ms)	1.49±0.02	4.03±0.27	3.70±0.21	2.81±0.15	2.46±0.2	2.02±0.32
M wave (mV)	61.6±1.2	2.2±0.5	6.7±0.7	14.1±1.2	20.1±1.3	16.2±1.3
H wave (mV)	7.5±1.1		1.4±0.3	4.8±0.83	5.0±1.2	5.2±0.9

Morphological evaluation of the regenerated nerves

The macroscopic examination during final dissection evidenced that in all animals the sciatic nerve had regenerated through the silicone guide and grown axons into the distal nerve stump. The silicone guide was covered by thin fibrous tissue, with light adherences to surrounding muscles. In the amputee group, the distal sciatic nerve segment was found inserted in the blind chamber (Fig. 2b), where a regenerative neuroma was observed under high magnification in all the rats. In the reinnervation group, the tibial branch remained attached to the gastrocnemius muscle into which regenerated axons had grown, whereas the peroneal branch did not show regenerative growth into the skin and in most cases ended in a neuroma.

Table 2. Cross-sectional area and number of myelinated fibers (MF) in the regenerated nerves at mid (inside the silicone guide) and distal (neuroma) levels found at 2.5, 6 and 9 months postinjury. Control values of rat intact sciatic nerves are also shown for comparison.

			Medial level		*Distal level*	
GROUP	Time	(n)	Nerve area (mm^2)	No MF	Nerve area (mm^2)	No MF
Intact nerve		(10)			0.66 ± 0.06	8237 ± 340
Silicone guide	2.5 mo	(6)			0.40 ± 0.03	13632 ± 1447
Amputee	2.5 mo	(4)	0.83 ± 0.15	21286 ± 2233	1.02 ± 0.22	27796 ± 2655 *
Reinnervation	2.5 mo	(4)	0.69 ± 0.01	13768 ± 824	0.45 ± 0.06	18814 ± 3762
Amputee	6 mo	(4)	0.93 ± 0.34	22467 ± 5760	0.79 ± 0.10	24569 ± 1280
Reinnervation	6 mo	(4)	0.85 ± 0.21	15838 ± 1857	0.62 ± 0.03	21018 ± 804
Amputee	9 mo	(4)	0.75 ± 0.09	18913 ± 3083	0.81 ± 0.04 *	26668 ± 2437 *
Reinnervation	9 mo	(4)	0.77 ± 0.14	17049 ± 3662	0.53 ± 0.02	20321 ± 942

* $p<0.05$ Amputee vs Reinnervation group at the same time interval

The No of MF was significantly increased in the Amputee group in comparison with intact nerves and Silicone guide group at all the intervals evaluated.

The main histological feature in the distal sciatic nerve of all the rats was the disorganization of the regenerated nerve structure, with microfasciculation that was more prominent at distal levels than at midtube. The nerve area was enlarged in the amputee model nerves, due to the large number of sprouts that formed a neuroma, in comparison with intact control nerves and nerves with distal reinnervation to normal or foreign targets. Regenerative axons were more densely packed at the periphery of the neuroma, whereas at central areas there was more extracellular matrix and blood vessels, and some zones of ongoing Wallerian degeneration even at the long term (Fig. 4a, c). At 9 months some areas showed a number of abnormal fibers (Fig. 4d) with increased diameter, dense axoplasm, and marked attenuation or disappearance of the myelin sheath.

The quantitative results of nerve cross sectional area and myelinated nerve counts obtained at 2.5, 6 and 9 months in the different experimental groups are shown in Table 2. At 2.5 months there were higher numbers of nerve profiles (regenerative sprouts) in the amputee

group than in the reinnervation group at both levels studied, although only at the distal level differences were statistically significant. At 6 and 9 months results were similar to those found at 2.5 months, with maintenance of a large number of axonal profiles (Fig. 4).

The main difference between nerve sections of mid and distal nerve levels studied is that whereas at mid level the numbers of myelinated axons tended to decrease slowly, at distal level regenerative sprouts were maintained over time without significant changes.

When the tibial and the peroneal nerve branches were transected and redirected to foreign muscle and skin targets, the nerve cross-section area and the number of myelinated fibers was decreased in comparison with the amputee groups, indicating that this surgical strategy is effective in reducing the formation of neuroma when the nerve is not allowed to reach its targets. Furthermore, the size of myelinated fibers was mildly increased in the reinnervation cases compared to the amputee model nerves (see Fig. 5).

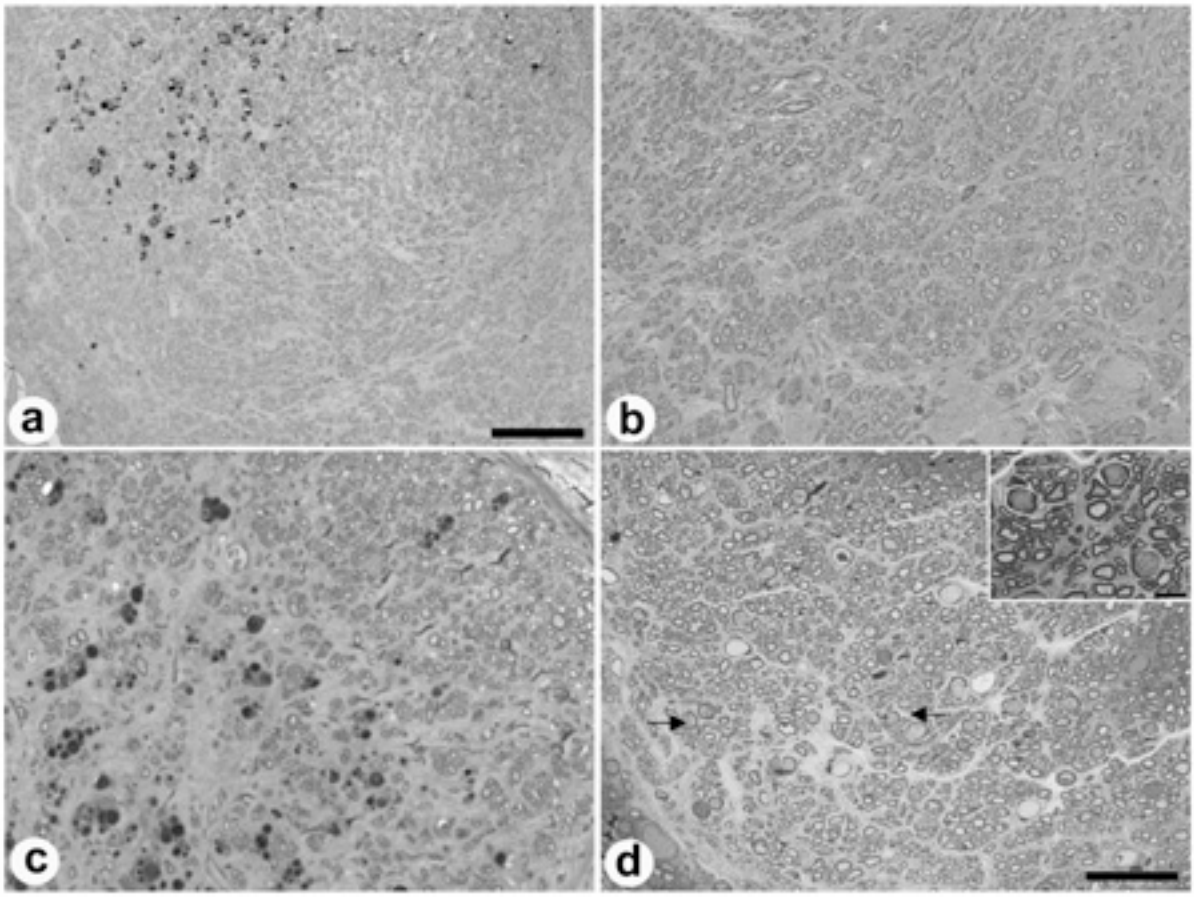

Figure 4. Semithin transverse sections of sciatic nerves representative of the amputee group at 2.5 months (a, b), 6 months (c) and 9 months (d). Note the appearance of zones with ongoing Wallerian degeneration at 2.5 and 6 months (a, c). At 9 months (d) some areas (arrows) showed abnormal fibers with swollen, dense axoplasm, and marked attenuation or disappearance of the myelin sheath (see also inset; bar=10μm). Bar = 100 μm in a, and 50 μm in b, c, d.

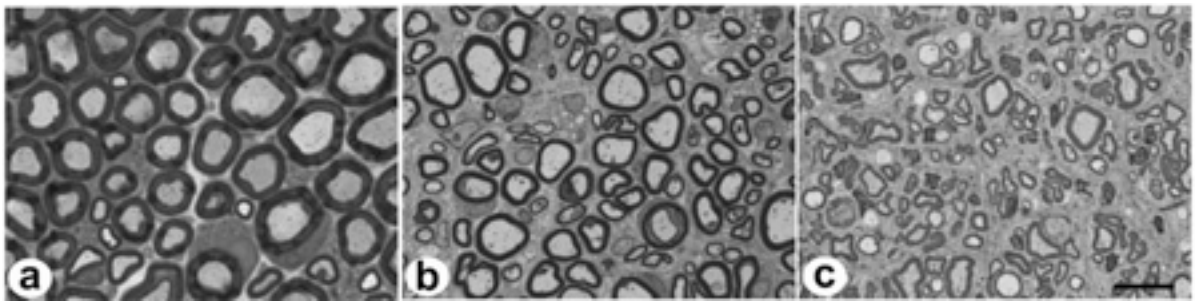

Figure 5. High magnification of sciatic nerve sections from an intact rat (a), a representative rat of the reinnervated group (b) and of the amputee group (c) at 6 months. Note the differences in the size of myelinated fibers between the amputee and the reinnervation nerve. Bar = 10 μm.

Immunohistochemistry

We performed the immunohistochemistry against ChAT, a marker of motor axons (Lago and Navarro, 2006) and CGRP, a marker of sprouting motor, and large and small sensory axons (Xu and Zochodne, 2002). At all times postlesion evaluated, we found large ChAT+ myelinated fibers at the nerve proximal level and inside the blind chamber. ChAT+ fibers were grouped in a fasciculated manner and not scattered as in regenerative nerves after transection and repair (Lago and Navarro, 2006; Lago et al., 2005). At 6 and 9 months postlesion there was a slight decrease in the density of ChAT+ profiles, but immunolabeling was still maintained in intensity (Fig. 6). CGRP-labeled axons were found scattered throughout the cross sectional area of the nerve at both levels evaluated. Immunolabeling against CGRP was observed in myelinated fibers and also in groups of unmyelinated axons at 2.5 months. The density of CGRP+ axons was clearly decreased at later time points evaluated, when CGRP+ fibers were mainly unmyelinated.

The expression of GAP-43 was assessed at 6 and 9 months postlesion. GAP-43 labeled axons were confined throughout the transverse section of the sciatic nerve (Fig. 6). No differences were found in GAP-43 immunoreactivity between samples taken at 6 (43.93 ± 1.47%) and 9 (43.25 ± 0.26 %) months. Moreover, a similar degree of immunoreactivity was observed in animals allowed for muscle reinnervation than in the amputee group.

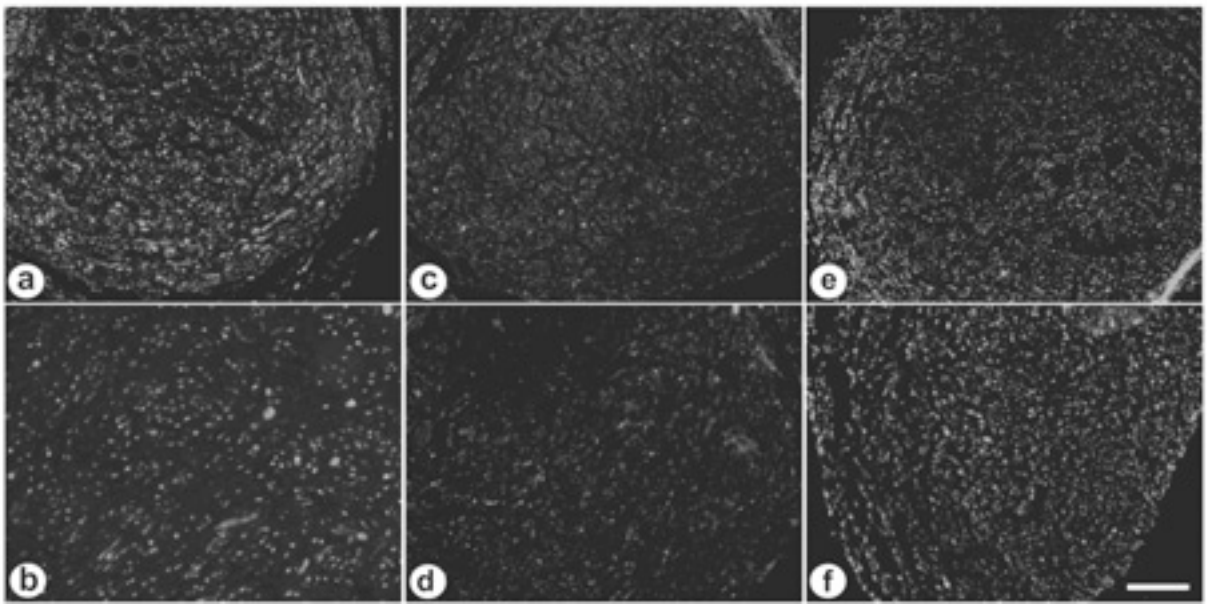

Figure 6. Immunohistochemical labeling against ChAT (a, b), CGRP (c, d) and GAP-43 (e, f) in transverse sections of the sciatic nerve neuroma in the amputee group at 6 (a, c, e) and 9 (b, d, f) months. Note the distribution of ChAT-positive profiles throughout the transverse section. CGRP-immunoreactivity was found throughout all the transverse section at lower density. GAP-43-immunoreactivity was expressed at high level scattered in the neuroma. Bar = 100 μm.

Size distribution of DRG neurons

To assess changes in the size distribution of L4 DRG neurons, we counted all the neuronal soma labeled against PGP9.5, a panneuronal marker, and classified them into small, medium and large size. The histogram in figure 7 shows the relative distribution of neuronal cell sizes in amputee (652 neurons measured), reinnervated (884 neurons) and control (1064 neurons) rats. There was a general reduction in neuronal size in the amputee group. The frequency of large neurons decreased from 18% in control DRG to 7% in amputee rats. In the reinnervation group the percentage of large neurons was maintained similar to controls, but there was a non significant decline of small neurons.

To investigate whether there was any population of DRG neurons selectively suffering atrophy, we also measured neurons immunolabeled against PV, predominantly present in large DRG neurons, CGRP, present in medium and small neurons, and IB4, a marker of non-peptidergic small DRG neurons (Fig. 7). In the amputee group there were significant changes with respect to controls, with reduction of large and increase of medium and small PV+ DRG cells (Fig. 8). In the reinnervated group the size distribution was maintained more similar to that of the control rats. For CGRP and IB4 immunoreactive neurons there were no significant differences between the different groups, although we did not find large CGRP+ neurons in the amputee group.

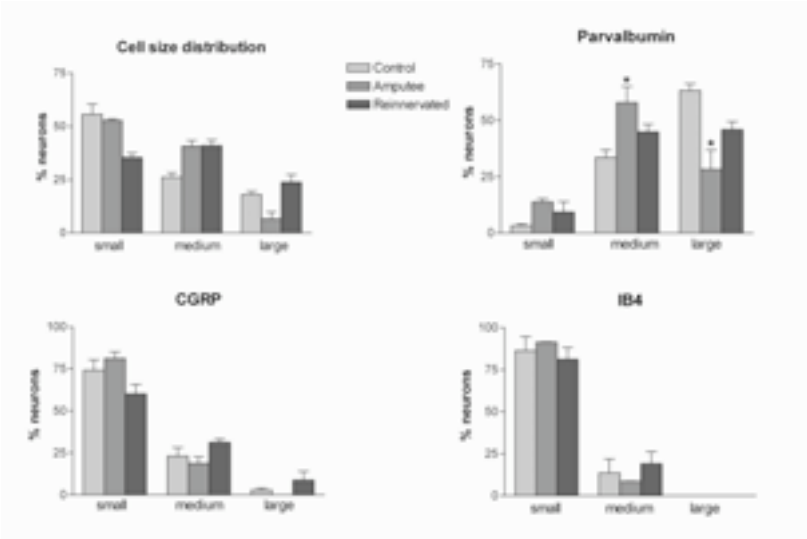

Figure 7. Neuronal cell size distribution in L4 DRG at 6 months postlesion, and size distribution of parvalbumin, CGRP and IB4 labeled neurons in the amputee group and the reinnervated group in comparison with control values. *$p<0.05$ vs control.

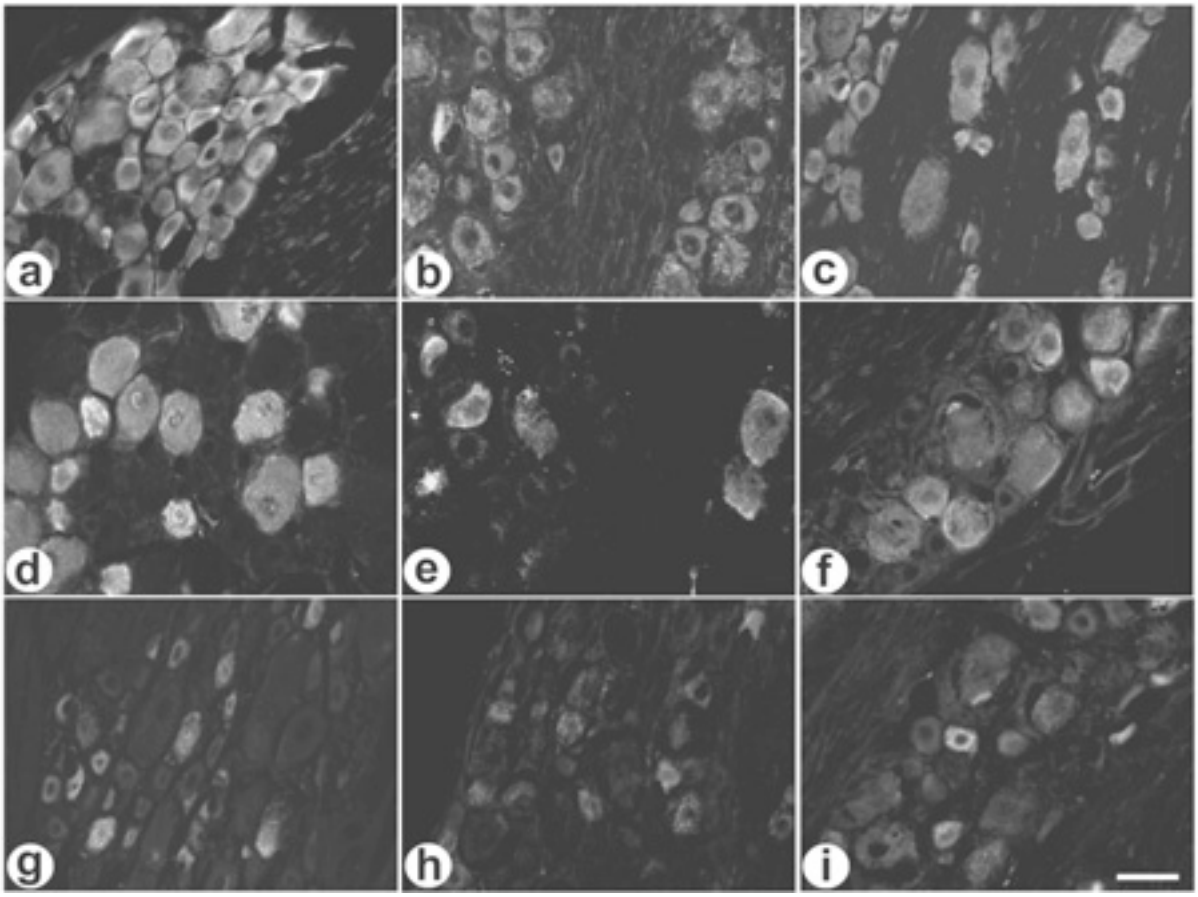

Figure 8. Immunohistochemical labeling against PGP9.5 (a, b, c), Parvalbumin (d, e, f) and CGRP (g, h, i) in DRG sections of a control rat (a, d, g) and of rats of the amputee group (b, e, h) and the reinnervated group (e, f, i) at 6 months postlesion. Note the expression of PGP9.5 in all neuronal profiles of the DRG, Parvalbumin mainly in large neurons, and CGRP in small and medium size neurons. Bar = 50 μm.

DISCUSSION

The present study was mainly aimed at examining the regenerative potential of amputee peripheral nerves, whose ending stump was inserted into a closed tube, thus isolating growing axons from regeneration and end organ interaction and producing a neuroma, compared with the situation in which regenerating axons could reach denervated tissue targets. The used experimental model of nerve amputation attempts to mimic the situation that can be expected after a limb amputation. The sectioned nerves in the proximal stump of the amputated limb eventually try to regenerate, but in the absence of a distal degenerating nerve and of targets (muscle, skin, vessels) to reinnervate, they end forming a neuroma. The design of the CYBERHAND prosthetic implantation includes interfacing sectioned nerves by means of regenerative electrodes, in order to take profit of the surviving axons for receiving efferent impulses that may contribute in the motor control of the prosthetic hand, and for stimulating sensory fibers to provide sensory feedback from the sensors embedded in the prosthetic hand.

For the severed axons to grow through the regenerative electrode a distal nerve segment shall be attached at the distal side of the electrode (Lundborg et al 1982; Lago et al 2005). More distally, this distal nerve segment has no continuity with muscle and skin targets since the limb is amputated.

The results found in this study show the expected features of a neuroma that is formed when regenerating axons are prevented from elongating in a degenerated distal nerve and, thus, from reaching the end organs (Aitken 1949; Fried et al 1993; Schmidt and Plurad 1985). They are characterized structurally as randomly oriented regenerating nerve fibers, of smaller than normal caliber, embedded in scar tissue (Aitken 1949; Fried et al 1991, 1993). Histological examination of biopsies collected from patients who suffered nerve injuries without repair during one to four years confirm that the morphology of neuroma and chronically denervated human peripheral nerves is essentially similar to that described in experimental models (Terenghi et al 1998).

Regeneration in the amputee model

After transection and repair, regenerative axonal sprouts readily emerge from the proximal nerve segment and grow to cross the suture gap and approach the distal segment. Sprouts which do not take an extraneural course may either approach a Schwann cell column, or may grow at random into the connective tissue layers of the nerve since an excess number of sprouts invade the distal Schwann cell columns (Aguayo et al 1973; Jenq and Coggeshall 1985). Each regenerating parent axon may give rise to over 10 axonal sprouts in the first few weeks (Witzel et al 2005). With time the number of axons decrease in the distal segment, as sprouts that do not make peripheral connections atrophy and eventually disappear. Nevertheless, even long time after injury (6 to 12 months), regenerating neurons support multiple sprouts, branching from the level of the lesion, in the distal stump of the nerve. This fact results in higher counts of distal fibers than the number of proximal fibers that really regenerate across the neuroma (Horch and Lisney 1981; Jenq and Coggeshall 1985; Mackinnon et al 1991). This increase in number involves myelinated axons, whereas unmyelinated axons are slightly reduced (Carter and Lisney 1991). A large number of axons counted in the distal segment does not necessarily indicate better regeneration; on the contrary, multiple branching may be a response to obstacles such as scars in the zone of axonal advance. The same process occurs, but more accentuated, when the nerve is not allowed to reinnervate the distal targets (Carter and Lisney 1991), as we found in the amputee model. Regenerative sprouts are not eliminated and continue to grow blindly within the

neuroma. Therefore, axonal counting in the distal nerve is considerably higher than the number of neurons actually regrowing axons due to sprouting and neuroma formation. Although at the distal level we found a high number of myelinated axons due to the neuroma formation, it is worth to note the high number of axons found also at the proximal level indicating a considerable immaturity of the regenerated nerve repaired with a silicone tube. Detailed histological studies have shown that following transection of a nerve, many sprouts arising within the neuroma are able to retrogradely grow relatively long distances proximally along the nerve trunk. The largest number of such sprouts was observed at 10 weeks after nerve section, with a decrease by 9 months (Scadding and Thomas 1983). This retrograde regeneration makes counts of nerve fibers larger than normal not only near the macroscopically defined neuroma but also at more proximal (mm to cm) levels of the nerve.

Ending neuroma are usually found to contain large numbers of small and haphazardly arranged regenerating nerve fascicles within a densely collagenous and fibroblastic stroma. We have studied the nerve amputation situation for 9 months. The numbers of axonal sprouts in the ending stump inserted in a capped tube did not change markedly over time. Nevertheless, there was evidence of loss of sprouts in avascular zones, whereas they remained steady in zones rich in nerve microfascicles associated with microvessels. Longstanding neuromas show nonuniform histological features, including zones of relative ischemia and limited axon penetration (Xu and Zochodne 2002), as we have found mostly localized at central areas of the neuroma, in the absence of distal regeneration and reinnervation. Abnormal axonal profiles, similar to regressive changes found in old regenerated fibers that may suffer from compressive and ischemic processes (Le Beau et al 1988) were also found at 9 months. All these features would limit the suitability of long term neuroma for delayed repair or interfacing.

We also evaluated the expression of ChAT and CGRP as indication of functionally defined nerve fibers. We found ChAT+ fibers at both levels analyzed with a fasciculated pattern, probably due to the fact that axonal sprouts from a motor parent axon grew together. Although a previous report showed that regenerating motor axons histochemically labeled by acetyl-choline esterase were non-myelinated at 90 days after transection and encapsulation of the distal nerve (Macias et al., 1998), we found that most ChAT+ fibers were myelinated at all the postinjury times studied. CGRP labeling was also present but at decreasing density in the longer term samples. Of interest is that still 9 months after injury there was prominent labeling of GAP-43, a marker of regenerating axons (Van Lookeren Campagne et al., 1999),

in the axonal sprouts in the neuroma, indicating that the regenerative potential is maintained even at this long time after the injury.

When we determined the DRG neurons size distribution in the amputee and forced reinnervation groups in comparison with the control rats, we found that there was a shift to smaller size neurons. This neuronal size reduction was mostly evident in the amputee group, and involving parvalbumin-positive large neurons, whereas the size of CGRP and IB4-positive cells was less affected. Reinnervation of foreign targets partially prevented neuronal atrophy. Although we did not make a quantitative numerical estimate, the decrease in the proportion of small DRG neurons in this group may be explained by a selective death of small-size neurons after nerve injury, which was compensated in the amputee group by the reduction in size. Previous studies (Groves et al 1996; Rich et al 1989; Tandrup et al 2000) have shown that a subset of small diameter sensory neurons may be particularly vulnerable to axotomy-induced changes. The period of neuronal death following axotomy peaks at 1–3 months and then gradually diminishes, over a period of six months. It is unclear why this axotomy-induced apoptosis continues for such a long time after axotomy, particularly if deprivation of target-derived neurotrophic factors is the cause.

Strategies to modulate the regenerative response and to reduce the neuroma formation

After nerve injury, when regeneration is not permitted, a bulbous swelling usually forms at the severed nerve end, constituting a traumatic neuroma. Significant pain and dysesthesia are frequently associated with the formation of neuroma. The development of a painful neuroma may be more disabling to the patient than an area of anesthesia or even loss of motor function (Vernadakis et al 2003). It must be taken into account that axons trapped in a neuroma tend to become abnormally sensitive to mechanical, chemical, physical and metabolic stimuli and some even fire spontaneously (Devor 2006), being the source of disesthesia and pain. Although our results show that neurons can regenerate their axons and maintain them over long time even in the absence of distal reinnervation, further studies should be done to know how to reduce the uncontrolled axonal growth in the end stump to reduce sprouting and neuropathic pain.

Capping the transected nerve stump within a tube, either of silicon or of collagen, has been shown to partially prevent an amputated neuroma from forming, and secondarily suppress the appearance of induced pain by ectopic firing of terminal sprouts in the neuroma (Danielsen et al 1986; Sakai et al 2005). Therefore, the amputee model used in this study already took into account this strategy. Thus, the features of ending neuroma may be expected

to be even increased if the nerve is just sectioned or ligated. It was also shown that by placing the ending nerve stumps into a silicone tube, survival of axotomized sensory neurons is improved even if axons do not regenerate across a long gap (Melville et al., 1989). However, when the transected sciatic nerve is placed in a blinded impermeable chamber filled with saline, other authors reported a 10-20% loss of DRG neurons (Rich et al 1987; Groves et al 1999). Neuronal death and atrophy could be prevented if neurotrophic factors, such as NGF (Rich et al 1987, 1989; Otto et al 1987) and NT3 (Groves et al 1999), are supplied to the axotomized neurons by local application into the blinded chamber.

By reimplanting a transected peripheral nerve within a muscle tissue, the formation of neuroma is limited. The minimal neuroma that formed had significantly less scar tissue and contained nerve fibers at a decreased density than when the proximal nerve stump was left free or apposed to the wound skin (Mackinnon et al 1985). The experimental evidences led to the clinical approach of implanting resected neuroma within nearby muscles, in attempts to reduce neuropathic pain development. Our results show that in the group of rats with forced muscle reinnervation the density of growing axons was reduced and the size of the myelinated fibers appeared to slightly increase, from samples taken at 2.5 to 9 months, when compared with the amputee situation. The motor fibers of the tibial nerve were able to reinnervate the gastrocnemius muscle, as evidenced by the electrophysiological tests. On the other hand, no evidence of skin reinnervation by the peroneal branch could be obtained. The partial effect of the forced reinnervation paradigm in preventing intense axonal sprouting and DRG neuronal atrophy in our model may be explained by the lack of target reinnervation by the peroneal and sural branches, as well as by cutaneous afferents of the tibial nerve in the muscle. Nevertheless, Wells et al (2001) suggested that this strategy could be used to obtain EMG signals, by using a small strip of a foreign muscle, to provide efferent peripheral nerve-based information for prosthetic devices.

CONCLUSIONS

Our results indicate that axons can regenerate through a short distal nerve segment, even if ending in a blinded chamber, and sustain distal branches without degenerating for a long time. These evidences are positive since they indicate that axons regenerated through a sieve electrode may be eventually interfaced with external input-output systems over long time. The planned continuing studies will be focused to reduce the degree of terminal sprouting (in order to reduce the proportion of distal sprouts vs. parent axons) and to increase the caliber of regenerated fibers (towards normal profiles).

Acknowledgments

This research was supported by grants IST-2001-35094 (CYBHERAND project) and IST-001917 (NEUROBOTICS project) from the EC. The authors thank Jessica Jaramillo for technical assistance in the morphological studies.

REFERENCES

Aguayo A.J, Peyronnard J.M, Bray G.M. A quantitative ultrastructural study of regeneration from isolated proximal stumps of transected unmyelinated nerves. J Neuropathol Exp Neurol 1973; 32: 256-270.

Aitken JT. The effect of peripheral connexions on the maturation of regenerating nerve fibres. J Anat 1949; 43:32-43.

Boucher TJ, Okuse K, Bennett DLH, Munson JB, Wood JN, McMahon SB. Potent analgesic effects of GDNF in neuropathic pain states. Science 2000; 290:124-127.

Branner A, Stein RB, Normann RA. Selective stimulation of cat sciatic nerve using an array of varying-length microelectrodes. J Neurophysiol 2001; 85:1585-1594

Carter DA, Lisney SJW. Changes in myelinated and unmyelinated axon numbers in the proximal parts of rat sural nerves after two types of injury. Restor Neurol Neurosci 1991; 3:65-73.

Ceballos D; Valero-Cabré A; Valderrama E; Schuttler M; Stieglitz T; Navarro X. Morphologic and functional evaluation of peripheral nerve fibers regenerated through polyimide sieve electrodes over long-term implantation. J Biomed Mater Res 2002; 60:517-528.

Danielsen N, Shyu BC, Dahlin LB, Lundborg G, Andersson SA. Absence of ongoing activity in fibres arising from proximal nerve ends regenerating into mesothelial chambers. Pain 1986; 26:93-104.

Devor M. Responses of nerves to injury in relation to neuropathic pain. In: McMahon SB, Koltzenburg M (eds), Wall and Melzack's Textbook of Pain. 5th ed. Elsevier Churchill Livingstone, 2006, p. 905-927.

Feltri M, Herer S.S, Wrabertz J, Kamholz J, Shy M.E. Mitogen-expanded Schwann cells retain the capacity to myelinate regenerating axons after transplantation into rat sciatic nerve. Proc Natl Acad Sci USA 1992; 89: 8827-8831.

Fried K, Govrin-Lippmann R, Devor M. Close apposition among neighbouring axonal endings in a neuroma. J Neurocytol 1993; 22:663-681.

Fried K, Govrin-Lippmann R, Rosenthal F, Ellisman MH, Devor M. Ultrastructure of afferent axon endings in neuroma. J Neurocytol 1991; 20:682-701.

Fu SY, Gordon T. Contributing factors to poor functional recovery after delayed nerve repair: Prolonged denervation. J Neurosci 1995; 15:3886-3895.

Fukuoka T, Kondo E, Dai Y, Hashimoto N, Noguchi K. Brain-derived neurotrophic factor increases in the uninjured dorsal root ganglion neurons in selective spinal nerve ligation model. J. Neurosci 2001; 21:4891–4900.

Gordon T, Sulaiman O, Boyd JG. Experimental strategies to promote functional recovery after peripheral nerve injuries. J Periph Nerv System 2003; 8:236–250.

Groves MJ, An SF, Giornetto B, Scaravilli F. Inhibition of sensory neuron apoptosis and prevention of loss by NT-3 administration following axotomy. Exp Neurol 1999; 155:284-294.

Groves MJ, Christopherson T, Giometto B, Scaravilli F. Axotomy-induced apoptosis in adult rat primary sensory neurons. J Neurocytol 1997; 26:615–624.

Groves MJ, Ng YW, Ciardi A, Scaravilli F. Sciatic nerve injury in the adult rat: comparison of effects on oligosaccharide, CGRP and GAP-43 immunoreactivity in primary afferents following two types of trauma. J Neurocytol 1996; 25:219-231.

Hall SM. The biology of chronically denervated Schwann cells. Ann N Y Acad Sci 1999; 883:215-233.

Horch KW, Lisney SJW. On the number and nature of regenerating myelinated axons after lesions of cutaneous nerves in the cat. J Physiol 1981; 313:275-286.

Jenq C-B, Coggeshall RE. Numbers of regenerating axons in parent and tributary peripheral nerves in the rat. Brain Res 1985; 326:27-40.

Klinge PM, Vafa MA, Brinker T, Brandis A, Walter GF, Stieglitz T, Samii M, Wewetzer K. Immunohistochemical characterization of axonal sprouting and reactive tissue changes after long-term implantation of a polyimide sieve electrode to the transected adult rat sciatic nerve. Biomaterials 2001; 22:2333-2343.

Lago N, Ceballos D, Rodríguez FJ, Stieglitz T, Navarro X. Long term assessment of axonal regeneration through polyimide regenerative electrodes to interface the peripheral nerve. Biomaterials 2005; 26:2021-2031.

Lago N, Navarro X. Correlation between target reinnnervation and distribution of motor axons in the injured rat sciatic nerve. J Neurotrauma 2006; 23:227-240.

Le Beau JM, Ellisman MH, Powell HC. Ultrastructural and morphometric analysis of long-term peripheral nerve regeneration through silicone tubes. J Neurocytol 1988; 17:161-172.

Lundborg G, Dahlin LB, Danielsen N, Gelberman RH, Longo FM, Powell HC, Varon, S. Nerve regeneration in silicone chambers: influence of gap length and of distal stump components. Exp Neurol 1982; 76:361-375.

Mackinnon SE, Dellon AL, Hudson AR, Hunter DA. Alteration of neuroma formation by manipulation of its microenvironment. Plast Reconstr Surg 1985; 76:345-353.

Mackinnon SE, Dellon AL, O'Brien JP.. Changes in nerve fiber numbers distal to a nerve repair in the rat sciatic nerve model. Muscle Nerve 1991; 14:1116-1122.

Melville S, Sherburn TE, Coggeshall RE. Preservation of sensory cells by placing stumps of transected nerve in an impermeable tube. Exp Neurol 1989; 105:311-315.

Navarro X, Butí M, Verdú E. Autotomy prevention by amitriptyline after peripheral nerve section in different strains of mice. Restor Neurol Neurosci 1994; 6:151-157.

Navarro X, Calvet S, Rodríguez FJ, Stieglitz T, Blau C, Butí M, Valderrama E, Meyer JU. Stimulation and recording from regenerated peripheral nerves through polyimide sieve electrodes. J Periph Nerv System 1998; 2:91-101.

Navarro X, Krueger T, Lago N, Micera S, Stieglitz T, Dario P. A critical review of interfaces with the peripheral nervous system for the control of neuroprostheses and hybrid bionic systems. J Periph Nerv System 2005; 10:229-258.

Obata K, Yamanaka H, Dai Y, Tachibana T, Fukuoka T, Tokunaga A. Differential activation of extracellular signal-regulated protein kinase in primary afferent neurons regulates brain-derived neurotrophic factor expression after peripheral inflammation and nerve injury. J Neurosci 2003; 23:4117- 4126.

Otto D, Unsicker K, Grothe C. Pharmacological effects of nerve growth factor and fibroblast growth factor applied to the transectioned sciatic nerve on neuron death in adult rat dorsal root ganglia. Neurosci Lett 1987; 83:156-160.

Rich KM, Luszczynski JR, Osborne PA, Johnson EM Jr. Nerve growth factor protects adult sensory neurons from cell death and atrophy caused by nerve injury. J Neurocytol 1987; 16:261-268.

Rich KM, Disch SP, Eichler ME. The influence of regeneration and nerve growth factor on the neuronal cell body reaction to injury. J Neurocytol 1989; 18:569-576.

Rodríguez FJ, Verdú E, Ceballos D, Navarro X. Neural guides seeded with autologous Schwann cells improve nerve regeneration. Exp Neurol 2000; 161:571-584.

Sakai Y, Ochi M, Uchio Y, Ryoke K, Yamamoto S. Prevention and treatment of amputation neuroma by an atelocollagen tube in rat sciatic nerves. J Biomed Mater Res B Appl Biomater 2005; 73:355-360.

Scadding JW, Thomas PK. Retrograde growth of myelinated fibres in experimental neuromas. J Anat 1983; 136:793-799.

Schmidt RE, Plurad SB. Ultrastructural appearance of intentionally frustrated axonal regeneration in rat sciatic nerve. J Neuropathol Exp Neurol 1985; 44:130-146.

Stieglitz T, Beutel H, Meyer J-U. A flexible, light-weight multichannel sieve electrode with integrated cables for interfacing regenerating peripheral nerves. Sensor Actuators 1997; 60:240-243.

Sulaiman OA, Gordon T. Effects of short- and long-term Schwann cell denervation on peripheral nerve regeneration, myelination and size. Glia 2000; 32:234-246.

Tandrup T, Woolf CF, Coggeshall RE. Delayed loss of small dorsal root ganglion cells after transection of the rat sciatic nerve. J Comp Neurol 2000; 422:172-180.

Terenghi G, Calder JS, Birch R, Hall SM. A morphological study of Schwann cells and axonal regeneration in chronically transected human peripheral nerves. J Hand Surg [Br] 1998; 23:583-587

Udina E, Rodríguez FJ, Verdú E, Espejo M, Gold BG, Navarro X. FK506 enhances regeneration of axons across long peripheral nerve gaps repaired with collagen guides seeded with allogeneic Schwann cells. Glia 2004; 47:120-129.

Van Lookeren Campagne M, Oestreicher AB, Van Bergen en Henegowen PM, Gispen WH. Ultrastructural immunocytochemical localization of B-50/GAP43, a protein kinase C substrate, in isolated presynaptic nerve terminals and neuronal growth cones. J Neurocytol 1989; 18:479-489.

Vernadakis AJ, Koch H, Mackinnon SE. Management of neuromas. Clin Plast Surg 2003; 30:247-268.

Verdú E, Navarro X. The role of Schwann cell in nerve regeneration. En Castellano B, González B, Nieto-Sampedro M (eds): Understanding Glial Cells. Kluwer Academic Pub, 1998, p. 319-359.

Wang Y, Chang CF, Morales M, Chiang YH, Hoffer J. Protective effects of glial cell line-derived neurotrophic factor in ischemic brain injury. Ann N Y Acad Sci 2002; 962:423-437.

Wells MR, Vaidya U, Ricci JL, Christie C. A neuromuscular platform to extract electrophysiological signals from lesioned nerves: a technical note. J Rehabil Res Develop 2001; 38:385-390.

Witzel C, Rohde C, Brushart TM. Pathway sampling by regenerating peripheral axons. J Comp Neurol 2005; 485:183-190.

Xu Q-G, Zochodne DW. Isquemia and failed regeneration in chronic experimental neuromas. Brain Res 2002; 946:24-30.

EFFECTS OF SCHWANN CELL TRANSPLANTATION IN AN EXPERIMENTAL AMPUTEE MODEL

Natalia Lago, Caty Casas, F. Javier Rodríguez, Elizabeth M. Muir *, John Rogers *, Xavier Navarro

Group of Neuroplasticity and Regeneration, Department of Cell Biology, Physiology and Immunology, and Institute of Neuroscience, Universitat Autònoma de Barcelona, Bellaterra, Spain

* Physiological Laboratory, University of Cambridge, Cambridge, United Kingdom.

INTRODUCTION

One of the sequelae that follow transection of a peripheral nerve is that a number of neurons whose axons project in that nerve die. Neuronal loss must be prevented if total functional recovery after repair of nerve lesions is to be attained. The proportion of neuronal death among sensory neurons of the dorsal root ganglia (DRG) after sciatic nerve injury has been reported varying between 10 and 30% in several studies (Arvidsson et al., 1986; Rich et al., 1987; Himes and Tessler, 1989; Ygge, 1989; Vestergaard et al., 1997; Groves et al., 1999). Regarding loss of motoneurons, a non-significant loss of 0-10% motoneurons has been reported after sciatic nerve injury (Vanden-Noven et al., 1993; Lowrie et al., 1994; Valero-Cabré et al., 2001). Varying results may to some extent be due to counting methodologies, but also reflect variations in age at lesion, postoperative survival time, and proximity of the lesion. The degree of DRG neuronal death after axonal injury in adult rats was found to be mainly dependent on the severity of the injury and on the distance from the axonal injury to the neuronal body (Ygge, 1989). The process of neuronal death is prolonged, and thus more severe if neuromas persist after permanent transection and ligation of nerves. Neuronal death following axotomy and failure of reinnervation is due to apoptosis and has a similar time course to that of neuronal vacuolation seen after axotomy (Groves et al., 1997), with a progressive increase during the first 1-3 months and then a gradual decline over a period of six months (Groves et al., 1999).

On another hand, when regenerating axons are prevented to reach appropriate target tissue, each axon is able to maintain numerous growing sprouts forming an ending neuroma over long time (see previous manuscript by Lago and Navarro). Six to twelve months after a nerve section left unrepaired or capped in a blinded chamber, the number of myelinated axons proximal to and at the neuroma is largely above normal, although the number of unmyelinated axons does not change significantly (Scadding and Thomas, 1983; Carter and Lisney, 1991). Without appropriate distal reconnection, maturation may be arrested and retrograde atrophy and degeneration may ensue (Gianini et al., 1989). Moreover, sectioned axons are able to regenerate up to 6 months of chronic denervation if subjected to delayed repair, by resuturing the proximal stump to a fresh or a degenerated distal nerve stump, but only a low proportion of neurons support regeneration (Fu and Gordon, 1995; Gordon et al., 2003).

The loss of a noticeable proportion of neurons and the retrograde atrophy and inability to sustain regeneration are two important problems to solve for the eventual chronic application of an interface with the injured nerves in amputee limbs to achieve a neural-based control of advanced cybernetic prostheses, like that developed in the CYBERHAND project.

In past years much attention was focused on the role of neurotrophic factors in the maintenance and survival of neurons and in promoting axonal regeneration after nerve injury (for reviews see Persson and Ibáñez, 1993; Terenghi, 1999; Boyd and Gordon, 2003). After peripheral nerve injury, the adult mammalian peripheral nervous system responds by increasing the availability of neurotrophic factors, either by autocrine or paracrine sources. Additional exogenous supply of neurotrophic factors may enhance the regenerative response of peripheral neurons, especially when their axons can not regain contact with target cells, in situations such as chronic denervation, nerve ligature or amputation. The spectrum of neurotrophic factors reported to stimulate axonal regeneration includes nerve growth factor (NGF), brain derived neurotrophic factor (BDNF), neurotrophin-3 (NT-3) and neurotrophin-4/5 (NT-4/5), insulin-like growth factors (IGF-I and IGF-II), ciliary neurotrophic factor (CNTF), basic fibroblast growth factor (FGF-2) and glial cell line-derived neurotrophic factor (GDNF). Local administration of NGF and of NT-3, but not of CNTF and FGF, to adult rat axotomized nerves inside a blinded impermeable chamber effectively prevented sensory neuronal loss (Otto et al, 1987; Rich et al., 1989; Groves et al., 1999). However, it has been suggested that a complex mixture of different neurotrophic factors and neurotropic molecules may potentiate peripheral nerve reaction and regeneration better than any one individual component.

Schwann cells (SCs) upregulate the expression and secretion of a variety of neurotrophic factors during Wallerian degeneration, and also secrete extracellular matrix components and basal lamina that provide permissive pathways through which regenerating axons grow in the degenerated distal nerve (Verdú and Navarro, 1998). Considering the importance of the SCs in creating an adequate microenvironment for nerve regeneration, the construction of cellular prostheses consisting in a nerve guide seeded with transplanted SCs has been successfully assayed in animal models for achieving nerve regeneration across long gaps which are not normally bridged (Feltri et al., 1992; Guénard et al., 1992; Rodríguez et al., 2000; Udina et al., 2004). One of the reasons for impaired regeneration into chronically denervated peripheral nerves is the inability of SCs to sustain enough trophic support and interaction with growing axons (Hall, 1999; Hoke et al., 2002). It has been shown that the longer the time of denervation, the lower the expression of c-erbB receptors and of GDNF in SCs, and the smaller the percentage of bands of Büngner reinnervated (Li et al., 1997; Höke et al., 2002).

By using a nerve amputee model of the rat sciatic nerve, we have tested a strategy to maintain and promote maturation of regenerated axons without distal target reinnervation by

transplanting SCs previously isolated in culture within the capped silicone chamber containing the ending nerve stump. We have evaluated by morphology and immunohistochemistry the effects of transplanted SCs on the fate of long-term neuroma formation. Under this experimental paradigm, we have also compared the effects of transplants of SCs obtained from primary cultures with SCs of an immortalized line, and SCs of the same line overexpressing GDNF.

MATERIAL AND METHODS

Surgical procedure

Operations were performed on female Sprague-Dawley rats, aged 2.5 months, under pentobarbital anesthesia (40 mg/kg i.p.). The sciatic nerve was exposed at the midthigh and sharply transected. Both nerve stumps were fixed into a silicone guide (2 mm i.d, 8 mm long), with one 10-0 suture at each end, leaving a short gap of 4 mm between the stumps. The lumen of the silicone guide was filled with saline solution. The distal sciatic nerve was transected again at a distance of 10 mm from the silicone guide and the ending nerve stump fixed inside a capped silicone chamber, with one stitch of 10-0 suture. The capped chamber was made with a piece of tube 6 mm long covered at one end with silicone adhesive. The capped chamber was filled either with saline solution (amputee group, n=12) or with a suspension of SCs (amputee+SC group, n=12). Four rats of each group were evaluated at 2.5, 6 and 9 months.

In another two groups the capped chamber was filled with SCs from the SCTM41 cell line (amputee+SCTM41 group, n=4) or with SCs overexpressing GDNF (amputee+SCTM41-GDNF group, n=4) (Wilby et al., 1999), and the nerves studied at 2.5 months. Because the SCs cells of these lines derived from CD rats (Charles River Laboratories, Margate, UK), to avoid immune rejection host animals were treated with FK506 (2mg/kg i.p.) daily for 15 days after surgery and transplantation and 2 days/week until the end of follow-up.

For comparisons, a group (tube repair group) in which the distal nerve was not transected but was in continuity to distal targets, and a group of intact rats (control) were used.

Schwann cell cultures

SCs from female Sprague-Dawley rats, aged 2 months, were isolated following a previously reported method (Verdú et al., 2000). Under anesthesia, the sciatic nerve was exposed and cut at the upper thigh. Seven days later animals were reanesthetized to remove

the *in vivo* degenerating nerves under aseptic conditions. The nerve segments were stored in Hanks's balanced solution (HBSS, Sigma) with Ca2+ and Mg2+. The epineurium and connective tissue were stripped of and the nerves were mechanically and enzymatically dissociated. After centrifugation (900 rpm, 7 min) the cell suspension was seeded onto microplates pre-coated with poly-lysine and incubated with a defined culture medium under 5% CO_2 at 37ºC. Seven days later, cells from confluent cultures with 80% SC purity were detached with trypsin-EDTA and the cell mixture recovered by centrifugation.

The SCTM41 cell line is based on the constitutive expression of a synthetic ligand-gated proto-oncogene, tamoxifen-regulated human c-Myc. The SCTM41 line expressing GDNF was produced as described in Wilby et al. (1999). The SCTM41 parent and SCTM41-GDNF cells were grown on poly-lysine-coated flasks in DMEM supplemented with 10% fetal calf serum, glutamine and pyruvate. The SCTM41 cells show more extensive cytoplasm than typical primary SCs *in vitro* and they divide rapidly in culture.

Before transplantation, cultures were removed from the flasks using trypsin-EDTA. The reaction was stopped with fresh culture medium and the cells were centrifuged. Cells were resuspended in DMEM mixed with Matrigel at a final concentration of 4 mg/ml. The volume was adjusted to obtain a final number of 200,000 cells per tube for SCs and of 100,000 per tube for both SCTM41 cells. Capped silicone tubes were filled with the Matrigel cell suspension and kept at 37ºC for 3-4 hours before implantation (Fig. 1).

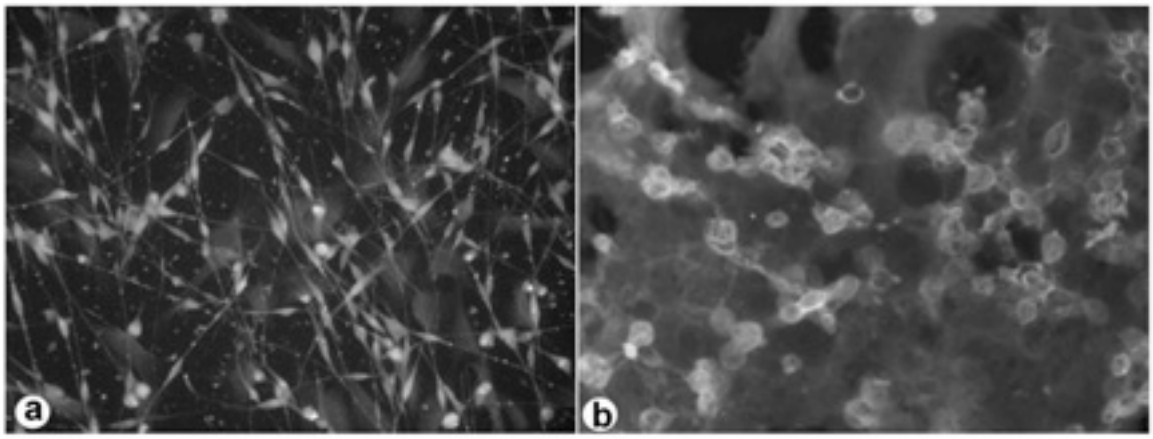

Figure 1. Immunolabeling against S-100. (a) Primary SC culture, showing the typical spindle-shape of the cells. (b) Immunolabeled SCs placed in a Matrigel scaffold before transplantation in the amputee nerve model.

Morphological evaluation

After postoperation intervals of 2.5, 6 and 9 months, the rats were deeply anesthetized and perfused transcardially with 4% paraformaldehyde in phosphate-buffer saline solution (PBS, 0.1M, pH 7.4). Then, the nerve was dissected out and sectioned in different segments: a

medial nerve segment (mid level) inside the silicone guide and a distal nerve segment (distal level) between the silicone guide and the ending chamber. These segments were postfixed with 3% glutaraldehyde-3% paraformaldehyde in cacodylate-buffer solution (0.1 M, pH 7.4), postfixed in osmium tetroxide (2%, 2 h, 4°C), dehydrated through ethanol series, contrasted with uranyl acetate (2.5%, overnight) and embedded in Agar 100 resin. Embedded nerves were sectioned using a LKB III 6802 ultramicrotome (Leica). Semithin sections (0.5 μm) were stained with toluidine blue and examined by light microscopy (Olympus BX-40). Images of the whole sciatic nerve were acquired at 4x with a digital camera (Olympus DP50), while sets of images chosen by systematic random sampling of squares representing at least 30% of the nerve cross-sectional area were acquired at 100x. Measurements of the cross-sectional area of the whole nerve, as well as counts of the number of myelinated fibers were carried out by using NIH Image 1.62b software.

Immunohistochemistry

Segments of the nerve inside the silicone guide and inside the ending chamber were collected and postfixed in the same perfusion solution for 4h. Samples were washed in phosphate-buffer (0.1M, pH 7.4) and processed for embedding in paraffin. Transverse sections (4 μm thickness) were cut with a microtome, mounted in (3-aminopropyl)triethoxysilane-coated slides and dried overnight. The sections were deparaffinized and rehydrated, and subjected to antigen retrieval with sodium citrate (pH 6.1) during 20 minutes at 95ºC. Then sections were washed with Trizma buffer solution (TBS, 0.05M, pH 7.4; Sigma) and TBS plus 0.05% Tween-20 (Fluka) (TBST) before blocking nonspecific binding sites with 2% BSA in TBST for 1 h at room temperature. After washes, sections were incubated for 24h at 4ºC with rabbit anti-GDNF (Santa Cruz Biotechnology; 1:50), and goat anti-human S100 (R&D Systems Inc; 1:200). Slides were washed with TBST and incubated with Cy3 and Cy2 secondary antibodies (Jackson Immunoresearch; 1:200) for 1h at room temperature. After further washing the slides were dehydrated and mounted with DPX (Fluka).

Statistical analysis

All results are expressed as mean±SEM. Statistical comparisons between groups and intervals were made by nonparametric tests, and differences were considered significant when $p<0.05$.

RESULTS

As indicated in the previous study, nerve regeneration occurred within the silicone guide across the short gap (4 mm) established in all the animals. Inside the guide, the regenerated nerve was round and occupied the center of the lumen. The microscopical appearance of nerve sections taken from the distal half of the guide (mid level) showed a thick perineurial layer surrounding the endoneurium composed of small fascicles of myelinated and unmyelinated axons and numerous blood vessels (Fig. 2), as usual in regenerated nerves repaired with impermeable tubes (Williams et al., 1983; Jenq and Coggeshall, 1985; Gómez et al., 1996). We did not observe degenerative axonal profiles in the sections at the tube level at any time interval evaluated after implantation (Fig. 3a). Transverse sections taken at the distal nerve segment showed also typical features of a neuroma; there were large numbers of small thinly myelinated and unmyelinated axonal profiles, numerous SCs and microvessels, embedded in connective tissue (Fig. 3b). The caliber of regenerated myelinated axons was smaller at the distal than at the mid level at the three postinjury times studied.

In comparison with nerves that were able to regenerate along the distal nerve to reinnervate targets (tube repair group), the nerves in the amputee model showed a larger cross-sectional area and about double numbers of myelinated fibers at 2.5 months (Table 1). The quantitative results showed a tendency to diminish the counts of myelinated fibers at 9 months at the mid level but not at the distal level. There were higher numbers of axonal profiles in the rats with SCs transplanted in comparison with those with only saline in the ending chamber at both levels studied, although differences were not statistically significant (Fig. 4).

Table 1. Cross-sectional area and number of myelinated fibers in the regenerated nerves at mid and distal levels at 2.5, 6 and 9 months postinjury in the group with the sciatic nerve sectioned and repaired with a silicone guide, and the distal nerve segment fixed to a capped tube filled with a suspension of SCs.

			Mid level		*Distal level*	
Group	time	(n)	Nerve area (mm^2)	No MF	Nerve area (mm^2)	No MF
Amputee+SC	2.5 mo	(4)	1.11 ± 0.08	24216 ± 1373	0.73 ± 0.07	26589 ± 2064
Amputee+SC	6 mo	(4)	0.79 ± 0.11	26743 ± 3436	0.71 ± 0.09	29212 ± 3489
Amputee+SC	9 mo	(4)	0.89 ± 0.08	23912 ± 1033	0.71 ± 0.07	28400 ± 1563

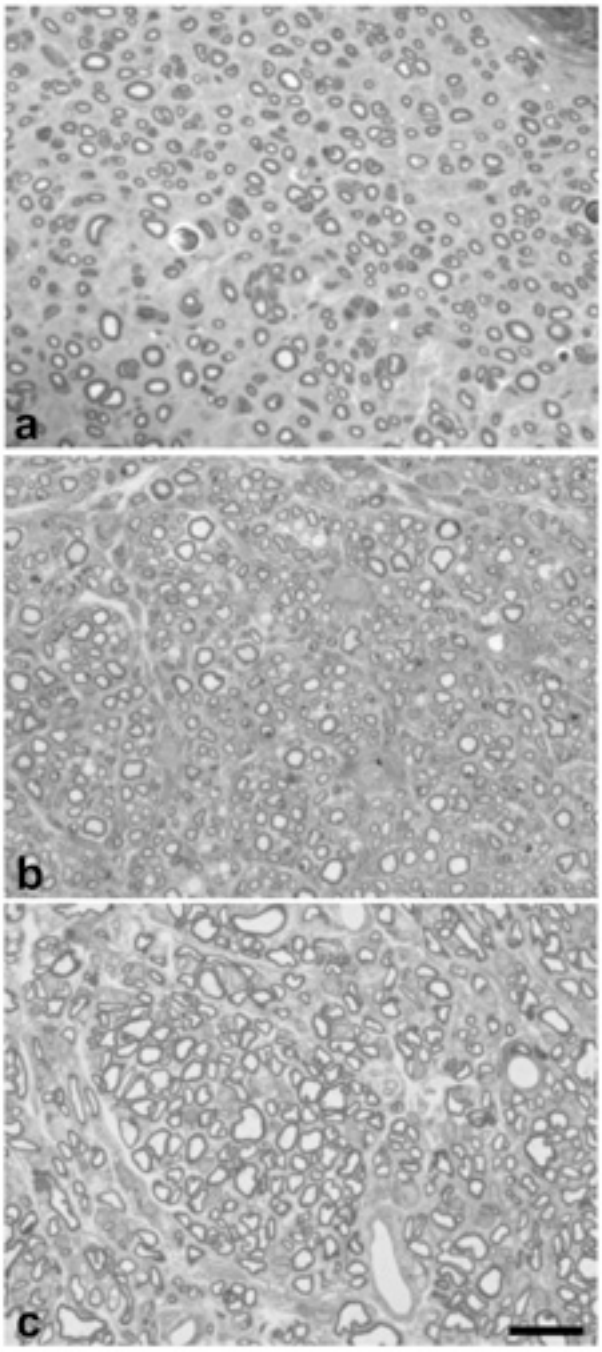

Figure 2. Semithin transverse sections of sciatic nerves representative of regenerated nerves at the mid level, inside the silicone tube after 2.5 months in one rat of the control tube repair group (a), the Amputee group (b), and the Amputee+SC group (c). Note the increased density of myelinated fibers in the Amputee model groups in comparison with the control injured group. Bar = 20 μm.

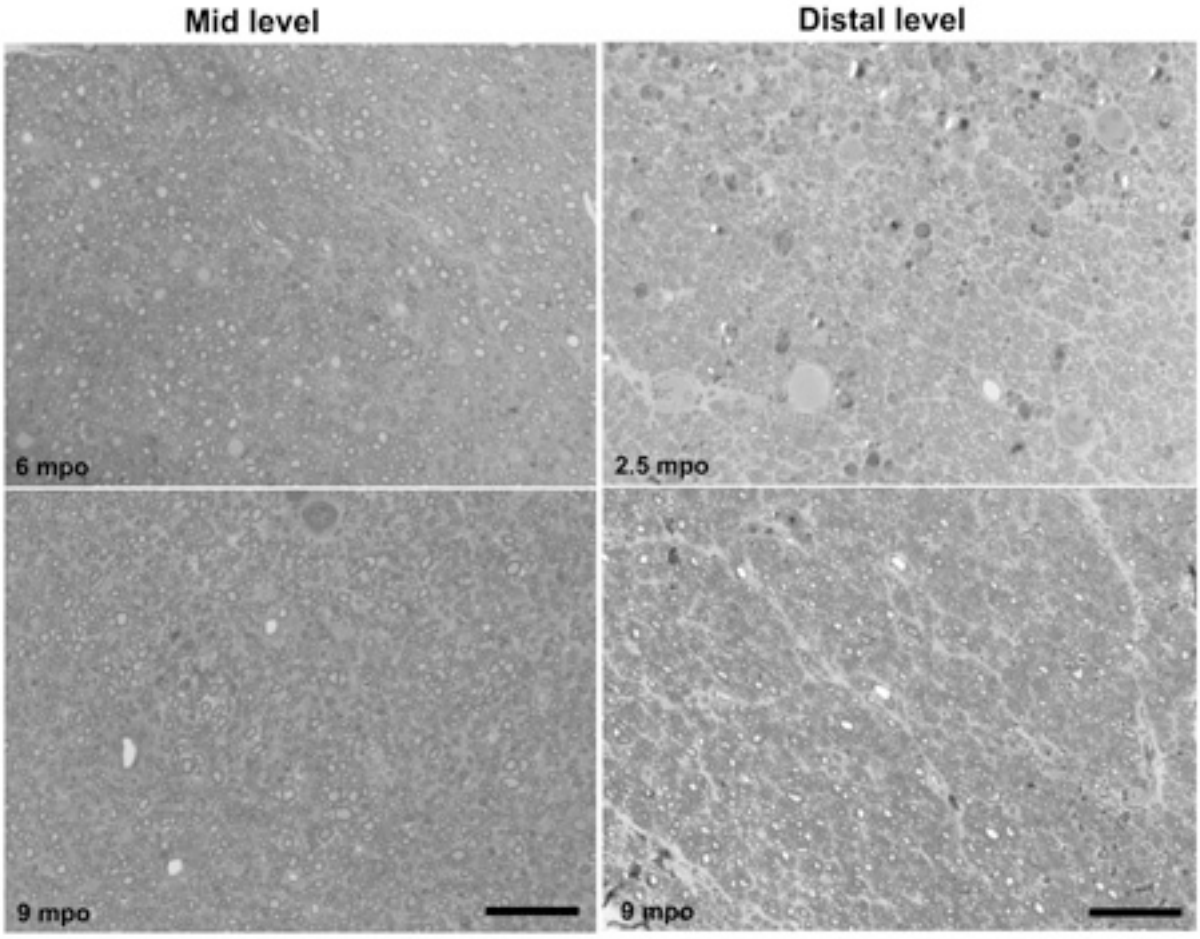

Figure 3. Semithin transverse sections of sciatic nerves representative of regenerated nerves at the mid level, inside the silicone tube, and distal to the silicone tube, at the neuroma after 2.5 and 9 months in rats of the Amputee+SC group. Note the high number and density of myelinated fibers maintained over time. At 2.5 months, there were some figures of Wallerian degeneration at the distal level. Bar = 50 µm.

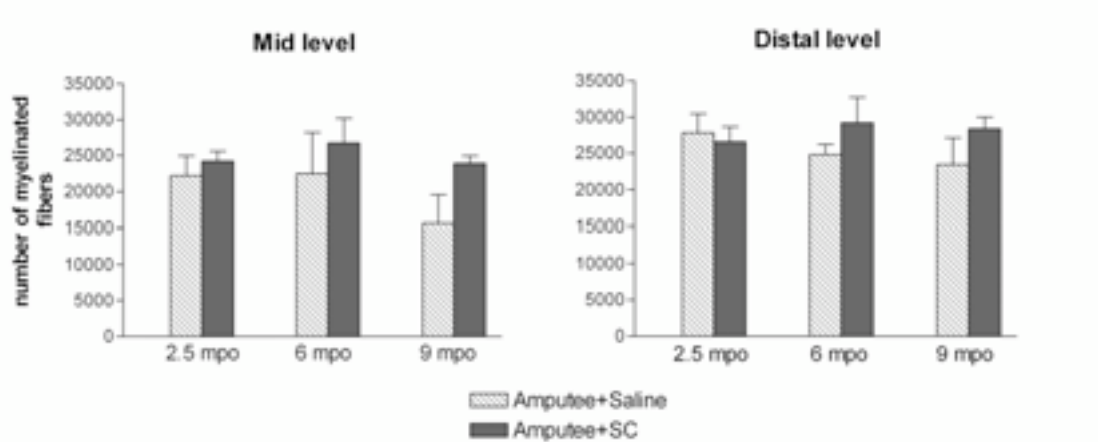

Figure 4. Histogram representation of the numbers of regenerated myelinated fibers (MF) counted on transverse semithin sections at the mid level (inside the silicone tube) and at the distal level (just proximal to the capped chamber) in groups with the capped ending chamber filled with saline or with a suspension of primary SCs.

In the following experiment, SCs from the SCTM41 line were transplanted in the ending chamber. In these groups regeneration occurred in the silicone tube similar to that described above for the Amputee group (see previous manuscript) and Amputee+SC group (Fig. 5). At the mid level the number of myelinated axons was similar in groups with SCTM41 cells and with SCTM41-GDNF cells, and in both slightly lower than in the group with primary SCs (Table 2). However, in one rat of group Amputee+SCTM41, the density of myelinated fibers was low, and the fibers were intermingled with numerous SCs, fibroblasts and some macrophages. This feature became more marked in this group at the distal level, where two of the rats showed only unmyelinated regenerating axons near the capped chamber (Fig. 5c, Fig. 6c). In contrast, in all the rats of group Amputee+SCTM41-GDNF there were a high number of small axons at the distal level, although some areas showed absence of axons and others signs of ongoing Wallerian degeneration (Fig. 5d). In the two groups it appeared to be a surplus of SCs, some in relation to regenerative units and others denervated (Fig. 6). No evidence of cell rejection was observed.

Table 2. Cross-sectional area and number of myelinated fibers in the regenerated nerves at mid and distal levels at 2.5 months postinjury in groups with the sciatic nerve sectioned and repaired with a silicone guide, and the distal nerve segment fixed into a capped tube filled with saline, or with a suspension of primary SCs, of SCTM41 cells or SCTM41-GDNF cells. Values from intact rat sciatic nerves and from nerves with a simple tube repair are also shown for comparison.

		Mid level		*Distal level*	
Group	(n)	Nerve area (mm^2)	Nº MF	Nerve area (mm^2)	Nº MF
Intact nerve	(10)			0.66 ± 0.06	8262 ± 258
Tube repair	(6)			0.40 ± 0.03	13000 ± 1121
Amputee	(4)	0.83 ± 0.15	22216 ± 2730	1.02 ± 0.22	27796 ± 2655
Amputee+SC	(4)	1.11 ± 0.08	24216 ± 1373	0.73 ± 0.07	26589 ± 2064
Amputee+SCTM41	(3)	1.31 ± 0.22	20233 ± 2169	0.87 ± 0.0	24405 ± 4566
Amputee+SCTM41-GDNF	(3)	1.48 ± 0.61	19179 ± 2232	1.06 ± 0.52	22357 ± 2553

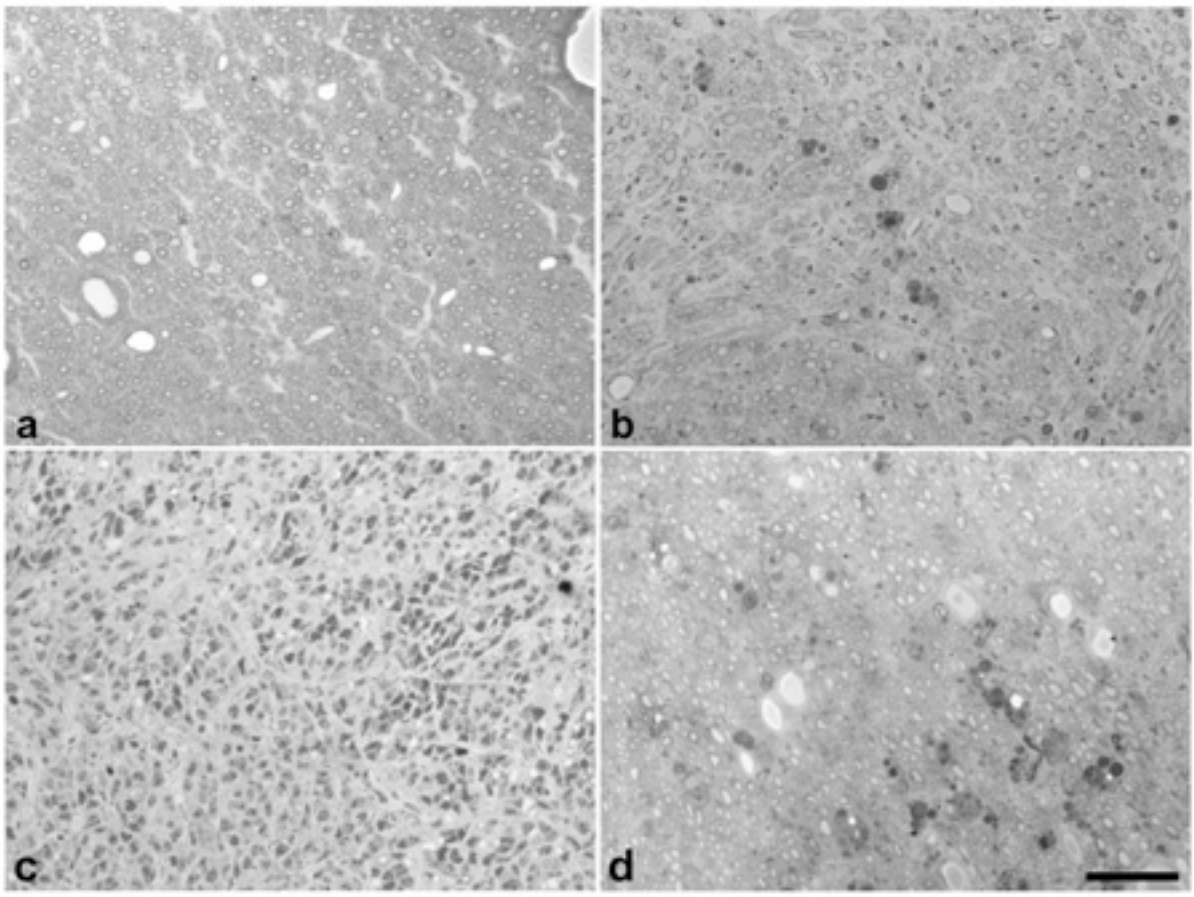

Figure 5. Photomicrographs of semithin transverse sections of regenerated sciatic nerves at mid (a, b) and distal levels (c, d) from Amputee+SCTM41 (a, c) and Amputee+SCTM41-GDNF (b, d) groups. Whereas at mid level the regenerated nerve of the Amputee+SCTM41 rat showed similar features to Amputee+SC rats (a), at the distal level there was a high density of cells filling the whole cross section area and few axons (c). The Amputee+SCTM41-GDNF rat maintained the same density of myelinated fibers at both levels (b, d). Bar = 50μm.

Immunohistochemistry against S100 showed a high number of labeled SCs surrounding axons at the mid level in all the groups (Fig. 7). At the distal level, there was a slight increase in S100 immunoreactive cellsity in groups with SCs compared with the amputee group with saline inside the blinded chamber inside the capped chamber in comparison with Amputee+Saline group (Fig. 8). Some areas of the transverse sections showed groups of denervated S100+ cells, particularly in the group Amputee+SCTM41 (Fig. 8c). Immunolabeling against GDNF did not allow to identify immunoreactive cells above background staining.

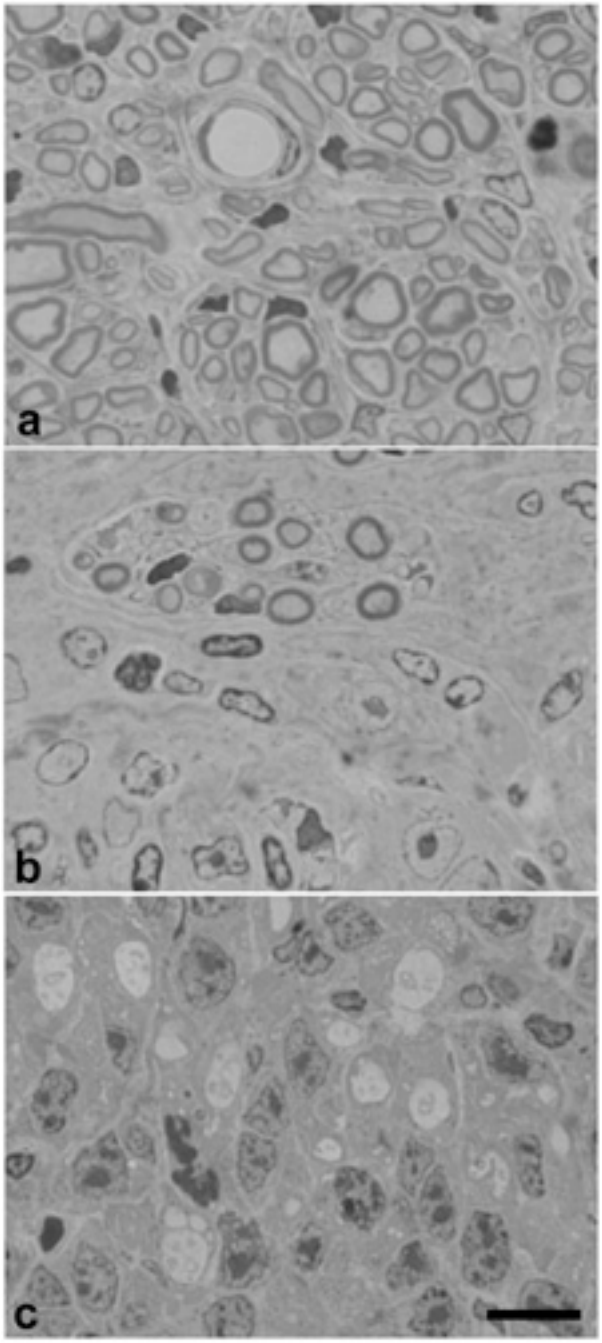

Figure 6. Main features observed in regenerated nerves with SCTM41 or SCTM41-GDNF cells transplanted in the capped chamber at the neuroma level. (a) Semithin transverse section with typical microfascicles in a rat from SCTM41-GDNF group. (b) A regenerative unit contained both myelinated (M) and unmyelinated fibers surrounded by numerous denervated SCs. (c) Unmyelinated fibers surrounded by a high density of cells in a rat from SCTM41 group. Bar = 10µm.

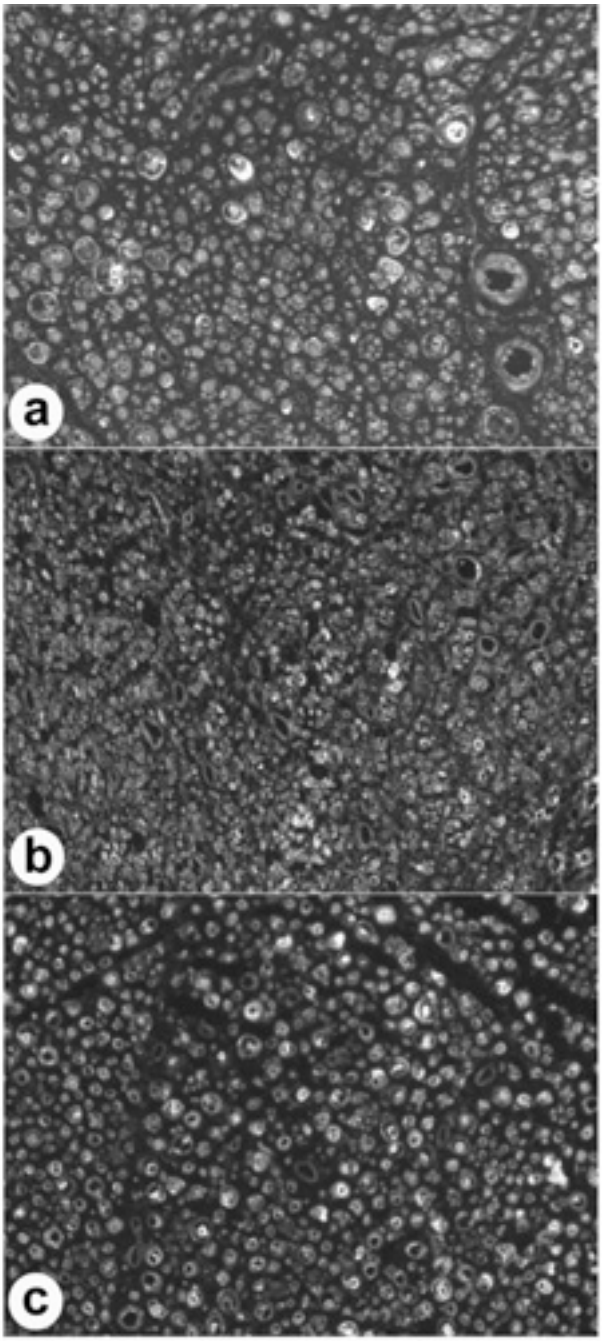

Figure 7. Immunohistochemistry against S100 in representative samples at the mid level of groups Amputee+SC (a), Amputee+SCTM41 (b) and Amputee+SCTM41-GDNF (c). S100-immunoreactivity was observed in all the groups with any noteworthy difference. Bar = 20 μm.

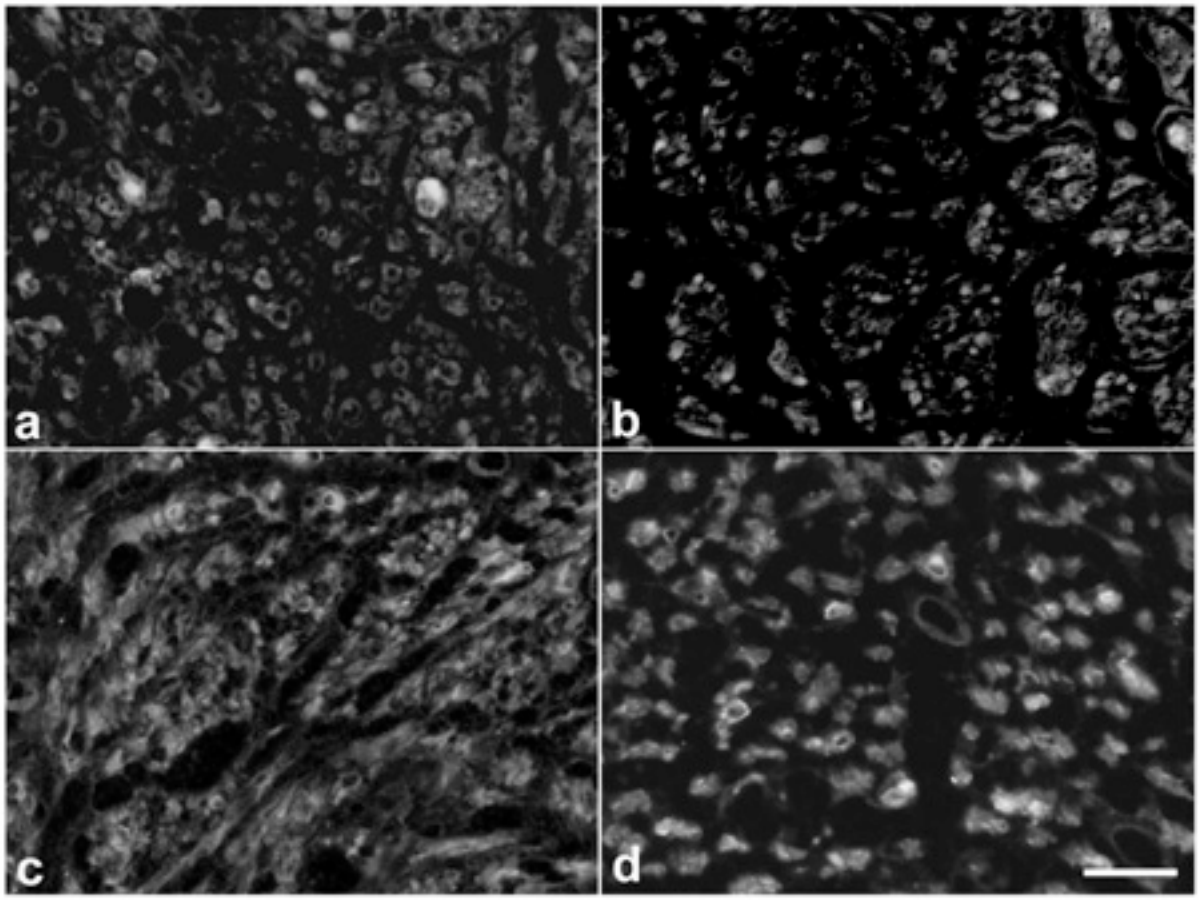

Figure 8. Immunohistochemistry against S100 in samples taken at the neuroma level of groups Amputee (a), Amputee+SC (b), Amputee+SCTM41 (c) and Amputee+SCTM41-GDNF (d). Bar = 20μm.

DISCUSSION

In this work we have assayed if by transplanting SCs in the ending capped chamber, axonal regeneration and maturation can be enhanced over long time without possible reconnection with target organs. Our results, together with those detailed in the previous manuscript, show that following transection and tube repair peripheral nerve fibers can regenerate through a short distal nerve segment, even if ending in a blinded chamber, and sustain distal branches without degenerating for a long time. Nevertheless, there is excessive axonal sprouting forming a neuroma, and the caliber of myelinated fibers remain far lower than normal during the 9 months investigated. With a distal transplant of primary SCs there were slightly more regenerated myelinated axons in the mid segment of the nerve (about 20%) and at the distal neuroma (about 10%) than in groups with saline, indicating that the transplanted cells stimulated the axonal growth response.

The number of myelinated fibers immediately distal to the silicone guide averaged 13000 in the tube repair group at 2.5 months. This value is the same that found in previous studies (Jenq and Coggeshall 1985) using a silicone tube to bridge a short 4 mm gap. Jenq and Coggeshall (1985) found that this number remains steady over 9 months, although the number at the mid-tube level increased from about 9000 at 2 months to 14000 at 9 months, when presumably axon numbers have stabilized. These data suggests that myelinated axons branch in the guide gap giving origin to the surplus axons in the distal stump, but also that regenerating myelinated axons continue growing into the gap for considerable time (Jenq and Coggeshall 1985). This situation is similar to that described after nerve section repaired with epineurial suture, in which the number of myelinated axons was found increased from 2 to 12 months (Mackinnon et al 1991).

Effects of primary SC transplants

In the absence of nerve continuity towards target tissues, the regenerative response is maintained over long term and the numbers of myelinated fibers almost doubled. By 9 months, however, we found a reduction in this number at the guide level, suggesting the elimination of supernumerary branches. The addition of transplanted SCs at the capped chamber seemed to stimulate the neuronal growth program. Reactive SCs in the denervated distal stump after a nerve lesion highly induce the expression of several neurotrophic factors and their receptors, including NGF (Heumann et al., 1987) and GDNF (Hoke et al., 2003). The increased neurotrophic support peaks at about 1 week postaxotomy and declines with time. In contrast, there is no upregulation in a chronically denervated nerve (Hoke et al.,

2003), thus suggesting that one of the reasons for impaired regeneration into chronically denervated peripheral nerves may be the inability of SCs to produce enough trophic support for both motor and sensory neurons. Our results indicate that, by increasing the amount of competent SCs in contact with growing axons, nerve regeneration is enhanced, similarly to what occurs when long gaps are repaired with guides filled with SCs (Guénard et al., 1992; Rodríguez et al., 2000; Udina et al., 2004). Although in the present study we did not investigate the fate of the implanted SCs, previous results from our laboratory (Rodríguez et al., 2000; Udina et al., 2004) and from others (Yu and Kocsis, 2005; Kimura et al., 2005) indicate that transplanted SCs are able to survive and migrate into the recipient nerve at least for a few months.

Peripheral nerve injury results in changes in action potential waveform, ion channel organization, and firing properties of primary afferent neurons (see Devor, 2006). It has been suggested that these changes are the result of reduction in basal trophic support from skin targets. Recently, Yu and Kocsis (2005) have reported on the effects of green fluorescent protein (GFP)-expressing SCs transplanted in a similar model to that used in this study. Two to three weeks after injury and SC injection, they found GFP-SCs extensively distributed throughout the neuroma, and oriented longitudinally along axons proximal to the neuroma. Interestingly, changes in action potential properties of cutaneous sensory neurons observed in a neuroma group (such as reduction of action potential duration and the amplitude and duration of spike afterhyperpolarizations) were attenuated in the GFP-SC group. Thus the engrafted SC procedure ameliorated electrophysiological changes of primary afferents associated with target disconnection and neuroma formation.

Effects of GDNF-expressing SCs

In order to provide the regenerating axons with an additional neurotrophic support, to improve survival of axotomized neurons as well as to promote growth of their axons, we transplanted in the same amputee nerve model SCs that are modified to secrete GDNF. GDNF was chosen because it appears to be involved in the regenerative support of neurons in the peripheral nervous system. Following transection of the sciatic nerve, GDNF mRNA is up-regulated rapidly in the distal denervated nerve along with the mRNA for one of its receptors, GFRalpha-1, in the nerve and in DRG neurons (Hoke et al., 2000, 2002). Administration of high doses of GDNF to adult rats induces SCs to proliferate and myelinate even normally unmyelinated axons (Höke et al., 2003), suggesting that GDNF can be a factor mediating axonal-glial interactions. It has been shown that SC-derived GDNF is taken up by DRG and

motor neurons and transported anterogradely along the axons for release from terminals, where it may act on glial cells expressing GDNF mRNA. GDNF may have other relevant effects in the modulation of neuropathic pain secondary to neuroma formation (Boucher et al., 2000; Wang et al., 2002).

The SCTM41 cell line used has been reported to closely resemble primary SCs, and does not form tumors. Nevertheless, in the group with SCTM41 cells we observed a hindering effect in comparison with the group with primary SCs. Regenerating axons were not found in half of those rats within the distal nerve segment, instead a noticeable increase of cells, mostly denervated SCs, appeared at the neuroma. These results suggest that the SCTM41 cell line by itself is not capable to induce axonal growth in a permissive environment such as the degenerated peripheral nerve. It is worth to comment that untransfected SCTM41 cells do not produce detectable quantities of GDNF, BDNF or NT3 (Wilby et al., 1999), and it may be hypothesized that when transplanted in vivo they may remain as quiescent cells and do not present the pro-regenerative phenotypic changes characteristic of reactive host SCs.

By transfection of the SCTM41 cells with the rat GDNF construct, a derived line overexpressing GDNF was obtained (Wilby et al., 1999). In vivo transplants of SCTM41-GDNF cells in degenerative animal models had a positive effect in enhancing survival and axonal growth of dopaminergic neurons (Wilby et al., 1999) and survival of retinal photoreceptors (Lawrence et al., 2004) in comparison with the parent line. In agreement with these reports, the engineered cells performed also better than the parent cell line in our nerve amputee model, suggesting that the GDNF production favorably influenced axonal regeneration. However, the numbers of myelinated fibers found at the mid and distal levels were lower than with a transplant of primary SCs. Considering that the general morphological features, in terms of axonal density and caliber, were not changed, we interpret that the SCTM41-GDNF improved the regenerative response with respect to the parent SCTM41 cells but did not reach the same potential as the primary SCs.

Individual clones of the SCTM41-GDNF line maintained in culture have been found by ELISA to secrete GDNF at a rate of 92 ng/10^6 cells/day (Wilby et al., 1999). Thus, the quantities of GDNF secreted by our grafts (assuming full survival of transplanted cells) would be 9 ng/day, which are lower than concentrations supplied in experiments in which direct injections of GDNF were given (Boucher et al., 2000; Barras et al., 2002; Fine et al., 2002). Nevertheless, the levels and timing of GDNF production by the SCTM41-GDNF cells once transplanted are unknown. In addition, it should be noted that the donor SCTM41 cells are allografts and, despite the immunosuppression by FK506, there may be a slow loss of cells

because of some form of rejection (Lawrence et al., 2004). Therefore, it is possible that secretion of the growth factor was too low and limited to a short time after transplant to influence the axonal response over the 2.5 months evaluated.

It remains to be seen whether axonal regeneration and maturation can be further improved by grafting a mixture of primary SCs and the GDNF-engineered cell line, or GDNF-engineered primary cells in the same model. Further research is also needed to characterize the long-term viability and response of grafted SCs in the peripheral nerve and in the neuroma.

Acknowledgments

This research was supported by grants IST-2001-35094 (CYBERHAND project) and IST-001917 (NEUROBOTICS project) from the EC. The authors thank the valuable help of Jessica Jaramillo in the morphological studies.

REFERENCES

Arvidsson J, Ygge J, Grant G. Cell loss in lumbar dorsal root ganglia and transganglionic degeneration after sciatic nerve resection in the rat. Brain Res 1986; 373:15-21.

Barras FM, Pasche P, Bouche N, Aebischer P, Zurn AD. Glial cell line-derived neurotrophic factor released by synthetic guidance channels promotes facial nerve regeneration in the rat. J Neurosci Res 2002; 70:746-755.

Boucher TJ, Okuse K, Bennett DLH, Munson JB, Wood JN, McMahon SB. Potent Analgesic effects of GDNF in neuropathic pain states. Science 2000; 290: 124-127

Boyd JG, Gordon T. Neurotrophic factors and their receptors in axonal regeneration and functional recovery after peripheral nerve injury. Mol Neurobiol 2003; 27:277-324.

Carter DA, Lisney SJW. Changes in myelinated and unmyelinated axon numbers in the proximal parts of rat sural nerves after two types of injury. Restor Neurol Neurosci 1991; 3:65-73.

Devor M. Responses of nerves to injury in relation to neuropathic pain. In: McMahon SB, Koltzenburg M (eds), Wall and Melzack's Textbook of Pain. 5th ed. Elsevier Churchill Livingstone, 2006, p. 905-927.

Feltri M, Herer S.S, Wrabertz J, Kamholz J, Shy M.E. Mitogen-expanded Schwann cells retain the capacity to myelinate regenerating axons after transplantation into rat sciatic nerve. Proc Natl Acad Sci USA 1992, 89:8827-8831.

Fine EG, Decosterd I, Papaloizos M, Zurn AD, Aebischer P. GDNF and NGF released by synthetic guidance channels support sciatic nerve regeneration across a long gap. Eur J Neurosci 2002; 15:589-601.

Fu SY, Gordon T. Contributing factors to poor functional recovery after delayed nerve repair: Prolonged denervation. J Neurosci 1995; 15:3886-3895.

Giannini C, Lais AC, Dyck PJ. Number, size, and class of peripheral nerve fibers regenerating after crush, multiple crush, and graft. Brain Res 1989; 500:131-138.

Gómez N, Cuadras J, Butí M, Navarro X. Histologic assessment of sciatic nerve regeneration following resection and graft or tube repair in the mouse. Restor Neurol Neurosci 1996; 10:187-196.

Gordon T, Sulaiman O, Boyd JG. Experimental strategies to promote functional recovery after peripheral nerve injuries. J Periph Nerv System 2003; 8:236-250.

Groves MJ, An SF, Giornetto B, Scaravilli F. Inhibition of sensory neuron apoptosis and prevention of loss by NT-3 administration following axotomy. Exp Neurol 1999; 155:284-294.

Groves MJ, Christopherson T, Giometto B, Scaravilli F. Axotomy-induced apoptosis in adult rat primary sensory neurons. J Neurocytol 1997; 26:615–624.

Guénard V, Kleitman N, Morrissey TK, Bunge RP, Aebischer P. Syngeneic Schwann cells derived from adult nerves seeded in semipermeable guidance channels enhance peripheral nerve regeneration. J Neurosci 1992, 12:3310-3320.

Hall SM. The biology of chronically denervated Schwann cells. Ann N Y Acad Sci 1999, 883:215-233.

Heumann R, Korsching S, Bandtlow C, Thoenen H. Changes of nerve growth factor synthesis in nonneuronal cells in response to sciatic nerve transection. J Cell Biol 1987; 104:1623-1631.

Himes BT, Tessler A. Death of some dorsal root ganglion neurons and plasticity of others following sciatic nerve section in adult and neonatal rats. J Comp Neurol 1989; 284:215-230.

Hoke A, Cheng C, Zochodne DW. Expression of glial cell line-derived neurotrophic factor family of growth factors in peripheral nerve injury in rats. Neuroreport. 2000; 11:1651-1654.

Hoke A, Gordon T, Zochodne DW, Sulaiman OA. A decline in glial cell-line-derived neurotrophic factor expression is associated with impaired regeneration after long-term Schwann cell denervation. Exp Neurol 2002; 173:77-85.

Hoke A, Ho T, Crawford TO, LeBel C, Hilt D, Griffin JW. Glial cell line-derived neurotrophic factor alters axon schwann cell units and promotes myelination in unmyelinated nerve fibers. J Neurosci 2003; 23:561-567.

Jenq C-B, Coggeshall RE. Long-term patterns of axon regeneration in the sciatic nerve and its tributaries. Brain Res 1985; 345:34-44.

Kimura A, Ajiki T, Takeuchi K, Hakamata Y, Murakami T, Hoshino Y, Kobayashi E. Transmigration of donor cells involved in the sciatic nerve graft. Transplant Proc 2005; 37:205-207.

Lawrence JM, Keegan DJ, Muir EM, Coffey PJ, Rogers JH, Wilby MJ, Fawcett JM, Lund RD. Transplantation of Schwann cell line clones secreting GDNF or BDNF into the retinas of dystrophic Royal College of Surgeons rats. Invest Ophthalmol Vis Sci 2004; 45:267-274.

Li H, Terenghi G, Hall SM. Effects of delayed re-innervation on the expression of c-erbB receptors by chronically denervated rat Schwann cells in vivo. Glia 1997; 20:333-347.

Lowrie MB, Lavalette D, Davies CE. Time course of motoneurone death after neonatal sciatic nerve crush in the rat. Dev Neurosci 1994; 16:279-284.

Mackinnon SE, Dellon AL, O'Brien JP.. Changes in nerve fiber numbers distal to a nerve repair in the rat sciatic nerve model. Muscle Nerve 1991; 14:1116-1122.

Otto D, Unsicker K, Grothe C. Pharmacological effects of nerve growth factor and fibroblast growth factor applied to the transectioned sciatic nerve on neuron death in adult rat dorsal root ganglia. Neurosci Lett 1987; 83:156-160.

Persson H, Ibáñez CF. Role and expression of neurotrophins and the trk family of tyrosine kinase receptors in neural growth and rescue after injury. Current Op Neurol Neurosurg 1993; 6:11-18.

Rich KM, Disch SP, Eichler ME. The influence of regeneration and nerve growth factor on the neuronal cell body reaction to injury. J Neurocytol 1989; 18:569-576.

Rich KM, Luszczynski JR, Osborne PA, Johnson EM Jr. Nerve growth factor protects adult sensory neurons from cell death and atrophy caused by nerve injury. J Neurocytol 1987; 16:261-268.

Rodríguez FJ, Verdú E, Ceballos D, Navarro X. Neural guides seeded with autologous Schwann cells improve nerve regeneration. Exp Neurol 2000, 161:571-584.

Scadding JW, Thomas PK. Retrograde growth of myelinated fibres in experimental neuromas. J Anat 1983; 136:793-799.

Terenghi G. Peripheral nerve regeneration and neurotrophic factors. J Anat 1999; 194:1-14.

Udina E, Rodríguez FJ, Verdú E, Espejo M, Gold BG, Navarro X. FK506 enhances regeneration of axons across long peripheral nerve gaps repaired with collagen guides seeded with allogeneic Schwann cells. Glia 2004; 47:120-129.

Valero-Cabré A, Tsironis K, Skouras E, Perego G, Navarro X, Neiss WF. Superior muscle reinnervation after autologous nerve graft or poly-l-lactide-ε-caprolactone (PLC) tube implantation in comparison to silicone tube repair. J Neurosci Res 2001; 63:214-223.

Vanden-Noven S, Wallace N, Muccio D, Turtz A, Pinter MJ. Adult spinal motoneurons remain viable despite prolonged absence of functional synaptic contact with muscle. Exp Neurol 1993; 123:147-156.

Verdú E, Navarro X. The role of Schwann cell in nerve regeneration. En Castellano B, González B, Nieto-Sampedro M (eds): Understanding Glial Cells. Kluwer Academic Pub, 1998, p. 319-359.

Verdú E, Rodríguez FJ , Gudiño-Cabrera G, Nieto-Sampedro M, Navarro X. Expansion of adult Schwann cells from mouse predegenerated peripheral nerves. J Neurosci Methods 2000; 99:111-117.

Verestergaard S, Tandrup T, Jakobsen J. Effect of permanent axotomy on number and volume of dorsal root ganglion cell bodies. J Comp Neurol 1997; 388:307-132.

Wang Y, Chang CF, Morales M, Chiang YH, Hoffer J. Protective effects of glial cell line-derived neurotrophic factor in ischemic brain injury. Ann NY Acad Sci 2002; 962:423-437.

Wilby MJ, Sinclair SR, Muir EM, Zietlow R, Adcock KH, Horellou P, Rogers JH, Dunnett SB, Fawcett JW. A glial cell line-derived neurotrophic factor-secreting clone of the Schwann cell line SCTM41 enhances survival and fiber outgrowth from embryonic nigral neurons grafted to the striatum and to the lesioned substantia nigra. J Neurosci 1999; 19:2301-2312.

Williams LR, Longo FM, Powell HC, Lundborg G, Varon S. Spatial-temporal progress of peripheral nerve regeneration within a silicone chamber. Parameters for a biossay. J Comp Neurol 1983; 218:160-170.

Ygge J. Neuronal loss in lumbar dorsal root ganglia after proximal compared to distal sciatic nerve resection: a quantitative study in the rat. Brain Res 1989; 478:193-195.

Yu K, Kocsis JD. Schwann cell engraftment into injured peripheral nerve prevents changes in action potential properties. J Neurophysiol 2005; 94:1519-1527.

4

Evaluación de la regeneración de axones motores en lesión del nervio periférico. Estrategias para promover la regeneración específica motora y sensorial.

Lago N, Navarro X.
Correlation between target reinnervation and distribution of motor axons in the injured rat sciatic nerve.
J Neurotrauma 2006, 23: 227-240.

Lago N, Rodríguez FJ, Jaramillo J, Navarro X.
Effects of motor and sensory nerve transplants on the amount and specificity of sciatic nerve regeneration.
(Manuscrito).

JOURNAL OF NEUROTRAUMA
Volume 23, Number 2, 2006

Pp. 227–240

Correlation between Target Reinnervation and Distribution of Motor Axons in the Injured Rat Sciatic Nerve

NATALIA LAGO and XAVIER NAVARRO

ABSTRACT

Peripheral nerve injuries are rarely followed by complete return of function. Deficits are particularly important for motor function, resulting in paralysis and muscle atrophy. In different groups, the sciatic nerve was either crushed or transected and repaired by direct suture or by tube repair using silicone or collagen tubes. After 60 days, nerve regeneration was assessed by electrophysiological and functional tests, nerve morphology and immunohistochemistry against choline acetyltransferase (ChAT) for labeling motor axons. Suture and tube repair resulted in similar levels of muscle reinnervation, but significantly lower than after nerve crush. Recovery of walking track pattern was poor in all groups after nerve section. The numbers of regenerated myelinated fibers and of ChAT+ fibers were similar to control values after nerve crush, but increased after section and repair. The normal fascicular architecture and grouping of ChAT+ fibers were maintained after nerve crush, but lost after section and repair, where motor fibers were scattered within small regenerated fascicles throughout the nerve. The loss of fascicular organization was related to the deficient recovery of locomotor function. Thus, labeling of motor axons by ChAT immunohistochemistry provides useful information for the study of the degree and specificity of nerve regeneration.

Key words: ChAT; immunohistochemistry; motor axons; nerve regeneration; peripheral nerve; reinnervation; tube repair

INTRODUCTION

PERIPHERAL NERVE REGENERATION continues to be intensively studied because successful reinnervation is essential for the return of useable function. Damage to peripheral nerves is rarely followed by a complete return of function. Deficits are particularly important for motor function, resulting in paralysis and atrophy of denervated muscles. Although peripheral motor and sensory axons usually survive trauma and are able to regenerate across the injury site and along the distal nerve stump, reinnervation of peripheral targets is usually incomplete and does not lead to recovery of functions in which the denervated organs were originally involved (Fu and Gordon, 1997; Lundborg 2003; Navarro et al., 1994b; Valero-Cabré et al., 2004). It has been shown that despite electrophysiological tests and histological methods show a good degree of target reinnervation, there is poor correlation with recovery of complex functions, such as the walking pattern after sciatic nerve injury in rodents (De

Group of Neuroplasticity and Regeneration, Department of Cell Biology, Physiology and Immunology, and Institute of Neuroscience, Universitat Autònoma de Barcelona, Bellaterra, Spain.

Medinacelli, 1988; Munro et al., 1998; Valero-Cabré and Navarro, 2002). The main reasons for remaining deficits and dysfunctions are: the limited number of axons that succeed in regenerating through the degenerated distal nerve, and the lack of specificity of target reinnervation by regenerated axons.

Differences in regeneration between motor nerves and purely sensory nerves have been investigated (Kawasaki, 2000), but it still remains unclear how the regeneration of motor and sensory axons differs after surgical nerve repair and whether regenerating motor or sensory axons grow faster (Guttmann et al., 1944; Krarup et al., 1988; Navarro et al., 1994b; Verdú and Navarro, 1997). A comparison using a single mixed nerve, in which every axon regenerates under the same conditions, is ideal for investigating the differences in regenerative capabilities of motor and sensory axons of similar caliber. It has been proposed that regeneration of sensory axons dominate that of motor axons, as detected by retrograde labeling, at least during the first weeks after nerve section and immediate suture (Suzuki et al., 1998) or tube repair (Negredo et al., 2004). In contrast, the levels of functional reinnervation achieved at longer term are similar for large myelinated motor and sensory fibers, as evaluated by electrophysiological methods, although for both lower than the levels achieved by thin sensory and sympathetic fibers (Navarro et al., 1994b; Valero-Cabré et al., 2001; Verdú and Navarro, 1997).

The different techniques applied for repairing injured peripheral nerves aim to obtain optimal reinnervation and full recovery of function. Although there have been great improvements in microsurgical techniques, after a complete nerve transection it is not possible to reach adequate target reinnervation because non-specific colonization of the original target by regenerating axons (Lundborg, 1988). This lack of specificity arises from topographic intrafascicular changes generated after the injury, and from the random growth of regenerating sprouts (Abernethy et al., 1992).

In order to correlate results of morphological and electrophysiological assessment of motor axons regeneration, we were interested in finding a reliable method to identify motor axons in the intact and injured peripheral nerve. In previous works, cholinesterase (CE) and carbonic anhydrase (CA) staining were applied for the study and identification of fascicles containing motor and sensory myelinated axons (Macias et al., 1998; Riley et al., 1988; Sanger et al., 1991). Nevertheless, Kawasaki et al. (2000) could identify only 60% of the myelinated sensory fibers and 50% of the myelinated motor fibers in control nerves at the microscopic level compared with the results based on ultraestructural study (Schmalbruch, 1986). In this work, we used immunohistochemistry against choline acetyltransferase (ChAT), which is present in somatic motor peripheral fibers, to compare the intact rat sciatic nerve with the regenerated sciatic nerve after different injuries, in terms of number of regenerated axons, distribution among nerve fascicles and degree of reinnervation. The results show how motor axons dispersion correlates with functional results and that immunohistochemistry against ChAT is a good method to assess the number and topographical specificity of regenerated motor axons after nerve lesions.

MATERIALS AND METHODS

Surgical Procedure and Experimental Design

Operations were performed under pentobarbital anesthesia (40 mg/kg i.p.) in five groups of adult female Sprague-Dawley rats, aged 2.5 months. All experimental procedures were approved by the Ethics Committee of our institution, and followed the European Communities Council Directive 86/609/EEC.

In the Crush group ($n = 5$) the sciatic nerve was crushed during 30 sec in three different orientations by means of a fine forceps (Dumont no. 5). A suture was placed in a neighbor muscle at the level of the crush for later recognition of the injury site. In other three groups the sciatic nerve was transected with sharp microscissors (Vannas-Tübingen spring scissors) and immediately repaired either by direct epineurial suture (four 10-0 atraumatic monofilament sutures, Ethicon) preserving the original alignment of the tibial and peroneal fascicles of the sciatic nerve trunk (group SUT, $n = 5$), or by tube repair leaving a 4-mm gap between the proximal and distal nerve stump bridged with a silicone tube (6 mm long, 2 mm inner diameter [i.d.], 0.5-mm wall thickness; Dicoinsa, Barcelona, Spain) (group SIL, $n = 5$) or with a collagen guide (COL; 6 mm, 1 mm i.d., 0.5 mm wall thickness; Integra LifeSciences, Plainsboro, NJ) (group COL, $n = 5$). In the latter two groups each nerve stump was introduced 1 mm into the end of the tube and was fixed with one 10-0 suture leaving a final interstump gap of 4 mm measured with a microruler. A control group ($n = 5$) was sham operated without injuring the sciatic nerve. The wound was sutured by planes and disinfected with povidone-iodine. In order to prevent neuropathic pain and avoid autotomy after denervation, animals were treated with amitriptyline (150 μg/mL in the drinking water) from two weeks before surgery (Navarro et al., 1994a). All the animals were kept under standard conditions, on soft adsorbent bedding, with access to standard laboratory food and water ad libitum and with a light-dark cycle of 12 h, during 2 months postoperation to allow for nerve regeneration and muscle reinnervation.

Functional Evaluation

At 60 days postoperation all the rats were evaluated by non-invasive tests to assess the success of distal target reinnervation by the regenerating sciatic nerve. Regeneration of large myelinated fibers was assessed by nerve conduction tests (Navarro et al., 1994b; Valero-Cabré et al., 2001, 2004). With the animals under anesthesia (pentobarbital 40 mg/kg i.p.), the nerve was stimulated through a pair of needle electrodes placed at the sciatic notch with single electrical pulses of 0.05 ms duration up to supramaximal intensity. The compound muscle action potentials (CMAPs) were recorded from the medial gastrocnemius muscle and from the plantar muscles (at the third interosseus space) with small needle electrodes. Similarly, sensory compound nerve action potentials (CNAPs) were recorded by electrodes placed near the tibial nerve at the ankle and near the digital nerves of the fourth toe. The evoked action potentials were displayed on a storage oscilloscope (Sapphire 4M, Medelec Vickers) at settings appropriate to measure the amplitude from baseline to peak and the latency to the onset. For normalization of the data, values obtained in the operated hindlimb were expressed as percentage of values of the contralateral limb for each animal.

Pain sensitivity in the hindpaw was tested by light pricking three times with a blunt needle in each of five areas, from the most proximal pawpad to the tip of the second digit on the plantar surface of the paw. The animal response was scored as no response (0), reduced (1) or normal reaction (2) in each area tested, and the 5 scores added into a pinprick score (PP) (Navarro et al., 1994b). Recovery of nociception was also quantitated by thermal algesimetry (Hargreaves et al., 1988) using a Plantar Algesimeter (Ugo Basile). Rats were placed into a plastic box with an elevated glass floor. The beam of a projection lamp was focused from the bottom of the box onto the plantar surface of the hindpaw. The time spent until withdrawal of the heated paw was measured through a time-meter coupled with IR detectors. The value for a test was the mean of three trials separated by 30-min resting periods. The values were normalized as the percentage of withdrawal latency of the operated versus the contralateral intact hindpaw each testing day.

The walking track test was carried out prior to surgery and at 30 and 60 days postoperation, to assess the recovery of locomotor function. The plantar surface of the rat hindpaws was painted with acrylic paint and the rat left to walk along a corridor with white paper at the bottom. Footprints corresponding to the operated and intact paws were easily identified. The print length (PL) and the distance between the 1st and 5th toes (TS) and between the 2nd and 4th toes (IT) were measured with a precision device. The three parameters were combined in the Sciatic Functional Index (SFI) (De Medinacelli et al., 1982; Bain et al., 1988) to quantify the changes in walking pattern. The SFI varies between 0 (for uninjured) and about −100 (for maximally impaired gait).

Morphological Evaluation

After functional testing, animals were deeply anesthetized and perfused transcardially with 4% paraformaldehyde in phosphate-buffer saline solution (PBS, 0.1 M, pH 7.4). The sciatic nerve was harvested and two segments sampled, one at 2 mm from the injury site for immunohistochemistry and another segment at 5 mm distal to the injury site in groups Crush and SUT, or just distal to the tube in groups SIL and COL for morphology. Control rats were perfused in the same solution, and a segment of the sciatic nerve from the same location at the midthigh was collected and processed in parallel. This segment was postfixed in glutaraldehyde-paraformaldehyde (3%/3%) in cacodylate-buffer solution (0.1 M, pH 7.4) overnight at 4°C, and then processed for embedding in Epon resin. Semithin sections 0.5 μm thick were stained with toluidine blue and examined by light microscopy. Images of the whole sciatic nerve were acquired at 10× with an Olympus DP50 camera attached to a computer, while sets of images chosen by systematic random sampling of squares representing at least 30% of the nerve cross-sectional area were acquired at 100×. Measurements of the cross-sectional area of the whole nerve, area of bundles of regenerated fibers, as well as counts of the number of myelinated fibers were carried out by using NIH Image software.

Immunohistochemistry

Segments of the regenerated sciatic nerves taken at 2 mm from the injury in groups Crush and SUT or inside the guide in groups with tube repair were collected and postfixed in the same perfusion solution for 4 h. Samples were washed in phosphate-buffer (PB; 0.1 M, pH 7.4) and stored in the same buffer with azide 0.1% for embedding in paraffin. Transverse sections (4 μm thickness) were cut with a microtome, mounted in (3-aminopropyl)triethoxysilane-coated slides and dried overnight. The sections were deparaffinized and rehydrated before staining. Antigen retrieval was performed with sodium citrate (pH 6.1) during 20 min at 95°C. Then sections were washed with Trizma buffer solution (TBS, 0.05M, pH 7.4; Sigma) and placed in 2% H_2O_2 in 70% methanol for 25 min at room temperature. After washing with TBS and TBS plus 0.05% Tween-20 (Fluka) (TBST) sections were incubated for 24 h at 4°C with primary antibodies: anti-NF200 (Chemicon; 1:400) which reacts with the 200-kDa neurofilament regions, and goat polyclonal antiserum to ChAT (AB144P, Chemicon;

Table 1. Neurophysiological Results of Target Reinnervation by Regenerated Nerves 60 Days after Injury and Repair of the Sciatic Nerve in the Different Groups of Rats Evaluated

	Intact nerves, n = 20	*Crush, n = 5*	*SUT, n = 5*	*SIL, n = 5*	*COL, n = 5*
Gastrocnemius muscle					
Latency (msec)	1.35 ± 0.04	2.18 ± 0.2[a]	2.49 ± 0.1[a]	3.0 ± 0.2[abc]	3.1 ± 0.2[abc]
CMAP (mV)	59.2 ± 1.7	47.9 ± 1.5[a]	18.0 ± 3.3[ab]	14.0 ± 1.3[ab]	15.8 ± 2.4[ab]
Plantar muscle					
Latency (msec)	2.8 ± 0.04	5.3 ± 0.2[a]	6.0 ± 0.5[a]	6.7 ± 0.5[a]	7.0 ± 1.1[a]
CMAP (mV)	7.59 ± 0.53	2.63 ± 0.36[a]	0.48 ± 0.09[ab]	0.37 ± 0.06[ab]	0.39 ± 0.07[ab]
Tibial nerve					
Latency (msec)	1.2 ± 0.03	1.7 ± 0.04[a]	1.5 ± 0.06[a]	1.6 ± 0.04[a]	1.6 ± 0.08[a]
CNAP (μV)	173.4 ± 13.9	123.0 ± 5.1	55.3 ± 8.3[ab]	39.5 ± 13.3[ab]	57.8 ± 13.4[ab]
Digital nerve					
Latency (msec)	2.2 ± 0.02	3.7 ± 0.3[a]	3.9 ± 0.6[a]	4.3 ± 0.9[a]	4.3 ± 0.6[a]
CNAP (μV)	15.4 ± 0.8	8.3 ± 1.8[a]	5.6 ± 0.7[a]	3.0 ± 0.3[abc]	3.9 ± 0.8[a]
Pinprick score	10 ± 0.0	10 ± 0.0	9.2 ± 0.6[a]	4.6 ± 1.0[abc]	4.8 ± 0.3[abc]
Algesimetry (% of contralateral limb)	104 ± 6	99 ± 4	157 ± 18[ab]	163 ± 20[ab]	146 ± 10[ab]

$p < 0.05$ vs. Intact nerves[a], vs. group Crush[b], and vs. group SUT[c].

SUT, epineurial suture repair; SIL, repair with a silicone tube; COL, repair with a collagen guide; CMAP, compound muscle action potential; CNAP, compound nerve action potential.

Values are mean ± SEM.

1:50). Slides were washed with TBST and incubated with biotinylated secondary antibodies (Vector; 1:200) for 1 h at room temperature. After further washing the slides were incubated with ABC (avidin-biotin complex, Vector; 1:200) for 1h at room temperature and incubated for 3 min with 3,3-diaminobenzidine tetrahydrochloride solution (D5637; Sigma), counterstained with hematoxylin, dehydrated and mounted with DPX (Fluka). Images of the whole sciatic nerve were acquired at 10×, while sets of systematic randomly chosen images representing at least 30% of the nerve cross-sectional area were acquired at 100×. Area measurements and counts of ChAT-positive axons were carried out by using NIH Image software. ChAT+ fibers were counted if brown staining was present in individual myelinated fibers, whereas small grouped fibers corresponding to unmyelinated sympathetic sudomotor fibers, discernible by the lack of myelin sheath, were not counted. To quantify the distribution of motor axons within the nerve, counts of the number of ChAT+ fibers within each of the chosen fields was used to calculate the coefficient of variation (CV; SD/mean ± 100%). The CV allows for the comparison of variability between populations with different means. A low CV indicates that the axons were distributed evenly across the cross section, whereas a high CV indicates more segregation (Franz et al., 2005).

Statistical Analysis

All results are expressed as mean ± SEM. Statistical comparisons between groups and intervals were made by

FIG. 1. Representative recordings of compound muscle action potentials from plantar muscles in rats of groups crush (**A**), epineurial suture repair (SUT; **B**), and repair with a silicone tube (SIL; **C**). Horizontal scale, 2 msec/square; vertical scale, 1 mV/square (A), 0.5 mV/square (B,C).

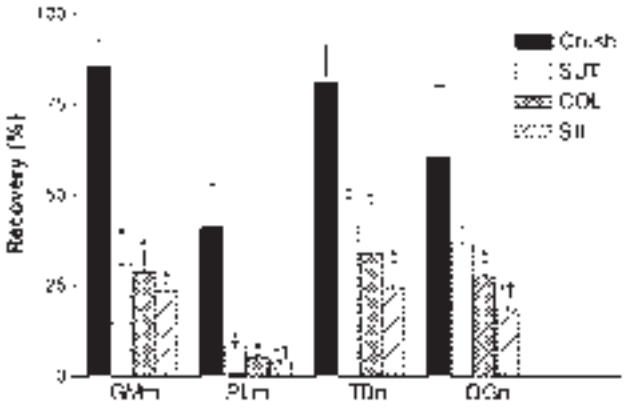

FIG. 2. Histogram of percentage recovery of compound muscle action potential (CMAP) amplitude of gastrocnemius and plantar muscles and compound nerve action potential (CNAP) amplitude of tibial and digital nerves in the four groups of rats after sciatic nerve injury. $^{*}p < 0.05$ versus group crush; $^{\dagger}p < 0.05$ versus group epineurial suture repair (SUT).

one-way ANOVA followed by posthoc Scheffé test and by non-parametric Kruskal-Wallis and Mann-Whitney *U* tests. The relationships between results of functional and morphological tests were analyzed using Pearson correlation tests. A value of $p < 0.05$ was considered to be statistically significant.

RESULTS

Functional Tests

Functional tests performed at 60 days postoperation indicated successful reinnervation of distal targets by the regenerating sciatic nerve in all the rats of the different groups evaluated. Table 1 shows the results of the neurophysiological tests for each group. In all rats stimulation of the injured right sciatic nerve evoked CMAPs and CNAPs in the tested muscles and nerves that were of longer latency and lower amplitude compared to the intact nerves (see Fig. 1). Rats of group Crush showed the highest values of CMAP amplitudes (about 85% of control values in the gastrocnemius muscle and 41% in the plantar muscle) and CNAP amplitudes (81% in the tibial nerve and 60 % in the digital nerve). These values were significantly higher than in groups SUT (31%, 8%, 41%, and 37%, respectively), COL (29%, 5%, 34%, and 28%) and SIL (23%, 4%, 24%, and 18%) (Fig. 2). For rats with nerve transection and surgical repair better recovery was found in group SUT than in groups with tube repair although differences did not reach significance for most values. The latency of CMAPs and CNAPs was significantly increased with respect to control values in all injured groups, showing group Crush the shortest mean latencies compared with the other injured groups.

Pain sensibility recovered in all the paw areas in groups Crush and SUT, but was incomplete in groups COL and SIL (about 50%; Table 1). The time to paw withdrawal found during the thermal algesimetry test was significantly longer (145–165%) in the operated hindlimb than in the intact contralateral hindlimb in rats with nerve transection and repair whereas in rats with nerve crush groups the values were close to normal.

Paw prints obtained in the walking track test showed reduced toe spreading (TS and IT factors) and longer PL in the operated paw compared to the intact paw in rats of groups SUT, COL, and SIL, yielding a SFI of −79 to −89. Rats of the group Crush were the only ones showing a noticeable recovery of walking track parameters to values that did not differ from those of control rats (Table 2).

Morphological Evaluation

The macroscopic examination during final dissection evidenced that, in all animals, the sciatic nerve had regenerated. The transverse nerve area was smaller than that of the intact sciatic nerve in all the experimental

TABLE 2. WALKING TRACK ANALYSIS AT 60 DAYS POSTINJURY

Group	*PL (%)*	*TS (%)*	*IT (%)*	*SFI*
Control	100.1 ± 2.1	100.1 ± 2.4	101.9 ± 4.5	−6.0 ± 3.2
Crush	100.3 ± 2.8	108.3 ± 3.2	103.7 ± 6.2	0.65 ± 5.0
SUT	137.5 ± 6.9[ab]	53.0 ± 4.9[ab]	70.4 ± 7.5[ab]	−78.5 ± 6.9[ab]
SIL	120.5 ± 8.0[a]	46.3 ± 4.2[ab]	49.1 ± 2.5[ab]	−81.6 ± 6.1[ab]
COL	129.4 ± 14.4[a]	42.2 ± 10.8[ab]	53.4 ± 3.2[ab]	−89.5 ± 9.7[ab]

$p < 0.05$, vs. group Control[a], and vs. group Crush[b].

PL, print length; TS, toe spreading, IT, intermediary toe spreading in percent of contralateral values; SFI, Sciatic Functional Index; SUT, epineurial suture repair; SIL, repair with a silicon tube; COL, repair with a collagen guide.

Values are mean ± SEM.

TABLE 3. CROSS-SECTIONAL AREA AND NUMBER OF MF COUNTED IN SEMITHIN SECTIONS UNDER LIGHT MICROSCOPY, AND TOTAL NUMBER OF MF COUNTED IN IMMUNOHISTOCHEMISTRY LABELING, NUMBER OF CHAT-LABELED MF, AND CV OF CHAT-LABELED MF AS A MEASUREMENT OF TOPOGRAPHICAL DISTRIBUTION IN THE REGENERATED NERVES AFTER SCIATIC NERVE INJURY

	Control, n = 5	*Crush, n = 5*	*SUT, n = 5*	*SIL, n = 5*	*COL, n = 5*
Light microscopy					
Nerve area (mm^2)	0.66 ± 0.06	0.49 ± 0.09	0.39 ± 0.03	0.42 ± 0.04	0.37 ± 0.02
No. MF	8371 ± 225	8219 ± 126	13937 ± 689[ab]	15132 ± 652[ab]	14187 ± 771[ab]
Immunohistochemistry					
No. MF	6991 ± 188	7639 ± 149	10521 ± 237[ab]	12645 ± 278[ab]	11183 ± 230[ab]
No. ChAT + fibers	1674 ± 64	1735 ± 67	2303 ± 150	3810 ± 293[a]	2492 ± 392
Distribution ChAT + (CV%)	85 ± 5	77 ± 5	57 ± 7	58 ± 9	42 ± 5[a]

$p < 0.05$ vs. group Control,[a] and vs. group Crush.[b]

MF, myelinated fibers; ChAT, choline acetyltransferase; CV, coefficient of variation; SUT, epineurial suture repair; SIL, repair with a silicone tube; COI, repair with a collagen guide.

Values are mean ± SEM.

groups. The number of myelinated fibers was significantly higher in groups SUT, SIL and COL than in group Crush and in control nerves (Table 3). In groups SUT, SIL and COL the regenerated nerve was organized in multiple small fascicles and the myelinated fibers were of small caliber, whereas the morphological appearance in rats subjected to a crush was similar to intact nerves (Fig. 3).

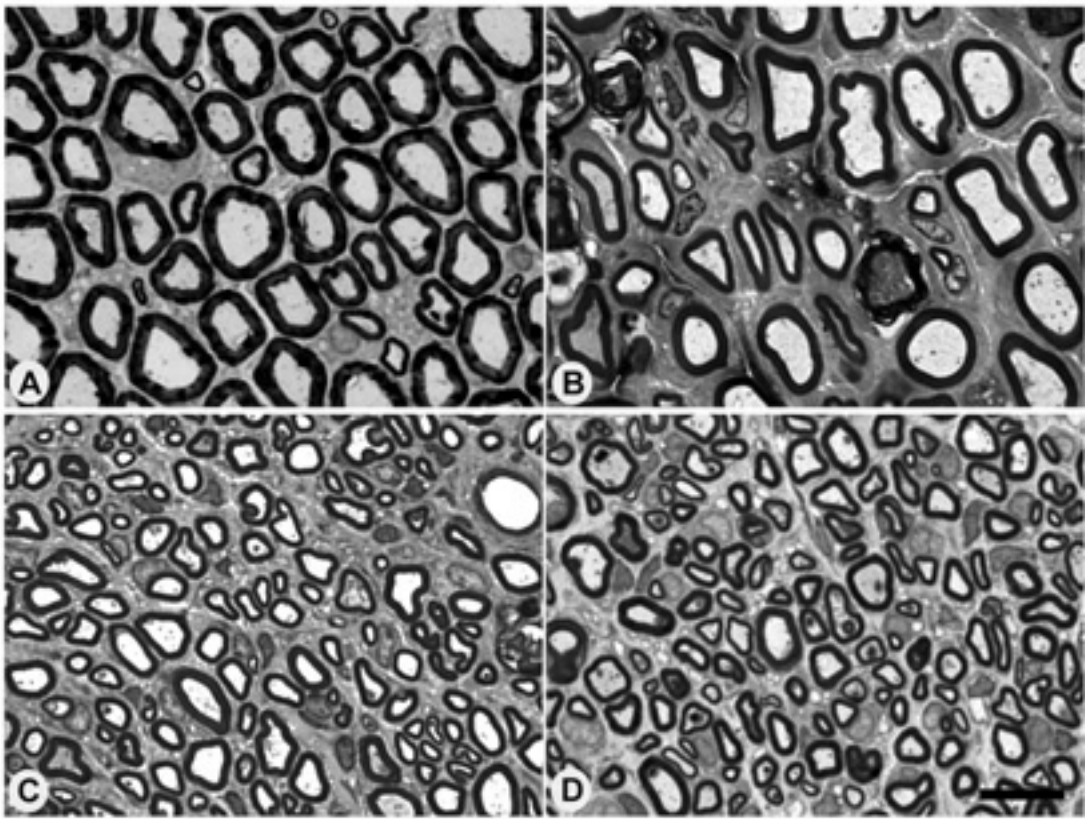

FIG. 3. Representative micrographs of transverse sections of the sciatic nerve in groups control (**A**), crush (**B**), epineurial suture repair (SUT; **C**) and repair with a collagen guide (COL; **D**) at 60 days postoperation. Note the increased density and decreased size of regenerated myelinated fibers in C and D in comparison with the control nerve. Scale bar = 10 μm.

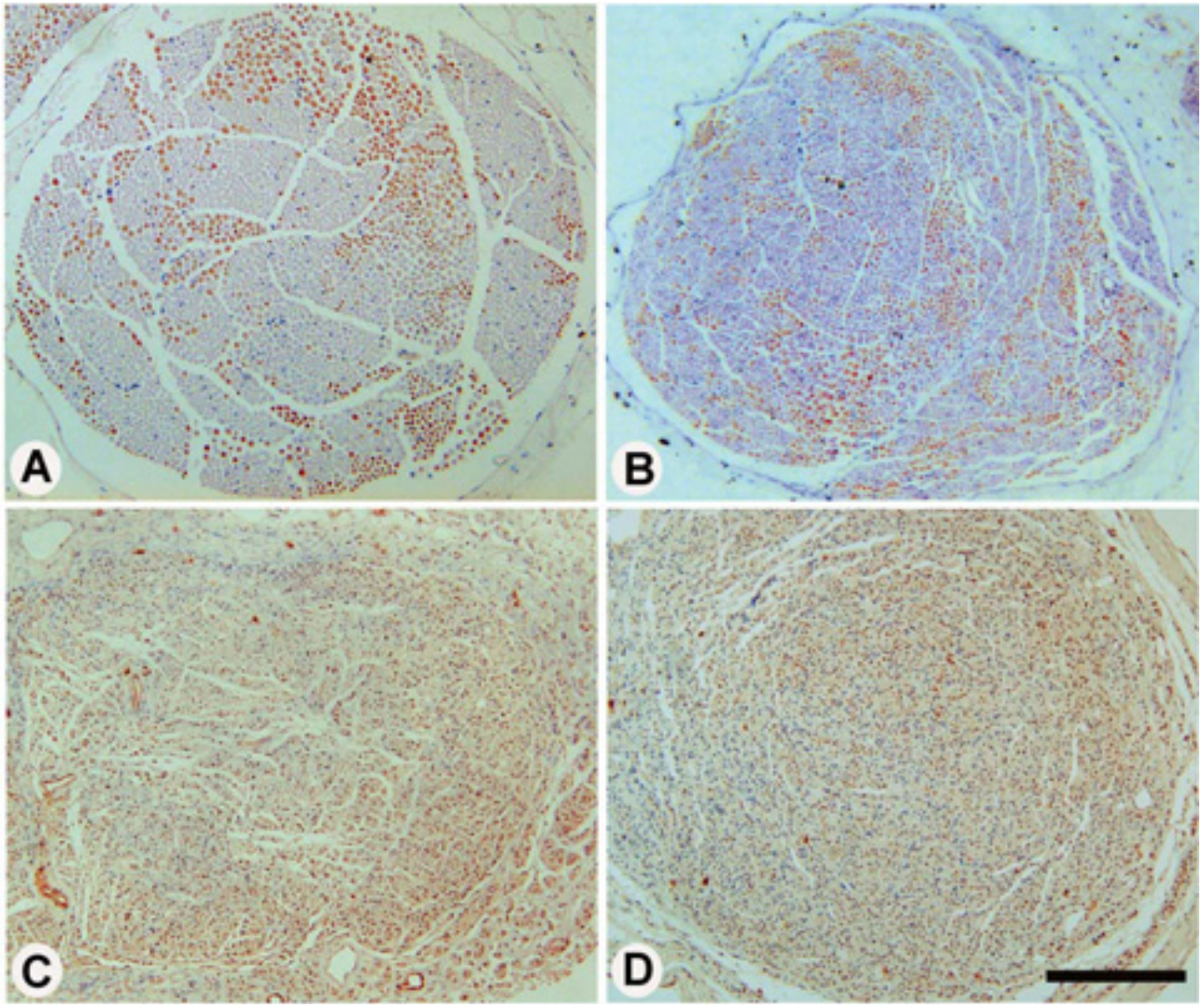

FIG. 4. Immunohistochemical labeling against choline acetyltransferase (ChAT) counterstained with hematoxylin in transverse sections of a control sciatic nerve (**A**), and a representative regenerated nerve of groups crush (**B**), epineurial suture repair (SUT; **C**), and repair with a silicone tube (SIL; **D**). Note the characteristic fasciculation pattern and motor fiber grouping in the control sciatic nerve (A), which is preserved after crush (B), and the scattered distribution of regenerated motor fibers after nerve section and repair, (C,D). Scale bar = 200 μm.

Immunohistochemistry

The number of ChAT+ axons counted in the intact rat sciatic nerve averaged 1674, that is, about 20% of the number of myelinated fibers. The number of ChAT+ fibers was similar to control in group Crush, but increased in groups with section and repair, with significant difference in group SIL compared with groups Control, Crush, and SUT (Table 3). When comparing the number of ChAT+ fibers with the total number of myelinated fibers counted by immunohistochemistry against NF-200, the proportion of motor axons averaged about 20–30% in the four injured groups, within the range of control nerves.

Regarding the distribution of ChAT-labeled fibers, the normal sciatic nerve showed a clear fasciculation pattern of motor axons. They tended to group together with other large myelinated fibers, likely muscular afferents. This organization was maintained in nerves regenerated after a crush injury (Fig. 4), whereas in groups SUT, SIL, and COL ChAT+ fibers regenerated dispersed throughout the cross-sectional area within the small fascicles. In spite of

this general disorganization, there were some microfascicles with prevalent ChAT+ fibers and others without (Fig. 5).

To characterize quantitatively the distribution of ChAT+ motor axons in an unbiased manner, we counted the number of labeled fibers in microscope fields covering an area of 30% of a single nerve cross section. The CVs were used to assess quantitatively the clustering of motor fibers. The CV was high (85%) in control intact sciatic nerves, indicating a clustered distribution of motor axons (Table 3). The mean CV 60 days after a crush injury was slightly decreased, whereas after transection and repair the CVs were substantially lower (<60%) than in control nerves. A low CV reflects the even distribution of regenerating sprouts in the distal nerve stump.

On another hand, there was a slight difference between counting myelinated fibers in resin-embedded semithin sections and in paraffin-embedded thin sections. Immunohistochemical labeling against NF-200 yielded numbers that were 75–93% of those counted in toluidine-stained semithin sections depending upon the group. The short distance between nerve segments taken for each method should not influence since at this level the sciatic nerve has no branches. The most likely reason is the lower resolution of immunohistochemical labeling on paraffin sections, so that a proportion of small axons with a thin myelin sheath are not clearly labeled and not counted. This problem accounts for a slightly higher proportion in regenerated nerve, where axons have smaller diameter for long time (Jenq and Coggeshall, 1985; Gómez et al., 1996).

Functional Recovery and Motor Axons Regeneration

When all animals were considered significant positive correlations were found between the measurements that mainly reflect motor functional recovery (CMAP of gastrocnemius and plantar muscles and the SFI) (Table 4). Moreover, negative significant correlations were also found between each of the measurements of functional recovery and the number of total regenerated myelinated fibers and the number of ChAT+ fibers, further indicating the presence of an excessive number of regenerative sprouts in animals with lower levels of reinnervation. On the contrary, positive significant correlations were found between functional recovery and the CV of ChAT+ fibers in the sciatic nerve.

DISCUSSION

The results of this study show that, after sciatic nerve section, repair with fascicular epineurial suture or with collagen or silicone guides provide similar levels of muscle reinnervation, as judged by the amplitude of CMAPs, that were significantly lower than after nerve crush. Despite evidence of hindlimb muscles reinnervation, recovery of the walking track pattern was very poor in all groups after sciatic nerve section. In contrast, the number of regenerated myelinated fibers 60 days after injury was similar to the control values after sciatic nerve crush, but significantly increased after section and repair. The number of ChAT-labeled motor axons was also higher than normal in the regenerated nerves after section and repair, although the most interesting finding was that the normal fascicular architecture was maintained after nerve crush but lost after section, and in these cases motor fibers were present scattered within small regenerated fascicles. The loss of fascicular organization was significantly correlated with the deficient recovery of motor function.

Motor Recovery after Different Types of Lesions

After peripheral nerve crush injury complete axotomy is produced, resulting in degeneration of the distal axonal segment, but the epineurial sheaths and the endoneurial tubes remain intact in continuity. Regenerating axons from the proximal stump are adequately guided by the intrinsic guidance provided by the endoneurial tubes, and reinnervation of the correct peripheral targets occurs (Valero-Cabré et al., 2004). This explains the satisfactory recovery in this group and the preservation of motor axons grouping observed in immunohistochemically labeled sections. Swett et al. (1990) showed by using retrograde labeling that all motoneurons survived after nerve crush injury, although about 16% were not labeled in the distal nerve; the unlabeled group was composed mainly of small motoneurons whose axons probably had not regenerated distal to the crushed zone. This possible deficit would explain the reduced CMAP amplitude found at distal plantar muscles, despite functional recovery for locomotion and pain responses appear almost complete in group Crush.

In contrast, after complete nerve transection epineurial, perineurial and endoneurial sheaths are disrupted, and the stumps retracted by elastic forces. The intrinsic guidelines, that is, basal lamina and Schwann cell columns, are interrupted and the regenerating fibers are not able to restore the original innervation pattern (Horch, 1970). Tube repair behaves similar to direct suture repair, although it may offer advantages in that it prevents fibrous entrapment of the injured nerve (Ashur et al., 1987) and is less affected by difficulties in the correct alignment of nerve fascicles (Evans et al., 1991). Target reinnervation, proved by neurophysiological tests, was slightly though not significantly lower after tube repair than after

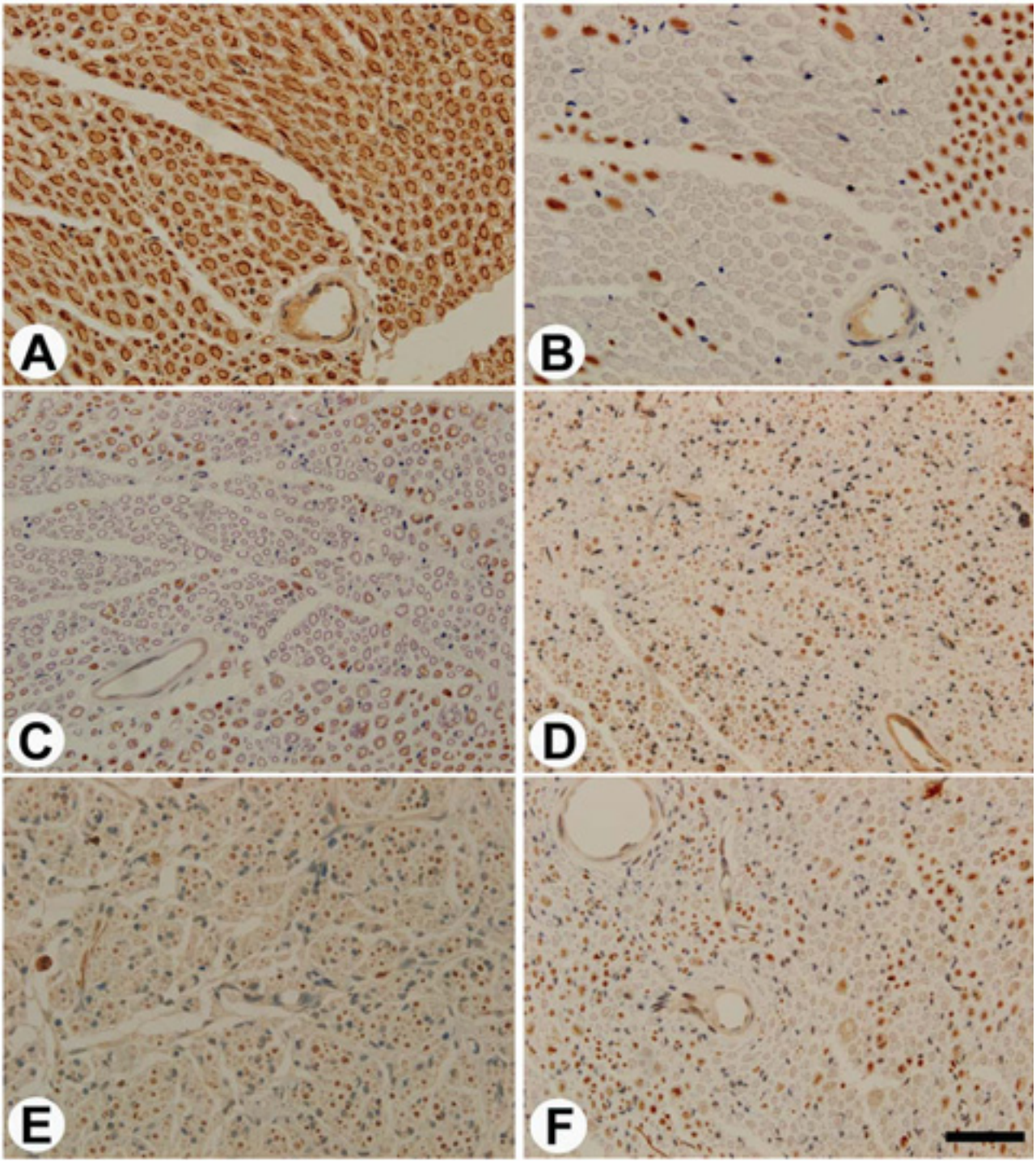

FIG. 5. Immunohistochemical labeling against NF200 in a control sciatic nerve (**A**) and against choline acetyltransferase (ChAT) in a consecutive section of the same control nerve (**B**) and in regenerated sciatic nerves of groups crush (**C**), epineurial suture repair (SUT; **D**), repair with a collagen guide (COL; **E**) and repair with a silicone tube (SIL; **F**). Samples were counterstained with hematoxylin. Scale bar = 40 μm.

Table 4. Correlation Analyses between Measurements of Motor Functional Recovery (Muscle Reinnervation and Walking Pattern [SFI]) and of Morphological Regeneration (Number of MF, Number and Distribution of ChAT-Labeled Motor Axons) in the Experimental Groups Evaluated

	CMAP plantar	*SFI*	*No. MF*	*No. ChAT + MF*	*CV ChAT + MF*
CMAP gastrocnemius	0.851^{**}	0.908^{**}	-0.781^{**}	-0.661^{**}	0.701^{**}
CMAP plantar	—	0.747^{**}	-0.699^{**}	-0.552^{*}	0.582^{**}
SFI	—	—	-0.822^{**}	-0.526^{*}	0.663^{**}
No. MF	—	—	—	0.479^{*}	-0.625^{**}
No. ChAT + MF	—	—	—	—	-0.486^{*}

Pearson correlation test: $^{*}p < 0.05$; $^{**}p < 0.01$.

Values are the correlation coefficient.

SFI, Sciatic Functional Index; MF, myelinated fibers; ChAT, choline acetyltransferase; CMAP, compound muscle action potential; CV, coefficient of variation.

epineurial suture, in agreement with previous reports comparing the same models (Navarro et al., 1994b; Valero-Cabré et al., 2004). Collagen guides allowed for similar levels of regeneration compared to silicone tubes for the short 4-mm gap left, although they have been shown to behave better when bridging long nerve gaps (Gómez et al., 1996; Navarro et al., 1996). Recovery of complex functions, such as coordinated walking, after peripheral nerve injury requires not only muscle reinnervation, but also its accuracy. Our results indicate that only when regeneration was intrinsically guided after nerve crush, there was an appreciable recovery of the walking track original pattern, whereas repair by direct suture or by a tube leaving a gap resulted in significant impairment of the walking track pattern (De Medinaceli et al., 1982; Shenaq et al., 1989; Valero-Cabré and Navarro, 2002).

Motor Axon Regeneration

Histological analyses of nerve regeneration using conventional light and electron microscopy can not differentiate between distinct functional types of axons, and thus would fail to reveal potentially important differences between motor and sensory axon regrowth. Most studies attempting to compare motor and sensory nerve regeneration have used labeling of neuronal somata at ventral horn and dorsal root ganglia, respectively, by using retrograde tracers applied to the regenerated nerve. Sensory fibers regenerate more dominantly than motor fibers in the early stage of nerve regeneration (Suzuki et al., 1998). At later stages after nerve section and epineurial suture the proportion of regenerating sensory and motor neurons has been shown to be similar or slightly higher for the former (Madorsky et al., 1998; Puigdellivol et al., 2002). However, motor neurons regenerate in significantly lower proportion than sensory ones in situations where regeneration is compromised, such as in synthetic nerve guides with a long gap (Bailey et al., 1993; Madorsky et al., 1998) or through sieve electrodes (Negredo et al., 2004; Lago et al., 2005). Nevertheless, methodological issues and variability among different combinations of retrotracers have to be taken into account in such studies (Puigdellivol et al., 2002). Using combined CE and CA histochemical staining it has been reported that CA+ sensory fibers grew earlier than CE+ motor fibers in the neuroma developed after cutting the sciatic nerve (Macias et al., 1998; Sanger et al., 1991). Intrinsic differences between sensory and motor neurons were corroborated in the median-ulnar nerves where the cell bodies were at similar distances from the injury site and revealed that motor axon lagged behind sensory axon regeneration (Macias et al., 1998).

We used immunohistochemistry against ChAT to label the motor axons population in the rat sciatic nerve. The method used allows labeling of ChAT+ myelinated alphamotor and unmyelinated sympathetic cholinergic fibers in peripheral nerves of a variety of animal species (Lago, unpublished observations). The number of ChAT+ motor fibers in control rat sciatic nerves corresponded well with the numbers found under ultrastructural (Schmalbruch, 1986) and in estimates of CE histochemical studies (Macias et al., 1998). Our results indicate that immunohistochemistry against ChAT labels with good resolution motor fibers in normal and regenerated nerves and can be used for the assessment of the amount and the topographical distribution of motor axons regeneration. Simultaneous labeling against other markers, such as NF-200 or CGRP, allows for comparison of motor and sensory fibers under different experimental conditions.

ChAT+ motor fibers were present in regenerated nerves after a crush in similar numbers to controls and maintained the normal spatial distribution. The total num-

ber of ChAT+ was significantly increased in regenerated nerves of groups SUT, COL and SIL, but representing a similar proportion (22–30%) of the total number of myelinated fibers that were also higher than normal. The number of regenerated ChAT+ motor fibers counted was about 1.5 times higher in groups SUT and COL and 2.3 times in group SIL than that found in control nerves, clearly indicating that regenerating motor fibers present profuse sprouting. After nerve transection regenerative axonal sprouts readily emerge from the proximal nerve stump and grow to cross the injury site and elongate in the distal segment. Each regenerating parent axon may give rise to over 10 axonal sprouts in the first days (Brushart and Witzel, 2003). Sprouts may either approach a Schwann cell column or may grow at random into the connective layers of the nerve since an excess number of sprouts invade the distal Schwann cell columns (Aguayo et al., 1973; Jenq and Coggeshall, 1985). Therefore, the total number of the axons in the distal nerve segment may considerably exceed the number in the nerve proximal to the lesion. With time the number of axons decreases in the distal segment, as sprouts that do not make peripheral connections atrophy and eventually disappear. Even long time after injury, regenerating neurons support multiple (averaging 1.5–2) sprouts in the distal stump of the nerve (Horch and Lisney, 1981; Jenq and Coggeshall, 1985). A large number of axons counted in the distal segment might not necessarily indicate better regeneration; on the contrary, multiple branching may be a response to obstacles to axonal advance. Because of random elongation of multiple sprouts, the same neuron can simultaneously reinnervate different muscles (Angelov et al., 1993; Valero-Cabré et al., 2001), resulting in defective recovery. The degree of sprouting that we found at 60 days postinjury is similar for motor and sensory myelinated axons despite the assumed delay in initial regeneration of motor axons.

The characteristic clustering of motor axons in the control nerves was also observed in the crush group indicating that when the injury preserves the continuity and architecture of the endoneurial tubes, regenerated axons retrace their former pathways to adequately reinnervate the original distal targets (Nguyen et al., 2002). However, the motor grouping pattern disappeared after nerve transection and either direct suture repair or tube repair with a short gap, with ChAT+ axons observed scattered in small reformed fascicles throughout the cross-sectional nerve area. The hypothesis of fascicular specificity of regeneration led to attempts to demonstrate that tube repair would be more beneficial than direct suture repair when the fascicular matching is not adequate, and that a minimum gap between nerve stumps would allow axonal sprouts to sense cues released from adequate distal endoneurial tubes to be guided towards their original distal target (Brushart and Seiler, 1987; Evans et al., 1991; Rende et al., 1991). However, more recent works found that tube repair of short or mid length gaps did not improve the outcome or the accuracy of reinnervation with respect to direct fascicular suture (Bodine-Fowler et al., 1997; Valero-Cabré et al., 2001; Valero-Cabré and Navarro 2003; Zhao et al., 1992). From the anatomical point of view, regenerating fibers belonging to peroneal or tibial branches of the sciatic nerve show a random distribution inside nerve guides with no evident segregation (Alzate et al., 2000; Brushart et al., 1995). This phenomenon indicates that axons grow in a disorganized fashion in the newly formed extracellular matrix inside the guide, during the initial phase of regeneration. Our study shows for the first time that fibers belonging to a certain functional type regenerate in a disorganized pattern inside a nerve guide and in the nerve distal to suture repair. This lack of organization in endoneurial topography will lead to non-specific reinnervation of distal targets by the regenerating fibers.

Specificity of target reinnervation, in terms of anatomical and functional matching, is a key unresolved problem to achieve full functional recovery after peripheral nerve injuries. The maintenance of the normal fasciculation pattern in the distal nerve after a nerve injury is important to allow for accurate topographic projection of regenerating axons to the original targets. In addition to refined microsurgical repair methods, neurobiological strategies to be investigated for enhancing regeneration and guidance of motor axons may include administration of neurotrophic factors (Boyd and Gordon, 2003), vector-mediated gene transfer to axotomized motoneurons (Natsume et al., 2003), application of guidance peptides related to motor axons (Simon-Haldi et al., 2002), or the use of transplants of Schwann cells engineered to selectively enhance motor axons regrowth.

ACKNOWLEDGMENTS

We thank Jessica Jaramillo for technical assistance in the morphological studies, and Drs. Martí Pumarola and José M. Vela for advice and support in the immunohistochemical methods. This research was supported by grants IST-2001-35094 and IST-001917 from the EC.

REFERENCES

ABERNETHY, D.A., RUD, A., and THOMAS, P.K. (1992). Neurotrophic influence of the distal stump of transected peripheral nerve on axonal regeneration: absence of topographic specificity in adult nerve. J. Anat. 180, 395–400.

AGUAYO, A.J., PEYRONNARD, J.M., and BRAY, G.M. (1973). A quantitative ultrastructural study of regeneration from isolated proximal stumps of transected unmyelinated nerves. J. Neuropathol. Exp. Neurol. **32,** 256–270.

ALZATE, L.H., SUTACHAN, J.J., and HURTADO, H. (2000). An anterograde degeneration study of the distribution of regenerating rat myelinated fibers in the silicone chamber model. Neurosci. Lett. **286,** 17–20.

ANGELOV, D.N., GUNKEL, A., STENNERT, E., and NEISS, W.F. (1993). Recovery of original nerve supply after hypoglossal-facial anastomosis causes permanent motor hyperinnervation of the whisker-pad muscles in the rat. J. Comp. Neurol. **338,** 214–224.

ASHUR, H., VILNER, Y., FINSTERBUSH, A., ROUSSO, M., WEINBERG, H., and DEVOR, M. (1987). Extent of fiber regeneration after peripheral nerve repair: silicone splint vs. suture, gap repair vs. graft. Exp. Neurol. **97,** 365–374.

BAILEY, S.B., EICHLER, M.E., VILLADIEGO, A., and RICH, K.M. (1993). The influence of fibronectin and laminin during Schwann cell migration and peripheral nerve regeneration through silicone chambers. J. Neurocytol. **22,** 176–184.

BAIN, J., MACKINNON, S., and HUNTER, D. (1988). Functional evaluation of complete sciatic, peroneal and posterior tibial nerve lesions in the rat. Plast. Reconstr. Surg. **83,** 129–136.

BODINE-FOWLER, S.C., MEYER, R.S., MOSCOWITZ, A., ABRAMS, R., and BOTTE, M. (1997). Innaccurate projection of rat soleus motoneurons: a comparison of nerve repair techniques. Muscle Nerve **20,** 29–37.

BOYD, J.G., and GORDON, T. (2003). Glial cell line-derived neurotrophic factor and brain-derived neurotrophic factor sustain axonal regeneration of chronically axotomized motoneurons *in vivo*. Exp. Neurol. **183,** 610–619.

BRUSHART, T.M., and SEILER, W.A. (1987). Selective reinnervation of distal motor stumps by peripheral motor axons. Exp. Neurol. **97,** 289–300.

BRUSHART, T.M., and WITZEL, C. (2003). The morphology of early peripheral axon regeneration. Soc. Neurosci. Abst. 2003 Viewer/Itinerary Planner 152.10.

BRUSHART, T.M., MATHUR, V., SOOD, R., and KOSCHORKE, G. (1995). Dispersion of regenerating axons across enclosed neural gaps. J. Hand. Surg. **20,** 557–564.

BRUSHART, T.M., HOFFMAN, P.N., ROYALL, R.M., MURINSON, B.B., WITZEL, C., and GORDON, T. (2002). Electrical stimulation promotes motoneuron regeneration without increasing its speed or conditioning the neuron. J. Neurosci. **22,** 6631–6638.

DE MEDINACELLI, L. (1988). Functional consequences of experimental nerve lesions: effects of reinnervation blend. Exp. Neurol. **100,** 166–178.

DE MEDINACELLI, L., FREED, W.J., and WYATT, R.J. (1982). An index of functional condition of rat sciatic nerve based on measurements made from walking track. Exp. Neurol. **77,** 634–643.

EVANS, P.J., BAIN, J.R., MACKINNON, S.E., MAKINO, A.P., and HUNTER, D.A. (1991). Selective reinnervation: a comparison of recovery following microsuture and conduit nerve repair. Brain Res. **559,** 315–321.

FRANZ, C.K., RUTISHHAUSER, U., and RAFUSE, V.F. (2005). Polysialylated neural cell adhesion molecule is necessary for selective targeting of regenerating motor neurons. J. Neurosci. **25,** 2081–2091.

FU, S.Y., and GORDON, T. (1997). The cellular and molecular basis of peripheral nerve regeneration. Mol. Neurobiol. **14,** 67–116.

GIANNINI, C., LAIS, A.C., and DYCK, P.J. (1989). Number, size, and class of peripheral nerve fibers regenerating after crush, multiple crush, and graft. Brain Res. **500,** 131–138.

GÓMEZ, N., CUADRAS, J., BUTÍ, M., and NAVARRO, X. (1996). Histologic assessment of sciatic nerve regeneration following resection and graft or tube repair in the mouse. Restor. Neurol. Neurosci. **10,** 187–196.

GUTMANN, E., GUTTMANN, L., MEDAWAR, P.B., and YOUNG, J.Z. (1944). The rate of regeneration of nerve. J. Exp. Biol. **19,** 14–44.

HARGREAVES, K., DUBNER, R., BROWN, F., and JORIS, J. (1988). A new and sensitive method for measuring thermal nociception in cutaneous hyperalgesia. Pain **32,** 77–88.

HORCH, K.W., and LISNEY, S.J.W. (1981). On the number and nature of regenerating myelinated axons after lesions of cutaneous nerves in the cat. J. Physiol. **313,** 275–286.

JENQ, C.-B., and COGGESHALL, R.E. (1985). Numbers of regenerating axons in parent and tributary peripheral nerves in the rat. Brain Res. **326,** 27–40.

KAWASAKI, Y., YOSHIMURA, K., and HARII, K. (2000). Identification of myelinated motor and sensory axons in a regenerating mixed nerve. J. Hand Surg. **25A,** 104–111.

KRARUP, C., LOEB, G.E., and PEZESHKPOUR, G.H. (1988). Conduction studies in peripheral cat nerve using implanted electrodes. II. The effects of prolonged constriction on regeneration of crushed nerve fibers. Muscle Nerve **11,** 933–944.

LAGO, N., CEBALLOS, D., RODRÍGUEZ, F.J., STIEGLITZ, T., and NAVARRO, X. (2005). Long-term assessment of axonal regeneration through polyimide regenerative electrodes to interface the peripheral nerve. Biomaterials **26,** 2021–2031.

LUNDBORG, G. (1988). *Nerve Injury and Repair.* Churchill-Livingstone: Edinburgh.

LUNDBORG, G. (2003). Nerve injury and repair—a challenge to the plastic brain. J. Peripher. Nerv. Syst. **8,** 209–226.

MACIAS, M.Y., LEHMAN, C.T., SANGER, J.R., and RILEY, D.A. (1998). Myelinated sensory and alpha motor axon regeneration in peripheral nerve neuromas. Muscle Nerve **21,** 1748–1758.

MADORSKY, S.J., SWETT, J.E., and CRUMLEY, R.L. (1998). Motor versus sensory neuron regeneration through collagen tubules. Plast. Reconstr. Surg. **102,** 430–436.

MARTINI, R., SCHACHNER, M., and BRUSHART, T.M. (1994). The L2/HNK-1 carbohydrate is preferentially expressed by previously motor axon-associated Schwann cells in reinnervated peripheral nerves. J. Neurosci. **14,** 7180–7191.

MOLANDER, C., and ALDSKOGIUS, H. (1992). Directional specificity of regenerating primary sensory neurons after peripheral nerve crush or transection and epineurial suture. A sequential double-labeling study in the rat. Restor. Neurol. Neurosci. **4,** 339–344.

MUNRO, C., SZALAI, J., MACKINNON, S., and MIDHA, R. (1998). Lack of association between outcome measures of nerve regeneration. Muscle Nerve **21,** 1095–1097.

NATSUME, A., WOLFE, D., HU, J., et al. (2003). Enhanced functional recovery after proximal nerve root injury by vector-mediated gene transfer. Exp. Neurol. **184,** 878–886.

NAVARRO, X., BUTÍ, M., and VERDÚ, E. (1994a). Autotomy prevention by amytriptiline after peripheral nerve section in different strains of mice. Restor. Neurol. Neurosci. **6,** 151–157.

NAVARRO, X., VERDÚ, E., and BUTÍ, M. (1994b). Comparison of regenerative and reinnervating capabilities of different functional types of nerve fibers. Exp. Neurol. **129,** 217–224.

NAVARRO, X., RODRÍGUEZ, F.J., LABRADOR, R.O., et al. (1996). Peripheral nerve regeneration through bioresorbable and durable nerve guides. J. Periph. Nerv. System **1,** 53–64.

NEGREDO, P., CASTRO, J., LAGO, N., NAVARRO, X., and AVENDAÑO, C. (2004). Differential growth of axons from sensory and motor neurons through a regenerative electrode: a stereological, retrograde tracer, and functional study in the rat. Neuroscience **128,** 605–615.

NGUYEN, Q.T., SANES, J.R., and LICHTMAN, J.W. (2002). Pre-existing pathways promote precise projection patterns. Nat. Neurosci. **5,** 861–867.

POLITIS, M.J., and STEISS, J.E. (1985). Electromyographic evaluation of a novel surgical preparation to enhance nerve-muscle specificity that follows mammalian peripheral nerve trunk transection. Exp. Neurol. **87,** 326–333.

POLITIS, M.J., EDERLE, K., and SPENCER, P.S. (1982). Tropism in nerve regeneration in vivo. Attraction of regenerating axons by diffusible factors derived from cells in distal nerve stumps of transected peripheral nerves. Brain Res. **253,** 1–12.

PUIGDELLÍVOL-SÁNCHEZ, A., VALERO-CABRÉ, A., PRATS-GALINO, A., NAVARRO, X., and MOLANDER, C. (2002). On the use of fast blue, fluoro-gold and diamidino yellow for retrograde tracing after peripheral nerve injury: uptake, fading, dye interactions, and toxicity. J. Neurosci. Methods **115,** 115–127.

RENDE, M., GRANATO, A., MANACO, M.L., ZELAGNO, G., and TOESCA, A. (1991). Accuracy of reinnervation by peripheral nerve axons regenerating across 10 mm gap within an impermeable chamber. Exp. Neurol. **111,** 332–339.

RILEY, D.A., SANGER, J.R., MATLOUB, H.S., YOUSIF, N.J., BAIN, J.L.W., and MOORE, G.H. (1988). Identifying motor and sensory myelinated axons in rabbit peripheral nerves by histochemical staining for carbonic anhydrase and cholinesterase activities. Brain Res. **453,** 79–88.

SANGER, J.R., RILEY, D.A., MATLOUB, H.S., YOUSIF, N.J., BAIN, J.L., and MOORE, G.H. (1991). Effects of axotomy on the cholinesterase and carbonic anhydrase activities of axons in the proximal and distal stumps of rabbit sciatic nerves: a temporal study. Plast. Reconstr. Surg. **87,** 726–738.

SCHMALBRUCH, H. (1986). Fiber composition of the rat sciatic nerve. Anat. Rec. **215,** 71–81.

SHENAQ, J.M., SHENAQ, S.M., and SPIRA, M. (1989). Reliability of sciatic function index in assessing nerve regeneration across a 1 cm gap. Microsurgery **10,** 214–219.

SIMON-HALDI, M., MANTEI, N., FRANKE, J., VOSHOL, H., and SCHACHNER, M. (2002). Identification of a peptide mimic of the L2/HNK-1 carbohydrate epitope. J. Neurochem. **83,** 1380–1388.

SUZUKI, G., OCHI, M., SHU, N., UCHIO, Y., and MATSUURA, Y. (1998). Sensory neurons regenerate more dominantly than motoneurons during the initial stage of the regenerating process after peripheral axotomy. Neuroreport **9,** 3487–3491.

SWETT, J.E., HONG C.-Z., and MILLER, P.G. (1991). All peroneal motoneurons of the rat survive crush injury but some fail to reinnervate their original targets. J. Comp. Neurol. **304,** 234–252.

VALERO-CABRÉ, A., and NAVARRO, X. (2002). Functional impact of axonal misdirection after peripheral nerve injuries followed by graft or tube repair. J. Neurotrauma **19,** 1475–1485.

VALERO-CABRÉ, A., TSIRONIS, K., SKOURAS, E., PEREGO, G., NAVARRO, X., and NEISS, W.F. (2001). Superior muscle reinnervation after autologous nerve graft and poly-L-lactide-ε-caprolactone (PLC) tube implantation in comparison to silicone tube repair. J. Neurosci. Res. **63,** 214–223.

VALERO-CABRÉ, A., TSIRONIS, K., SKOURAS, E., NAVARRO, X., and NEISS, W.F. (2004). Peripheral and spinal motor reorganization after nerve injury and repair. J. Neurotrauma **21,** 95–108.

VERDÚ, E., and NAVARRO, X. (1997). Comparison of immunohistochemical and functional reinnervation of skin and muscle after peripheral nerve injury. Exp. Neurol. **146,** 187–198.

ZHAO, Q., DAHLIN, L.B., KANJE, M., LUNDBORG, G., and SHI-BI, L.U. (1992). Axonal projections and functional recovery following fascicular repair of the rat sciatic nerve with y-tunelled silicone chambers. Restor. Neurol. Neurosci. **4,** 413–419.

Address reprint requests to:
Xavier Navarro, M.D., Ph.D.
Group of Neuroplasticity and Regeneration
Faculty of Medicine
Universitat Autònoma de Barcelona
E-08193 Bellaterra, Spain

E-mail: xavier.navarro@uab.es

EFFECTS OF MOTOR AND SENSORY NERVE TRANSPLANTS ON THE AMOUNT AND SPECIFICITY OF SCIATIC NERVE REGENERATION

Natalia Lago, F. Javier Rodríguez, Jéssica Jaramillo, Xavier Navarro

Group of Neuroplasticity and Regeneration, Department of Cell Biology, Physiology and Immunology, and Institute of Neuroscience, Universitat Autònoma de Barcelona, Bellaterra, Spain.

INTRODUCTION

After nerve transection resulting in a nerve gap, neurotropic factors and Schwann cells emerging from the distal nerve stump attract nerve sprouts from the proximal stump, that are able to grow through the gap between the two nerve stumps (Ansselin et al., 1997; Lundborg et al., 1982; Politis and Spencer, 1983; Zhang et al., 1997) and regenerate along the denervated distal nerve stump long distances and reestablish functional connections. However, in most cases, even when regeneration itself is robust, functional recovery is poor, mainly due to lack of specificity of peripheral regeneration, so axons can synapse on inappropriate targets. This is due to the fact that, after complete severance of the nerve, many regenerating axons fail to enter correct bands of Büngner causing a neuron-target mismatch (Thomas, 1989). Functional outcome of peripheral nerve repair depends on the amount and the precision of end organ reinnervation. The misdirection of regenerated axons occurs between motor and sensory pathways (endoneurial tubes) during mixed-nerve regeneration, between different muscles during motor axon regeneration, and between different sensory areas and different corpuscles during sensory axon regeneration. When motor axons reinnervate incorrect muscles, it results in uncoordinated movements and synkinesia, whereas misrouted regenerating sensory axons can not correctly transduce sensory stimuli and may cause sensory disturbances and mislocalization (Hendry et al., 1986; Aldskogius and Molander, 1990; Sumner, 1990; Gramsbergen et al., 2000; Maki, 2002; Valero-Cabré et al., 2002).

After complete transection of a peripheral nerve in adult rats, regenerated motor axons do not show selectivity for reinnervating their own target muscle, thus resulting in a distorted representation of the motoneuronal spinal nuclei (Hardman and Brown, 1987; Valero-Cabré et al., 2001). However, in rats injured postnatally, distal muscles are reinnervated by motoneurons mainly distributed in the normal spinal nuclei, although topographical selectivity is not quite to the degree found in controls (Hardman and Brown, 1987; DeSantis et al., 1992). In contrast to adult animals, selectivity exists in newborns from the start rather than being a more random reinnervation subsequently sharpened by elimination of inappropriate connections. Nonetheless, it has been reported that motor axons have the ability to reinnervate motor pathways more accurately than sensory axons to cutaneous pathways, a phenomenon called *preferential motor reinnervation* (PMR) (Brushart, 1988; 1993). This process has been related to the differential expression of certain surface molecules, such as the carbohydrate epitope L2/HNK-1 in Schwann cells (SCs) accompanying motor axons and NCAM in non-myelin-forming Schwann cells of sensory nerves (Martini et al., 1992; 1994;

Saito et al., 2005). However, when a peripheral nerve is injured, denervated SCs proliferate and change their morphological and phenotypic characteristics (Jessen and Mirsky, 1992). Previously myelin-forming SCs loss their myelin sheaths and reexpress molecules normally confined to immature and nonmyelinating SCs of newborn and adult animals, respectively (Jessen and Mirsky, 1992). Lesion-induced changes, including upregulation of nerve growth-promoting molecules, appear to be important prerequisites for SC-mediated axonal regrowth (Martini, 1994). Moreover, denervated Schwann cells exhibit a high degree of phenotypic plasticity, suggesting that the SC phenotype is mainly reflection of the accompanying axonal properties (Aguayo et al., 1976).

Initial findings in favor of fascicular specificity of regeneration (Politis et al., 1982; Politis and Steiss, 1985) led to attempts to demonstrate that tube repair leaving a short gap between nerve stumps would allow axons to be guided towards their original distal fascicle by means of neurotropic diffusible factors (Evans et al., 1991; Brushart and Seiler, 1987; Rende et al., 1991). However, recent works have demonstrated that tubulization of short or mid long gaps by itself does not improve the accuracy of reinnervation with respect to direct suture when correct alignment between proximal and distal stumps was achieved (Bodine-Fowler et al., 1997; Valero-Cabré et al., 2001, 2002).

In the present work, we have assessed if, by introducing an implant of pure motor or sensory nerve into a silicone guide, axons can regenerate more specifically by cues delivered by the grafted motor or sensory SCs. For this purpose, we repaired a mid length gap of the rat sciatic nerve with a silicone guide containing a transplant of either ventral or dorsal root. Reinnervation of muscle and skin targets was evaluated during three months postinjury, followed by final morphological study of the regenerated nerves. Our results show that regeneration was mildly enhanced by the nerve root transplant, but there was not a significant degree of motor and sensory preferential reinnervation with this strategy. Nevertheless, functional results indicated that a dorsal root graft helped sensory axons to regrowth to target organs.

MATERIALS AND METHODS

Experimental design and surgical procedure

Dorsal and ventral L4 to L6 roots were aseptically harvested from anesthetized female Sprague-Dawley rats, aged 2 months. The root segments were placed in Dulbecco's minimum essential medium (DMEM) supplemented with 10% fetal calf serum to allow for in vitro predegeneration. Seven days later, the root explants, about 3 mm long, were introduced in the

middle of a silicone guide and fixed with one stitch of 10-0 monofilament suture at one level, maintaining a longitudinal orientation. Then the guide was filled with saline.

Operations were performed in 20 female Sprague-Dawley rats, aged 2.5 months under pentobarbital anesthesia (40 mg/kg i.p.). Under a dissecting microscope, the sciatic nerve was exposed at the midthigh and carefully freed from surrounding tissues from the sciatic notch to the knee. The sciatic trunk was sharply transected and the nerve stumps placed 1 mm into the ends of the silicone guide (10 mm long, 2 mm i.d., 0.5 mm wall thickness), with one stitch of 10-0 monofilament suture at each end, leaving a gap of 8 mm (measured with a microruler) between the stumps (Fig. 1a). In eight rats the silicone guide contained a segment of ventral root (group VR), and in other eight a segment of dorsal root (group DR). In a control group the guide was filled with saline solution (group S; n=4). The wound was sutured by planes and disinfected with povidone-iodine. In order to avoid autotomy after denervation, animals were treated with amitriptyline (Navarro et al., 1994a). All the animals were kept under standard conditions during 3 months postoperation to allow for nerve regeneration.

Functional evaluation

At 60 and 90 days postoperation (dpo) rats were evaluated by non-invasive tests to assess distal target reinnervation by the regenerating sciatic nerve. Regeneration of large myelinated fibers was assessed by nerve conduction tests (Navarro et al., 1994b; Valero-Cabré et al., 2001, 2004). With the animals under anesthesia (pentobarbital 30 mg/kg i.p.), the nerve was stimulated through a pair of needle electrodes placed at the sciatic notch with single electrical pulses of 0.05 ms duration up to supramaximal intensity. The compound muscle action potentials (CMAPs) were recorded from the medial gastrocnemius muscle and from the plantar muscles (at the third interosseus space) with small needle electrodes. Similarly, sensory compound nerve action potential (CNAP) was recorded by electrodes placed near the digital nerves of the fourth toe. The evoked action potentials were displayed on a storage oscilloscope (Sapphire 4M, Medelec Vickers) at settings appropriate to measure the amplitude from baseline to peak and the latency to the onset. For normalization of the data, values obtained in the operated hindlimb were expressed as percentage of values of the contralateral limb for each animal.

For motor unit number estimation (MUNE) we used the incremental technique. Starting from subtreshold stimulation levels, the sciatic nerve was stimulated with single pulses of gradually increased intensity until a response was seen, representing the first motor unit activated. With further stimulus intensity increases, quantal increases in the response

were recorded (Fig. 1). We assumed that each increment, higher than 25 μV, represented the addition of one motor unit. The amplitude of the resultant response was divided by the number of increments to yield an estimate of the mean amplitude of single units; this value was divided into the maximum CMAP to give the estimate of the number of motor units (Azzouz et al., 1997; Shefner, 2001).

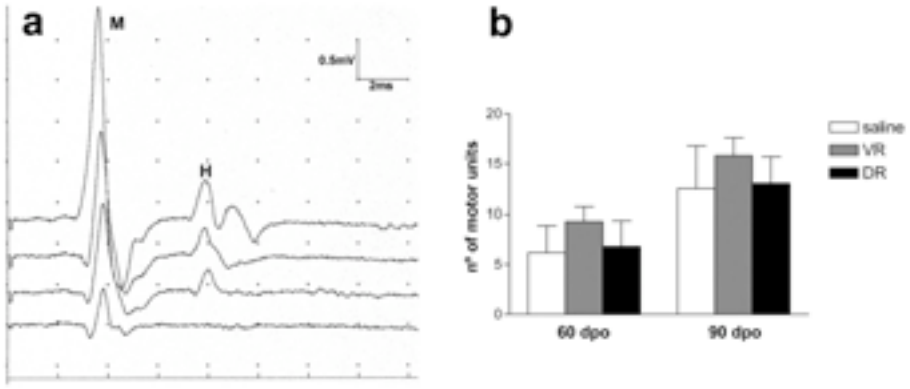

Figure 1. (a) Representative recordings of compound muscle action potentials from plantar muscles in a control rat during the incremental MUNE technique. By increasing the intensity of stimulation, new motor units are activated and add to the M wave amplitude. (b) Histogram of the number of motor units of plantar muscle estimated in groups S, VR and DR at 60 and 90 days. Note that the MUNE of plantar muscle in control rats average 54.

The extension of recovery of pain sensitivity in the hindpaw was tested by light pricking with a needle in five areas, from the most proximal pawpad to the tip of the fourth digit on the plantar surface. The animal response was scored as no response (0), reduced (1) or normal reaction (2) in each area tested, and the 5 scores added into a pinprick score (PP). Recovery of nociception was also quantitated by thermal algesimetry (Hargreaves et al., 1988) using a Plantar Algesimeter apparatus (Ugo Basile). Rats were placed into a plastic box with an elevated glass floor. The beam of a projection lamp was focused from the bottom of the box onto the plantar surface of the hindpaw. The time spent until withdrawal of the heated paw was measured through a time-meter coupled with IR detectors. The value for a test was the mean of three trials separated by 30 min resting periods. The values were normalized as the percentage of withdrawal latency of the operated versus the contralateral intact hindpaw each testing day.

Morphological evaluation

At three months postoperation, animals were deeply anesthetized and perfused transcardially with 4% paraformaldehyde in phosphate-buffer saline solution. The sciatic nerve was harvested and a segment of the nerve just distal to the tube was postfixed in glutaraldehyde-paraformaldehyde (3%-3%) in cacodylate-buffer solution overnight at 4°C, and then processed for embedding in Epon resin. Semithin sections 0.5 μm thick were stained with toluidine blue and examined by light microscopy (Olympus BX40). Images of the whole sciatic nerve were acquired at 10x with an Olympus DP50 camera attached to a computer, while sets of images chosen by systematic random sampling of squares representing at least 30% of the nerve cross-sectional area were acquired at 100x. Measurements of the cross-sectional area of the whole nerve, and counts of the myelinated fibers were carried out by using NIH Image software.

Segments of the regenerated sciatic nerves taken from inside the guide (distal half) were collected and postfixed in the same perfusion solution for 4 h. Samples were washed in phosphate-buffer and embedded in paraffin. Transverse sections (4 μm thick) were cut with a microtome, mounted in silane-coated slides and dried overnight. The sections were deparaffinized and rehydrated before staining. Antigen retrieval was performed with sodium citrate (pH 6.1) during 20 minutes at 95ºC. Then sections were washed with Trizma buffer solution (TBS, 0.05M, pH 7.4; Sigma) and placed in 2% H_2O_2 in 70% methanol for 25 minutes at room temperature. After washes in TBS and TBS with 0.05% Tween-20 (Fluka), sections were incubated for 24h at 4ºC with primary antibody goat polyclonal antiserum to ChAT (AB144P, Chemicon; 1:50). Slides were washed and incubated with biotynilated secondary antibody (Vector; 1:200) for 1h at room temperature. After further washing the slides were incubated with ABC (avidin-biotin complex, Vector; 1:200) for 1h at room temperature and incubated for 3 min with 3,3-diaminobenzidine tetrahydrochloride solution (D5637; Sigma), counterstained with hematoxylin, dehydrated and mounted with DPX (Fluka). Images of the whole sciatic nerve were acquired at 10x, and sets of systematic randomly chosen images representing at least 30% of the nerve cross-sectional area were acquired at 100x. Area measurements and counts of ChAT+ axons were carried out by using NIH Image software. ChAT+ fibers were counted if clear staining was present in individual myelinated fibers, whereas small grouped fibers corresponding to unmyelinated sudomotor fibers, discernible by the lack of myelin sheath, were not counted.

Control rats were perfused and equivalent segments of the sciatic nerve collected and processed in parallel.

Statistical analysis

All results are expressed as mean ± SEM. Statistical comparisons between groups and intervals were made by non-parametric Kruskal-Wallis and Mann-Whitney *U* tests. A value of $p < 0.05$ was considered to be statistically significant.

RESULTS

Functional results

Functional tests performed during follow-up after operation indicated successful reinnervation of distal targets by the regenerating sciatic nerve in all the rats of the three groups evaluated. Nevertheless, the degree of reinnervation achieved was significantly lower in the three groups in comparison with control values.

Table 1 shows the values for the electrophysiological tests performed at two and three months postoperation. The latency of compound action potentials, indicative of the conduction velocity of impulses by the regenerated fibers, was longer than normal in the three groups. Between groups comparisons showed that the latency in the gastrocnemius muscle at 90 dpo was significantly shorter in group VR than in the group S, whereas the latency for the digital nerve was shorter in group DR than in group S.

Table 1. Neurophysiological results of target reinnervation by regenerated nerves 60 and 90 days after injury and repair of the sciatic nerve in the different groups of rats evaluated. Values are mean ± SEM.

			60 dpo			**90 dpo**		
	Group	Baseline	S	VR	DR	S	VR	DR
	(n)	*(14)*	*(4)*	*(8)*	*(8)*	*(4)*	*(8)*	*(8)*
Gastrocnemius muscle	Latency (ms)	1.19 ± 0.08	3.47 ± 0.69	2.79 ± 0.12	3.11 ± 0.16	3.30 ± 0.68	2.37 ± 0.07 *	2.6 ± 0.13
	CMAP (mV)	58.4 ± 2.5	11.6 ± 2.5	20.8 ± 0.8 *	20.0 ± 2.8 *	20.9 ± 5.09	28.9 ± 1.64	27.8 ± 3.22
Plantar muscle	Latency (ms)	2.6 ± 0.09	6.97 ± 0.79	6.83 ± 0.42	6.91 ± 0.71	4.50 ± 0.23	4.41 ± 0.18	4.47 ± 0.12
	CMAP (mV)	9.80 ± 0.42	0.43 ± 0.18	0.61 ± 0.10	0.53 ± 0.16	0.91 ± 0.36	1.72 ± 0.23 *	1.62 ± 0.38
Digital nerve	Latency (ms)	2.0 ± 0.07	4.99 ± 0.63	4.70 ± 0.6	4.54 ± 0.43	4.83 ± 0.25	4.20 ± 0.2	4.10 ± 0.24 *
	CNAP (μV)	15.9 ± 0.96	3.33 ± 1.51	2.55 ± 0.72	2.21 ± 1.13	4.54 ± 1.73	3.91 ± 0.60	6.17 ± 1.82
Nociception	PP score	10 ± 0.0	4.5 ± 1.7	4.8 ± 0.8	6.1 ± 0.5	7.2 ± 1.1	7.3 ± 0.6	7.9 ± 0.5
	Algesimetry		153 ± 51	135 ± 31	121 ± 14	152 ± 38	131 ± 15	115 ± 16

* $p<0.05$ vs group S.

S, saline; VR, ventral root; DR, dorsal root; CMAP, compound muscle action potential; CNAP, compound nerve action potential; PP, pinprick score.

Regarding the amplitude of the CMAPs, there were no differences between groups VR and DR, although both groups showed higher mean values than the S group, with significant differences for the gastrocnemius muscle at 60 dpo and for the plantar muscle at 90 dpo. The amplitude of CNAPs recorded in the digital nerve was higher in group DR, that achieved up to 55% of control values, than in groups VR and S (about 35%). All rats in group VR showed reinnervation of the distal targets, i.e. plantar muscle and digital nerve, whereas one rat of each group DR and S did not.

The number of motor units estimated and the mean amplitude of their action potentials were also significantly reduced compared with contralateral control values (Table 2, Fig 1). The MUNE of the gastrocnemius muscle averaged about 60% of control numbers in groups VR and DR and only 35% in group S at 60 dpo, and increased slightly at 90 dpo. In the more distal plantar muscles the numbers increased more markedly with time from 60 to 90 dpo; at 60 dpo we found about 17% of normal in group VR for 12% in groups DR and S, although by 90 dpo differences were reduced. Despite no significant differences were found because the large variability between animals in each group, group VR showed an earlier increase in the number of reinnervated motor units.

Table 2. Amplitude and estimated number of motor units of plantar and gastrocnemius muscles recorded at 60 and 90 dpo in the different groups of rats evaluated. Values are mean ± SEM.

			60 dpo			**90 dpo**		
		Control *(n=6)*	S *(n=4)*	VR *(n=6)*	DR *(n=6)*	S *(n=4)*	VR *(n=6)*	DR *(n=6)*
Plantar muscle	MUAP (μV)	184.2 ± 17.8	79.3 ± 17.5	68.0 ± 11.5	97.2 ± 17.1	72.5 ± 15.3	95.9 ± 9.2	122.1 ± 14.1
	MUNE	53.7 ± 6.1	6.2 ± 2.7	9.3 ± 1.4	6.8 ± 2.6	12.5 ± 4.2	15.8 ± 1.8	13.0 ± 2.7
Gastrocnemius muscle	MUAP (μV)	297.0 ± 31.5	210.6 ± 30.3	203.5 ± 34.6	212.2 ± 25.6	253.9 ± 32.7	242.7 ± 29.6	214.5 ± 20.5
	MUNE	205.8 ± 23.9	71.3 ± 18.1	124.7 ± 30.9	123.0 ± 12.1	78.8 ± 9.3	135.7 ± 21.1	154.5 ± 15.5

S, saline; VR, ventral root; DR, dorsal root; MUAP, motor unit action potential; MUNE, motor units number estimation.

Pain sensibility was incomplete in all the groups, whereas the time to paw withdrawal found in the thermal algesimetry test was shorter in the group DR in comparison with groups VR and S (Table 1).

Morphological results

The morphological evaluation performed at 90 dpo showed that the sciatic nerve was regenerated through the 8 mm gap in all the animals evaluated. The transverse nerve area was smaller than that of the intact sciatic nerve in all the experimental groups. The number of myelinated fibers was significantly higher in the 3 injured groups in comparison with the intact nerve (Table 3) but no differences were found between them. In all the rats studied the regenerated nerve was organized in multiple small fascicles, and the myelinated fibers were of smaller caliber than normal (Fig. 2).

The number of ChAT+ myelinated axons counted in the intact rat sciatic nerve averaged 1674±64, i.e. about 20% of the total number of myelinated fibers. In the regenerated nerves, the number of ChAT+ fibers was lower in the group with a ventral root implant (11%) in comparison with the group with a dorsal root implant (14%) and with saline (17%), but differences were not statistically significant. The distribution of ChAT-labeled axons was scattered throughout the regenerated nerves, in contrast with the fascicular grouping seen in intact sciatic nerves (Fig. 3). In the regenerated nerves ChAT+ axons were found within most of the reformed fascicles intermingled with other small myelinated axons and with unmyelinated axons.

Table 3. Cross-sectional area and number of myelinated fibers counted in semithin sections, and total number of ChAT labeled myelinated fibers in the regenerated sciatic nerves 90 days after tube repair in the three groups studied. Values are mean ± SEM.

	Control	S	VR	DR
(n)	*(4)*	*(4)*	*(4)*	*(4)*
Nerve area (mm^2)	0.66 ± 0.06	0.35 ± 0.01	0.37 ± 0.04	0.31 ± 0.04
No. Myelinated fibers	8371 ± 225	10955 ± 615	10798 ± 770	11291 ± 575
No. ChAT+ fibers	1674 ± 64	1908 ± 180	1340 ± 361	1525 ± 410

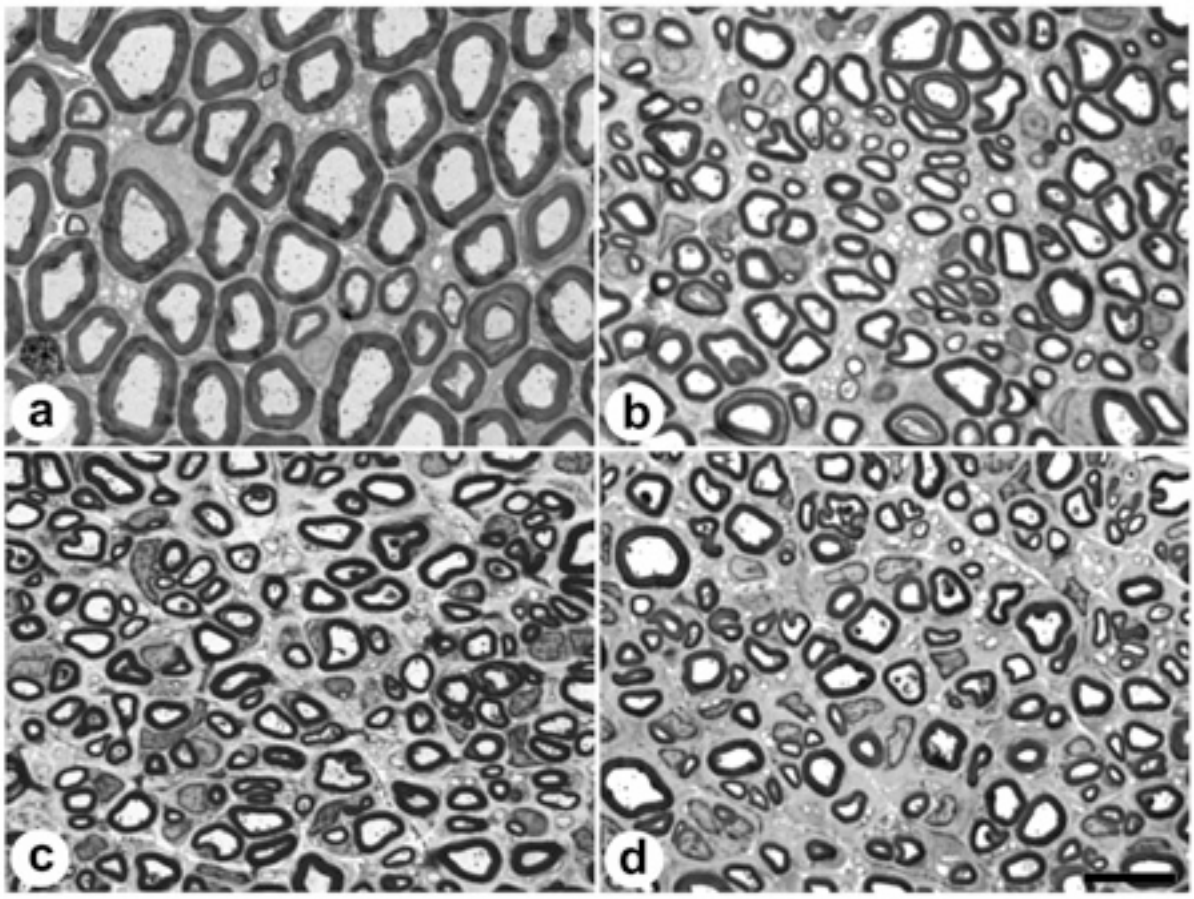

Figure 2. Photomicrographs of transverse sections of the sciatic nerve from representative sample of control rats (a), group S (b), group VR (c) and group DR (d) rats. Note the increased density and the reduced size of myelinated fibers in all the regenerated nerves (b-d) in comparison with the intact nerve (a). Bar = 10 μm.

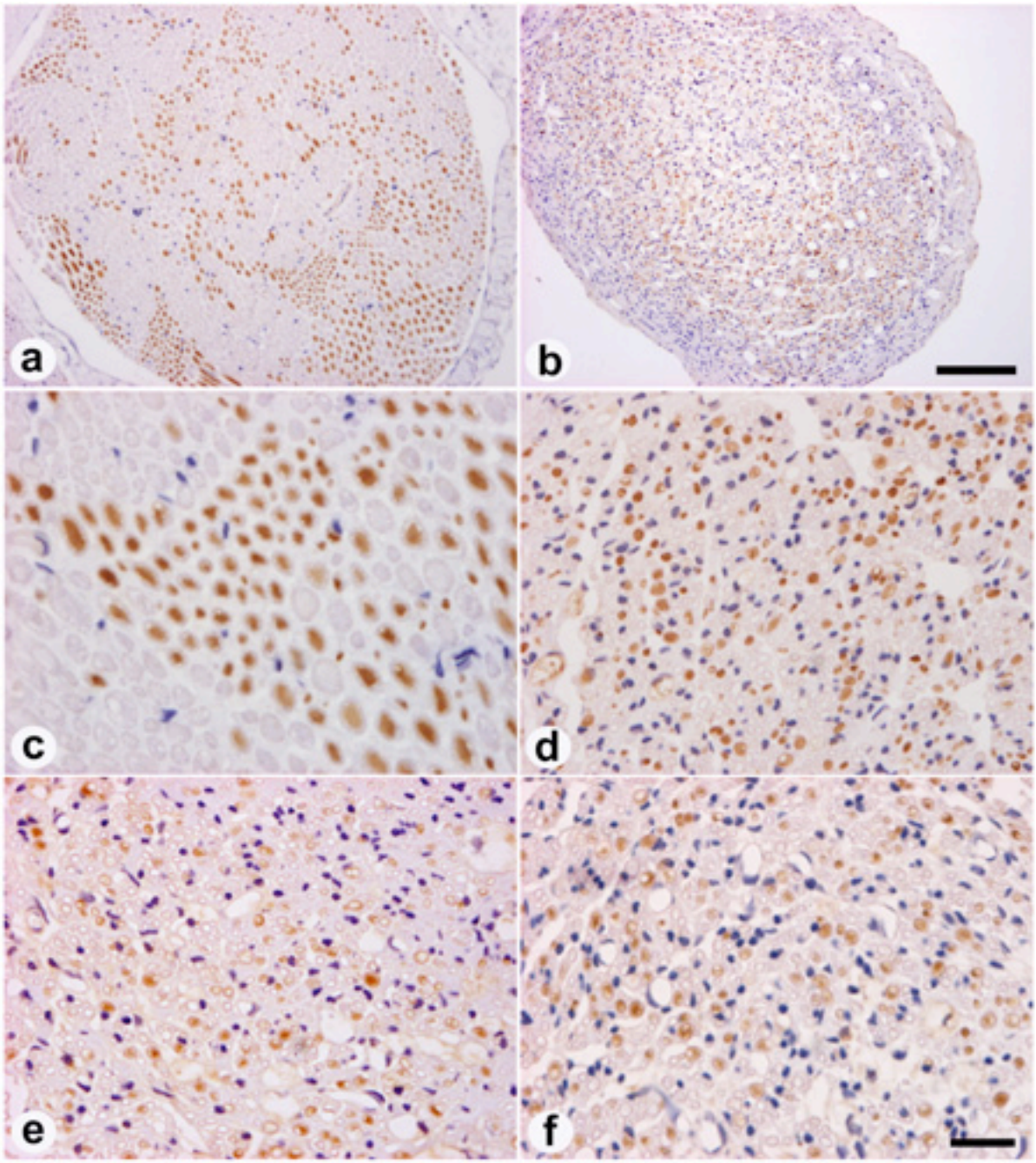

Figure 3. Immunohistochemical labeling against choline acetyltransferase (ChAT) counterstained with hematoxylin in transverse sections of a control sciatic nerve (a) and of a regenerated nerve after silicone tuber repair (b, group VR). Higher magnification of fascicles containing ChAT-labeled axons in a control nerve (c), and in regenerated nerves of groups S (d), VR (e) and DR (f). Note that in ChAT-positive axons are myelinated fibers. Whereas in the intact nerve motor axons are distributed confined in muscular fascicles, in the regenerated nerves they appear scattered throughout all the transverse nerve section. Bar = 100 μm in a-b, and 20 μm in c-f.

DISCUSSION

The results of this study show that by transplanting a small nerve segment inside a silicone guide, axonal regeneration is enhanced, leading to slightly faster and higher levels of target reinnervation. The present results also show that there is not clear preferential reinnervation promoted when the nerve segment transplanted is of pure sensory or motor origin, harvested from dorsal or ventral roots of syngeneic animals. Nevertheless, we found evidences suggesting that regeneration of motor axons was promoted at earlier times by the motor graft, whereas reinnervation of sensory pathways was increased in the presence of the sensory graft.

Effects of a nerve transplant in tube repair

A proposed strategy in order to improve the results of tube repair of mid and long nerve gaps, making them closer to the results provided by classical autologous nerve graft, consists in the introduction of a small isolated nerve segment inside the tube (Navarro and Verdú, 2004). The interposition of a nerve transplant within a synthetic guide would ensure an enhanced source of reactive SCs in its lumen, thus enhancing the formation of the new regenerating nerve structure. Such a transplant obviates potential problems and limitations associated with the addition and delivery of exogenous factors and agents (Rich et al 1989, Labrador et al 1998, Midha et al 2003) or cultured SCs (Guénard et al 1992, Levi et al 1997, Rodríguez et al 2000). Previous studies have shown that tube repair with such a nerve transplant results in a slightly faster regeneration rate without histological differences in short gaps, but a higher percentage of successful regeneration and a higher number of myelinated and unmyelinated axons in long gaps with respect to empty chambers (Smahel and Jentsch 1986; Jenq and Coggeshall, 1986, 1987; Navarro and Kennedy 1991; Rodríguez et al., 1999). In addition, nerve segments of different caliber allowed for similar improvement of regeneration (Jenq and Coggeshall, 1987). Predegenerated implants improved regeneration in comparison with fresh implants, whereas freeze-thawed acellular nerve transplants did not favor regeneration (Rodríguez et al., 1999), indicating that the presence of SCs and their dedifferentiation (during predegeneration in vitro) are relevant factors to be taken into account to promote effective regeneration. Using a Y chamber model, Maki and coworkers (2002) demonstrated that SC migration from the distal nerve stump was more important for axonal regeneration in a gap (4 mm) model than neurotropic diffusible factors released from the distal nerve segment. Moreover, one-week denervated nerve segments inserted into one of the distal Y channels showed stronger regenerative attraction than fresh nerve segments inserted

into the other Y channel. Although in the present study we did not investigate the fate of the implanted SCs, previous results using similar experimental models from our laboratory (Rodríguez et al., 2000; Udina et al., 2004) and from others (Yu and Kocsis, 2005; Kimura et al., 2005) indicate that transplanted SCs are able to survive and migrate into the recipient nerve for at least two months.

The beneficial effect of nerve transplants was reported to be more marked within long than in mid nerve gaps in the mouse (Rodríguez et al., 1999). Accordingly, with the 8 mm gap used in the rat we found that muscle and nerve reinnervation was improved with the nerve root transplants compared with the empty guide, although differences were smoothed with time, and by 3 months after injury there were no differences in the counts of regenerated myelinated fibers. Morphological evaluation performed at earlier times might probably show some differences.

Selective reinnervation by ventral and dorsal root transplants

By inserting a small segment of ventral or dorsal root in the repair tube we attempted to investigate if the SCs normally accompanying efferent and afferent axons in the peripheral nervous system could preferentially stimulate regeneration of the corresponding populations of axons. The functional results obtained indicate that selectivity of regeneration was mildly promoted at early time points, but it was obscured as regeneration and target reinnervation progresses. Regarding reinnervation of proximal (gastrocnemius) and distal (plantar) muscles, despite the M wave amplitude followed a similar course, the number of motor units estimated in the plantar muscle was higher in group VR at 60 dpo but similar at 90 dpo compared with group DR. Differences were more noticeable for sensory reinnervation; the digital CNAP and the response to nociceptive stimuli showed higher responses in group DR than in group VR during the 3 months follow-up. These results suggest that sensory axons regenerated better when the sensory root graft was interposed between the nerve stumps.

The fact that we only found slight, not significant differences could be explained by the large interindividual variability and because the evaluations were performed at a relatively late time, when regenerated nerve fibers had reinnervated target organs. It is possible that at earlier time points before regenerating fibers reach target organs, differences in the rate and amount of regenerating axons of different types might be observed (Nichols et al., 2004). The morphological evaluation did not show differences in the number of regenerated myelinated nerve fibers. Of interest, the number of ChAT+ motor fibers was slightly lower in group VR than in group DR, and in both lower than in group S; this finding can be interpreted as a

reduced selectivity of motor axons to grow with the ventral root transplant, but is more likely due to an enhanced rate of regeneration of motor axons that by 3 months were already undergoing pruning of supernumerary sprouts (Brushart, 1988, 1990).

Maki et al. (2005) reported that distal nerves derived from a sensory fascicle induced more regenerating axons than those from a motor fascicle. They suggested that sensory and motor nerve segments have different effects on axonal regeneration. On another hand, our results are in contradiction with those found by Nichols et al. (2004), who assessed preferential regeneration when a 5 mm graft from a cutaneous (sensory), a muscular (motor), or a mixed nerve graft was directly sutured between the injured tibial nerve stumps. In that study, more regenerative axons were found through the motor and the mixed grafts than through the sensory graft. Nevertheless, the need in that study to graft three sensory graft cables for only two motor cables and one mixed graft to match for the cross-sectional graft area, might have introduced differences in the scar tissue formed at the repair site. Indeed, it has been shown in the smaller mouse model that surgical coaptation, such as use of fibrin sealant versus sutures, can influence preferential motor regeneration (Robinson and Madison, 2003).

Factors influencing the selectivity of regeneration

One of the problems of studying selective regeneration is the use of adequate models. Weiss and Edds (1945) introduced the rat femoral nerve as a model system to study the fate of regenerating axons that originally innervated muscle or skin. The femoral model has been largely used, and neuronal retrolabeling the most usual technique to count the number of motoneurons that reconnect with correct end organs (Rodríguez et al., 2004). The femoral nerve divides at the groin in a muscular (motor) branch to the quadriceps muscle and a cutaneous (sensory) branch, the saphenous nerve, to the skin. Previous work in the rat femoral nerve has shown that regenerating motor neurons preferentially reinnervate a terminal nerve branch to muscle as opposed to skin. This process was termed preferential motor reinnervation (PMR) and interpreted as evidence that regenerating motor axons can differentiate between SC tubules present in muscle versus cutaneous pathways (Brushart, 1993; Brushart and Seiler, 1987). Similar findings were later reported for selective regeneration of sensory axons (Madison et al., 1996). However, part of this previous work has been confounded by motor axons having access to target muscle during the regeneration period. When muscle reinnervation by regenerating motor axons was prevented, significantly more motor neurons reinnervated the cutaneous pathway rather than the original muscular

pathway (Robinson and Madison, 2004), therefore suggesting that skin and muscle pathways are not inherently different in terms of their ability to support regeneration of motor neurons. Rather, it would be the relative level of trophic support provided by each nerve branch that determines whether motor (and sensory) axons will regenerate in that particular branch. Relevant to this point would be the differences in number of SCs between the so-called motor and sensory terminal pathways; in the quadriceps nerve there are about 350-500 myelinated fibers vs 1500 in the saphenous nerve. Similarly, the sciatic nerve conveys about 3-4 times more myelinated sensory than motor fibers, and more than double numbers of unmyelinated sensory than sympathetic axons (Schmalbruch, 1986; Prodanov, 2006). These data indicate that cutaneous sensory distal pathways contain considerably more numbers of SCs than muscular counterparts. Regarding the L4 and L5 spinal roots, similar differences exist between efferent and afferent axons (Prodanov, 2006). Therefore, the dorsal root graft used in this study contributed with at least double number of denervated SCs than the ventral root grafts of the same size.

In addition, it has to be taken into account that the muscular nerves also contain sensory axons (for example, the quadriceps nerve has about 50-60% sensory axons), and thus motor axons regenerating into sensory SC tubes in the distal motor branch are incorrectly counted as correct regeneration, when evaluated by retrograde tracing. To avoid this problem, Maki and colleagues (Maki, 2002; Maki et al., 2005) designed a silicone Y-chamber model, in whose proximal opening they inserted either the L5 ventral root or the saphenous nerve, and in the distal openings a segment of L5 ventral root as a pure motor branch and a segment of saphenous nerve as a pure sensory nerve. By counting the numbers of axons regenerated into each of the distal pathways, they found higher numbers of both motor and sensory axons in the sensory distal pathway than in the motor distal pathway. They proposed that whereas sensory axons showed preferential growth toward the distal sensory channel, motor axons did not.

Besides methodological considerations, the site of injury and the type of repair, the type of nerve, the age and the animal species has been shown to influence the results on motor specific regeneration (Le et al., 2002; Robinson and Madison, 2003; Franz et al., 2005). After transection made at a proximal level in the femoral nerve, where motor and sensory axons are scattered throughout the nerve, regenerating axons can not grow separately into the saphenous and quadriceps branch. The sciatic nerve is in the majority of its length a mixed, sensory-motor nerve. This fact will make particularly difficult to obtain significant differences in the selectivity of regeneration between motor and sensory fibers in this model. In the present

study we found that a dorsal root graft improved sensory recovery, probably reflecting enhanced regeneration of sensory axons, whereas a ventral root graft had only a small positive effect on motor recovery at early time of reinnervation. The numbers of myelinated axons distal to the silicone guide were similar in the three groups studied, indicating that the amount of axonal regeneration was not the cause for the differences in selective reinnervation.

Preferential reinnervation is thought to be due to collaboration between the regenerating axons and the appropriate pathway type (Brushart, 1993; Madison et al., 1996). After peripheral nerve lesion, SCs in the degenerating nerve undergo dedifferentiation and start proliferation. The de-differentiated daughter cells downregulate myelin-associated proteins (Trapp et al., 1988; Mitchell et al., 1990) and upregulate the expression of numerous regeneration-associated genes as cell-adhesion molecules N-CAM and L1 (Jessen and Mirsky 1992; Martini and Schachner, 1988). After recontact with regenerated axons, some of the differentiating cells upregulate expression of myelin-related mRNAs (Mitchell et al., 1990; Gupta et al., 1993) and start to produce myelin sheaths. The mechanisms by which regenerating motor axons interact with appropriate SCs are not completely known. They may depend on both receptors and their ligands on the interacting partner cells, as well as on neural patterns of activity (Stevens et al., 1998). Previous results indicated that the HNK-1 carbohydrate epitope is expressed more strongly in myelin-forming SCs of motor axons in the adult rodent, but rarely by those of the sensory axons (Martini et al., 1994; Saito et al., 2005). On the other hand, NCAM-positive cells exist exclusively in sensory nerve fascicles and not in motor fascicles, and they have been identified as non-myelin forming SCs of sensory unmyelinated fibers (Saito et al., 2005). Both markers appear distinctly by about three weeks postnatally, suggesting that they play a role during development of nerve fasciculation. The differential expression of these SC surface molecules has been repeatedly cited as one possible molecular mechanism leading to preferential regeneration. However, HNK-1 and NCAM immunoreactivity is lost within days after nerve transection in motor and sensory fascicles, respectively (Saito et al., 2005), although it may reappear after recontact with the appropriate axons (Martini et al., 1994), indicating that their expression in SCs is related to the type of axon in contact with the glial cell. Furthermore, no immunoreactivity for these markers was seen in cultured SCs from either motor or sensory adult mouse nerves (Saito et al., 2005). No labeling in rat SCs has been successful because the available antibodies against HNK-1 react very faintly with rat cells (personal observations). Therefore, the lack of expression of selective markers in reactive SCs after nerve degeneration talks against an effective role in offering distinct pathways promoting initial selective axonal regrowth.

Until presently there are no effective neurobiological strategies to allow for a significant degree of specificity of regeneration and target reinnervation by motor or sensory axons after transection of peripheral nerves in adult mammals. Procedures that increase the regeneration and reinnervation rate, like nimodipine treatment (Angelov et al., 1996), surgical repair with predegenerated grafts (Brushart et al., 1998) or early electrical stimulation (Al-Majed et al., 2000), have been shown to reduce polyinnervation and misdirected reinnervation. Faster nerve regeneration would decrease the expression of target-derived neurotrophic factors, which stimulate axonal terminal sprouting (Covault and Sanes, 1985), and accelerate pruning of misdirected collaterals (Brushart, 1990, 1993).

Acknowledgments

This research was supported by grants IST-2001-35094 (CYBERHAND project) and IST-001917 (NEUROBOTICS project) from the EC. The authors thank the technical help of Tabaré Moreyra.

REFERENCES

Aguayo AJ, Chavron L, Bray GM. Potential of Schwann cells from unmyelinated nerves to produce myelin: a quantitative ultrastructual and radiographic study. J Neurocytol 1976; 5:565–573.

Aldskogius H, Molander C. Specificity in regenerative outgrowth and target reinnervation by mammalian peripheral axons. Restor Neurol Neurosci 1990; 1:275-280.

Al-Majed AA, Neumann CM, Brushart TM, Gordon T. Brief electrical stimulation promotes the speed and accuracy of motor axonal regeneration. J Neurosci 2000; 20:2602-2608.

Angelov DN, Neiss WF, Streppel M, Andermahr J, Mader K, Stennert E. Nimodipine accelerates axonal sprouting after surgical repair of rat facial nerve. J Neurosci 1996; 16: 1041-1048.

Ansselin AD, Fink T, Davey DF. Peripheral nerve regeneration through nerve guides seeded with adult Schwann cells. Neuropathol Appl Neurobiol 1997; 23:387-398.

Azzouz M, Leclerc N, Gurney M, Warter JM, Poindron P, Borg J. Progressive motor neuron impairment in an animal model of familial amyotrophic lateral sclerosis. Muscle Nerve 1997; 20:45-51.

Bodine-Fowler SC, Meyer RS, Moscowitz A, Abrams R, Botte M. Innaccurate projection of rat soleus motoneurons: a comparison of nerve repair techniques. Muscle Nerve 1997; 20:29-37.

Brushart TM. Preferential reinnervation of motor nerves by regenerating motor axons. J Neurosci 1988; 8:1026-1031.

Brushart TM. Preferential motor reinnervation: a sequential double-labeling study. Restor Neurol Neurosci 1990; 1:281-287.

Brushart TM. Motor axons preferentially reinnervate motor pathways. J Neurosci 1993; 13:2730-2738.

Brushart TM, Gerber J, Kessens P, Chen YG, Royall RM. Contributions of pathway and neuron to preferential motor reinnervation. J Neurosci 1998; 18:8674-8681.

Brushart TM, Seiler WA. Selective reinnervation of distal motor stumps by peripheral motor axons. Exp Neurol 1987; 97:289-300.

Covault J, Sanes JR. Neural adhesion molecule (N-CAM) accumulates in denervated and paralyzed skeletal muscles. Proc Natl Acad Sci 1985; 82:4544-4548.

DeSantis M, Berger PK, Laskowski MB, Norton AS. Regeneration by skeletomotor axons in neonatal rats is topographically selective at an early stage of reinnervation. Exp Neurol 1992; 116:229-239.

Evans PJ, Bain JR, Mackinnon SE, Makino AP, Hunter DA. Selective reinnervation: a comparison of recovery following microsuture and conduit nerve repair. Brain Res 1991; 559:315-321.

Franz CK, Rutishauser U, Rafuse VF. Polysialylated neural cell adhesion molecule is necessary for selective targeting of regenerating motor neurons. J Neurosci 2005; 25: 2081-2091.

Guenard V, Kleitman N, Morrissey TK, Bunge RP, Aebischer P. Syngeneic Schwann cells derived from adult nerves seeded in semipermeable guidance channels enhance peripheral nerve regeneration. J Neurosci 1992; 12: 3310-3320.

Gupta SK, Pringle J, Poduslo JF, Mezei C. Induction of myelin genes during peripheral nerve remyelination requires a continuous signal from the ingrowing axon. J Neurosci Res 1993; 34: 14-23.

Gramsbergen A, IJkema-Paassen J, Meek MF. Sciatic nerve transection in the adult rat: abnormal EMG patterns during locomotion by aberrant innervation of hindleg muscles. Exp Neurol 2000; 161:183-193.

Hardman VJ, Brown MC. Accuracy of reinnervation of rat internal intercostal muscles by their own segmental nerves. J Neurosci 1987; 7:1031-1036.

Hendry IA, Hill CE, Watters DJ. Long-term retention of Fast Blue in sympathetic neurones after axotomy and regeneration--demonstration of incorrect reconnections. Brain Res 1986; 376:292-298.

Jenq C, Coggeshall RE. The effects of an autologous transplant on patterns of regeneration in rat sciatic nerve. Brain Res 1986; 364:45-56.

Jenq C, Coggeshall RE. Sciatic nerve regeneration after autologous sural nerve transplantation in the rat. Brain Res 1987; 406:52-61.

Jessen KR, Mirsky R. Schwann cells: early lineage, regulation of proliferation and control of myelin formation. Curr Opin Neurobiol 1992; 2:575-581.

Kimura A, Ajiki T, Takeuchi K, Hakamata Y, Murakami T, Hoshino Y, Kobayashi E. Transmigration of donor cells involved in the sciatic nerve graft. Transplant Proc 2005; 37:205-207.

Labrador R, Buti M, Navarro X. Influence of collagen and laminin gels concentration on nerve regeneration after resection and tube repair. Exp Neurol 1998; 149: 243-252.

Lago N, Navarro X. Correlation between target reinnnervation and distribution of motor axons in the injured rat sciatic nerve. J Neurotrauma 2006; 23:227-240.

Le TB, Aszmann O, Chen YG, Royall RM, Brushart TM. Effects of pathway and neuronal aging on the specificity of motor axon regeneration. Exp Neurol 2001; 167:126-132.

Levi AD, Sonntag UK, Dickman C, Mather J, Li RH, Cordoba SC, Bichard B, Berens M. The role of cultured Schwann cell grafts in the repair of gaps within the peripheral nervous system of primates. Exp Neurol 1997; 143:25-36.

Lundborg G. Regeneration of peripheral nerves--a biological and surgical problem. Scand J Plast Reconstr Surg Suppl 1982; 19:38-44.

Madison RD, Archibald SJ, Brushart TM. Reinnervation accuracy of the rat femoral nerve by motor and sensory neurons. J Neurosci 1996; 16: 5698-5703.

Maki Y. Specificity in peripheral nerve regeneration: a discussion of the issues and the research. J Orthop Sci 2002; 7:594-600.

Maki Y, Yoshizu T, Tsubokawa N. Selective regeneration of motor and sensory axons in an experimental peripheral nerve model without endorgans. Scand J Plast Reconstr Surg Hand Surg 2005; 39:257-260.

Martini R, Xin Y, Schmitz B, Schachner M. The L2/HNK-1 carbohydrate epitope is involved in the preferential outgrowth of motor neurons on ventral roots and motor nerves. Eur J Neurosci 1992; 4:628–639.

Martini R, Schachner M. Immunoelectron microscopic localization of neural cell adhesion molecules (L1, N-CAM, and myelin-associated glycoprotein) in regenerating adult mouse sciatic nerve. J Cell Biol 1988; 106: 1735-1746.

Martini R, Schachner M, Brushart TM. The L2/HNK-1 carbohydrate is preferentially expressed by previously motor axonassociated Schwann cells in reinnervated peripheral nerves. J Neurosci 1994; 14:7180– 7191.

Midha R, Munro CA, Dalton PD, Tator CH, Shoichet MS. Growth factor enhancement of peripheral nerve regeneration through a novel synthetic hydrogel tube. J Neurosurg 2003; 99:555-565.

Mitchell LS, Griffiths IR, Morrison S, Barrie JA, Kirkham D, McPhilemy K. Expression of myelin protein gene transcripts by Schwann cells of regenerating nerve. J Neurosci Res 1990; 27:125-135.

Navarro X, Butí M, Verdú E. Autotomy prevention by amytriptiline after peripheral nerve section in different strains of mice. Restor Neurol Neurosci 1994; 6:151-157.

Navarro X, Kennedy WR. The effects of autologous nerve transplants on motor and sudomotor reinnervation by regenerative axons. Brain Res 1991; 565:181-187.

Navarro X, Verdú E. Cell transplants and artificial guides for nerve repair. In Herdegen T, Delgado-García JM (eds): Brain Damage and Repair. Dordrecht (NL), Kluwer Academic Pub, 2004, pp. 451-471.

Navarro X, Verdú E, Butí M. Comparison of regenerative and reinnervating capabilities of different functional types of nerve fibers. Exp Neurol 1994; 129:217-224.

Nichols CM, Brenner MJ, Fox IK, Tung TH, Hunter DA, Rickman SR, Mackinnon SE. Effect of motor versus sensory nerve grafts on peripheral nerve regeneration. Experimental Neurology 2004; 190:347-355.

Politis MJ, Ederle K, Spencer PS.Tropism in nerve regeneration in vivo. Attraction of regenerating axons by diffusible factors derived from cells in distal nerve stumps of transected peripheral nerves. Brain Res 1982; 253:1-12.

Politis MJ, Spencer PS. An in vivo assay of neurotropic activity. Brain Res 1983; 278:229-231.

Politis MJ, Steiss JE. Electromyographic evaluation of a novel surgical preparation to enhance nerve-muscle specificity that follows mammalian peripheral nerve trunk transection. Exp Neurol 1985; 87:326-333.

Prodanov D. Morphometric analysis of the rat lower limb nerves – Anatomical data for neural prosthesis design. Thesis, University of Twente, 2006.

Rende M, Granato A, Manaco ML, Zelagno G, Toesca A. Accuracy of reinnervation by peripheral nerve axons regenerating across 10 mm gap within an impermeable chamber. Exp Neurol 1991; 111:332-339.

Rich KM., Disch SP, Eichler ME. The influence of regeneration and nerve growth factor on the neuronal cell body reaction to injury. J Neurocytol 1989; 18: 569-576.

Robinson GA, Madison RD. Motor neurons can preferentially reinnervate cutaneous pathways. Exp Neurol 2004; 190:407-413.

Robinson GA, Madison RD. Preferential motor reinnervation in the mouse: comparison of femoral nerve repair using a fibrin sealant or suture. Muscle Nerve 2003; 28:227-231.

Rodríguez FJ, Gómez N, Labrador RO, Butí M, Ceballos D, Cuadras J, Verdú E, Navarro X. Improvement of regeneration with predegenerated nerve transplants in silicone chambers. Restor Neurol Neurosci 1999; 14:65-79

Rodríguez FJ, Valero-Cabré A, Navarro X. Regeneration and functional recovery following peripheral nerve injuries. Drug Discovery Today: Disease Models 2004; 1:177-185.

Rodriguez FJ, Verdu E, Ceballos D, Navarro X. Nerve guides seeded with autologous schwann cells improve nerve regeneration. Exp Neurol 2000; 161: 571-584.

Saito H, Nakao Y, Takayama S, Toyama Y, Asou H. Specific expression of an HNK-1 carbohydrate epitope and NCAM on femoral nerve Schwann cells in mice. Neurosci Res 2005; 53:314-322.

Schmalbruch H. Fiber composition of the rat sciatic nerve. Anat Rec 1986; 215:71-81.

Shefner JM. Motor unit number estimation in human neurological diseases and animal models. Clin Neurophysiol 2001; 112:955-964.

Smahel J, Jentsch B. Stimulation of peripheral nerve regeneration by an isolated nerve fragment. Ann Plast Surg 1986; 16:494-501.

Stevens B, Tanner S, Fields RD. Control of myelination by specific patterns of neural impulses. J Neurosci 1998; 18:9303-9311.

Sumner AJ. Aberrant reinnervation. Muscle Nerve 1990; 13:801-803.

Trapp BD, Hauer P, Lemke G. Axonal regulation of myelin protein mRNA levels in actively myelinating Schwann cells. J Neurosci 1988; 8:3515-3521.

Udina E, Rodriguez FJ, Verdu E, Espejo M, Gold BG, Navarro X. FK506 enhances regeneration of axons across long peripheral nerve gaps repaired with collagen guides seeded with allogeneic Schwann cells. Glia 2004; 47: 120-129.

Valero-Cabré A, Navarro X. Functional impact of axonal misdirection after peripheral nerve injuries followed by graft or tube repair. J Neurotrauma 2002; 19:1475-1485.

Valero-Cabré A, Tsironis K, Skouras E, Perego G, Navarro X, Neiss WF. Superior muscle reinnervation after autologous nerve graft or poly-l-lactide-ε-caprolactone (PLC) tube implantation in comparison to silicone tube repair. J Neurosci Res 2001; 63:214-223.

Weiss P, Edds MV. Sensory-motor nerve crosses in the rat. J Neurophysiol 1945; 30:173-193.

Yu K, Kocsis JD. Schwann cell engraftment into injured peripheral nerve prevents changes in action potential properties. J Neurophysiol 2005; 94:1519-1527.

DISCUSIÓN GENERAL

Regeneración axonal a través de electrodos regenerativos

La evaluación de la regeneración del nervio ciático a través de los electrodos regenerativos de poliamida demuestra que los axones son capaces de regenerar a través de los micro-orificios de tales electrodos regenerativos y mantenerse funcionales tras implante crónico de hasta 12 meses en la rata. Todas las ratas implantadas presentaron regeneración del nervio ciático a través de los electrodos regenerativos, alcanzando la máxima reinervación distal a los 6 meses postimplante, resultados que se corresponden con el número de fibras mielínicas que alcanza cifras similares a las del nervio control. Sin embargo, de los 7 a los 12 meses encontramos un descenso en la reinervación funcional más distal en algunos de los animales y a nivel morfológico un descenso en el número de fibras mielínicas distales al electrodo. Esta pérdida de reinervación distal a largo plazo es probablemente debida a una axonopatía compresiva a nivel del electrodo, causada por compresión de los axones al progresar su maduración y aumentar su calibre dentro de los orificios delimitados.

Si se comparan los resultados obtenidos a los 2,5 meses post-implante, en los animales con electrodo regenerativo (Trabajo 1) y los animales sin electrodo en la guía de silicona (Trabajo 6), el número de fibras mielínicas a nivel distal es de 4940 ± 1455 vs 15132 ± 652. Esto significa que una tercera parte de los axones presentarían dificultades para atravesar el electrodo regenerativo. El diámetro medio de las fibras mielínicas en los animales implantados con el electrodo regenerativo es de 1,86 ± 0,13 µm, mientras que en ratas con sección y reparación por sutura directa es de aproximadamente 3,2 µm (Mackinnon et al., 1991). Por tanto, la colocación de un electrodo regenerativo entre los extremos del nervio seccionado determina una apreciable dificultad para la regeneración de axones, lo que se traduce en un menor número de axones mielínicos y un menor diámetro de éstos distalmente, así como en un retraso y menores niveles de reinervación de dianas, musculares o nerviosas, distales.

El diseño ideal de un electrodo regenerativo implica el poder acceder a un número elevado de axones, es decir, disponer de tantos orificios como axones de forma que se alcanzara una proporción electrodo:axón de 1:1, mediante orificios de diámetros entre 1 y 12 µm. Sin embargo, este diseño no resulta biológicamente

efectivo, ya que la regeneración falla cuando los orificios son demasiado pequeños (Navarro et al., 1996; Wallman et al., 2001), debiendo, por tanto, establecer un equilibrio entre el número de agujeros y su diámetro. Estudios previos han indicado que, para favorecer la regeneración axonal y aún poder registrar señales de grupos relativamente pequeños de axones, se debe aceptar un equilibrio entre el número de orificios en el electrodo y su tamaño, siendo para ello el diámetro de los orificios más adecuado entre 40 y 65 μm (Kovacs et al., 1994; Navarro et al., 1996; Wallman et al., 2001). Desde el punto de vista eléctrico, se ha calculado que diámetros de los orificios-electrodo superiores a 30 μm serían necesarios para mejorar la relación señal-ruido en el registro (Edell, 1986). El electrodo regenerativo de poliamida empleado en este proyecto dispone de 281 orificios circulares de 40 μm de diámetro, en mayor número de lo que es posible realizar, para las mismas dimensiones totales, sobre otros materiales, como silicio. A pesar de haberse demostrado la regeneración de las fibras nerviosas a través de este tipo de electrodos, los resultados obtenidos en el presente trabajo sugieren que sería conveniente un aumento en el diámetro de los orificios con el fin que la remielinización no encuentre un obstáculo físico una vez reinervados los tejidos. El aumento de diámetro de los orificios o del número de orificios, y correspondientemente de la transparencia o espacio total abierto, favorecería la regeneración axonal (Navarro et al., 1996; Wallman et al., 2001). Sin embargo, si se aumenta mucho el diámetro de los orificios, se perdería el objetivo fundamental del diseño del electrodo regenerativo, que es la mejora de la selectividad de interfase neural, con lo que se debe buscar un equilibrio entre el mantenimiento de la selectividad con diámetros entre 40-65 μm y el aumento del área libre para el paso de los axones regenerativos.

A partir de nuestros resultados tras implante *in vivo* y, gracias a continuas mejoras en el proceso tecnológico de la fabricación de electrodos basados en poliamida, se ha desarrollado un nuevo modelo de electrodo regenerativo (Ramachandran et al., 2006). En este siguiente diseño de electrodo regenerativo, utilizado para la obtención de señales neurales, se aumentó el número de orificios a 571 sin variar el diámetro de los mismos (40 μm) . La tabla siguiente muestra los resultados de los tests electrofisiológicos realizados a los 2 meses y 7 meses post-implante y la evaluación morfológica realizada a los 7 meses en algunos de estos animales (Ramachandran et al., 2006).

		2 meses	7 meses
M. Gastrocnemio	Latencia (ms)	3.9 ± 0.1	1.9 ± 0.05
	PAMC (mV)	8.0 ± 1.8	26.2 ± 5.9
M. Plantar	Latencia (ms)	12.3 ± 2.1	4.7 ± 0.2
	PAMC (mV)	0.16 ± 0.03	1.9 ± 0.5
Area del Nervio	(mm^2)		0.633 ± 0.181
Fibras Mielínicas	(n^o)		13079 ± 3433

Si comparamos estos resultados con los obtenidos con el primer diseño del electrodo (Trabajo 1), vemos como la reinervación distal (músculo plantar) es ligeramente mayor con el segundo diseño que con el anterior a los 2 meses (0.16 vs 0.09 mV) y a los 6-7 meses post-implante. Pero donde más diferencias se observan es en el número de fibras mielínicas que atraviesan el electrodo regenerativo. Mientras que con el diseño anterior a los 6 meses el número era de 8848 ± 1033, con el diseño actual el número alcanza las 13000. Por tanto, el aumento en el número de agujeros estaría mejorando las capacidades del diseño anterior.

Estimulación y registro de señales neurales a través del electrodo regenerativo

La aplicación de interfases neurales para el control de prótesis artificiales pretende conseguir la comunicación bidireccional entre el sistema nervioso del sujeto y la prótesis mecánica. Así, el registro de señales motoras eferentes puede ser usado para el control motor de la prótesis mecánica (Edell, 1986) mientras que las señales registradas a partir de sensores táctiles y angulares pueden ser utilizadas para proveer al paciente de retroalimentación propioceptiva y táctil por medio de la estimulación de fibras nerviosas aferentes (Riso, 1999).

Para los estudios de estimulación y registro, se utilizó un diseño mejorado del electrodo regenerativo. Se aumentó el número de orificios de 281 a 571 sin disminuir el diámetro de cada uno de ellos, con lo que aumentó la denominada transparencia o espacio abierto. Otro de los cambios en el diseño fue el aumento en el número de electrodos activos alrededor de los orificios, que pasó de 9 a 27, más 2 electrodos de referencia externos colocados en la pared de la guía de silicona.

La estimulación eléctrica mediante pulsos individuales de baja intensidad aplicados a través de los electrodos activos consigue la excitación de localizados

grupos de fibras nerviosas (Ceballos et al., 2002). Mediante el registro de la actividad muscular evocada se ha comprobado que la estimulación es selectiva en función del electrodo activo empleado. Así, la estimulación de algunos electrodos activos, pero no la de otros, induce la excitación de un determinado músculo.

Técnicamente más difícil resulta el registro de los impulsos axonales, especialmente en el caso de electrodos neurales implantados crónicamente (Navarro et al., 2005). Tras estimulación funcional y eléctrica, las señales registradas mediante los electrodos regenerativos corresponden seguramente a fibras de tipo Aβ –rápidas, altamente excitables– que conducen impulsos de amplitud elevada. Cuando utilizamos un patrón de estimulación eléctrica desde los tejidos distales a diferentes frecuencias y el registro de señales nerviosas subdivididas por latencias (Qtrac software; H. Bostock, copyright Institute of Neurology, London, UK), sólo encontramos fibras de latencia corta que se comportan como fibras Aβ (observaciones propias).

Las principales limitaciones en la función de interfase, particularmente para el registro de señales neurales, del electrodo regenerativo radican en la pérdida de conductividad por el aumento de la impedancia de los electrodos, a medida que aumenta el tiempo de implantación (observaciones propias; Roitbak y Sykova, 1999), y en la pérdida de continuidad por la baja resistencia de todo el sistema (electrodo, cinta y conector) a las tracciones mecánicas durante la actividad del animal.

En otros trabajos también se ha observado como, tras implantar un electrodo penetrante, con el tiempo se produce un descenso en el registro de señales neurales (Branner et al., 2004). En un caso de implante del mismo tipo de electrodo en el nervio mediano de un humano voluntario, a los 3 meses sólo 3 electrodos de un total de 20 permanecían activos, debido a la degradación de las conexiones por tensión mecánica en el punto de salida y al aumento de la impedancia de los electrodos (Warwick et al., 2003). El aumento de impedancia puede ser debido a la reacción inflamatoria y el crecimiento fibrótico alrededor de los electrodos, que aisla al electrodo de las fibras nerviosas, o al deterioro del material conductor de los electrodos activos (Liu et al., 1999; Turner et al., 1999; Murphy et al., 2004). En el caso de nervios regenerados, las dificultades metodológicas para el registro de potenciales de acción individuales, se acentúan debido a la reducción de la amplitud de tales potenciales (Loeb et al., 1977), ya que los axones regenerados son, incluso

a largo plazo, de menor calibre de lo normal y presentan cambios crónicos en las propiedades de excitabilidad de su membrana (Fields y Ellisman, 1986a, 1986b).

Por otra parte, para una correcta interconexión funcional nervio-prótesis es necesario poder distinguir la función que representan los impulsos nerviosos registrados por los diversos electrodos activos del electrodo regenerativo. Así, deben poder diferenciarse selectivamente los impulsos conducidos por axones motores para alimentar las órdenes de actuación a la prótesis. En este sentido, la pérdida de la normal arquitectura fascicular y el crecimiento desorganizado de los axones tras una sección completa del nervio periférico, presentan problemas adicionales en la identificación y clasificación de las señales registradas (Alzate et al., 2000; Brushart et al. 1995).

Mediante los electrodos regenerativos no se puede alcanzar un grado de selectividad ideal debido a que por cada orificio del electrodo crecen un número variables de axones (entre 20 y 90 fibras mielínicas; Ceballos et al., 2002) y, como hemos observado en el presente trabajo (Trabajo 1 y 3), estos axones pertenecen a poblaciones diferentes. Sin embargo, el procesamiento de las señales registradas por cada electrodo activo (que pueden incluir distintas clases funcionales), mediante algoritmos de reconocimiento de patrones, puede permitir una diferenciación suficiente de los tipos de impulsos (Jezernik et al., 2001; Cavallaro et al., 2003; Micera et al., 2003). Con la aplicación de algoritmos de reconocimiento de patrones, se realizará la separación, en una primera fase, de las señales aferentes de las eferentes, para después poder clasificar diferentes tipos de aferencias y de eferencias.

Desde el punto de vista neurobiológico, como no se puede disminuir el diámetro de los orificios por debajo de unas 30 μm dado que la regeneración falla, una opción de interés radica en conseguir separar axones de diferentes poblaciones para que regeneren por diferentes orificios-electrodos. Una de las posibles estrategias es la de tratar de separar mediante un tubo en Y, las aferencias de las eferencias neurales mediante moléculas guía, o mediante el tratamiento con esas moléculas de los diferentes agujeros.

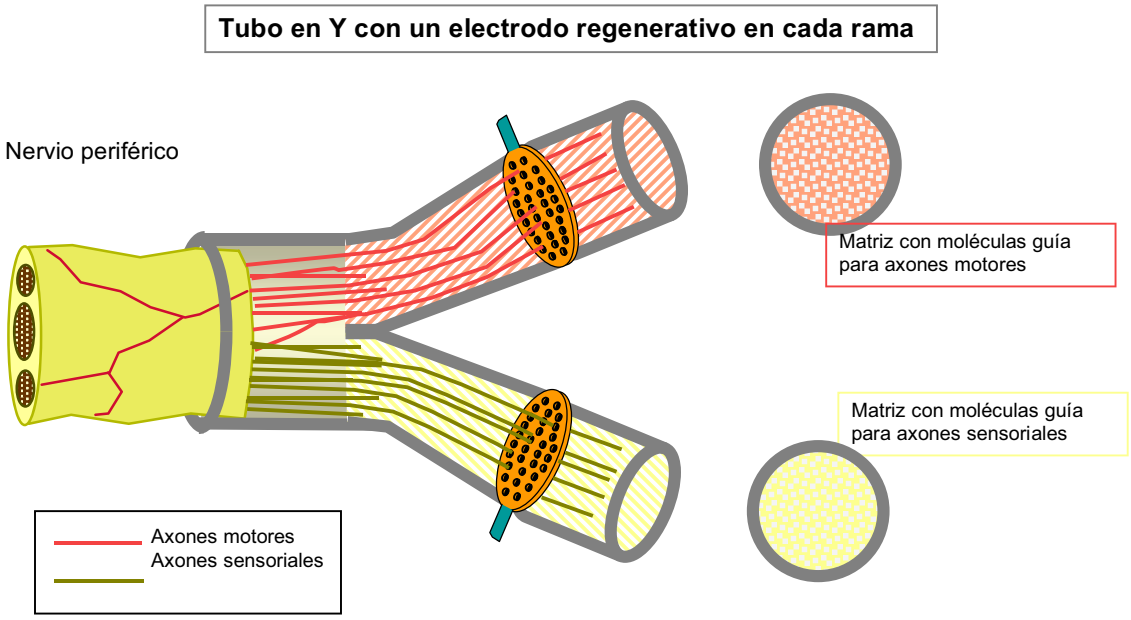

Regeneración y mantenimiento de axones en el modelo de amputación

El diseño de la neuroprótesis CYBERHAND incluye el implante del electrodo regenerativo entre los muñones del nervio seccionado en la extremidad amputada.

Tras lesión y reparación por tubulización, los axones pueden regenerar a través del tubo y mantenerse sin degenerar a lo largo del tiempo, sin que haya reconexión con los tejidos distales. La característica principal que se observa en el modelo de amputación es la formación de un neuroma a nivel distal, con un elevado número de fibras nerviosas delgadas orientadas de forma aleatoria, típica de un nervio periférico que se ha incapacitado para regenerar (Fried et al., 1991, 1993). La elevada densidad axonal a nivel distal también se encuentra a nivel proximal debido a la ramificación colateral que se produce (Gutmann y Sanders, 1943; Toft et al., 1988). Sin embargo, al no haber contacto con los tejidos distales y, por tanto, reinervación, este mayor número de axones se mantiene a lo largo del tiempo en lugar de ir disminuyendo (Mackinnon et al., 1991).

En el modelo de amputación hemos observado la formación de neuroma y el mantenimiento de éste a lo largo del tiempo. La densidad axonal no varía significativamente entre los 2,5 meses y los 9 meses indicando que no hay un descenso del número de colaterales axónicos a lo largo del tiempo como cabría esperar después de sección y reparación del nervio (Scadding y Thomas, 1983).

Otro de los hechos remarcables es la presencia de inmunoreactividad para CGRP, ChAT y GAP-43 a nivel proximal y distal a los 6 y 9 meses. Estos resultados indican que los axones, a pesar de no estar reconectando con los tejidos distales, expresan neurotransmisores y marcadores de axones en regeneración como el GAP-43 (Van Lookeren Campagne et al., 1999) a nivel del neuroma, indicando que el potencial regenerativo se mantiene a largo plazo a pesar de no haber reinervación distal.

Efecto del transplante de células de Schwann

En los grupos de amputación con transplante de CS se siguen observando las características típicas de un neuroma. En este caso, la densidad axonal tanto a nivel proximal como a nivel distal es mayor que en los grupos de amputación sin el transplante, y también se mantiene elevado a lo largo del tiempo.

Tras lesión del nervio, las CS denervadas proliferan y expresan una variedad de moléculas, desde factores neurotróficos hasta componentes de la matriz extracelular y de la lámina basal con tal de proveer de un ambiente favorable a la regeneración axonal (Verdú y Navarro, 1998). Sin embargo, las CS que quedan denervadas durante mucho tiempo son morfológica y funcionalmente diferentes; desciende la expresión de $p75^{NTR}$ (You et al., 1997) y se reduce la liberacion de factores tróficos (Fu y Gordon, 1995), hecho que podría explicar porqué las CS denervadas van perdiendo la capacidad para sostener la regeneración axonal (Hall, 2005). La función del transplante de CS es el de mejorar la regeneración axonal (Guénard et al., 1992; Rodríguez et al., 2000; Udina et al., 2004b), pero también se ha observado que un transplante de CS afecta al patrón de excitabilidad de los axones atrapados en un neuroma (Yu y Kocsis, 2005). En resumen, un transplante de CS en el modelo de amputación resulta beneficioso para el mantenimiento axonal a lo largo del tiempo.

Por el contrario, el transplante de CS de una linea inmortalizada obstaculiza la regeneración y reduce el mantenimiento de los axones en el modelo de amputación. En cambio, cuando se transplantan CS inmortalizadas que sobreexpresan GDNF, los resultados mejoran en cuanto al número de fibras mielínicas a nivel distal, en comparación con su grupo control, pero no alcanzan la densidad axonal observada para el transplante de CS primarias. Es probable que las CS inmortalizadas no induzcan la respuesta regenerativa axonal al mantenerse en un estado quiescente y sólo la mayor expresión de factores neurotróficos remedaría esta situación.

Aplicabilidad del modelo de amputación al Cyberhand

Los electrodos regenerativos estan pensados para ser implantados en los extremos seccionados de un nervio proximal a una amputación. Es de vital importancia conocer el comportamiento de los axones a nivel distal y a nivel proximal puesto que, pensando en la aplicación en humanos, primero se daría una amputación de una extremidad y luego la sección proximal para el implante del electrodo. A pesar de la formación del neuroma, los resultados muestran como los axones son capaces de sobrevivir y mantenerse funcionales a lo largo del tiempo. Además, el transplante de CS aumenta la regeneración axonal por lo que cabría esperar que en el caso de una denervación crónica en la que las CS distales pierden la capacidad regenerativa (Fu y Gordon, 1995), cuando se seccionara el nervio a nivel proximal habría dificultades para la regeneración axonal. El transplante en ese momento de CS daría un aporte trófico y trópico adecuado para reanudar la regeneración a nivel proximal.

Otra estrategia interesante es la de enterrar el segmento distal en un músculo denervado. Los resultados que obtuvimos fueron que la regeneración axonal es buena y el número de colaterales supernumerarios disminuye respecto al modelo de amputación simple. El hecho que haya un menor número de colaterales y que se puedan registrar potenciales compuestos del músculo reinervado, significa que algunos de los axones reinervan el músculo mientras que otros se quedan formando el neuroma. Si pensamos en el registro de señales eferentes y aferentes desde el electrodo regenerativo, se podría diseñar una estrategia consistente en implantar el electrodo en el nervio y, a nivel distal enterrar el nervio en un músculo. A su vez, se puede implantar un electrodo en el músculo (epimisial o intramuscular) para conseguir el registro diferencial de señales eferentes (Wells et al., 2001).

Regeneración de axones motores

La distribución topográfica de los axones motores en un nervio control sigue un patrón fascicular, es decir, hay una densidad diferente de axones motores dependiendo de la zona del nervio. Tras lesión del nervio ciático, este patrón se mantiene cuando no hay una disrupción de los túbulos endoneurales, como es el caso de la lesión por aplastamiento. El mantenimiento de la fasciculación motora se corresponde con un buen grado de regeneración y reinervación funcional (Nguyen et

al., 2002; Valero-Cabré et al., 2004). Sin embargo, cuando se produce la interrupción completa por sección del nervio, el nervio regenerado muestra una pérdida del patrón normal de fasciculación y, en correspondencia, la reinervación distal no alcanza los valores anteriores. El marcaje inmunohistoquímico contra el enzima acetilcolin-transferasa (ChAT) es de utilidad tanto para evaluar el patrón de fasciculación de los axones motores como para analizar el número de axones motores que se encuentran en el nervio regenerado. Hemos observado como mediante el marcaje contra ChAT, se obtiene el mismo porcentaje de axones motores que el obtenido por técnicas de microscopía óptica (Schmalbruch, 1986), sobre un 20% en el nervio ciático de rata. Tras lesión y reparación del nervio ciático, el porcentaje se mantiene en el mismo rango indicando que, a pesar que hay un aumento en el número de fibras mielínicas por colateralización (Jenq y Coggeshall, 1985; Mackinnon et al., 1991), este aumento es similar tanto para la población sensorial como para la motora.

Si comparamos los datos obtenidos entre la regeneración a través de un tubo de silicona simple o con un electrodo regenerativo, vemos que mientras que en el primero se mantiene la proporción de axones motores en un 25%, en el segundo es de un 14-18% indicando que hay una mayor pérdida de axones motores que sensoriales. Estos datos se corroboran al realizar el contaje de motoneuronas y neuronas sensoriales marcadas con retrotrazadores, que demuestra un descenso en el número de motoneuronas marcadas retrógradamente (Negredo et al., 2004), datos que a la vez se corresponden con una menor reinervación distal del músculo plantar comparada con la del nervio digital.

Tras lesión de un nervio periférico mixto, los axones sensoriales regeneran más rápidamente en estadíos tempranos de regeneración en comparación con los axones motores (Macias et al., 1998; Suzuki et al., 1998). Por tanto, dependiendo del momento en el que se realice la valoración morfológica y funcional se podrá observar la diferencia en la regeneración de las dos poblaciones axonales. En nuestros trabajos se ha valorado la regeneración y reinervación distal tras lesiones del nervio a los dos meses postlesión. En las lesiones generadas, a los 30 días se ha iniciado ya la reinervación de dianas distales en la pata de la rata, y a los 60 días la reinervación distal se ha empezado a consolidar (Valero-Cabré y Navarro, 2002); por tanto, a este tiempo no esperamos encontrar diferencias marcadas de la regeneración entre las dos poblaciones. Sin embargo, en el caso de la implantación

del electrodo regenerativo, cuando los axones regeneran se encuentran con un "cedazo" que limita su elongación, es decir, tal y como van regenerando los axones van ocupando los diferentes agujeros del electrodo por lo que los últimos en llegar no tendrán espacio para pasar. Esto explica el menor número de axones mielínicos a nivel distal comparado con los encontrados en un tubo de silicona simple. Dado que los axones motores presentan un retraso en las etapas iniciales de la regeneración, se explicaría la menor proporción de axones motores con respecto a los sensoriales que llegan a nivel distal al electrodo.

Estrategias para mejorar la regeneración de diferentes poblaciones axonales

Uno de los determinantes más importantes de la recuperación funcional tras lesiones de nervio es la precisión en la reinervación distal. Los mecanismos por los cuales los conos de crecimiento axonales seleccionan los túbulos endoneurales por los que elongarse, todavía no son conocidos. En un nervio mixto, la especificidad de la reinervación motora y sensorial parece producirse por un *prunning* o retracción selectiva de los colaterales axónicos que inicialmente crecen hacia tejidos inapropiados (Brushart, 1988; Madison et al., 1996). Este *prunning* puede estar influenciado por niveles de factores neurotróficos (Robinson y Madison, 2004) o por moléculas expresadas en las células de Schwann como el glucopéptido L2/HNK-1 (Martini et al., 1992, 1994) y la molécula de adhesión celular neural (NCAM) (Saito et al., 2005). No obstante, hay que tener en cuenta que en la mayoría de trabajos de regeneración selectiva se utiliza el nervio femoral como modelo de regeneración y reinervación periférica. El nervio femoral es un nervio mixto que se bifurca en el nervio safeno, rama sensorial, y en el nervio que inerva el músculo cuadriceps, rama muscular o motora. De los trabajos realizados con este modelo hay que considerar una serie de variables. La primera es que en la mayoría de estos trabajos utilizan la aplicación de distintos retrotrazadores en las ramas sensorial y motora para ver la regeneración por cada una de las ramas. Sin embargo, un mayor marcaje de motoneuronas desde la rama muscular no significa que haya una reinervación motora preferencial sino que los axones motores pueden estar ocupando túbulos endoneurales pertenecientes a axones sensoriales propioceptivos. El número de axones motores que están entrando en la rama muscular así como su patrón fascicular puede ser la medida más directa y eficaz de la regeneración selectiva. Otras variables a tener en consideración, en el modelo de nervio femoral, son la

especie animal, la edad del animal, el punto de lesión y el tipo de reparación nerviosa (Madison et al., 1996; Le et al., 2001; Robinson y Madison, 2003; Franz et al., 2005). La principal diferencia entre el nervio femoral y el ciático es que este último es mixto en prácticamente toda su longitud. En el modelo del nervio femoral se ha observado que a mayor distancia entre la lesión y el punto de bifurcación, los axones tienen menor capacidad para alcanzar sus dianas originales (Madison et al., 1996), es decir, si se lesiona el nervio cuando es mixto y no se da una clara división topográfica sensorial-motora, es más difícil observar regeneración selectiva. Esto puede explicar por qué en el nervio ciático no se obtienen los mismos resultados que los conseguidos en el nervio femoral al aplicar diferentes estrategias utilizadas para mejorar la regeneración específica (Maki, 2002).

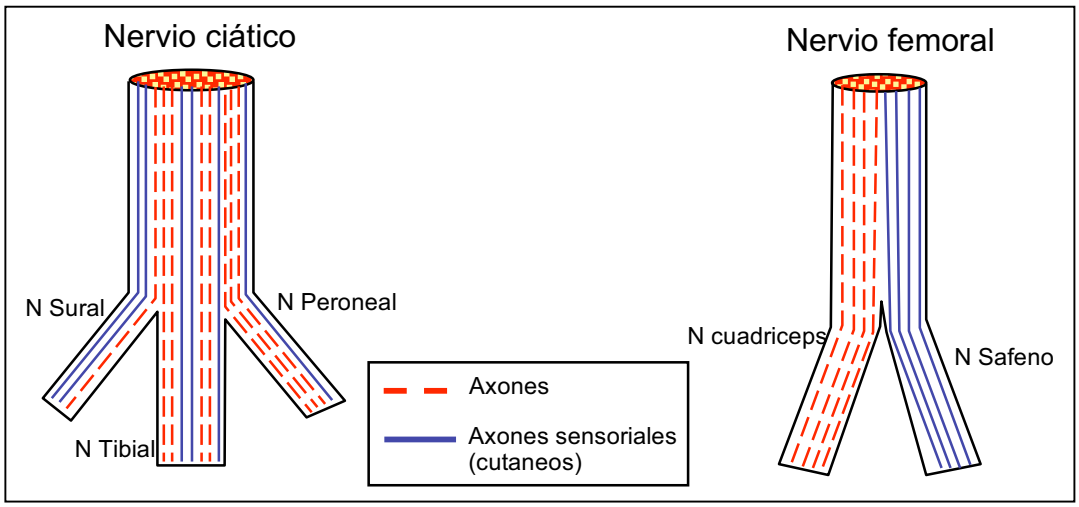

Nuestros resultados muestran como el transplante de un injerto de raíz dorsal o ventral no aumenta significativamente la regeneración sensorial y motora respectivamente, a los 3 meses postlesión. Sin embargo, sí que se observan pequeñas diferencias en estadíos iniciales de la regeneración de axones motores a través de injertos de raíz ventral, y una mayor reinervación sensorial a tiempo final en el grupo DR. Una de las explicaciones a estos resultados es que los conos de crecimiento entrarían en contacto de forma temprana con factores de membrana o difusibles, a cortas distancias, secretados por el nervio distal en degeneración, y que atraerían a los axones regenerativos. En el caso del modelo del nervio femoral explicaría que, si la lesión se produce muy cerca de la bifurcación, los axones, ya prácticamente segregados, entrarían en contacto con una fuente de factores específica para cada población axonal, y en mayor concentración que si los axones

están mezclados. En nuestro caso, el hecho que los axones motores y sensoriales estén contactando dentro de la guía de reparación con una fuente de factores secretados por CS motoras o sensoriales, podría estar ayudando a la regeneración selectiva en los primeros estadíos.

Se desconocen los mecanismos que pueden intervenir en una posible regeneración selectiva. Ya se ha comentado con anterioridad que las CS que acompañan a los axones motores expresan L2/HNK1 (Martini et al., 1992, 1994). En observaciones de nuestro laboratorio hemos constatado la expresión del péptido en raíz ventral predegenerada en cultivo hasta los 7 días post-denervación (resultados propios; Saito et al., 2005). Por tanto, en el momento de los transplantes, el injerto de raíz ventral todavía está expresando L2/HNK-1. Se desconoce, no obstante, si esta molécula está implicada directamente en el aumento de la tasa de regeneración axonal motora observada en estadíos iniciales. Lo que se ha observado es que el aumento de BDNF por estimulación eléctrica del nervio femoral aumenta la expresión de HNK1 en el nervio regenerado y se corresponde con una mayor reinervación muscular distal (Eberhardt et al., 2006). A pesar de que existen evidencias de que la presencia del péptido HNK1 aumenta selectivamente la regeneración de axones motores (Irintchev y Schachner, comunicación personal; observaciones propias), sería el conjunto de factores neurotróficos secretados, por las CS en proliferación (Lobsiger et al., 2002; An et al., 2003) o por las motoneuronas (Al-Majed et al., 2004), el que podría estar afectando, por diversos mecanismos, la selectividad de la regeneración axonal.

CONCLUSIONES

1. Los electrodos regenerativos de poliamida permiten la regeneración de los axones de un nervio periférico seccionado a través de los orificios del electrodo.
   1.1. De los 2 a los 6 meses post-implante hay un aumento en el número de axones que regeneran a través del electrodo junto con una progresiva maduración axonal y una apariencia tìpica de un nervio regenerado (vaina de mielina más delgada y fibras de menor diámetro).
   1.2. En algunos casos aparecen signos de axonopatía compresiva de los 6 a los 12 meses post-implante, causando una pérdida de fibras regeneradas y un descenso de la reinervación distal.
   1.3. Comparado con una guía de silicona sin electrodo regenerativo, la regeneración nerviosa está limitada por la interposición del electrodo, que representa un obstáculo para la elongación axonal.
   1.4. Los axones motores y sensoriales regeneran juntos a través del electrodo regenerativo. No obstante, los axones motores regeneran con retraso y presentan una mayor dificultad para atravesar el electrodo que los axones sensoriales.

2. Los electrodos regenerativos son útiles para el registro de señales neurales cuando se estimulan, funcional o eléctricamente, dianas distales. No obstante, los registros se obtuvieron en un 50% de los electrodos implantados, indicando que existen limitaciones en el registro, principalmente atribuídas al aumento de impedancia de los electrodos y a las tracciones mecánicas a las que está sometido todo el sistema tras implante crónico.

3. Los axones del nervio ciático son capaces de regenerar entre los extremos seccionados separados por una distancia corta a través de una guía de silicona, a pesar de mantener el extremo distal en una cámara ciega y sin capacidad de reconectar con los tejidos distales, remedando una situación de amputación.
   3.1. El número de fibras mielínicas regeneradas, en comparación con un nervio control y con un nervio regenerado en condiciones normales, está aumentado, y son de calibre pequeño y poco mielinizadas, debido a la profusa ramificación y a la formación de un neuroma. Los axones apenas

muestran signos de degeneración a largo plazo y mantienen características funcionales.

3.2. La reconexión del extremo distal a un músculo previamente denervado, permite su reinervación e induce un descenso del número de colaterales axonales y un aumento en el calibre de los axones regenerados.

3.3. El transplante de células de Schwann primarias en la cámara ciega distal tiene efectos positivos sobre la regeneración y el mantenimiento de los axones en el modelo de amputación, estimulando el crecimiento axonal y la ramificación distal.

3.4. Células de Schwann inmortalizadas no son capaces, por ellas mismas, de inducir el crecimiento axonal en un ambiente permisivo como es el nervio degenerado. La producción de GDNF por estas células influye favorablemente la regeneración axonal.

4. La topografía y el patrón fascicular normales de los axones motores se mantienen después de una lesión dels nervio ciático por aplastamiento, pero se pierde tras sección del nervio y reparación. El número de axones motores aumenta de forma proporcional al de fibras sensoriales, manteniéndose la proporción de ambas poblaciones. La pérdida de la organización fascicular tras neurotmesis se correlaciona de forma significativa con el déficit de recuperación de la función motora. El marcaje inmunohistoquímico contra ChAT es un buen método para evaluar el número y la especificidad topográfica de los axones motores regenerados tras lesiones nerviosas.

5. El transplante de un segmento nervioso predegenerado dentro de una guía de silicona aumenta la regeneración axonal y la reinervación distal. No se observa un efecto claro sobre la reinervación selectiva o preferencial cuando se realiza un tranplante de un segmento de raíz espinal ventral o dorsal proveniente de animales singénicos. No obstante, la regeneración de los axones motores es promovida en fases iniciales con el tranplante de raíz ventral, mientras que la reinervación de vías sensoriales aumenta en presencia del injerto de raíz dorsal.

6. La viabilidad de los electrodos regenerativos como interfase para el control neural de una prótesis mecánica y para la retroalimentación sensorial del sujeto requiere de avances combinados de la microtecnología y de la neurobiología.
   6.1. Los resultados de este trabajo indican la conveniencia de aumentar la transparencia y la robustez de los electrodos regenerativos de poliamida, de forma que mejoren las posibilidades de regeneración axonal y la resistencia del sistema de interfase en implantes a largo plazo.
   6.2. La regeneración axonal debe ser estimulada, particularmente para los axones mielínicos gruesos, y selectívamente guiada, de forma que se pueda obtener un patrón diferencial de la regeneración de axones motores y sensoriales del nervio.
   6.3. El mantenimiento de los axones regenerados en situaciones de amputación de la extremidad requiere de estrategias para el aporte de factores diana que promuevan la respuesta axonal y reduzcan la formación de neuromas terminales.

CONCLUSIONS

1. Polyimide sieve electrodes implanted in a transected peripheral nerve allowed regeneration of axons through the array of via holes.
   1.1. With increasing implantation time from 2 to 6 months there is increasing number and progressive maturation of regenerated axons.
   1.2. At longer term postimplantation, from 6 to 12 months, there are signs of compressive axonopathy causing loss of regenerated fibers and decline in target reinnervation in some cases.
   1.3. When compared with a silicone guide without the sieve electrode, nerve regeneration is limited by the interposition of the electrode, that acts as an obstacle for axonal growth.
   1.4. Motor and sensory axons grow together through the sieve electrode without a clear distribution of muscular nerve fascicles. However, motor fibers regenerating with more delay are confined to the periphery and have more difficulties to find paths across the sieve perforations than sensory axons.

2. The regenerative electrodes are an useful interface to record neural signals after functional or electrical stimulation of targets. Nevertheless, signal recordgins were obtained with 50% of the implanted electrodes. Failures are mainly attributed to increase of the electrodes impedance and to breaks due to mechanical traction affecting the whole system during chronic implants.

3. Sciatic nerve axons are able to regenerate through a short gap bridged by a silicone guide despite the distal nerve is enclosed inside a capped chamber avoiding reconnection with distal targets, mimiking an amputation model.
   3.1. Axons can sustain distal regenerated branches without degenerating for a long time and express functional features. The amputee model shows the expected features of a neuroma that is formed when regenerating axons are prevented from reaching end organs.
   3.2. Distal reconnection to a denervated muscle allows for its reinnervation, and induces a reduction in the number of axonal sprouts and an increase in the caliber of regenerated axons.

3.3. A transplant of primary Schwann cells in the distal capped chamber of the amputee model has positive effects, by stimulating the axonal growth response and the number of regenerating axons.

3.4. Schwann cells of an immortalized line are not able to induce axonal growth in a permissive environment such as the degenerated peripheral nerve. GDNF production by these cells favorably influences axonal regeneration.

4. The normal fascicular architecture and facicular pattern of motor axons are maintained after a sciatic nerve crush, but there are lost after nerve section and repair, when motor axons are scattered within small regenerated fascicles throughout the nerve. The loss of the fascicular organization significantly correlates with the deficient recovery of motor function. Immunohistochemical labeling against ChAT is a good method to assess the number and the topographical specificity of regenerated motor axons after nerve lesions.

5. Transplantation of a small predegenerated nerve segment inside a silicone guide enhances axonal regeneration, leading to slightly faster and higher levels of target reinnervation. There is not clear preferential reinnervation promoted when the nerve segment transplanted is of pure sensory or motor origin. Nevertheless, regeneration of motor axons is promoted at early times by the motor graft, whereas reinnervation of sensory pathways is increased in the presence of the sensory graft.

6. La viability of regenerative electrodes as an effective interface for the neural control of a mechanical prosthesis and for the sensory feedback to the subject requires combined advances of microtechnology and neurobiology.

6.1. The resultads of this work indicate the need to increase the transparency and the robustness of the polyimide regenerative electrodes, in order to improve the possibilties of axonal regeneration and the resistence of the whole system during long-term implantation.

6.2. Axonal regeneration must be enhanced, particularly for large myelinated axons, and selectively guided, so that a differential pattern of regeneration of motor and sensory axons present in the nerve could be achieved.

6.3. Maintenance of regenerated axons in cases of limb amputation requires the application of strategies to provide target factors that promote the axonal response and reduce the neuroma formation.

BIBLIOGRAFÍA

Abernethy DA, Thomas PK, Rud A, King RHM (1994) Mutual attraction between emigrant cells from transected denervated nerve. J Anat 184:239.

Agnew WF, McCreery DB (1990) Considerations for safety with chronically implanted nerve electrodes. Epilepsia 31 Suppl 2:S27-32.

Akin T, Najafi K, Smoke RH, Bradley RM (1994) A micromachined silicon sieve electrode for nerve regeneration applications. IEEE Trans Biomed Eng 41:305-313.

Al Majed AA, Tam SL, Gordon T (2004) Electrical stimulation accelerates and enhances expression of regeneration-associated genes in regenerating rat femoral motoneurons. Cell Mol Neurobiol 24:379–402.

Alzate LH, Sutachan JJ, Hurtado H (2000) An anterograde degeneration study of the distribution of regenerating rat myelinated fibers in the silicone chamber model. Neurosci Lett 286:17-20.

An YH, Wan H, Zhang ZS, Wang HY, Gao ZX, Sun MZ, Wang ZC (2003) Effect of rat Schwann cell secretion on proliferation and differentiation of human neural stem cells. Biomed Environ Sci 16:90-94.

Ann ES, Mizoguchi A, Okajima S, Ide C (1994) Motor axon terminal regeneration studied by protein gene product 9,5 immunohistochemistry on the rat. Arch Histol Cytol 57:317-330.

Archibald SJ, Shefner J, Krarup C, Madison RD (1995) Monkey median nerve repaired by nerve graft or collagen nerve guide tube. J Neurosci 15:4109-4123.

Atkins DJ, Heard DCY, Donovan WH (1996) Epidemiologic overview of individuals with upper limb loss and their reported research priorities. J Prosthetic and Orthotics 8:2-11.

Atroshi I, Rosberg HE (2001) Epidemiology of amputations and severe injuries of the hand. Hand Clin 17:343-350.

Bixby JL, Harris WA (1991) Molecular mechanisms of axon growth and guidance. Ann Rev Cell Biol 7:117-159

Bloch J, Fine EG, Bouche N, Zurn A, Aebischer P (2001) Nerve growth factor and neurotrophin-3 releasing guidinance channels promote regeneration of the transected rat dorsal root. Exp Neurol 172:425-432.

Bowe MA, Fallon JR (1995) The role of agrin in synapse formation. Annu Rev Neurosci 18:443-462.

Boyd JG, Gordon T (2003) Glial cell line-derived neurotrophic factor and brain-derived neurotrophic factor sustain the axonal regeneration of chronically axotomized motoneurons in vivo. Exp Neurol 183:610-619.

Bradley RM, Cao X, Akin T, Najafi K (1997) Long term chronic recordings from peripheral sensory fibers using a sieve electrode array. J Neurosci Methods 73:177-186.

Branner A, Stein RB, Normann RA (2001) Selective stimulation of cat sciatic nerve using an array of varying-length microelectrodes. J Neurophysiol 85:1585-1594.

Branner A, Stein RB, Fernandez E, Aoyagi Y, Normann RA (2004) Long-term stimulation and recording with a penetrating microelectrode array in cat sciatic nerve. IEEE Trans Biomed Eng 51:146-157.

Brindley GS, Polkey CE, Rushton DN, Cardozo L (1986) Sacral anterior root stimulators for bladder control in paraplegia: the first 50 cases. J Neurol Neurosurg Psychiatry 49:1104-1114.

Brushart TM (1988) Preferential reinnervation of motor nerves by regenerating motor axons. J Neurosci 8:1026-1031.

Brushart TM (1990) Preferential motor reinnervation: a sequential double-labeling study. Restor Neurol Neurosci 1:281-287.

Brushart TM (1993) Motor axons preferentially reinnervate motor pathways. J Neurosci 13:2730-2738.

Brushart TM (1991) The mechanical and humoral control of specificity in nerve repair. In: Operative nerve repair and reconstruction (Gelberman RH, ed), pp 215. Philadelphia: JB Lippincott Company.

Brushart TM, Mathur V, Sood R, Koschorke G (1995) Dispersion of regenerating axons across enclosed neural gaps. J Hand Surg 20:557-564.

Brushart TM, Gerber J, Kessens P, Chen YG, Royall RM (1998) Contributions of pathway and neuron to preferential motor reinnervation. J Neurosci 18:8674-8681.

Bunge RP (1993) Expanding roles for the Schwann cell: ensheathment, myelination, trophism and regeneration. Curr Opin Neurobiol 3:805-809.

Butí M, Verdu E, Labrador RO, Vilches JJ, Fores J, Navarro X (1996) Influence of physical parameters of nerve chambers on peripheral nerve regeneration and reinnervation. Exp Neurol 137:26-33.

Cajal SRy (1928) Degeneration and regeneration of the nervous system. Hafner, London (Facsimile of the 1928 edition).

Cannon WB (1939) A law of denervation. Am J Med Sci 198:739-750.

Cavallaro E, Micera S, Dario P, Jensen W, Sinkjaer T (2003) On the intersubject generalization ability in extracting kinematic information from afferent nervous signals. IEEE Trans Biomed Eng 50:1063-1073.

Ceballos D, Valero-Cabré A, Valderrama E, Schüttler M, Stieglitz T, Navarro X (2002) Morphological and functional evaluation of peripheral nerve fibers regenerated through polyimide sieve electrodes over long term implantation. J Biomed Mater Res 60:517-528.

Chao K, An W, Cooney I, Linschied R (1989) Biomechanics of the hand. (World Scientific, ed).

Chapin JK, Moxon KA (2000) Neural prosthesis for restoration of sensory and motor function. CRC Press. Boca Raton.

Chen ZL, Strickland S (2003) Laminin gamma1 is critical for Schwann cell differentiation, axon myelination, and regeneration in the peripheral nerve. J Cell Biol 163:889-899.

Chiu DT (1999) Autogenous venous nerve conduits. A review. Hand Clin 15:667-671.

Cutkosky MR (1985) Robotic grasping and fine manipulation. Kluwer academic publishers. Boston.

Dario P, Garzella P, Toro M, Micera S, Alavi M, Meyer U, Valderrama E, Sebastiani L, Ghelarducci B, Mazzoni C, Pastacaldi P (1998) Neural interfaces for regenerated nerve stimulation and recording. IEEE Trans Rehabil Eng 6:353-363.

Della Santina CC, Kovacs GT, Lewis ER (1997) Multi-unit recording from regenerated bullfrog eighth nerve using implantable silicon-substrate microelectrodes. J Neurosci Methods 72:71-86.

Dellon AL, Mackinnon SE (1988) Basic scientific and clinical applications of peripheral nerve regeneration. Surg Annu 20:59-100.

Dent EW, Gertler FB (2003) Cytoskeletal dynamics and transport in growth cone motility and axon guidance. Neuron 40:209-227.

Devor M, Govrin-Lippmann R, Angelides K (1993) Na+ channel immunolocalization in peripheral mammalian axons and changes following nerve injury and neuroma formation. J Neurosci 13:1976-1992.

Dickson BJ (2002) Molecular mechanisms of axon guidance. Science 298:959-964.

Doolabh VB, Hertl MC, Mackinnon SE (1996) The role of conduits in nerve repair: a review. Rev Neurosci 7:47-84.

Eberhardt KA, Irintchev A, Al-Majed AA, Simova O, Brushart TM, Gordon T, Schachner M (2006) BDNF/TrkB signaling regulates HNK-1 carbohydrate expression in regenerating motor nerves and promotes funtional recovery after peripheral nerve repair. Exp Neurol 198:500-510.

Edell DJ (1986) A peripheral nerve information transducer for amputees: long-term multichannel recordings from rabbit peripheral nerves. IEEE Trans Biomed Eng 33:203-214.

Fawcett JW, Keynes RJ (1990) Peripheral nerve regeneration. Annu Rev Neurosci 13:43-60.

Fields RD, Ellisman MH (1986a) Axons regenerated through silicone tube splices. I. Conduction properties. Exp Neurol 92:48-60.

Fields RD, Ellisman MH (1986b) Axons regenerated through silicone tube splices. II. Functional morphology. Exp Neurol 92:61-74.

Fields RD, Le Beau JM, Longo FM, Ellisman MH (1989) Nerve regeneration through artificial tubular implants. Prog Neurobiol 33:87-134.

Fine EG, Decosterd I, PapaloõÈzos M, Zurn AD, Aebischer P (2002) GDNF and NGF released by synthetic guidance channels support sciatic nerve regeneration across a long gap. Eur J Neurosci 15:589-601.

Franz CK, Rutishauser U, Rafuse VF (2005) Polysialylated neural cell adhesion molecule is necessary for selective targeting of regenerating motor neurons. J Neurosci 25:2081-2091.

Fried K, Govrin-Lippmann R, Rosenthal F, Ellisman MH, Devor M (1991) Ultrastructure of afferent axon endings in a neuroma. J Neurocytol 20:682-701.

Fried K, Govrin-Lippmann R, Devor M (1993) Close apposition among neighbouring axonal endings in a neuroma. J Neurocytol 22:663-681.

Frisen J, Risling M, Fried K (1993) Distribution and axonal relations of macrophages in a neuroma. Neuroscience 55:1003-1013.

Fu SY, Gordon T (1995) Contributing factors to poor functional recovery after delayed nerve repair: prolonged denervation. J Neurosci 15:3886-3895.

Fu SY, Gordon T (1997) The cellular and molecular basis of peripheral nerve regeneration. Mol Neurobiol 14:67-116.

Goodall EV, Horch KW (1992) Separation of action potentials in multiunit intrafascicular recordings. IEEE Trans Biomed Eng 39:289-295.

Goodrum JF, Bouldin TW (1996) The cell biology of myelin degeneration and regeneration in the peripheral nervous system. J Neuropathol Exp Neurol 55:943-953.

Grimes JH, Nashold BS (1974) Clinical application of electronic bladder stimulation in paraplegics. Br J Urol 46:653-657.

Guénard V, Kleitman N, Morrissey TK, Bunge RP, Aebischer P (1992) Syngeneic Schwann cells derived from adult nerves seeded in semipermeable guidance channels enhance peripheral nerve regeneration. J Neurosci 12:3310-3320.

Gutmann E, Sanders FK (1943) Recovery of fiber numbers and diameters in the regeneration of peripheral nerve. J Physiol 101:489-518.

Hall S (2005) The response to injury in the peripheral nervous system. J Bone Joint Surg 87:1309-1319.

Hausman MR, Masters J, Panozzo A (2003) Hand transplantation: current status. Mt Sinai J Med 70:148-153.

Henry EW, Chiu TH, Nyilas E, Brushart TM, Dikkes P, Sidman RL (1985) Nerve regeneration through biodegradable polyester tubes. Exp Neurol 90:652-676.

Herndon JH (2000) Composite-tissue transplantation-a new frontier. N Engl J Med 343:503-505.

Heumann R (1987) Regulation of the synthesis of nerve growth factor. J Exp Biol 132:133-150.

Jenq C-B, Coggeshall RE (1985) Long-term patterns of axon regeneration in the sciatic nerve and its tributaries. Brain Res 345:34-44.

Jezernik S, Grill WM, Sinkjaer T (2001) Neural network classification of nerve activity recorded in a mixed nerve. Neurol Res 23:429-434.

Jones KJ, Brown TJ, Damaser M (2001) Neuroprotective effects of gonadal steroids on regenerating peripheral motoneurons. Brain Res Rev 37:372-382.

Kapandji A (1982) The physiology of the joints. In: Upper Limb (Livingstone C, ed). Edinburgh.

Korner L (1979) Afferent electrical nerve stimulation for sensory feedback in hand prostheses. Clinical and physiological aspects. Acta Orthop Scand Suppl 178:1-52.

Kovacs GT, Storment CW, Rosen JM (1992) Regeneration microelectrode array for peripheral nerve recording and stimulation. IEEE Trans Biomed Eng 39:893-902.

Kovacs GT, Storment CW, Halks-Miller M, Belczynski CR, Jr., Della Santina CC, Lewis ER, Maluf NI (1994) Silicon-substrate microelectrode arrays for parallel recording of neural activity in peripheral and cranial nerves. IEEE Trans Biomed Eng 41:567-577.

Kuffler DP (1986) Isolated satellite cells of a peripheral nerve direct the growth of regenerating frog axons. J Comp Neurol 249:57-64.

Kuffler DP (1989) Regeneration of muscle axons in the frog is directed by diffusible factors from denervated muscle and nerve tubes. J Comp Neurol 281:416-425.

Lanzetta M, Petruzzo P, Vitale G, Lucchina S, Owen ER, Dubernard JM, Hakim N, Kapila H (2004) Human hand transplantation: what have we learned? Transplant Proc 36:664-668.

Lawrence SM, Larsen JO, Horch KW, Riso RR, Sinkjaer T (2002) Long-term biocompatibility of implanted polymer-based intrafascicular electrodes. J Biomed Mater Res 63:501-506.

Le TB, Aszmann O, Chen YG, Royall RM, Brushart TM (2001) Effects of pathway and neuronal aging on the specificity of motor axon regeneration. Exp Neurol 167:126-132.

Le Beau JM, Ellisman MH, Powell HC (1988) Ultrastructural and morphometric analysis of long-term peripheral nerve regeneration through silicone tubes. J Neurocytol 17:161-172.

Lefurge T, E. G, Horch KW, Stensaas L, Schoenberg AA (1991) Chronically implanted intrafascicular recording electrodes. Ann Biomed Eng 19:197-207.

Letorneau P, Shattuck TA (1989) Distribution and possible interactions of actin-associatted proteins and cell adhesion molecules of nerve growth cones. Development 195:505-519.

Letorneau PC, Condic ML, Snow DM (1994) Interactions of developing neurons with the extracellular matrix. J Neurosci 14:915-928.

Lieberman AR (1971) The axon reaction: a review of the principal features of perikaryal responses to axon injury. Int Rev Neurobiol 14:49-124.

Lindholm D, Heumann R, Meyer M, Thoenen H (1987) Interleukin-1 regulates synthesis of nerve growth factor in nonneuronal cells of rat sciatic nerve. Nature 330:658-659.

Liu HM (1996) Growth factors and extracellular matrix in peripheral nerve regeneration, studied with a nerve chamber. J Peripher Nerv Syst 1:97-110.

Liu X, McCreery DB, Carter RR, Bullara LA, Yuen TG, Agnew WF (1999) Stability of the interface between neural tissue and chronically implanted intracortical microelectrodes. IEEE Trans Rehabil Eng 7:315-326.

Llinás R, Nicholson C, Johnson K (1973) Implantable monolithic wafer recording electrodes for neurophysiology. In: Brain Unit Activity during behaviour (MI P, ed), pp 105-110: Charles Thomas IL.

Lobsiger CS, Taylor V, Suter U (2002) The early life of a Schwann cell. Biol Chem 383:245-253.

Loeb GE, Marks WB, Beatty PG (1977) Analysis and microelectrode design of tubular electrode arrays intended for chronic, multiple single-unit recording from captured nerve fibres. Med Biol Eng Comput 15:195-201.

Loeb GE, Peck RA (1996) Cuff electrodes for chronic stimulation and recording of peripheral nerve. J Neurosci Methods 64:95-103.

Low PA, Ward K, Schmelzer JD, Brimijoin S (1985) Ischemic conduction failure and energy metabolism in experimental diabetic neuropathy. Am J Physiol 248:457-462.

Lundborg G (1982a) Regeneration of peripheral nerves--a biological and surgical problem. Scand J Plast Reconstr Surg Suppl 19:38-44.

Lundborg G, Gelberman RH, Longo FM, Powell HC, Varon S (1982b) In vivo regeneration of cut nerves encased in silicone tubes: growth across a six-millimeter gap. J Neuropathol Exp Neurol 41:412-422.

Lundborg G (2003) Richard P. Bunge memorial lecture. Nerve injury and repair--a challenge to the plastic brain. J Peripher Nerv Syst 8:209-226.

Lundborg G (2004) Alternatives to autologous nerve grafts. Handchir Mikrochir Plast Chir 36:1-7.

Lunn ER, Brown MC, Perry VH (1990) The pattern of axonal degeneration in the peripheral nervous system varies with diffrenet types of lesion. Neuroscience 35:157-165.

Macias MY, Lehman CT, Sanger JR, Riley DA (1998) Myelinated sensory and alpha motor axon regeneration in peripheral nerve neuromas. Muscle Nerve 21:1748-1758.

Mackinnon SE, Dellon AL (1990) A study of nerve regeneration across synthetic (Maxon) and biologic (collagen) nerve conduits for nerve gaps up to 5 cm in the primate. J Reconstr Microsurg 6:117-121.

Mackinnon SE, Dellon AL, O'Brien JP (1991) Changes in nerve fibre numbers distal to nerve repair in the rat sciatic nerve model. Muscle Nerve 14:1116-1122.

Madison RD, Archibald SJ, Brushart TM (1996) Reinnervation accuracy of the rat femoral nerve by motor and sensory neurons. J Neurosci 16:5698-5703.

Maki Y (2002) Specificity in peripheral nerve regeneration: a discussion of the issues and the research. J Orthop Sci 7:594-600.

Malagodi MS, Horch KW, Schoenberg AA (1989) An intrafascicular electrode for recording of action potentials in peripheral nerves. Ann Biomed Eng 17:397-410.

Malmstrom JA, McNaughton TG, Horch KW (1998) Recording properties and biocompatibility of chronically implanted polymer-based intrafascicular electrodes. Ann Biomed Eng 26:1055-1064.

Mannard A, Stein RB, Charles D (1974) Regeneration electrode units: implants for recording from single peripheral nerve fibers in freely moving animals. Science 183:547-549.

Martini R, Schachner M (1988) Immunoelectron microscopic localization of neural cell adhesion molecules (L1, N-CAM, and myelin-associated glycoprotein) in regenerating adult mouse sciatic nerve. J Cell Biol 106:1735-1746.

Martini R, Xin Y, Schmitz B, Schachner M (1992) The L2/HNK-1 Carbohydrate Epitope is Involved in the Preferential Outgrowth of Motor Neurons on Ventral Roots and Motor Nerves. Eur J Neurosci 4:628-639.

Martini R, Schachner M, Brushart TM (1994) The L2/HNK-1 carbohydrate is preferentially expressed by previously motor axon-associated Schwann cells in reinnervated peripheral nerves. J Neurosci 14:7180-7191.

McNaughton TG, Horch K (1994) Action potential classification with dual channel intrafascicular microelectrodes. IEEE Trans Biomed Eng 41:609-616.

McNaughton TG, Horch KW (1996) Metallized polymer fibers as leadwires and intrafascicular microelectrodes. J Neurosci Methods 70:103-110.

Meek MF, Coert JH (2002) Clinical use of nerve conduits in peripheral-nerve repair: review of the literature. J Reconstr Microsurg 18:97-109.

Mensinger AF, Anderson DJ, Buchko CJ, Johnson MA, Martin DC, Tresco PA, Silver RB, Highstein SM (2000) Chronic recording of regenerating VIIIth nerve axons with a sieve electrode. J Neurophysiol 83:611-615.

Meyer M, Matsuoka I, Wetmore C, Olson L, Thoenen H (1992) Enhanced synthesis of brain-derived neurotrophic factor in the lesioned peripheral nerve: different mechanisms are responsible for the regulation of BDNF and NGF mRNA. J Cell Biol 119:45-54.

Micera S, Cavallaro E, Carrozza MC, Dario P (2003) Processing of the efferent ENG signals recorded using sieve electrodes: Open issues and possible approaches. CYBERHAND EU Project Technical Report.

Moore FD (2000) Ethical problems special to surgery: surgical teaching, surgical innovation, and the surgeon in managed care. Arch Surg 135:14-16.

Murphy B, Krieger C, Hoffer JA (2004) Chronically implanted epineural electrodes for repeated assessment of nerve conduction velocity and compound action potential amplitude in rodents. J Neurosci Methods 132:25-33.

Nannini N, Horch K (1991) Muscle recruitment with intrafascicular electrodes. IEEE Trans Biomed Eng 38:769-776.

Navarro X, Calvet S, Butí M, Gómez N, Cabruja E, Garrido P, Villa R, Valderrama E (1996) Peripheral nerve regeneration through microelectrode arrays based on silicon technology. Restor Neurol Neurosci 9:151-160.

Navarro X, Calvet S, Rodriguez FJ, Stieglitz T, Blau C, Buti M, Valderrama E, Meyer JU (1998) Stimulation and recording from regenerated peripheral nerves through polyimide sieve electrodes. J Peripher Nerv Syst 3:91-101.

Navarro X, Krueger TB, Lago N, Micera S, Stieglitz T, Dario P (2005) A critical review of interfaces with the peripheral nervous system for the control of neuroprostheses and hybrid bionic systems. J Peripher Nerv Syst 10:229-258.

Negredo P, Castro J, Lago N, Navarro X, Avendano C (2004) Differential growth of axons from sensory and motor neurons through a regenerative electrode: a

stereological, retrograde tracer, and functional study in the rat. Neuroscience 128:605-615.

Nguyen QT, Sanes JR, Lichtman JW (2002) Pre-existing pathways promote precise projection patterns. Nat Neurosci 5:861-867.

Omer GE, Spinner M, Van Beek AL (1998) Management of peripheral nerve problems. In: WB Saunders Company (edition S, ed). Philadelphia.

Perry VH, Brown MC (1992) Role of macrophages in peripheral nerve degeneration and repair. Bioessays 14:401-406.

Pollard TD, Borisy GG (2003) Cellular motility driven by assembly and disassembly of actin filaments. Cell 112:453-465.

Prochazka A, Mushahwar VK, McCreery DB (2001) Neural prostheses. J Physiol 533:99-109.

Ramachandran A, Schuettler M, Lago N, Doerge T, Koch KP, Navarro X, Stieglitz T, Hoffmann KP (2006) Design, in vitro and in vivo assessment of a multi-channel sieve electrode with integrated multiplexer. J Neural Eng.

Rathjen FG (1988) A neurite outgrowth-promoting molecule in developing fiber tracts. Trends Neuroscience 11:183-184.

Riso RR (1999) Strategies for providing upper extremity amputees with tactile and hand position feedback-moving closer to the bionic arm. Technol Health Care 7:401-409.

Robinson GA, Madison RD (2003) Preferential motor reinnervation in the mouse: comparison of femoral nerve repair using a fibrin sealant or suture. Muscle Nerve 28:227-231.

Robinson GA, Madison RD (2004) Motor neurons can preferentially reinnervate cutaneous pathways. Exp Neurol 190:407-413.

Rodríguez FJ, Verdú E, Ceballos D, Navarro X (2000) Neural guides seeded with autologous Schwann cells improve nerve regeneration. Exp Neurol 161:571-584.

Roitbak T, Sykova E (1999) Diffusion barriers evoked in the rat cortex by reactive astrogliosis. Glia 28:40-48.

Rosen JM, Grosser M, Hentz VR (1990) Preliminary experiments in nerve regeneration through laser-drilled holes in silicon chips. Restor Neurol Neurosci 2:89-102.

Rutishauser U, Acheson A, Hall AK, Mann DM, Sunshine J (1988) The neural cell adhesion molecule (NCAM) as a regulator of cell-cell interactions. Science 240:53-59.

Rutishauser U, Landmesser L (1996) Polysialic acid in the vertebrate nervous system: a promoter of plasticity in cell– cell interactions. Trends Neurosci 19:422– 427.

Sah DW, Ossipov MH, Rossomando A, Silvian L, Porreca F (2005) New approaches for the treatment of pain: the GDNF family of neurotrophic growth factors. Curr Top Med Chem 5:577-583.

Saito H, Nakao Y, Takayama S, Toyama Y, Asou H (2005) Specific expression of an HNK-1 carbohydrate epitope and NCAM on femoral nerve Schwann cells in mice. Neurosci Res 53:314-322.

Scadding JW, Thomas PK (1983) Retrograde growth of myelinated fibres in experimental neuromas. J Anat 136:793-799.

Scaravilli F (1984) The influence of distal environment on peripheral nerve regeneration across a gap. J Neurocytol 13:1027-1041.

Schmalbruch H (1986) Fiber composition of the rat sciatic nerve. Anat Rec 215:71-81.

Schmidt RA (1986) Advances in genitourinary neurostimulation. Neurosurgery 19:1041-1044.

Seddon HJ (1943) Three types of nerve injury. Brain 66:237-288.

Selzer ME (1980) Regeneration of peripheral nerve. In: The physiology of peripheral nerve disease (AJ S, ed), pp 358-431. Philadelphia: Saunders.

Sheng M, Greenberg M (1990) The regulation and function of c-fos and other immediate early genes in the nervous system. Neuron 4:477-485.

Shirley DM, Williams SA, Santos PM (1996) Brain-derived neurotrophic factor and peripheral nerve regeneration: a functional evaluation. Laryngoscope 106:629-632.

Skene JHP (1989) Axonal growth-associated proteins. Annu Rev Neurosci 12:127-156.

Stein RB, Peckham PH, Popovic DP (1992) Prostheses. Replacing motor function after diseases or disability. New York.

Sterne GD, Brown RA, Green CJ, Terenghi G (1997) Neurotrophin-3 delivered locally via fibronectin mats enhances peripheral nerve regeneration. Eur J Neurosci 9:1388-1396.

Stieglitz T, Beutel H, Meyer JU (1997) A flexible, light-weight multichannel sieve electrode with integrated cables for interfacing regenerating peripheral nerves. Sensors Actuators 60:240-243.

Strittmatter SM, Igarashi M, Fishman MC (1994) GAP-43 amino terminal peptides modulate growth cones morphology and neurite outgrowth. J Neurosci 14:5503-5513.

Sunderland S (1951) A classification of peripheral nerve injuries producing loss of function. Brain 74:491-516.

Sunderland S (1991) Nerve injury and their repair. A critical appraisal. Livingstone C.

Suzuki G, Ochi M, Shu N, Uchio Y, Matsuura Y (1998) Sensory neurons regenerate more dominantly than motoneurons during the initial stage of the regenerating process after peripheral axotomy. Neuroreport 9:3487-3492.

Tessier-Lavigne M, Goodman CS (1996) The molecular biology of axon guidance. Science 274:1123-1133.

Toft PB, Fugleholm K, Schmalbruch H (1988) Axonal branching following crush lesions of peripheral nerves of rat. Muscle Nerve 11:880-889.

Turner JN, Shain W, Szarowski DH, Andersen M, Martins S, Isaacson M, Craighead H (1999) Cerebral astrocyte response to micromachined silicon implants. Exp Neurol 156:33-49.

Udina E, Gold BG, Navarro X (2004a) Comparison of continuous and discontinuous FK506 administration on autograft or allograft repair of sciatic nerve resection. Muscle Nerve 29:812-822.

Udina E, Rodríguez FJ, Verdú E, Espejo M, Gold BG, Navarro X (2004b) FK506 enhances regeneration of axons across long peripheral nerve gaps repaired with collagen guides seeded with allogeneic Schwann cells. Glia 47:120-129.

Utley DS, Lewin SL, Cheng ET, Verity AN, Sierra D, Terris DJ (1996) Brain-derived neurotrophic factor and collagen tubulization enhance functional recovery after peripheral nerve transection and repair. Arch Otolaryngol Head Neck Surg 122:407-413.

Uzman BG, Villegas GM (1983) Mouse sciatic nerve regeneration through semipermeable tubes: A quantitative model. J Neurosci Res 9:325-338.

Valero-Cabre A, Tsironis K, Skouras E, Navarro X, Neiss WF (2004) Peripheral and spinal motor reorganization after nerve injury and repair. J Neurotrauma 21:95-108.

Valero-Cabré A, Navarro X (2002) Functional impact of axonal misdirection after peripheral nerve injuries followed by graft or tube repair. J Neurotrauma 19:1475-1485.

Van Lookeren Campagne M, Oestreicher AB, Van Bergen en Henegowen PM, Gispen WH (1989) Ultrastructural immunocytochemical localization of B-50/GAP43, a protein kinase C substrate, in isolated presynaptic nerve terminals and neuronal growth cones. J Neurocytol 18:479-489.

Verdú E, Navarro X (1998) The role of Schwann cell in nerve regeneration. In Castellano B, González B, Nieto-Sampedro M (eds): Understanding glial cells. Kluwer Academic Pub pp 319-359.

Wallman L, Zhang Y, Laurell T, Danielsen N (2001) The geometric design of micromachined silicon sieve electrodes influences funcional nerve regeneration. Biomaterials 22:1187-1193.

Warwick K, Gasson M, Hutt B, Goodhew I, Kyberd P, Andrews B, Teddy P, Shad A (2003) The application of implant technology for cybernetic systems. Arch Neurol 60:1369-1373.

Waxman SG, Dib-Hajj S, Cummins TR, Black JA (1999) Sodium channels and pain. Proc Natl Acad Sci USA 96:7635–7639.

Wells MR, Vaidya U, Ricci JL, Christie C (2001) A neuromuscular platform to extract electrophysiological signals from lesioned nerves: a technical note. J Rehabil Res Dev 38:385-390.

Werner A, Willem M, Jones LL, Kreutzberg GW, Mayer U, Raivich G (2000) Impaired axonal regeneration in alpha7 integrin-deficient mice. J Neurosci 20:1822-1830.

Whitworth IH, Brown RA, Dore CJ, Anand P, Green CJ, Terenghi G (1996) Nerve growth factor enhances nerve regeneration through fibronectin grafts. J Hand Surg [Br] 21:514-522.

Williams LR, Longo FM, Powell HC, Lundborg G, Varon S (1983) Spatial-temporal progress of peripheral nerve regeneration within a silicone chamber: parameters for a bioassay. J Comp Neurol 218:460-470.

Williams LR, Varon S (1985) Modification of fibrin matrix formation in situ enhances nerve regeneration in silicone chambers. J Comp Neurol 231:209-220.

Yoshida K, Horch K (1993) Selective stimulation of peripheral nerves using dual intrafascicular electrodes. IEEE Trans Biomed Eng 40:492-494.

Yoshida K, Jovanovic K, Stein RB (2000) Intrafascicular electrodes for stimulations and recording from mudpuppy spinal roots. J Neurosci Methods 96:47-55.

You S, Petrov T, Chung PH, Gordon T (1997) The expression of the low affinity nerve growth factor receptor in long-term denervated Schwann cells. Glia 20:87-100.

Yu K, Kocsis JD (2005) Schwann cell engraftment into injured peripheral nerve prevents changes in action potential properties. J Neurophysiol 94:1519-1527.

Zalewski AA (1970) Effects of reinnervation on denervated skeletal muscle by axons of motor, sensory, and sympathetic neurons. Am J Physiol 219:1675-1679.

Zhang Y, Campbell G, Anderson PN, Martini R, Schachner M, Lieberman AR (1995) Molecular basis of interactions between regenerating adult rat thalamic axons and Schwann cells in peripheral nerve grafts. II. Tenascin-C. J Comp Neurol 361:210-224.

Zhao Q, Drott J, Laurell T, Wallman L, Lindström K, Bjursten LM, Lundborg G, Montelius L, Danielsen N (1997) Rat sciatic nerve regeneration through a micromachined silicon chip. Biomaterials 19:75-80.

Zimmermann M (2001) Pathobiology of neuropathic pain. Eur J Pharmacol 429:23-37.